

27622



National Library
of Canada

Bibliothèque nationale
du Canada

CANADIAN THESES
ON MICROFICHE

THÈSES CANADIENNES
SUR MICROFICHE

NAME OF AUTHOR NOM DE L'AUTEUR ODNEY STUART BROWN
TITLE OF THESIS TITRE DE LA THÈSE COMPUTER ANALYSIS OF SAND AND
PETROLEUM DISTRIBUTION IN THE MANVILLE
GROUP, TURIN AREA, SOUTHERN ALBERTA
UNIVERSITY UNIVERSITÉ U of ALBERTA
DEGREE FOR WHICH THESIS WAS PRESENTED
GRADE POUR LEQUEL CETTE THÈSE FUT PRÉSENTÉE M SC
YEAR THIS DEGREE CONFERRED ANNÉE D'OBTENTION DE CE GRADE 1976
NAME OF SUPERVISOR NOM DU DIRECTEUR DE THÈSE DR. G D WILLIAMS

Permission is hereby granted to the NATIONAL LIBRARY OF
CANADA to microfilm this thesis and to lend or sell copies
of the film.

The author reserves other publication rights, and neither the
thesis nor extensive extracts from it may be printed or other-
wise reproduced without the author's written permission.

L'autorisation est, par la présente, accordée à la BIBLIOTHÈ-
QUE NATIONALE DU CANADA de microfilmer cette thèse et
de prêter ou de vendre des exemplaires du film.

L'auteur se réserve les autres droits de publication ni la
thèse ni de longs extraits de celle-ci ne doivent être imprimés
ou autrement reproduits sans l'autorisation écrite de l'auteur.

DATED DATE 26 April 76 SIGNED / SIGNÉ R S Brown

PERMANENT ADDRESS RÉSIDENCE FIXE C/O IMPERIAL OIL LIMITED
500 SIXTH AVE S.W.,
CALGARY ALTA T2P 0S1

INFORMATION TO USERS

THIS DISSERTATION HAS BEEN
MICROFILMED EXACTLY AS RECEIVED

This copy was produced from a microfiche copy of the original document. The quality of the copy is heavily dependent upon the quality of the original thesis submitted for microfilming. Every effort has been made to ensure the highest quality of reproduction possible.

PLEASE NOTE: Some pages may have indistinct print. Filmed as received.

Canadian Theses Division
Cataloguing Branch
National Library of Canada
Ottawa, Canada K1A 0N4

AVIS AUX USAGERS

LA THESE A ETE MICROFILMEE
TELLE QUE NOUS L'AVONS RECUE

Cette copie a été faite à partir d'une microfiche du document original. La qualité de la copie dépend grandement de la qualité de la thèse soumise pour le microfilmage. Nous avons tout fait pour assurer une qualité supérieure de reproduction.

NOTA BENE: La qualité d'impression de certaines pages peut laisser à désirer. Microfilmée telle que nous l'avons reçue.

Division des thèses canadiennes
Direction du catalogage
Bibliothèque nationale du Canada
Ottawa, Canada K1A 0N4

THE UNIVERSITY OF ALBERTA

COMPUTER ANALYSIS OF SAND AND PETROLEUM DISTRIBUTION IN THE
MANNVILLE GROUP, TIRIN AREA, SOUTHERN ALBERTA

by

(C)

RODNEY S. BROWN B.Sc.(Hons.)

A THESIS

SUBMITTED TO THE FACULTY OF GRADUATE STUDIES AND RESEARCH
IN PARTIAL FULFILMENT OF THE REQUIREMENTS FOR THE DEGREE
OF MASTER OF SCIENCE

DEPARTMENT OF GEOLOGY

EDMONTON, ALBERTA

SPRING, 1976

THE UNIVERSITY OF ALBERTA

FACULTY OF GRADUATE STUDIES AND RESEARCH

The undersigned certify that they have read, and recommend to the Faculty of Graduate Studies and Research for acceptance, a thesis entitled "COMPUTER ANALYSIS OF SAND AND PETROLEUM DISTRIBUTION IN THE MANNVILLE GROUP, TURIN AREA, SOUTHERN ALBERTA", submitted by Rodney S. Brown B.Sc. (Hons.), in partial fulfilment of the requirements for the degree of Master of Science.

[Handwritten signature]

Supervisor

[Handwritten signature]
[Handwritten signature]
[Handwritten signature]

DATE 26 April 1976

ABSTRACT

Sand distribution in the Mannville Group in the Turin area was determined using computer generated sand percentage slice maps, structure contour maps and isopach maps. Trend surface analysis was used to separate local anomalies from regional trends within the structural and lithologic data.

Continental Mannville Group sediments were deposited on an eroded surface of southwesterly-dipping Mississippian and Jurassic strata. Initial deposition consisted mainly of sand, and was restricted to stream channels on the pre-Mannville surface, the configuration of which reflected the northwesterly strike of the bedding. Infilling of valleys and the denudation of ridges produced a landscape of low relief by late Lower Mannville time. Maturation of the Cordilleran source area resulted in the progressive decrease in the volume of sand deposited within the Lower Mannville sequence, culminating in the widespread deposition of shales of the Ostracode Zone. Differential compaction of Lower Mannville sediments produced an Upper Mannville topography similar to, yet more subdued than that of the pre-Mannville surface. During late Mannville time, predominantly fine-grained clastics were deposited. Periodic uplift and erosion of the source area resulted in the influx of sand, which was more variably distributed than in the Lower Mannville Group. Drainage channels frequently coalesced to form wide valleys and floodplains of meandering and braided streams. Mannville sedimentation was halted by the transgression of the Colorado Sea.

Petroleum distribution is a function of pre-Mannville topography, sand distribution and post-depositional northwesterly-tilting of the basin. Traps are predominantly stratigraphic, formed by shaling out of channel sands. Oil and gas pools occur in the updip portion of sands

which accumulated along the flanks and crests of structural highs corresponding to topographic highs in the pre-Mannville surface. Production occurs mainly from the Lower Mannville Group and the Glauconitic Sandstone Equivalent.

ACKNOWLEDGEMENTS

The author wishes to thank Dr. G.D. Williams, project supervisor, for advice and financial support given during the preparation of the thesis. Messrs. D. Flint, T. Lam, and D. Proudfoot of the Western Canada Coal Resource Data Base, and Mr. K. McDonell of the Computing Science Department, University of Alberta, assisted in the application and creation of computer programs used in the study. Their help is greatly appreciated.

The Alberta Research Council made available microfilm facilities for the examination of electric well logs.

Special thanks go to Linda for assistance rendered throughout the year and for typing the manuscript.

Financial assistance was provided by a University of Alberta Graduate Teaching Assistantship and a Province of Alberta Graduate Studies Scholarship.

TABLE OF CONTENTS

	PAGE
ABSTRACT	iv
ACKNOWLEDGEMENTS	vi
LIST OF TABLES	ix
LIST OF FIGURES	ix
 CHAPTER	
I. INTRODUCTION	1
A. PURPOSE AND LOCATION OF STUDY	1
B. PREVIOUS WORK	1
II. METHOD OF STUDY	7
A. COMPILATION OF GEOLOGIC DATA	7
B. COMPUTER TECHNIQUES	8
(1) Gridding and Contouring	8
(2) Trend Surface Analysis	11
III. REGIONAL GEOLOGY	15
IV. GEOLOGY OF THE MANNVILLE GROUP	19
V. GEOLOGY OF THE TURIN AREA	28
A. PRE-MANNVILLE GEOLOGY	28
B. LOWER MANNVILLE GEOLOGY	36
C. UPPER MANNVILLE GEOLOGY	42
D. POST-MANNVILLE GEOLOGY	45
VI. SAND DISTRIBUTION IN THE MANNVILLE GROUP	51
A. INTRODUCTION	51
B. LOWER MANNVILLE GROUP	53

TABLE OF CONTENTS (cont'd)

CHAPTER	PAGE
C. UPPER MANNVILLE GROUP	66
D. QUANTITATIVE ANALYSIS OF SAND DEPOSITION	75
E. CONCLUSION	84
VII. PETROLEUM DISTRIBUTION	85
A. INTRODUCTION	85
B. LOWER MANNVILLE GROUP	87
C. GLAUCONITIC SANDSTONE EQUIVALENT	91
D. UPPER MANNVILLE GROUP (POST-GLAUCONITIC SANDSTONE EQUIVALENT)	92
E. POST-MANNVILLE GROUP	95
VIII. SUMMARY AND CONCLUSIONS	97
IX. REFERENCES	100

LIST OF TABLES

TABLE		PAGE
1.	Thickness and Volume Parameters of Sand Intervals	80
2.	Volume Parameters for the Mannville Group	81

LIST OF FIGURES

FIGURE		PAGE
1.	Location Map	2
2.	Location Map - Turin area (showing location of wells)	3
3.	Regional Geology Map - Western Canada Sedimentary Basin	16
4.	Neocomian (Pre-Mannville) Paleogeography	21
5.	Early Upper Mannville Paleogeography	22
6.	Lower Cretaceous Correlation Chart - Western Canada and Montana	23
7.	IES Log Correlation; cross section X-Y	29
8.	IES Log Correlation; cross section A-B	30
9.	Structure Map: Top of Mississippian	31
10.	Isopach Map: Jurassic	33
11.	Structure Map: Base of Mannville Group	35
12.	Trend Surface Map: Base of Mannville Group	37
13.	Structure Map: Top of Lower Mannville Group	38
14.	Isopach Map: Lower Mannville Group	39
15.	Diagrammatic Cross sections - Turin Area	41
16.	Structure Map: Top of Mannville Group	43
17.	Trend Surface Map: Top of Mannville Group	44

LIST OF FIGURES (cont'd)

FIGURE		PAGE
18.	Isopach Map: Upper Mannville Group	46
19.	Isopach Map: Mannville Group	47
20.	Dip section across the Turin Area; cross section X-Y	49
21.	Strike section across the Turin Area; cross section A-B	50
22.	Diagrammatic subdivision of the Mannville Group	54
23.	Subdivision of Mannville Group into intervals for Sand Calculations	55
24.	Sand Percentage Map: Interval 15	56
25.	Sand Percentage Map: Interval 14	58
26.	Sand Percentage Map: Interval 13	59
27.	Sand Percentage Map: Interval 12	61
28.	Trend Surface Map: Interval 12	63
29.	Sand Percentage Map: Interval 11	64
30.	Sand Percentage Map: Interval 10	65
31.	Sand Percentage Map: Interval 9	67
32.	Trend Surface Map: Interval 9	68
33.	Sand Percentage Map: Interval 8	70
34.	Sand Percentage Map: Interval 7	71
35.	Sand Percentage Map: Interval 6	72
36.	Sand Percentage Map: Interval 5	73
37.	Sand Percentage Map: Interval 4	74
38.	Sand Percentage Map: Interval 3	76
39.	Sand Percentage Map: Interval 2	77
40.	Sand Percentage Map: Interval 1	78

LIST OF FIGURES (cont'd)

FIGURE		PAGE
41.	Trend Surface Map: Interval 1	79
42.	Sand Volume Distribution, Mannville Group	83
43.	Petroleum Distribution: Lower Cretaceous	86
44.	Petroleum Distribution: Lower Mannville Group	88
45.	Petroleum Distribution: Glauconitic Sandstone Equiv.	93
46.	Petroleum Distribution: Upper Mannville Group	94
47.	Petroleum Distribution: Bow Island Formation	96

LIST OF APPENDICES

Computer printout of structural and lithologic data used in this study is held by the Geology Department library, University of Alberta.

Chapter I
INTRODUCTION

A. PURPOSE AND LOCATION OF STUDY

The purpose of the study was threefold:

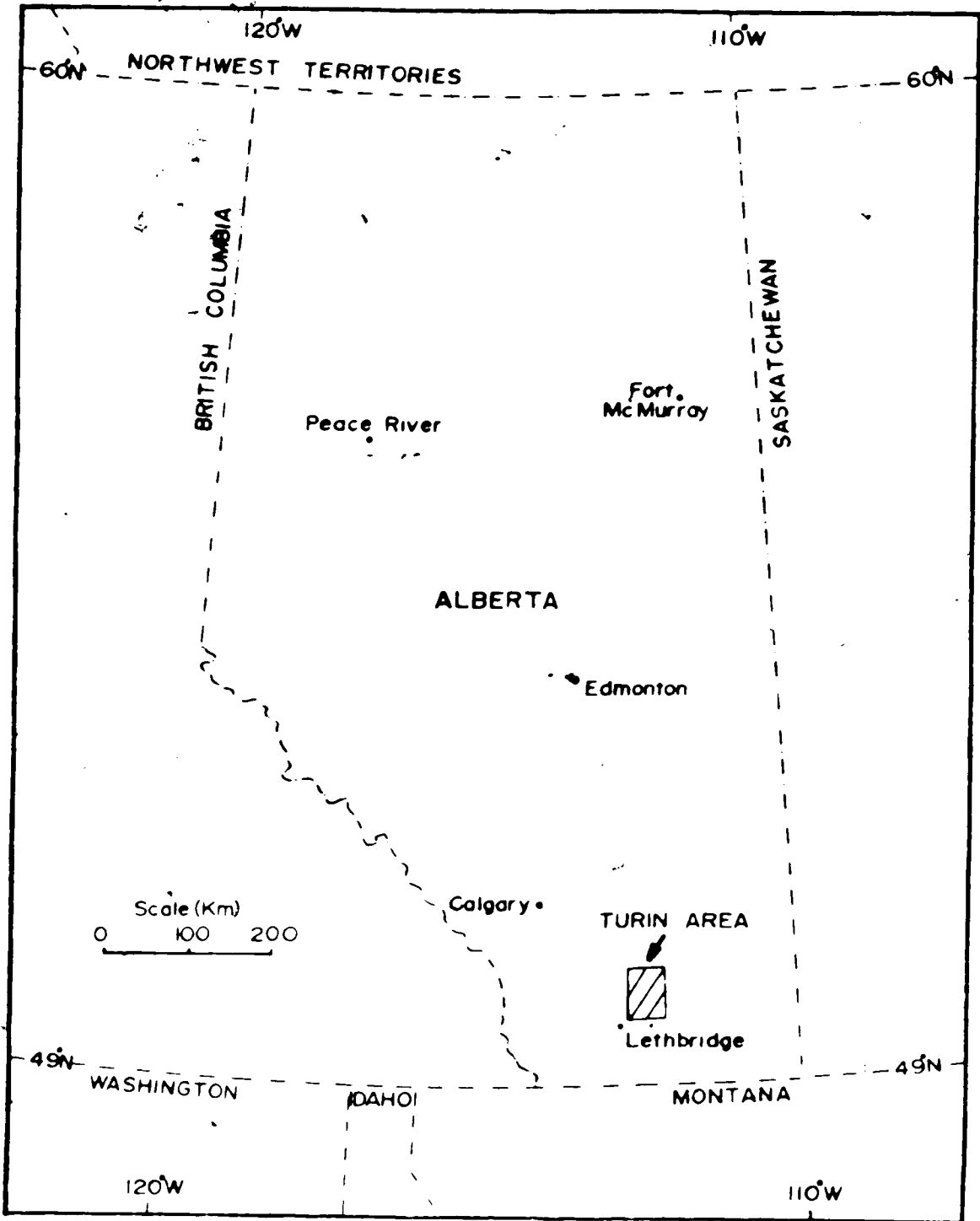
1. To map the distribution of sandstones in the Mannville Group using numerical techniques. This method was seen as a viable alternative to conventional interpretive log correlation, particularly within a continental sequence where sandstones are laterally discontinuous and exhibit considerable variation in log response.

2. To find reasons for the distribution of sandstones in the succession.

3. To determine the factors controlling the occurrence of oil and gas in the sandstones.

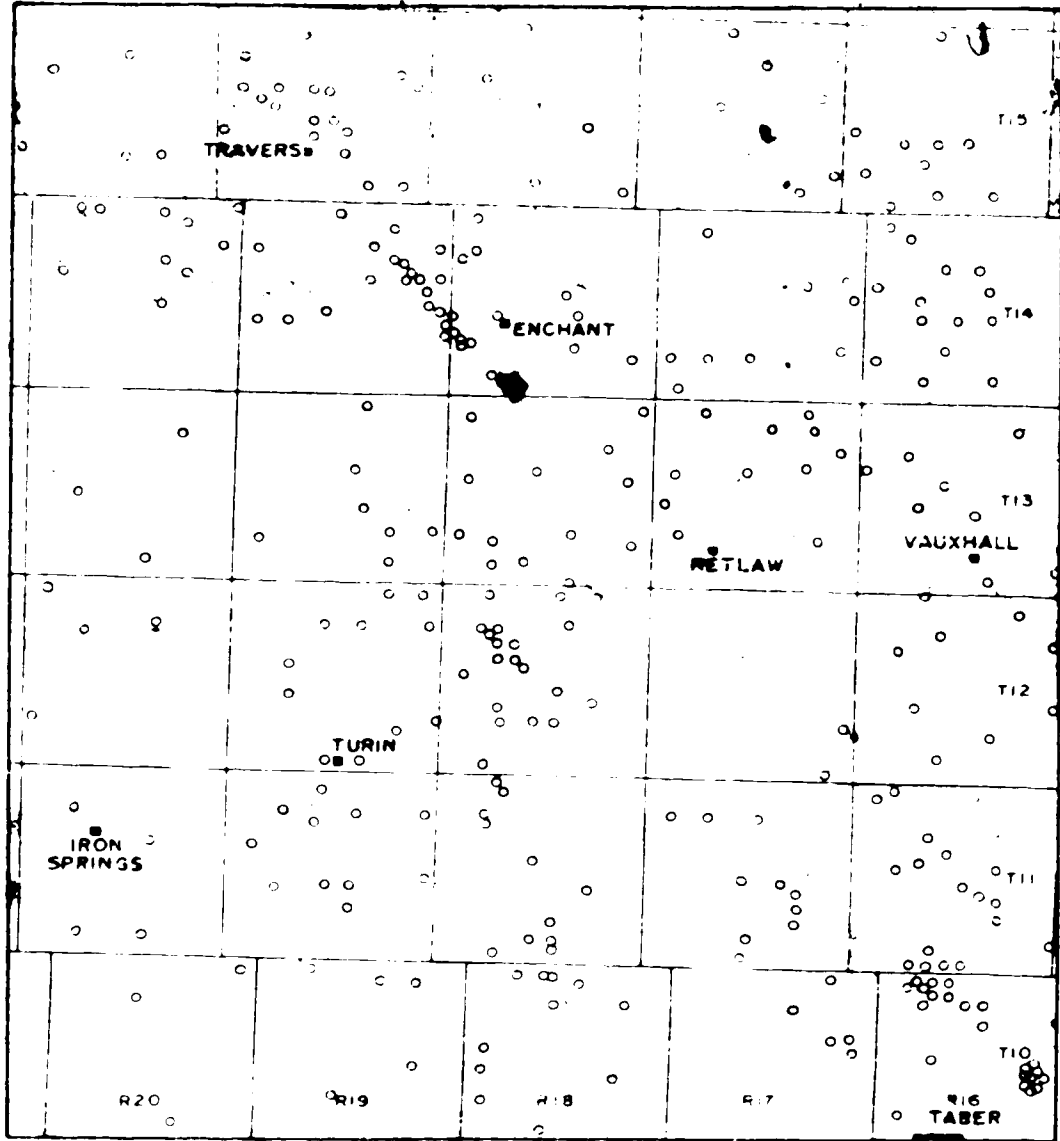
The Turin area is located in the southern Alberta plains (Fig. 1) within Townships 10 to 15, Ranges 16 to 20 west of the Fourth Meridian (Fig. 2), and covering approximately 1,100 square miles (2,850 square kilometres).

This area was chosen because the Mannville Group is entirely continental, and has oil and gas production from a number of sandstones within the sequence (the Little Bow, Enchant, Retlaw, Turin and Taber North fields). The shape and distribution of these fields suggested a fluvial origin for the reservoirs. Well density and distribution was sufficient to enable detailed lithologic analysis.



LOCATION MAP

FIGURE 1



LOCATION MAP - TURIN AREA

(SHOWING WELL DISTRIBUTION)

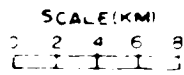


FIGURE 2

Poor Copy

B. PREVIOUS WORK

A chronological review of publications on the Mannville Group and its equivalents in Alberta, from McLearn's (1932, 1944) initial attempts at a regional correlation of the Lower Cretaceous, to the definitive, localized, sedimentological studies of the 1960's, is given in Acham (1971). Supplemental to this is Mellon's (1967) geographic subdivision of previous work, and a listing of important paleontological and sedimentological studies. The Lower Cretaceous correlations of Rudkin (1964) for western Canada and north central United States remain generally accepted to this date.

The Mannville Group and its equivalents in southwestern Saskatchewan were described by Maycock (1967) and Christopher (1975), and in southeastern Saskatchewan by Price (1963). Stelck (1975) discussed basement control of Cretaceous sand sequences in western Canada.

Correlations between Cretaceous formations of Montana and sequences in the western interior of the United States were presented by Cobban and Reeside (1952) and Gill and Cobban (1966), and a synthesis of the Cretaceous of central western United States was given by McGookey (1972). A recent attempt at reconstructing the Cretaceous palaeogeography of North America was made by Williams and Stelck (1975).

The Jurassic succession in Alberta and Saskatchewan was described by Weir (1954), Milner and Thomas (1954), Thompson and Crookford (1958) and Milner and Blaklee (1958). An overview and collation of previous work occurs in Springer *et al.* (1964). Peterson (1972) described the Jurassic of Montana and its correlatives in the central western United States. The Mississippian stratigraphy of western Canada is presented in Macauley *et al.* (1964), and in Craig (1972) for Montana.

Petroleum occurrences in the Lower Cretaceous of southern Alberta are documented in White (1960), Century (1966), and Larson (1969). Berry (1974) described the geology and development of the Grand Forks oil field, 15 miles (25 kilometres) east of the Turin area which produces from sandstones of the Mannville Group. The petroleum geology of the Alberta portion of the Sweetgrass arch is discussed in Herbaly (1974), and Cox (1966) described Jurassic and Cretaceous stratigraphic traps associated with the structure.

The composition, form, and depositional environments of fluvial sandstone bodies were described by Allen (1965), Potter (1967), Visher (1972) and Schumm (1972).

Computer application to geology during the decade following the pioneering work of the late 1950's was briefly outlined by Krumbein (1969). Krumbein's (1956) study into the separation of regional and local components in facies maps was the forerunner to his use of trend surface analysis of contour maps (Krumbein, 1959). Merriam and Harbaugh (1963) applied trend surface analysis to structural data in several areas of the central United States, and showed the relationship between trend anomalies and the distribution of oil and gas fields. Whitten (1969) described the use of computers in handling directional variables measured in structural geology.

Statistical analysis of data and computer modelling of sedimentary and stratigraphic features were discussed by Harbaugh and Bonham-Carter (1970). Davis (1973) contains useful sections on contouring and trend surface analysis, and Chayes (1970) discussed the significance of higher order trend surfaces.

Robinson et al. (1969) used spatial filtering to analyse stratigraphic horizons in southeastern Alberta, and defined structural trends in the Turin area similar to those mapped by trend surface analysis in the present study. A comparable investigation to that of the author was conducted by Wermund and Jenkins (1970), in which trend surface analysis was used to recognize deltaic sand bodies in the Upper Pennsylvanian of north central Texas.

Chapter II
METHOD OF STUDY

A. COMPILATION OF GEOLOGIC DATA

Stratigraphic correlations were established between the base of the Fish Scale Sandstone and top of the Mississippian, using IES, gamma-sonic and density logs from one well in each of the thirty townships in the study area. The tops of the Upper Mannville Group, Lower Mannville Group, Jurassic and Mississippian were then picked in 302 wells. Elevations relative to mean sea level were used in the generation of computer-contoured structure and isopach maps. Trend surface analysis was applied to the top and base of the Mannville Group to separate anomalous structural and depositional features from regional trends. These maps formed the basis for determining the degree of structural control on the distribution of sandstone in the Mannville Group.

For mapping purposes the Upper Mannville Group was proportionately subdivided into nine slices, each approximately fifty feet (fifteen metres) thick, and the Lower Mannville Group into slices of constant thickness (fifty feet), the total number of slices depending on the total isopach of the group. Sandstone thickness in each slice was picked from gamma logs. The gamma radiation response of sandstone ranges from 35 to 160+ API units, depending upon clay content (Wood et al., 1974), with an "average" response of 85 API units. In this study, a 60 API unit cutoff was used to indicate clean fluvial sands within the Mannville sequence.

Computer-contoured sandstone percentage maps were produced for each slice, and stacking of these maps showed the changing depositional pattern during Mannville time. Trend surface analysis of the sand isolith maps was used to separate regional sand distribution from anomalously thick accumulations, and thereby to enhance the outline of individual sandstone bodies. Changes in the influx of sand during deposition were ascertained by calculating the volume of sandstone per unit of thickness in each slice, and these data were used to make inferences regarding erosion of the source area and regional sedimentation.

Petroleum occurrences in the Turin area were plotted according to type and stratigraphic position, and comparison of these plots with the lithologic and structural maps led to the formulation of an hypothesis regarding the entrapment of petroleum in the Mannville Group.

B. COMPUTER TECHNIQUES

1. Gridding and Contouring

Uniformity of distribution and the density of data points determine the reliability of contour maps. The type of distribution of wells in the Turin area was checked according to the procedure of Davis (1973, pp. 301-307) — a chi-square method to test for uniformity and a Poisson distribution to test for randomness. A uniform distribution of points is one in which the density of points in one subarea is equal to the density of points in another of the same size. Such a distribution may be random (where any subarea is as likely to receive a point as any other subarea, with the placement of a point having no influence on the position of any other) or regular (where points occur at the nodes of a grid). A minimum of five data points in each subarea were required for the chi-square method used to be valid.

The Turin area was divided into 30 subareas of equal size, with the expected number of data points (wells) in each subarea being:

$$E = \frac{\text{total number of data points}}{\text{number of subareas}} = \frac{302}{30} = 10$$

A chi-square test of goodness-of-fit of the expected (uniform) distribution to the observed distribution is given by:

$$\chi^2 = \sum \frac{(O-E)^2}{E}$$

where O is the observed number of data points in a subarea. The test has $(m-2)$ degrees of freedom, where m is the number of subareas. The computed chi-square value exceeded the critical value of chi-square at the 5% significance level and so the data were not uniformly distributed.

The non-random distribution of points in the Turin area was verified by the Poisson distribution test. For n points to be randomly distributed within an area consisting of m subareas of equal size, the probability, Pr , that r points will fall into a subarea is:

$$Pr = \frac{e^{-\gamma} \gamma^r}{r!}$$

where γ is the expected number of points per subarea and e is the base of natural logarithms. The expected number of subareas that contain r points is:

$$E(r) = Pr \cdot m$$

The expected number of subareas that contained from zero to the maximum number of points in any subarea was calculated, and the observed number of subareas containing r points was determined. The observed and expected values were compared by a chi-square test, and the computed chi-square value was found to exceed the critical value of chi-square at the 5% significance level.

The high density of wells at producing fields resulted in an overall distribution intermediate between random and clustered. Because clustered data exert greater influence on contouring programs than those that are widely spaced, a gridding routine was used to produce a regular distribution of data points. The University of Alberta Computing Services' gridding program CGRID1 and contouring program CONTUR were used in the generation of structure and isopach maps. CGRID1 computes data values at the nodes of a grid superimposed on Z scattered points, and uses either Laplacian or Spline interpolation or varying degrees of both, depending on the value of C in the equation:

$$[D^2X + D^2Y - C(D^4X + D^4Y)]Z = 0$$

$$(D = \text{delta})$$

If $C = 0.0$, Laplacian interpolation takes place, and the computed surface has sharp peaks and dips at the data points, with no chance of spurious peaks occurring in areas devoid of data (Fox, 1962). By increasing C , Spline interpolation predominates over Laplacian and the surface passes

more smoothly through the data points; however, the possibility of spurious peaks and steep extrapolation in areas lacking data increase. A value of $C = 5.0$ was used in the present study.

In performing the interpolation, the program initially moved data points to the nearest grid points, and then shifted them back to their proper positions as the shape of the surface became evident. Values were computed at the nodes of a 40×34 grid, thereby producing a grid cell to data point ratio of 5:1, with each grid cell approximately equivalent in size to one township section. Reducing the grid cell size produced a smoother, more aesthetically pleasing contour map; however, such a reduction increased the number of gridded values to be calculated and hence the cost of the operation. Isopach map grids were created by subtracting the gridded elevations of the intervals' upper and lower structural surfaces.

The contouring method used in CONTUR is a modified version of the one described by Dayhoff (1963). The program interpolates between the gridded data points since a required contour line will usually not pass through the corners of the grid cells. All grid cells are searched for each contour value required and the points of intersection with the grid are written on a scratch file prior to contouring.

2. Trend Surface Analysis

The structural configuration of a stratigraphic horizon may be thought of in terms of a regional component, such as the depositional or structural dip within a sedimentary basin, and a local component caused by subsequent phases of deformation or localized sedimentologic variations (Krumbein, 1956). Similarly, a regionally distributed

lithologic facies may show local thickness or compositional variations which are distinguishable from, or superimposed upon, the regional trend. Trend surface analysis was used to separate local and regional elements in structural and lithologic data in the Turin area. This method, described by Krumbein (1959), Merriam and Harbaugh (1963) and Whitten (1969), involves the simulation of the regional trend by fitting a polynomial surface to the data. A first order polynomial fit is a plane, and the complexity of the surface increases with increasing order. The observed value at each data point is expressed in terms of its predicted value (on the surface) and an error component. Points lying above the predicted surface are considered positive residuals and those below negative. A best fit of the surface to the data is achieved using the least squares method, that is, the sum of the squares of the residuals is a minimum.

Trend surfaces are expressed algebraically as:

$$z = c_0 + \sum_{i=1}^n (c_i x^i + c_{i+n} y^i) + \sum_{i=1}^n (c_{2n+i} x^{n-i} y^i) + c_{3n} xy$$

where x and y are the map coordinates, z is the mapping parameter (e.g., structural elevation), n is the order of the surface fitted, and $i = 0, 1, 2, \dots, n$ (modified after Wernund and Jenkins (1970, p. 260)).

Once the coefficients c , that satisfy the least squares criterion for the specified order of polynomial, are determined, the predicted values of z can be calculated. The error term or residual equals the difference between the predicted and observed values. For the purpose

of contouring the trend surface and the residuals, a gridding routine was applied to ensure regular data distribution. As the grid cell size approximated that of one township section, residuals smaller than this could not be resolved.

First to eighth order surfaces were calculated for each set of data, and plots were generated for surfaces showing high statistical fit (indicated by the percent sum of squares accounted for) and good separation of regional and local components. A shortcoming of trend surface analysis was the subjectivity involved in deciding which order of polynomial gave the best resolution of meaningful anomalies. For progressively higher order polynomials, goodness of fit increased, resulting in progressively smaller deviations of the observed surface from the fitted surface. For the structural data, the observed surfaces so closely corresponded to the fifth to eighth order predicted surfaces, that few residuals existed, and the purpose of the exercise was defeated. The significance of progressively higher order surfaces was discussed by Chayes (1970), with reference to petrographic data.

Merriam and Harbaugh (1963) fitted trend surfaces of varying order to structural data from sedimentary basins of the central United States. Residuals were shown to correspond to areas of known petroleum occurrence; however, the trend surface chosen was done so by direct comparison of the various residual maps with the petroleum distribution plots, and not according to whether it showed the best statistical fit to the data. Without subjectively determining which order of surface produces the most meaningful anomalies for a given area, the residuals alone are of limited interpretative value.

For the uniformly dipping structural surfaces of the Turin area, second order polynomials were used (with 94% sum of squares accounted for) to enhance local topographic variations and hence determine the position of channels within the surfaces. Sand percentage data did not exhibit a regional distribution to which a valid mathematical surface could be applied (15% sum of squares accounted for with eighth order surfaces). Positive residuals (which corresponded to thick sand accumulations) resembled the raw data plot of sand distribution; however, the use of fourth order surfaces (with 13% sum of squares accounted for) led to a more accurate interpretation of the position of the distributaries in which most of the sand was deposited.



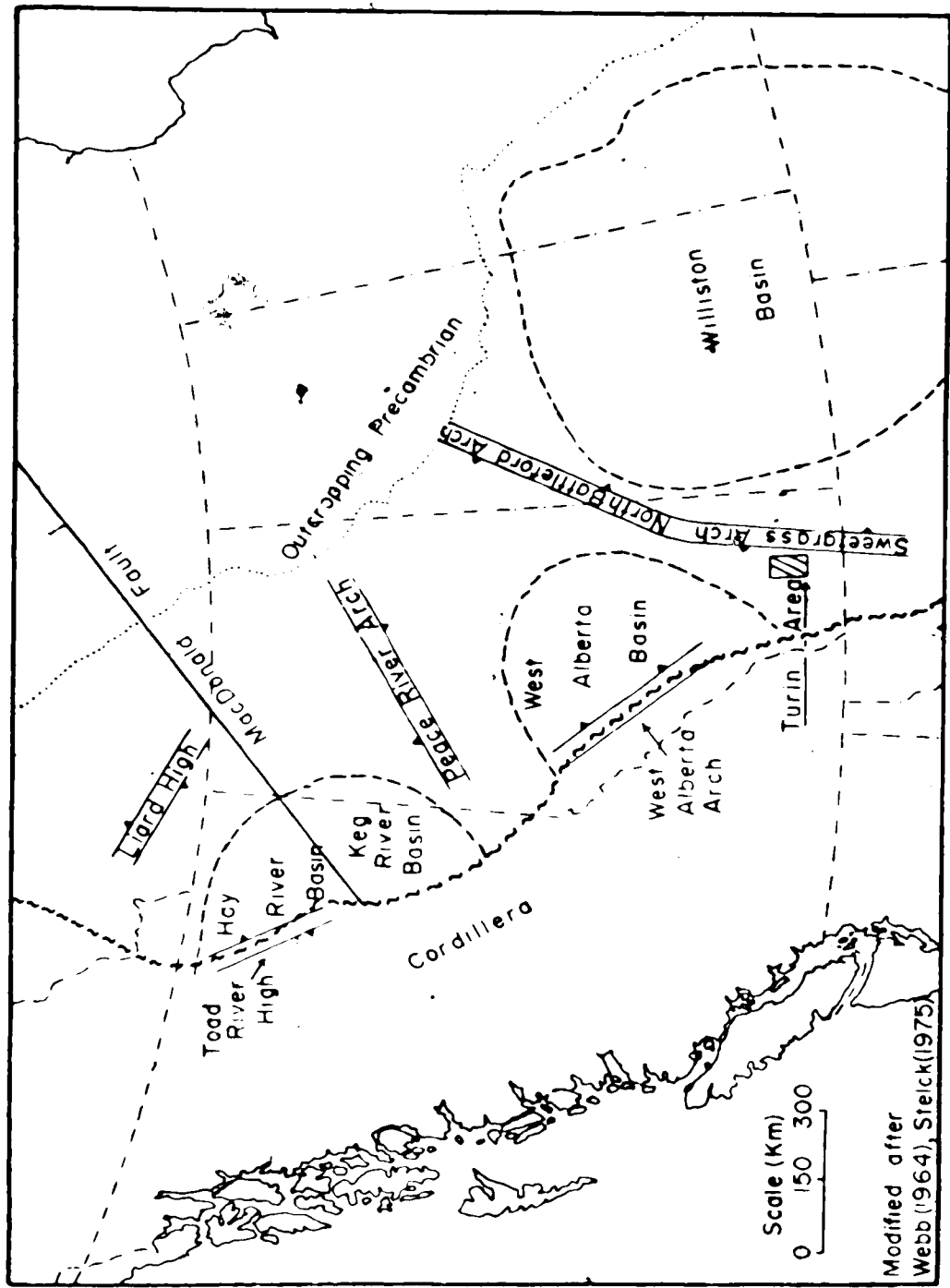
Chapter III

REGIONAL GEOLOGY

The Turin area lies in the southwestern part of the western Canada sedimentary basin, a northwesterly-trending Phanerozoic feature, flanked to the northeast by the Precambrian Canadian Shield (Fig. 3). The western margin is structural, and corresponds to the eastern edge of the Cordillera. The Palaeozoic and Mesozoic depositional basin extended farther west, but was subject to severe deformation during Mesozoic and Tertiary orogenies. Sediments thicken towards the Cordillera and attain a maximum thickness of approximately 16,000 feet (4,900 metres).

The Precambrian basement extends beneath the sedimentary cover and has had a profound effect upon the distribution and type of overlying sediments. Burwash *et al.* (1964, p. 14) stated that "... since the beginning of Palaeozoic time, movements in the basement have been epeirogenic, with localized vertical displacements subordinate to broad regional arching and subsidence". The arches are thought by Burwash and Krupicka (1969, 1970), Burwash *et al.*, (1973) to be the loci of potassium metasomatism of basement gneisses. The associated decrease in specific gravity has caused regional, periodic, isostatic readjustments to occur, forming a number of depositional sub-basins between the arches.

The Peace River arch forms the northern limit, and the West Alberta arch the western limit of the West Alberta basin (Stelck, 1975). In the southern part of the basin, the Sweetgrass arch extends northwards from Montana, across southeastern Alberta and meets the southward-plunging North Battleford arch extending from the Shield. This composite feature



REGIONAL GEOLOGY MAP - WESTERN CANADA SEDIMENTARY BASIN

FIGURE 3

separates the West Alberta basin from the Williston basin of Saskatchewan and Montana.

A summary of the depositional history of the western Canada sedimentary basin was given by Webb (1964). Early Palaeozoic deposition was confined to the Cordilleran miogeosyncline along the subsiding western margin of the craton. Periodic transgressions of the craton, followed by epeirogenic uplift and erosion, occurred during middle Cambrian to late Jurassic time. Cratonic sediments were predominantly shallow marine, and their eroded subcrop edges in Alberta subparallel the margin of the Shield.

Carbonate, evaporite, and clastic sequences were deposited over the Williston basin, western plains and Rocky Mountain region during the Devonian and Mississippian. Regional uplift occurred in the Pennsylvanian, and Middle Palaeozoic formations were erosionally truncated in a northeasterly direction (Webb, 1964). The interior cratonic region remained uplifted during the Permian and Triassic while miogeosynclinal sedimentation occurred along the craton's western margin.

Thin Jurassic marine shelf deposits occur over the western plains and thicken westwards, grading to deep water shales in the eastern Cordilleran region (Springer et al., 1964). Marine transgressions extended into the West Alberta basin from the west and south, resulting in the accumulation of shales and localized beach sands. Red beds were initially deposited in the Williston basin, followed by a shallow marine sequence in the middle Jurassic. Epeirogenic uplift and withdrawal of the sea in the late Jurassic is marked by a basinwide depositional hiatus.

Cretaceous beds overlie eroded Jurassic, Mississippian and Devonian strata with slight angular unconformity, overlapping progressively older beds in a northeasterly direction across the western plains (Rudkin, 1964). Incursions of the northern Boreal Sea and the southern Gulfian Sea onto the central North American continent occurred during the Lower Cretaceous (Williams and Stelck, 1975), and coalesced in the late Early Cretaceous to form a continuous seaway. The source of clastics was mainly from the central Cordilleran region, where granitic intrusion and vulcanism occurred throughout the Cretaceous. Upper Cretaceous rocks of the plains and Rocky Mountain foothills are mainly marine shales at the base, and become sandy and continental upwards (Williams and Burk, 1964).

Tertiary sedimentation in the western Canada sedimentary basin was continental. Uplift and deformation of the Rocky Mountains culminated in the Eocene (Taylor et al., 1964), following which the mountains and the region to the east underwent intense erosion, and coarse fluvial sands and gravels were deposited over the western plains. The western basin remained uplifted during the Quaternary and was the site of Pleistocene glaciation.

Chapter IV
GEOLOGY OF THE MANNVILLE GROUP

The Mannville Group represents the initial Cretaceous sedimentation on an uplifted erosional surface of Devonian, Carboniferous and Jurassic strata in the central and southern plains of the western Canada sedimentary basin. Deposition commenced in the Aptian and continued until early Late Albian, at which time the northern Boreal ocean and the Gulfian sea in the south transgressed, resulting in widespread deposition of Colorado Group marine sediments (Williams and Stelck, 1975).

Nauss (1945) named the Mannville Formation in the Vermilion area of east-central Alberta, and correlated it with the McMurray, Clearwater and Grand Rapids Formations of the lower Athabasca River. The unit was raised to group status by Badgley (1952), and subdivided by Glaister (1959) into two parts, with the boundary placed at the top of the Ostracode Zone of Loranger (1951). The Lower Mannville Group of central Alberta was defined by Williams (1963) as being equivalent to the McMurray Formation, comprising a basal Deville Member or "Detrital Zone" which was mainly restricted to topographic lows on the sub-Mannville surface; the Eilerslie Member or "Basal Quartz", a thick quartz sandstone and siltstone unit; and an upper "Calcareous" Member or "Ostracode Zone". Williams (1963) also divided the Upper Mannville Group into a basal Clearwater Formation (containing the Glauconitic Sandstone or Wabiskaw Member), and an upper Grand Rapids Formation. These formations overlie the McMurray Formation in the lower Athabasca River area. The Clearwater Formation was deposited during a southerly transgression of

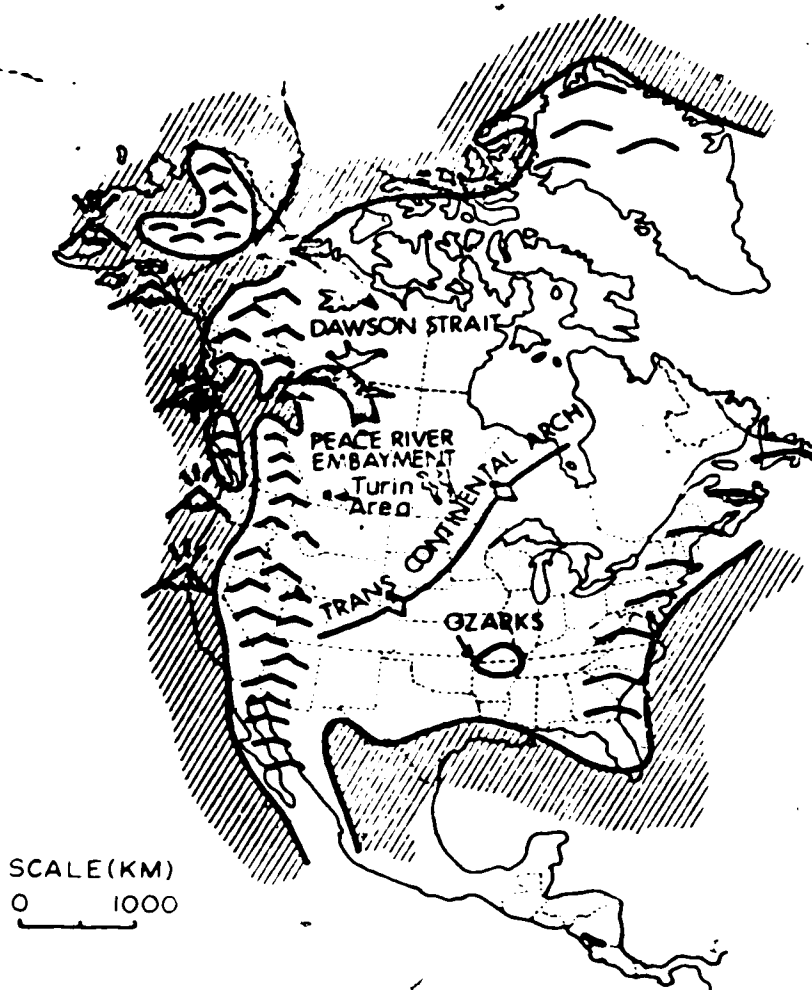
the Boreal sea. It grades laterally and vertically into the continental Grand Rapids Formation. The contact between the two is diachronous. Mellon (1967) did not consider the lithologies of the two formations sufficiently diverse in central Alberta, and renamed the correlative sequence the Fort Augustus Formation. At the end of Mannville time, the Clearwater sea retreated northwards and established a strand line on the northern side of the Peace River arch.

North American palaeogeography prior to Mannville deposition, and during early Upper Mannville time is shown in Figures 4 and 5 (after Williams and Stelck, 1975).

Lower Cretaceous strata thicken westward, and are called the Blairmore Group in the Alberta foothills (Fig. 6). Sedimentation in this area predated that in the plains, with deposition of the Cadomin Formation, a conglomerate averaging ten feet in thickness. The Blairmore Group in the southern foothills was divided by Mellon and Wall (1963) and Mellon (1967) into three units, the lower two of which were equivalent to the Mannville Group and an upper unit equivalent to the Bow Island Formation of the Colorado Group.

The Gladstone Formation (Mellon, 1967) constitutes the lower Blairmore Group, and consists of a basal conglomerate, equivalent to the Cadomin Formation in the north, a middle sequence of siltstone, shale and fine sandstone, and an upper "Calcareous" member of silty freshwater limestone and calcareous shale. The formation is correlated with the Lower Mannville Group.

Mellon (1967) proposed the name Beaver Mines Formation for the middle Blairmore Group, and correlated it with the Upper Mannville of



NEOCOMIAN (PRE-MANNVILLE) PALAEOGEOGRAPHY
After Williams and Stelck (1975)

FIGURE 4



SCALE (Km)
0 1000

EARLY UPPER MANNVILLE PALAEOGEOGRAPHY
After Williams and Stelck (1975)

FIGURE 5

SOUTHERN ALTA. FOOTHILLS	LOWER ATHABASCA RIVER	CENTRAL ALTA. PLAINS	SOUTHERN ALTA. PLAINS	MONTANA	SOUTHERN SASKATCHEWAN
Mellon (1967)	Williams (1963)	Mellon (1967)	This Paper	Rudkin (1964)	Christopher (1975)
M. BLAIRMORE GP L. BLAIRMORE GP GLADSTONE FM Calcareous M. Cadomin Eqv.	L. MANNVILLE GP Mc MURRAY FORMATION Deville Mbr.	L. MANNVILLE GP FORT AUGUSTUS McMURRAY FM Wabiskaw Mbr. Calcareous M.	L. MANNVILLE GP SUNBURST SANDSTONE Ostracod Zone Glouc. Sst. Equiv.	KOOTENAI GROUP BLACKLEAF MEMBER LAKOTA FM SUNBURST SANDSTONE CUTBANK SANDSTONE	MANNVILLE GROUP CANTUAR FM Aftos Mbr. Dimmock Crk Mbr. McCloud Mbr. SUCCESS FORMATION
M. BLAIRMORE GP BEAVER MINES FORMATION	U. MANNVILLE GP GRAND RAPIDS FORMATION CLEARWATER Wabiskaw Mbr.	VIKING FORMATION JOLI FOU FORMATION	BOW ISLAND FORMATION	NEWCASTLE SANDSTONE SKULL CREEK SHALE FALL RIVER SANDSTONE FUSON FORMATION	PENSE FM.
M. BLAIRMORE GP U. BLAIRMORE GP MILL CREEK FORMATION	COLORADO GP VIKING FORMATION JOLI FOU FORMATION	VIKING FORMATION JOLI FOU FORMATION	BOW ISLAND FORMATION	NEWCASTLE SANDSTONE SKULL CREEK SHALE FALL RIVER SANDSTONE FUSON FORMATION	PENSE FM.

LOWER CRETACEOUS CORRELATION CHART - WESTERN CANADA AND MONTANA

FIGURE 6

the plains. It consists of a lower shaly unit and an upper sandy section, and is conformable with the underlying Gladstone Formation. The succession is continental, and represents sedimentation on a western landmass during the transgression and regression of the Clearwater sea.

A widespread depositional hiatus occurred within the western Canada sedimentary basin following the regression of the Clearwater sea. Subsequent inundation of the basin by the southern and northern seas resulted in the deposition of the marine Colorado Group sediments. The Rocky Mountain foothills area initially remained the site of continental sedimentation, but was gradually overlapped by the Colorado sea. The Mill Creek Formation constitutes the continental Upper Blairmore sequence of the foothills. It consists mainly of argillites and thin interbeds of quartzose sandstone, in contrast to the feldspathic sandstones of the Beaver Mines Formation. Tuff beds and bentonite partings occur in the upper 300 feet of the Mill Creek Formation. In the southernmost area, the formation is overlain by, and possibly correlative in part with, the Crownsnest Volcanics. The Upper Blairmore Group of the foothills interfingers eastwards with the Bow Island Formation of the plains. During latest Lower Cretaceous time, the foothills area was finally transgressed by the Colorado sea and the Blairmore Group was overlain by shales of the Blackstone Formation, in part equivalent to the Upper Colorado Group.

The composition and depositional history of the Mannville Group in southern Saskatchewan has been recently revised by Christopher (1975). This area lay to the east of the Sweetgrass-North Battleford Arch, the drainage system of which initially flowed southward through the Williston

basin. Christopher (1975) showed a threefold subdivision of the group. The lowest unit is the Success Formation, a quartz sandstone succession of possible Neocomian age, equivalent to the Deville and part of the Ellerslie Members of the Lower Mannville Group of central Alberta. The Success Formation is divisible into two depositional units, resulting from two phases of uplift and erosion of the Shield source area. The basal coarse textured unit with interbedded mudstones and siltstones occurs in the deeper channels and is overlain by channel sandstones which were the products of meandering streams which periodically underwent braiding.

Uplift of the Swift Current region to the south resulted in the termination of Success sedimentation and a change in the direction of streams towards the west-northwest, to join the Mannville drainage pattern of Alberta. The Cantuar Formation (equivalent to the Upper Mannville Group) was deposited at this time, with early Cantuar streams channelling through the Success Formation into the underlying Devonian and Mississippian strata in some areas. The McCloud Member represents these initial deposits. The overlying Dimmock Creek Member was deposited under swampy, estuarine and marine conditions during the southern transgression of the Boreal sea (Clearwater time). Christopher (1975) stated that the sea extended into the Dakotas, apparently conflicting with Williams and Stelck (1975) who showed the southeastern extent of the Clearwater sea limited by the North Battleford arch. Christopher's Dimmock Creek Member may represent a subsequent transgression across Saskatchewan as the North Battleford arch ceased to act as a barrier.

During the final phase of Upper Mannville deposition (Atlas Member of the Cantuar Formation), southern Saskatchewan was a low-relief plain,

and the site of predominantly argillaceous deposition with periodic influxes of sand from the rising Rocky Mountain region. The Pense Formation was deposited during the inundation of the Colorado sea, which brought Mannville continental sedimentation to an end. Christopher (1975) has chosen to include this lower Colorado Group equivalent within the Mannville Group.

In Montana, the Kootenai Group is equivalent to the Mannville Group, with the Lakota Formation correlative with the Lower Mannville and the Fuson Formation and Fall River Sandstone with the Upper Mannville Group (Rudkin, 1964). The Lower Kootenai Group is divisible into a lower Cutbank Sandstone, an overlying Sunburst Sandstone, and an upper shale, equivalent to the Ostracode Zone. The Cutbank Sandstone is about 50 feet thick and thins northwards into Alberta. It consists of coarse sandstones and conglomerates and is depositonally continuous with the Sunburst Sandstone. It is either absent, or indistinguishable from the Sunburst Sandstone over most of southern Alberta. Its upper part is equivalent to the Deville and Eilerslie Members of central Alberta, while the lower conglomerate is correlated with the Cadomin Formation of the foothills. The Sunburst Sandstone consists of medium-grained sandstones, becoming finer at the top, and grading upwards into shales equivalent to the Ostracode Zone. These in turn are overlain by fluvial sandstones and shales of the Fuson Formation and Fall River Sandstone. Fall River continental sedimentation was followed by the deposition of the Skull Creek Shale (basal Colorado equivalent).

The southern Alberta plains lie at the centre of the five above-mentioned areas. Lithologically, the sequence resembles more closely that of the Mannville Group of the central Alberta plains.

In the Turin area, the Lower Mannville is continental, and consists of a lower sandy member (Sunburst Sandstone) and an overlying, thin (ten to thirty feet), shaly Ostracode Zone. A basal detrital unit equivalent to the Deville Member, or thin remnants of the Cutbank Sandstone, are not readily discernible.

Williams and Stelck (1975) show the southern limit of the Clearwater sea at the latitude of Calgary (Fig. 5). This is substantiated by the uniformity of the Upper Mannville section in the Turin area, and the absence of Grand Rapids and Clearwater components on well logs.

The author was reluctant to extend the term Fort Augustus Formation from central Alberta into the southern plains (no comparative study was attempted), and has used the term Upper Mannville Group for the beds above the Ostracode Zone. A high resistivity sandstone at the base of the Upper Mannville appears to be correlative with the Glauconitic Sandstone in the north, and is referred to as Glauconitic Sandstone Equivalent.

The marine Colorado Group overlies the Mannville in the southern plains. A thin sandstone at the base is generally included in the Basal Colorado Sandstone; however, the distinction drawn between it and sandstones at the top of the Mannville Group is highly subjective.

Chapter V

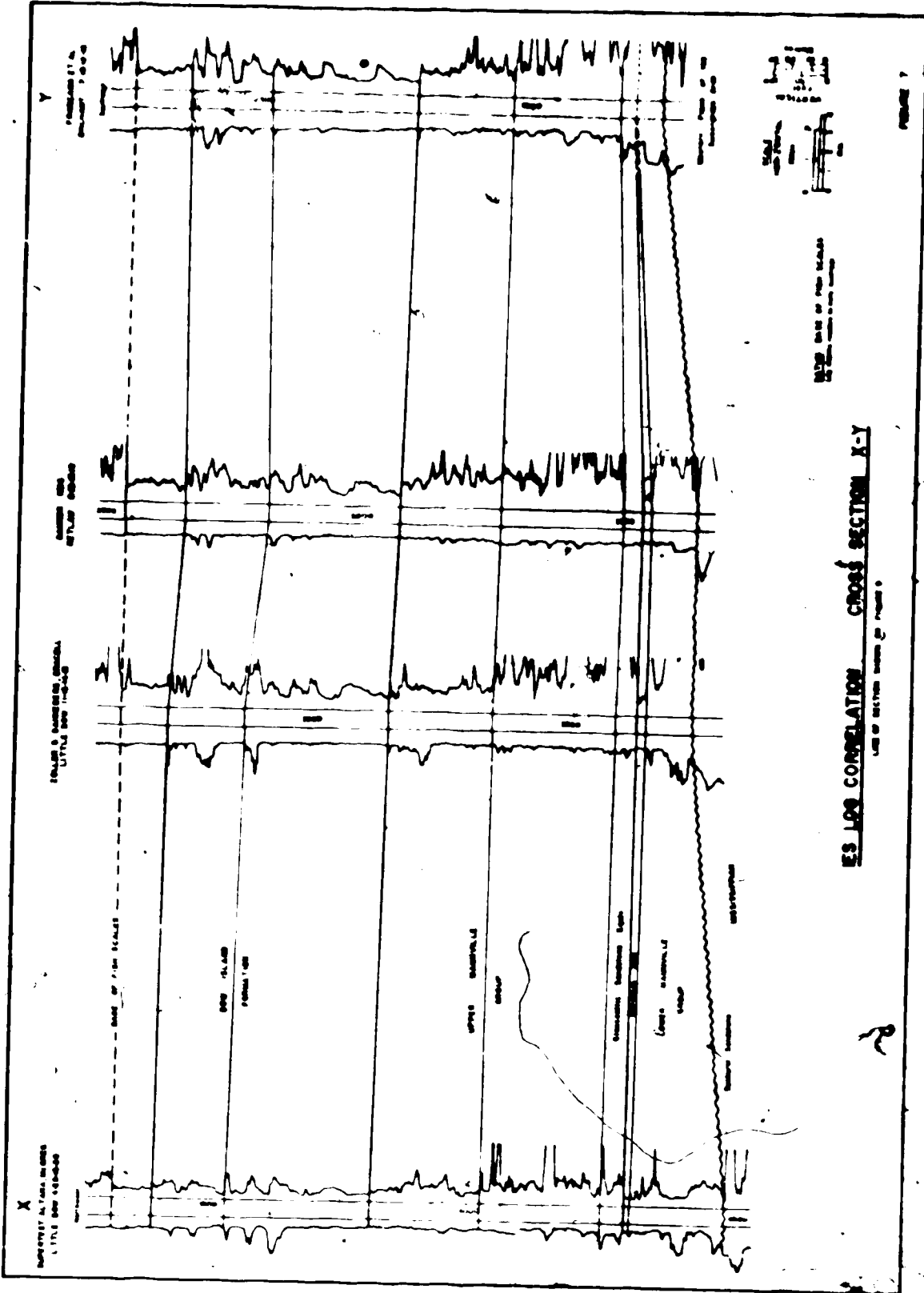
GEOLOGY OF THE TURIN AREA

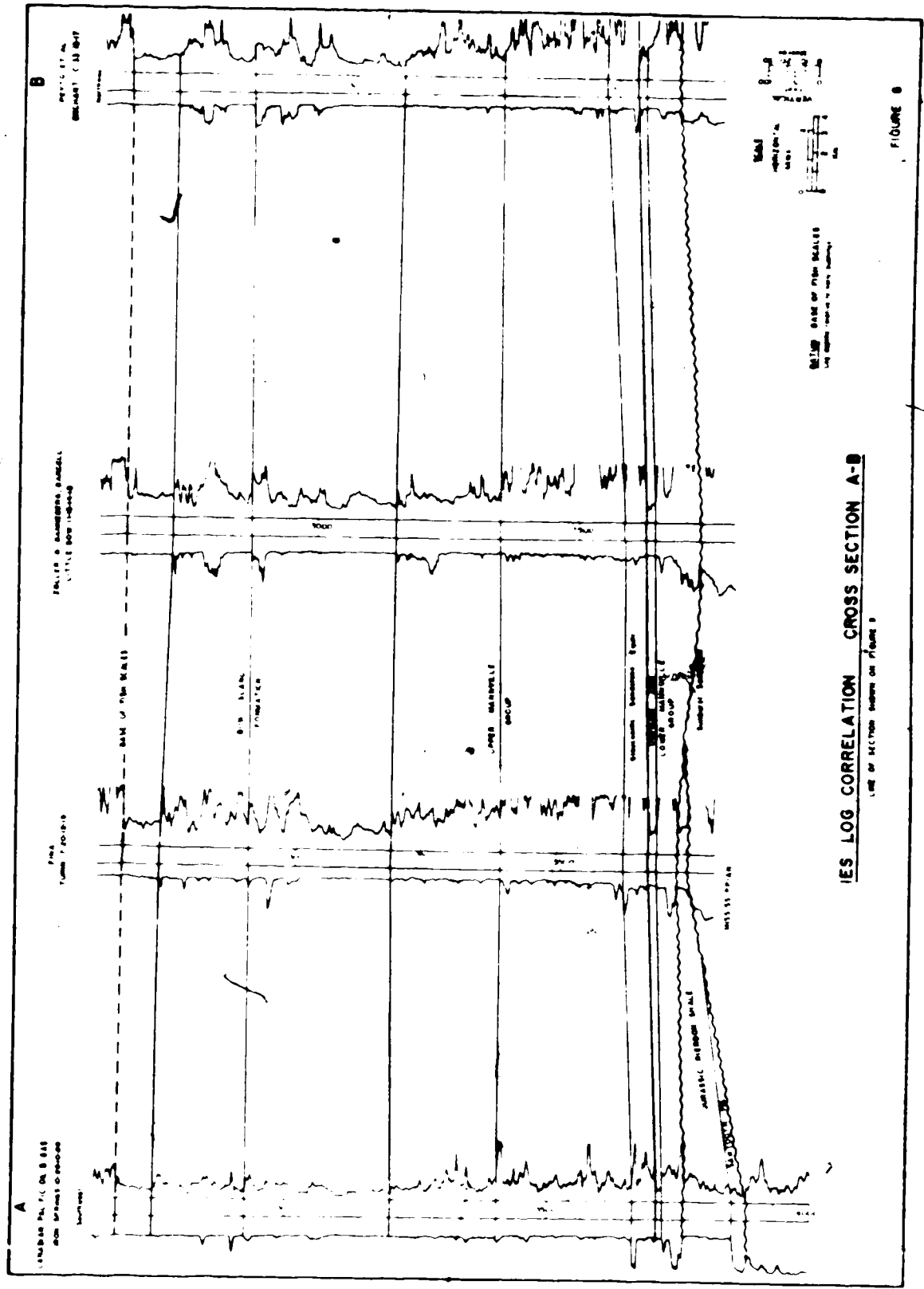
The Turin area lies on the margin of the West Alberta basin and the Sweetgrass arch. As shown by Herbaly (1974), the arch in southern Alberta may be divided into four northerly-plunging axes, the westernmost of which, the Taber-Enchant Axis, passes through the Turin area.

Strata dip gently from the arch towards the northwest, having attained the present structural configuration as a result of tilting associated with the Cordilleran Laramide orogeny. Electric log correlations (Figs. 7 and 8) of the interval from the top of the Mississippian to base of the Upper Cretaceous (base of Fish Scales) illustrate the pre-Tertiary southwesterly dip of the Mississippian and Jurassic strata and a northwesterly component of dip away from the Sweetgrass arch. The Lower Cretaceous succession is of fairly uniform thickness which is influenced mainly by pre-Cretaceous surface topography.

A. PRE-MANNVILLE GEOLOGY

The top of the Mississippian (Fig. 9) is homoclinal, dipping at approximately $0^{\circ}15'$ to the northwest. Mississippian sediments were deposited on a shallow cratonic shelf, thickening towards the southwest (Macauley *et al.*, 1964). Uplift, and the northeasterly truncation of the sequence during Pennsylvanian to Triassic time is evidenced in the Turin area by the subcrop of progressively older formations towards the northeast - from the Turner Valley and Shunda Formations in the southwest to the Pekisko Formation in the northeast.





WELLS LOG CORRELATION CROSS SECTION A-B

LINE OF SECTION between well 7-2019-10 and 7-2019-13

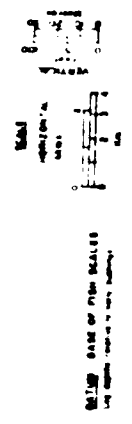
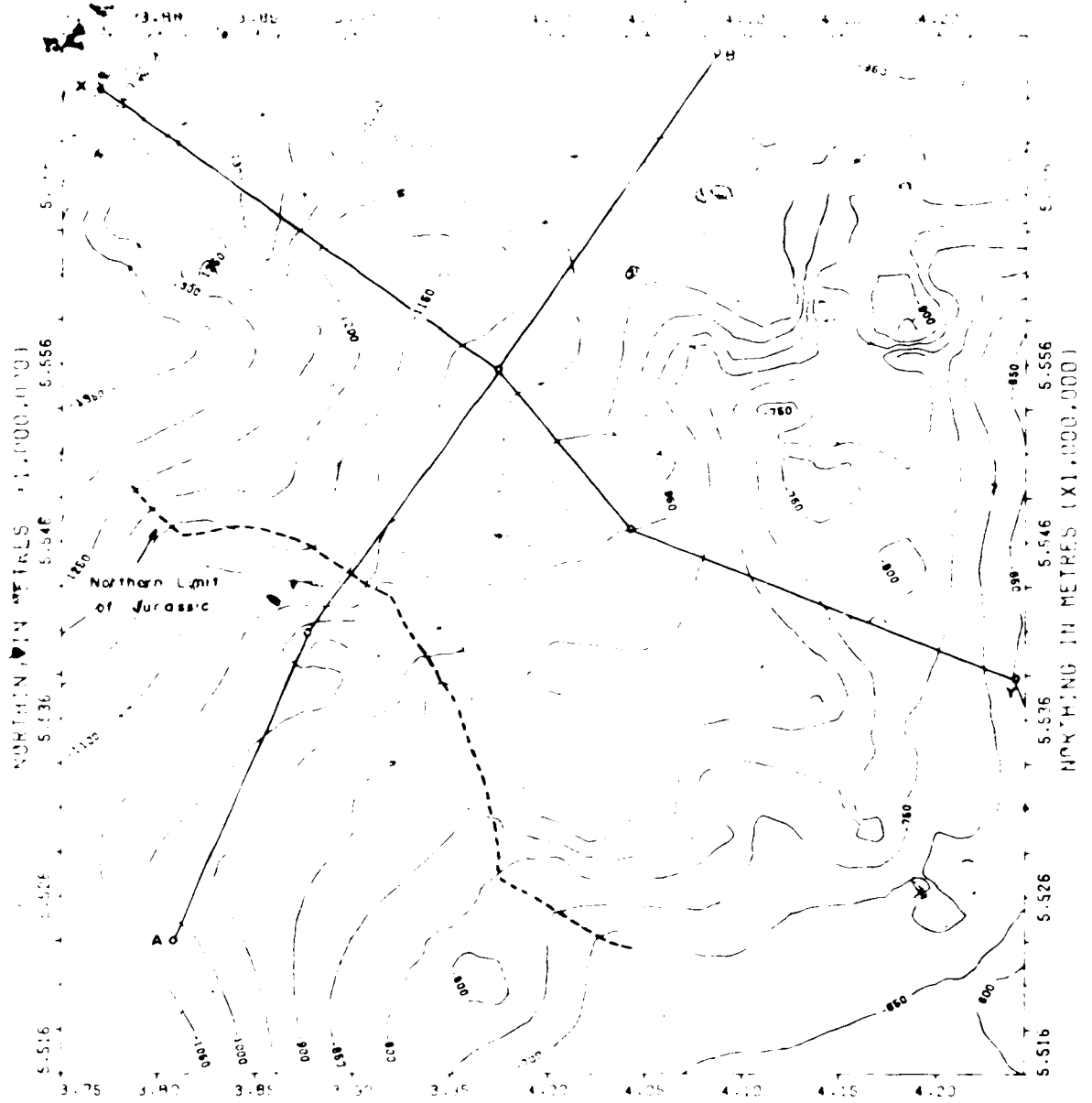


FIGURE 8



STRUCTURE MAP : TOP OF MISSISSIPPIAN
 AREA : T10N15R16D0W4
 CONTOUR INTERVAL : 50 FT.
 DATE : 1952

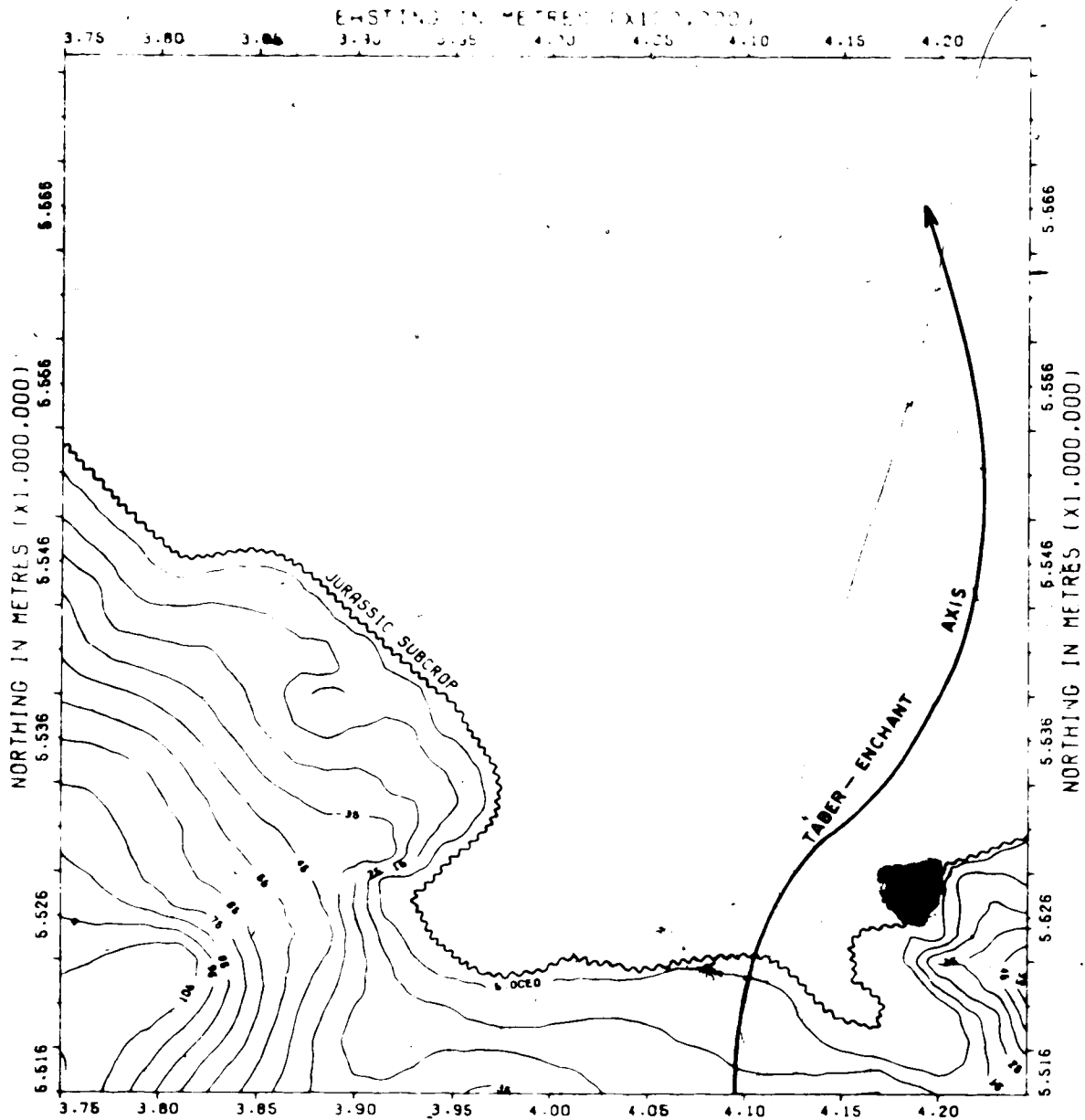
SCALE (FT.)
 0 2 4 6 8

FIGURE 3

The Mississippian surface was overlapped by a southern sea in Middle Jurassic time. The Sweetgrass arch was undergoing uplift at this time (Springer et al., 1964), and was the source of beach sands (Sawtooth Formation) deposited along its western margin, including the Turin area. The sea retreated to the south in late Middle Jurassic time. The Arch subsided in the early Late Jurassic and was covered by marine Rierdon shales. Subsequent uplift and erosion of the central and northern plains area resulted in the deposition of marine shales and sandstones of the Swift Formation across southern Alberta and Montana. The sea again retreated from the Turin area in latest Jurassic time and erosion of Jurassic and Mississippian strata continued until the onset of Mannville deposition.

The Jurassic subcrop edge (Fig. 10) is therefore erosional, although the Jurassic palaeogeographic maps of Springer et al. (1964) show the depositional limits to be approximately coincident with the erosional edge mapped in the Turin area. Rierdon shales constitute most of the Jurassic section in the map area, with only scattered remnants of Sawtooth and Swift Formations.

The Taber-Enchant Axis (Herbaly, 1974) probably extended northwards through the Jurassic subcrop embayment in Rierdon time (see Jurassic isopach map - Fig. 10). Sediments thicken rapidly to the southwest and southeast, while a more gradual increase occurs along the axis to the south. Jurassic sediments are restricted to the southern side of a broad, northwest-trending Mississippian ridge, indicated on Fig. 9. This southwesterly-dipping cuesta dominated the physiography of the southwest part of the Turin area in pre- and only Mannville times.



ISOPACH MAP : JURASSIC

AREA : T10-15.R16-20 W4

ISOPACH INTERVAL : 10FT.

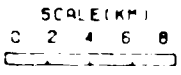


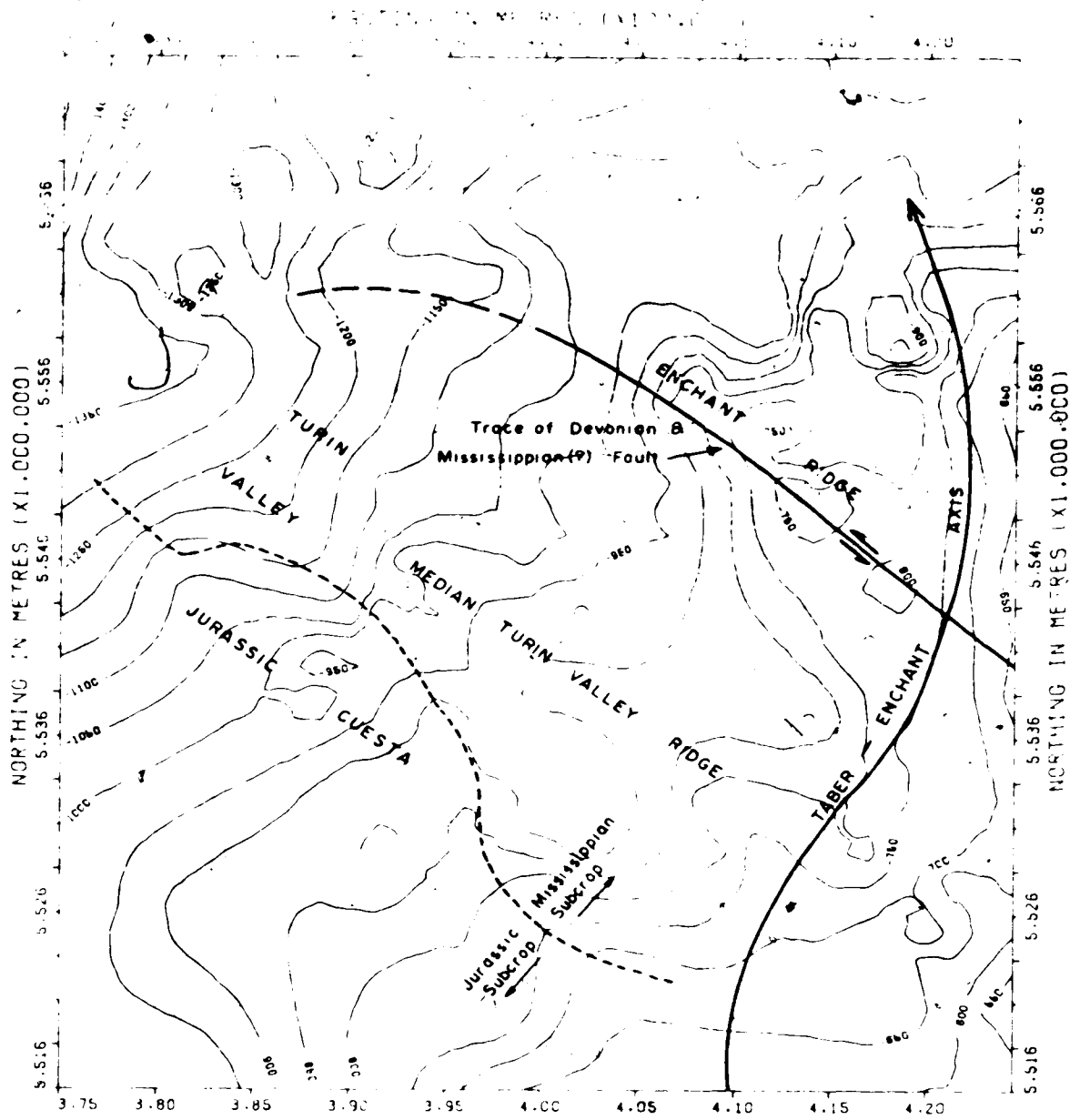
FIGURE 10

The structure map on the base of the Mannville Group (Fig. 11) represents the composite Jurassic and Mississippian surface onto which Mannville sediments were deposited. Surface relief, deduced from the Lower Mannville isopach map (Fig. 14), is of the order of 175 feet (53 metres). The inferred drainage pattern is northwesterly following the depositional strike of the bedding.

Herbaly (1974) shows a northwesterly-striking, sinistral transcurrent fault on the Devonian structure map of the Sweetgrass arch. This dislocation is present at the top of the Mississippian in the eastern Turin area, but whether structure at this level was due to post-Mississippian movement or control of Mississippian sedimentation by the underlying faulted Devonian surface was not determined.

The drainage pattern of the pre-Mannville surface was influenced significantly by the fault described above. The offset Taber-Enchant Axis forms a prominent ridge (here named the Enchant Ridge) on the northern side of the fault while a large, northwesterly-trending valley (the Turin Valley) developed to the south. The southwestern margin of the valley was formed by a cuesta of Mississippian limestone overlain by Jurassic strata. The valley is 11 miles (18 kilometres) wide in the central Turin area, and narrows towards the arch in the southeast. A low ridge (the median Turin Valley Ridge) divides the valley into two parallel channels which coalesce in the western part of the map area.

In the northeastern corner of the map area, north of the Enchant Ridge, two northerly-directed channels developed, separated by a small ridge. In the south, a shallow, westerly-trending valley formed at the base of the dip slope of the Jurassic cuesta.



STRUCTURE MAP : BASE OF MANNVILLE GROUP
 AREA : T10 15.R.G 25 W4 SCALE 1/2" = 100' (1:1250)
 CONTOUR INTERVAL : 50 FEET
 DATUM : MSL

FIGURE 11

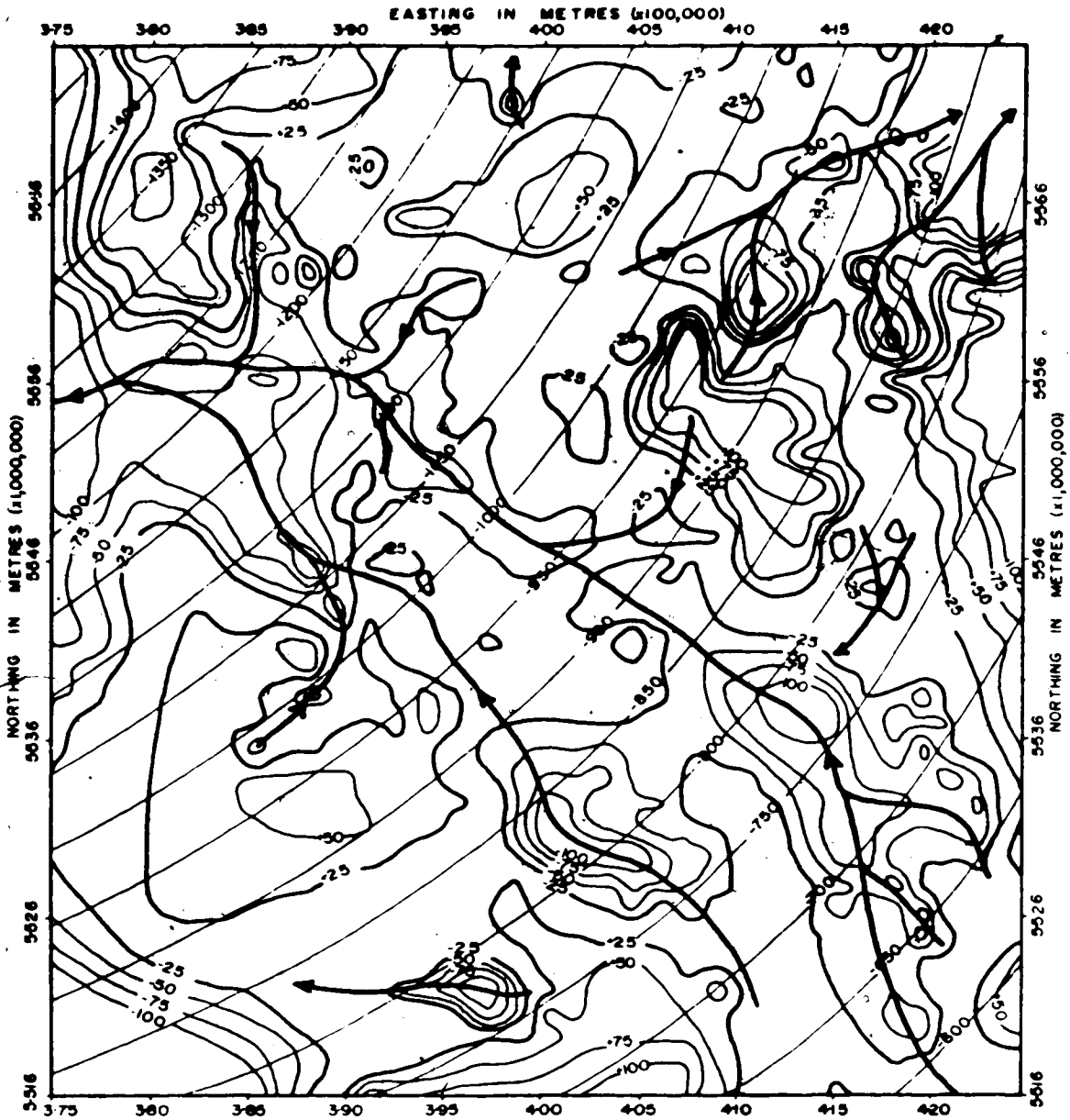
The above-mentioned topographic features were enhanced by fitting a second-order trend surface to the structure on the base of the Mannville Group (Fig. 12). The trend surface is a uniform northwesterly-dipping homocline showing a slight "spoon effect". This surface accounted for 94 percent of the variance in the original surface.

The Jurassic cuesta, Enchant Ridge and the Taber-Enchant Axis are represented as positive residuals. Relief on the Enchant Ridge becomes more subdued to the northwest, beyond the limit of the transcurrent Devonian fault.

B. LOWER MANNVILLE GEOLOGY

The dip on top of the Lower Mannville Group (Fig. 13) is similar to that on the pre-Mannville surface, but irregularities are less pronounced. The isopach map of the Lower Mannville strata (Fig. 14) reflects the topographic features discussed previously. Thickest Lower Mannville sections occur in pre-Mannville channels and lows, and isopach thins overlie topographic highs. Sediments thin towards the Sweetgrass Arch.

It is assumed that relief on the pre-Mannville surface, as presently mapped, was accentuated by the downcutting of pre-Mannville water courses by Lower Mannville streams. Unlike the pre-Mannville streams, the rate of deposition of Lower Mannville streams exceeded the rate of erosion, due to the abundant sediment supply from the uplifted Corilleran area, and preservation of deposits through regional subsidence. Channels were progressively filled with detritus.

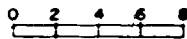


TREND SURFACE MAP : BASE OF MANNVILLE GROUP

AREA : T10-15, R16-20 W4

SCALE (KM)

TREND SURFACE ORDER : 2ND



TREND SURFACE CONTOUR INTERVAL : 50 FT

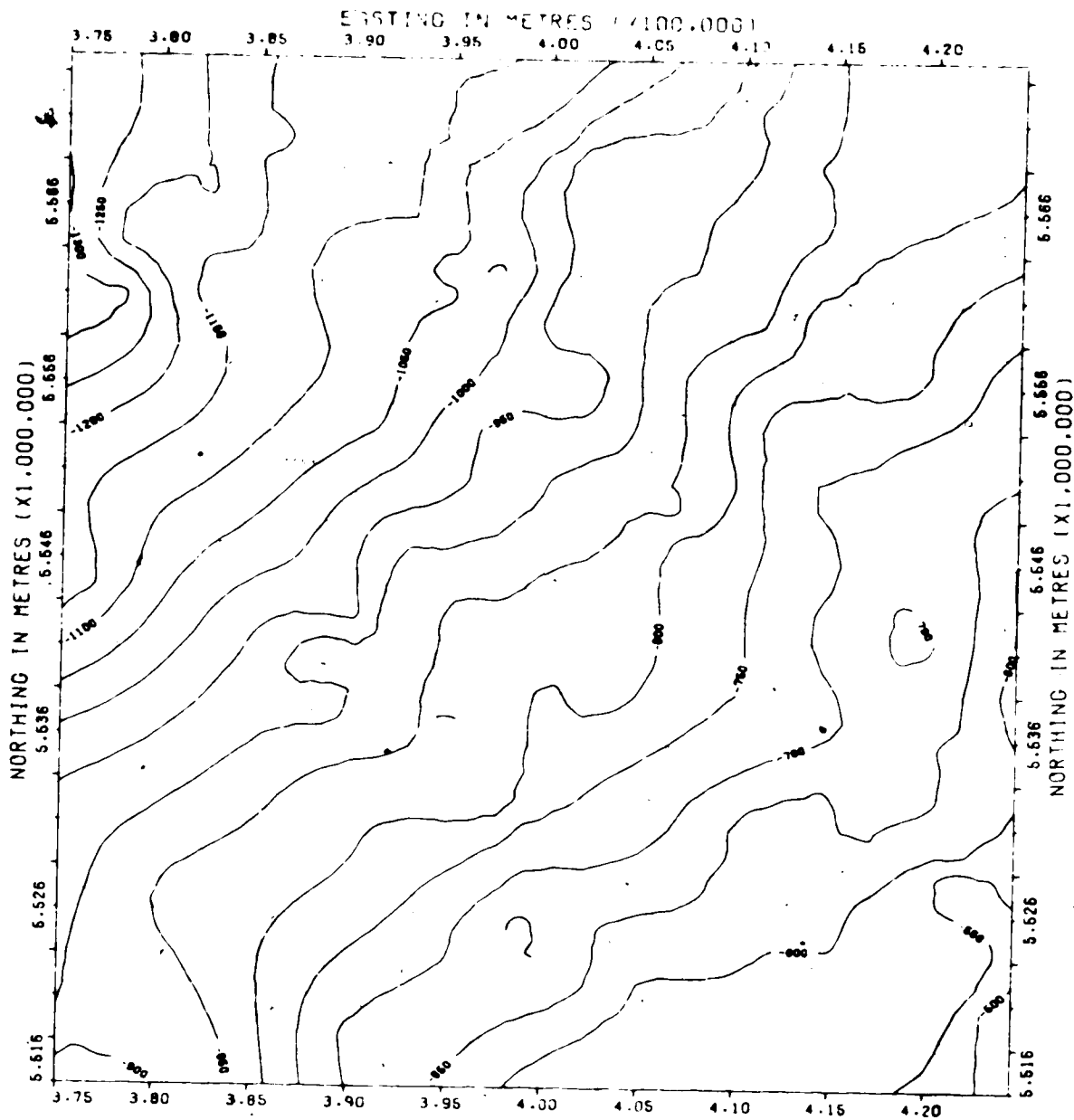
RESIDUALS CONTOUR INTERVAL : 25 FT

RESIDUALS

- POSITIVE
- NEGATIVE

INFERRED STREAMS

FIGURE 12



STRUCTURE MAP : TOP OF LOWER MANNVILLE GP.

AREA : T10-15.R16-20 W4

CONTOUR INTERVAL : 50 FT.

DATUM : MSL

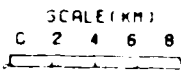
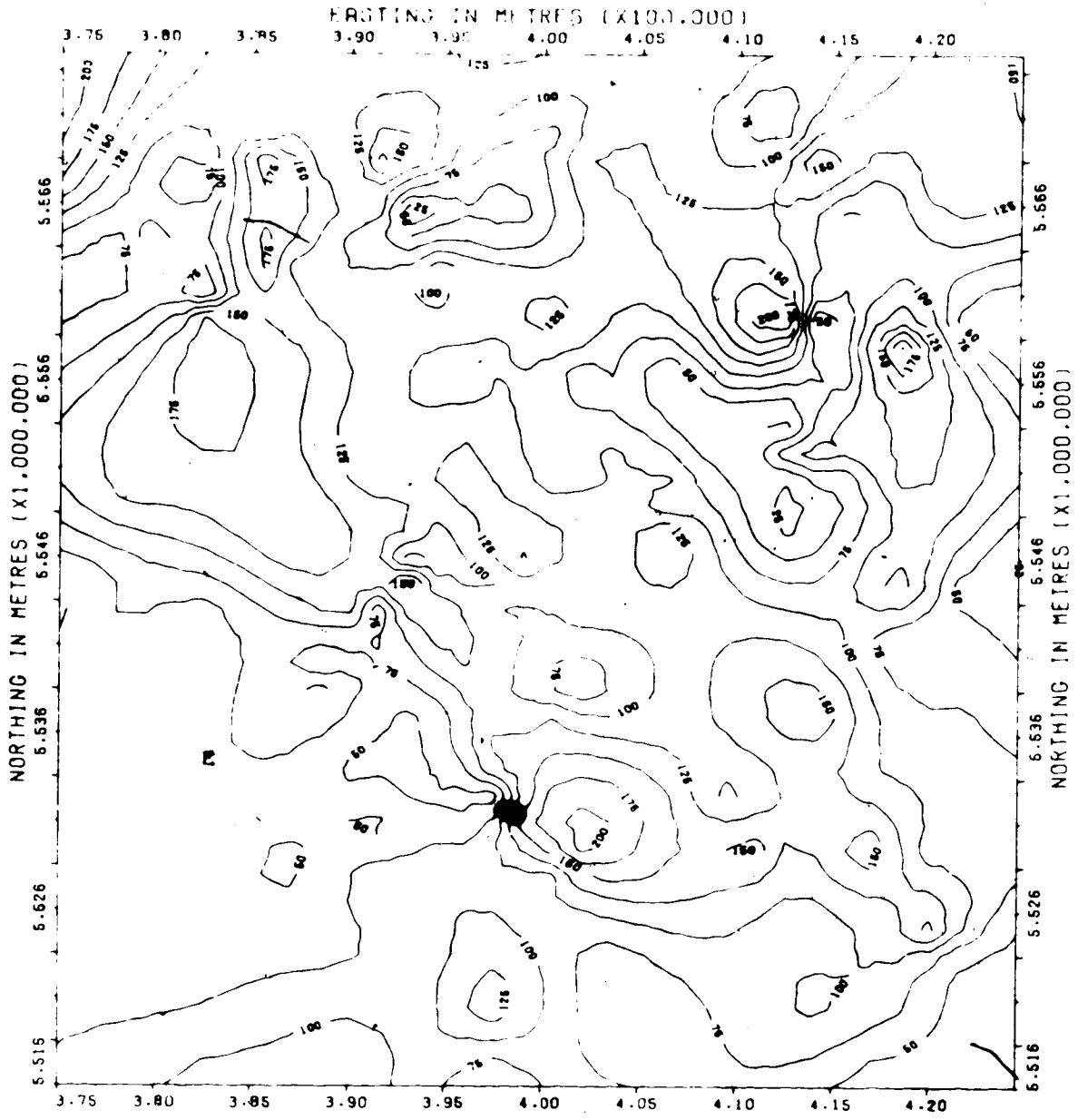


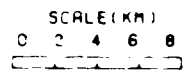
FIGURE 13



ISOPACH MAP : LOWER MANNVILLE GROUP

AREA : T10-15.R16-20 W4

ISOPACH INTERVAL : 25FT.



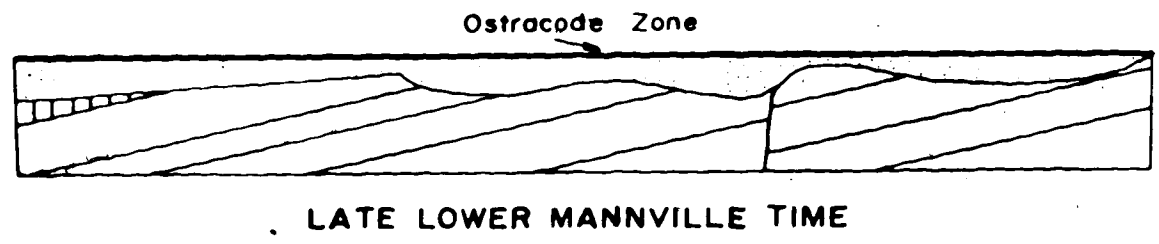
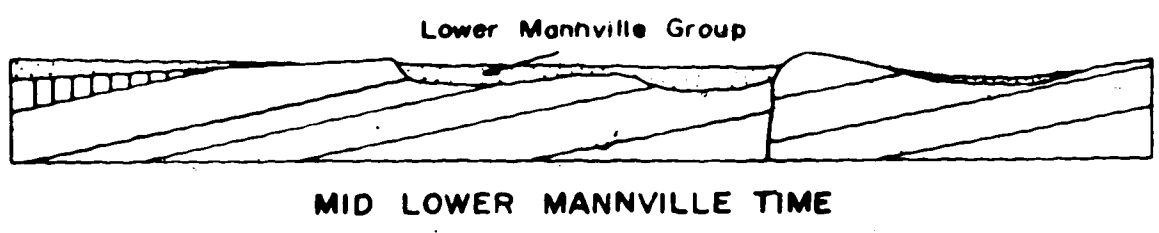
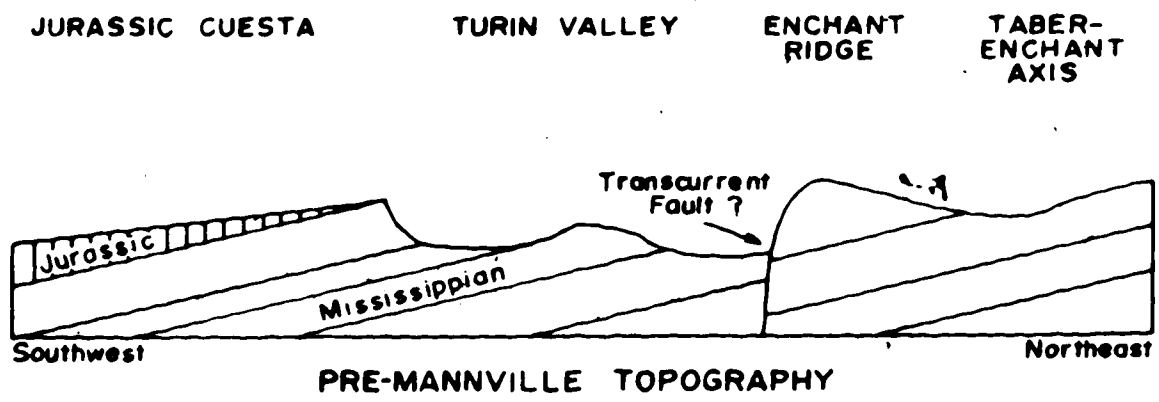
□ THICK
□ THIN

FIGURE 14

Towards the end of early Mannville time, the denudation of Jurassic and Mississippian highs, plus the infilling of channels with clastic material, had resulted in the formation of an extensive plain across the Turin area. Highs were eventually covered with sediment (25 to 50 feet of Lower Mannville strata occur over the highest parts of the Sweetgrass arch in the map area), until little expression remained of the pre-Mannville topography. Lakes and swamps developed, in which muds were deposited as a result of waning sediment supply from a maturing western source area. These muds constitute the Ostracode Zone and vary in thickness from 10 to 30 feet, with the thickest sections occurring above lows on the pre-Mannville surface. A thin limestone (two feet) occurs at the top of the Ostracode Zone in several places.

The Sweetgrass arch remained high, as evidenced by the easterly thinning of the Ostracode Zone towards the arch, and its absence from the top of the arch in the southeastern corner of the map area (Fig. 7). A diagrammatic representation of the changing topography and depositional pattern throughout early Mannville time is shown on Figure 15.

Relief on the top of the Lower Mannville Group is similar to, yet more subdued than that of the pre-Mannville surface. The relief is a function of "remnant" relief from the pre-Mannville (as shown by the absence of the Ostracode Zone on the Sweetgrass arch) and more importantly, differential compaction of Lower Mannville sediments. Minor variations in thickness of the Ostracode Zone over most of the Turin area indicate negligible relief at that time. A period of exposure and non-deposition occurred prior to the onset of Upper Mannville sedimentation, during which time compaction of Lower Mannville sediments took



DIAGRAMMATIC CROSS SECTIONS - TURIN AREA

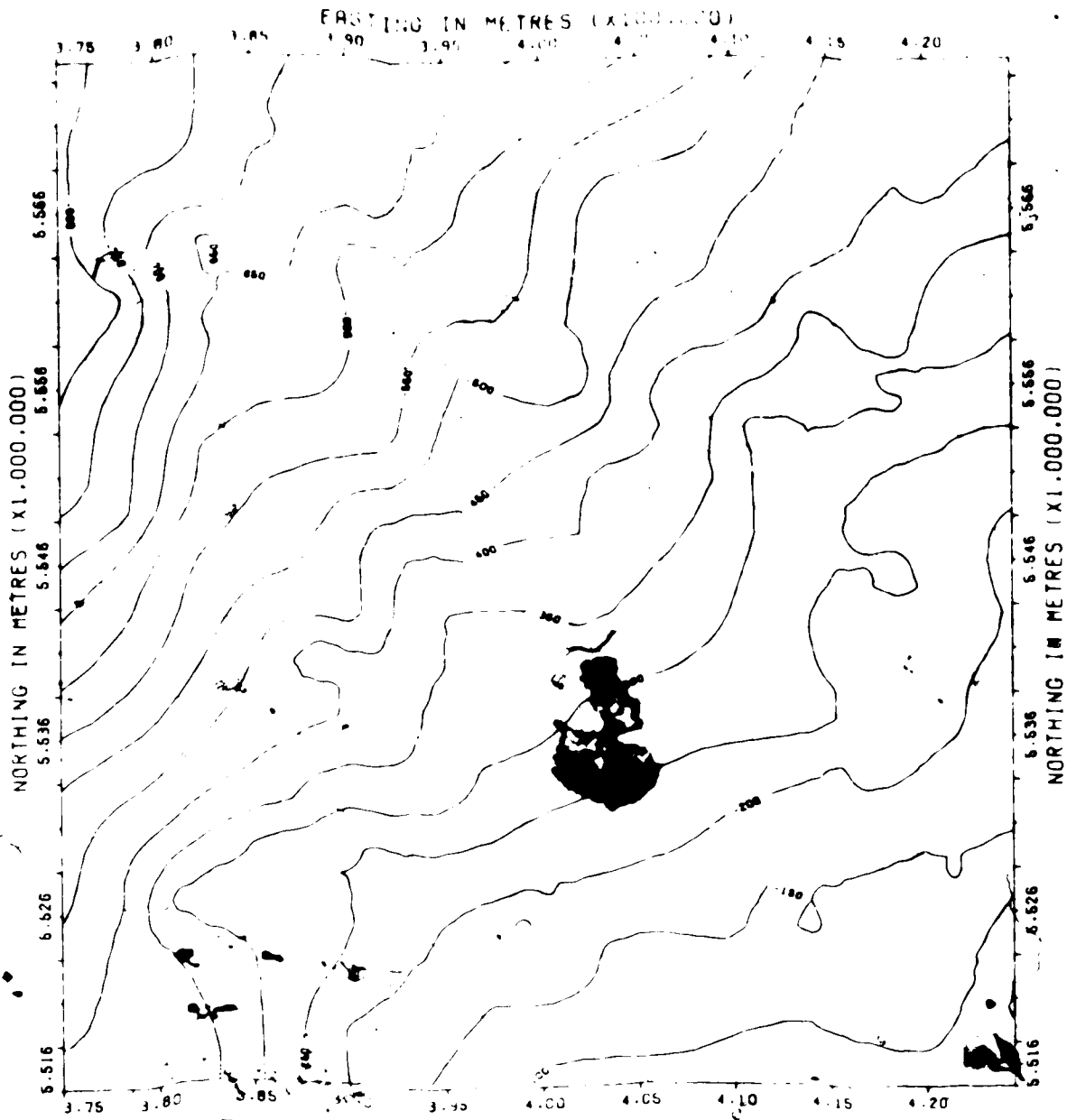
FIGURE 15

plate, producing a topographic surface comparable to that of early Mannville time (as discussed later in Chapter VII, the early late Mannville streams maintained courses similar to those of the early Mannville).

C. UPPER MANNVILLE GEOLOGY

The structure contour map on the top of the Mannville Group (Figure 16) is virtually identical to that on the top of the Lower Mannville (Figure 13), with the surface dipping at $0^{\circ}15'$ to the northwest. A second order trend surface accounted for 98 percent of the variance in elevations on the top of the Mannville. This surface dips towards the northwest (Figure 17), with positive residuals lying above the Taber-Enchant Axis, the Enchant Ridge and the Jurassic cuesta. Small, scattered negative residuals mark the position of the Turin Valley and a broad depression north of the Enchant Ridge. The structure map on the top of the Mannville was overlain by the trend surface map in plotting the courses of Upper Mannville streams shown on Figure 17.

The Turin Valley was wider during late Mannville time than it was during the deposition of the Lower Mannville Group. The position of channels is indefinite, suggestive of a floodplain traversed by braided and meandering streams. The high area to the northwest of the Enchant Ridge was breached by the northern Turin Valley stream, which cut a broad meander belt across the northern map area. The position of the southern Turin Valley stream is imprecise, and the structural maps fail to indicate whether the stream maintained its western course, or veered towards the northern valley.



STRUCTURE MAP : TOP OF MANVILLE GROUP

AREA : T10 15 R. 6 T20 W4

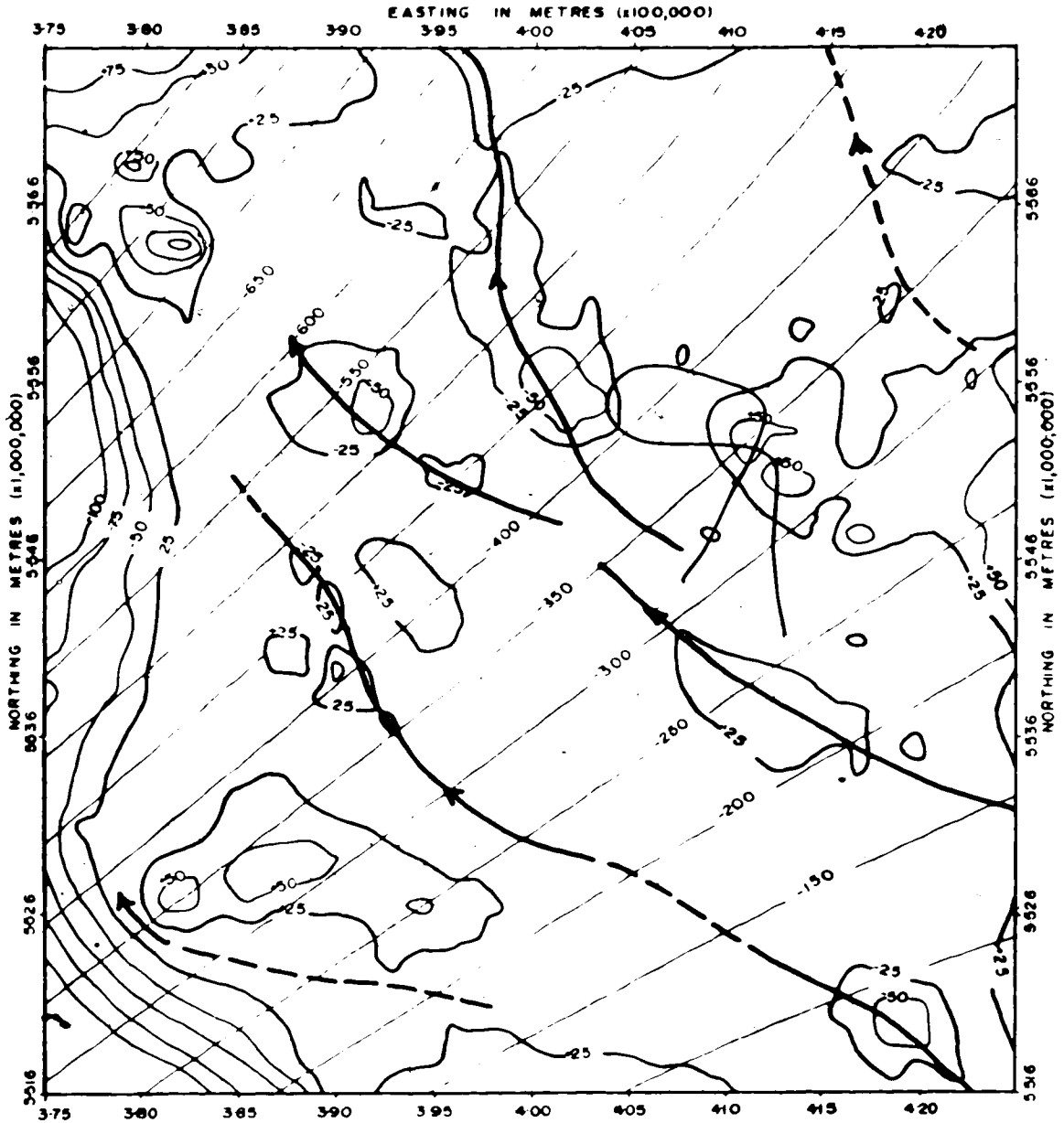
CONTOUR INTERVAL : 20 FT.

DATUM : MSL

SCALE (KM)



FIGURE 16



TREND SURFACE MAP : TOP OF MANNVILLE GROUP

AREA T10-15, R16-20 W4

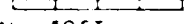
TREND SURFACE ORDER 2ND

TREND SURFACE CONTOUR INTERVAL 50 FT

RESIDUALS CONTOUR INTERVAL 25 FT

SCALE (KM)

0 2 4 6 8



RESIDUALS

- POSITIVE
- NEGATIVE

INFERRED STREAMS

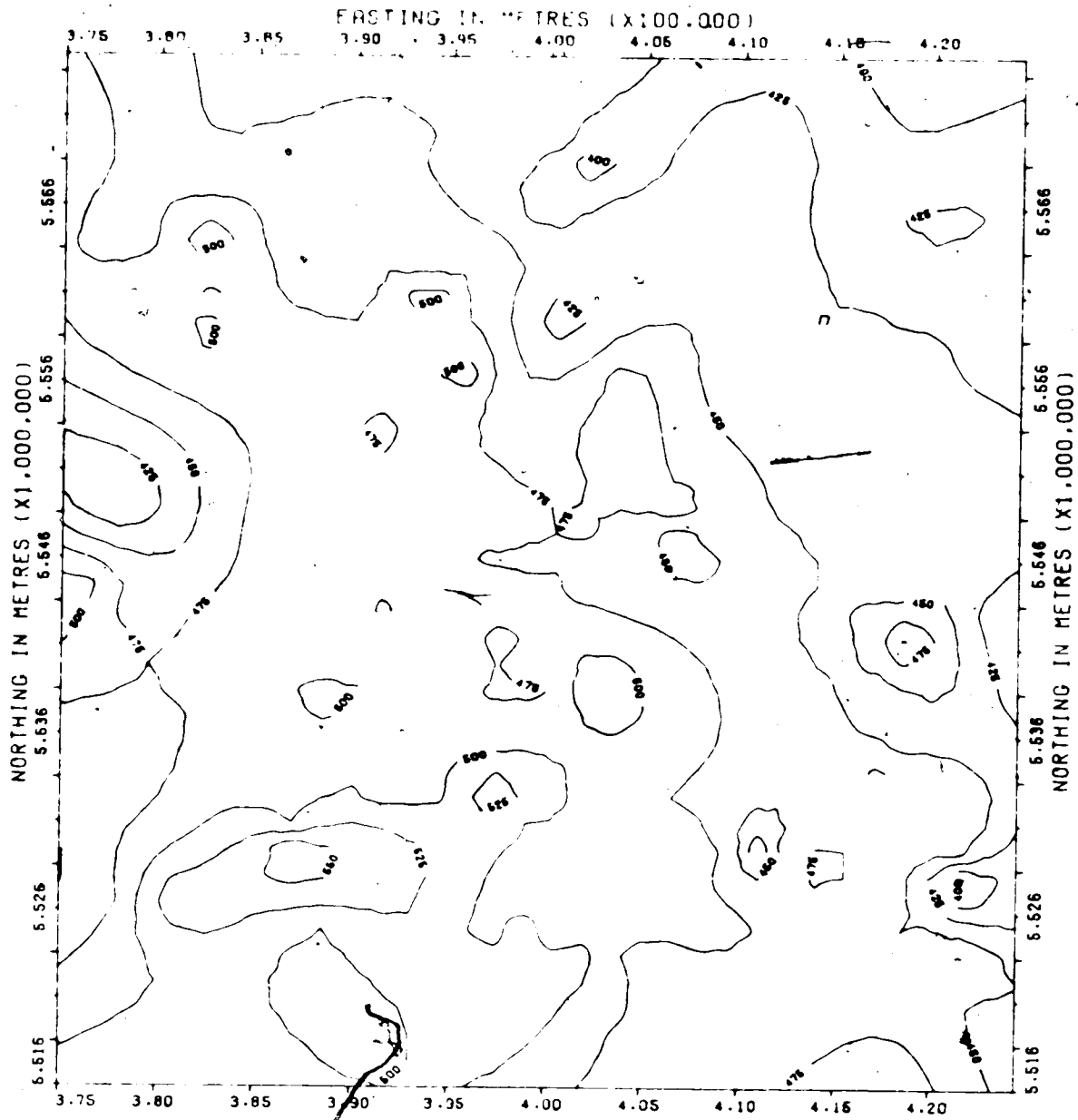
FIGURE 17

A fundamental depositional change occurred during late Mannville time. The Upper Mannville isopach (Figure 18) shows little resemblance to that of the Lower Mannville, as it thickens uniformly to the southwest, with depositional trends less influenced by pre-Mannville topography.

The isopach of the total Mannville Group (Figure 19) shows a regional southwesterly thickening, with areas of anomalously thick sediments along the Turin Valley and other smaller pre-Mannville channels. Thinning is evident over the Sweetgrass arch and pre-Mannville highs. Local variations in thickness are caused primarily by changes in thickness of the Lower Mannville Group.

D. POST-MANNVILLE GEOLOGY

Continental sedimentation in the Turin area terminated with deposition of marine shales and interbedded sandstone (Bow Island Formation) associated with the transgression of the Colorado sea in the late Early Albian. A thin sand occurs locally at the top of the Mannville Group, and has been variously identified in well files as Basal Colorado Sand, or included in the Upper Mannville Group. It is generally interpreted (G.D. Williams, personal communication) as a beach deposit derived from the reworking of Upper Mannville sandstones by the onlapping Colorado sea. Other than showing a high resistivity peak on electric logs, the sand appears to differ little from underlying sandstones; the interval was not cored in the Turin area. The sand is usually less than three feet thick, and has been included in the Colorado Group in the present study.



ISOPACH MAP : UPPER MANNVILLE GROUP

AREA : T10-15.R:6-20 W4
ISOPACH INTERVAL : 25FT.

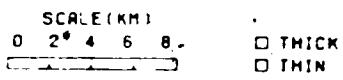
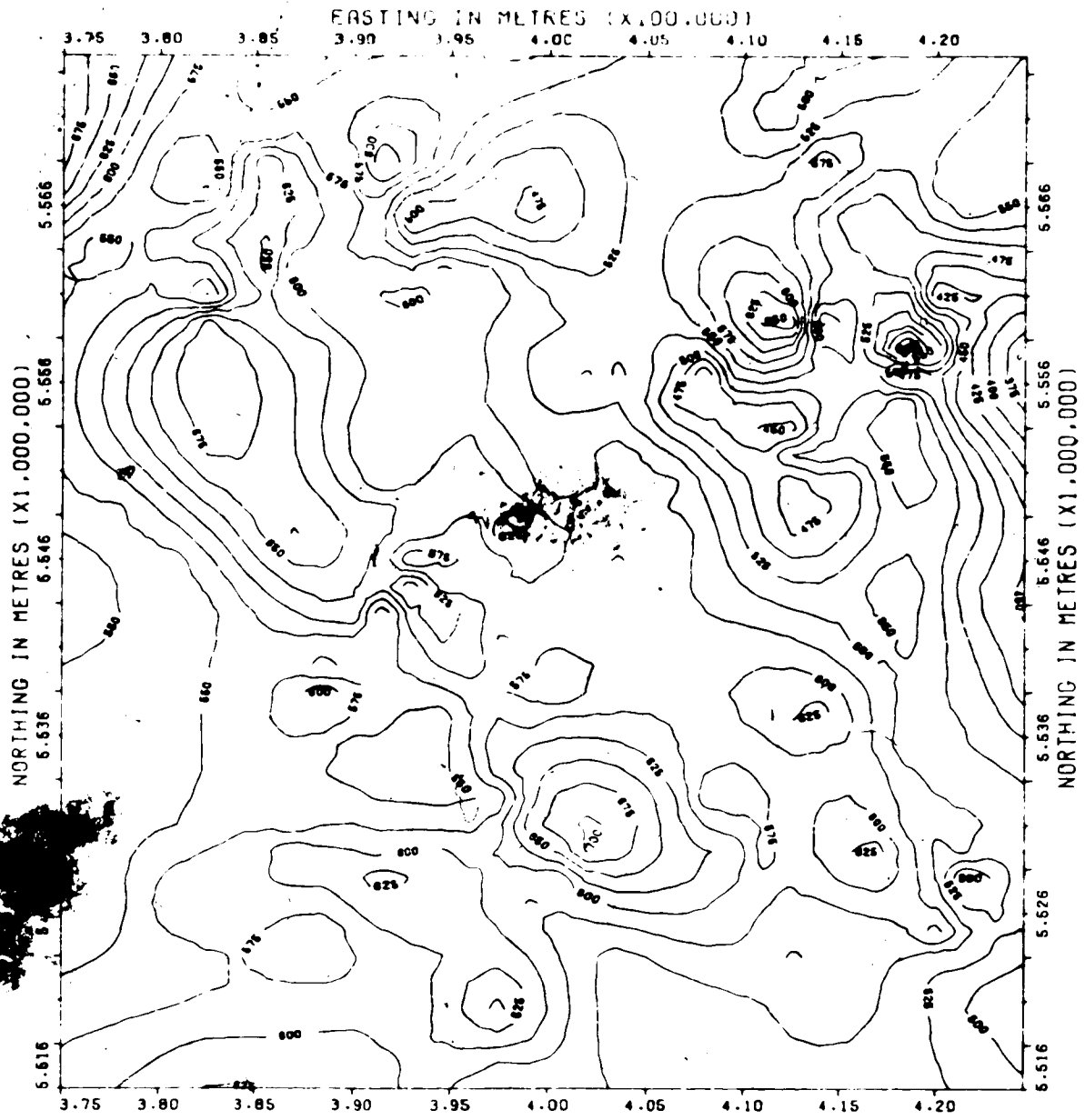


FIGURE 18



ISOPACH MAP : MANNVILLE GROUP

AREA : T10-15.R16-20 W4
ISOPACH INTERVAL : 25FT.

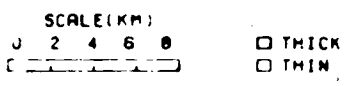
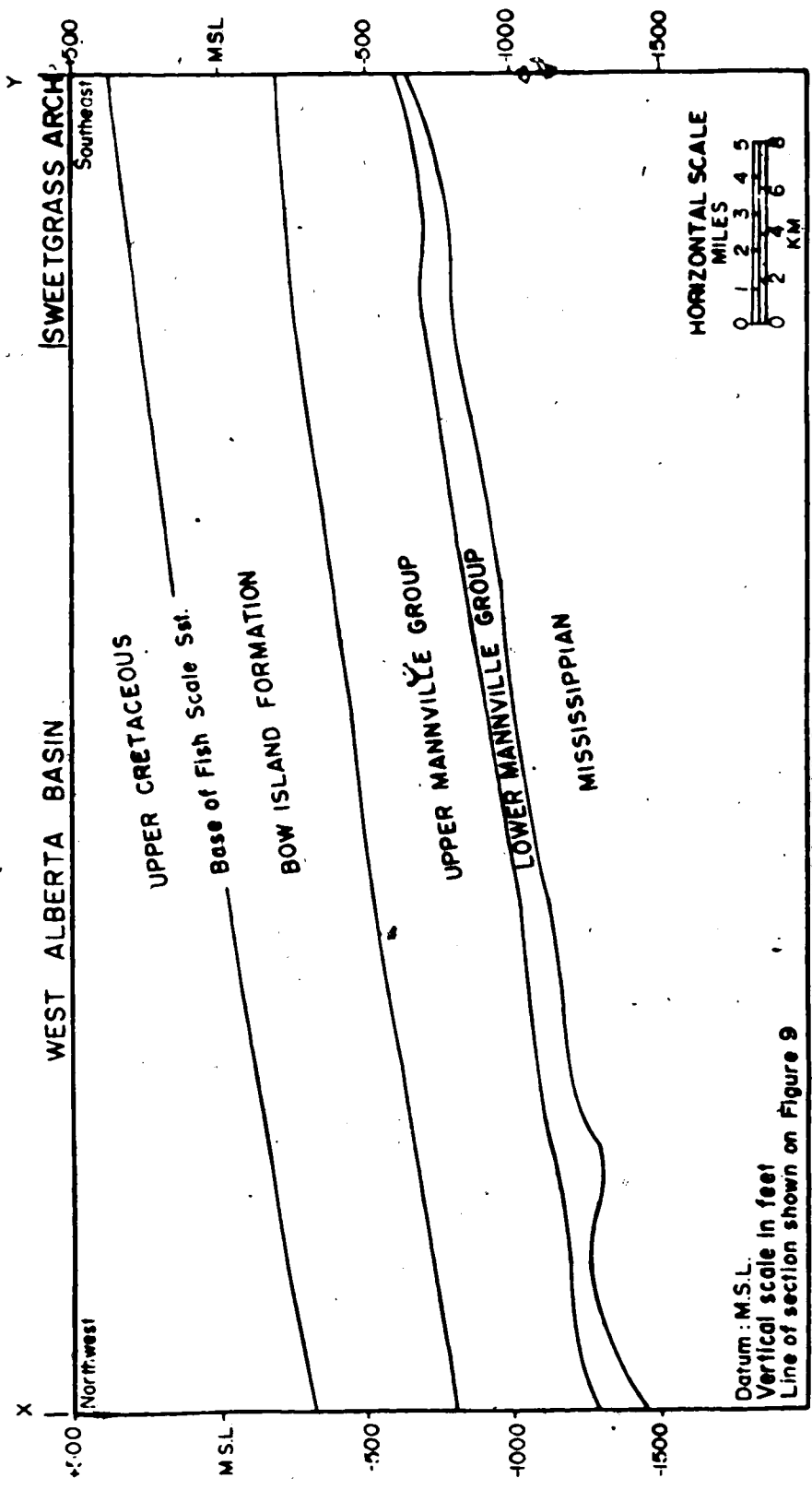


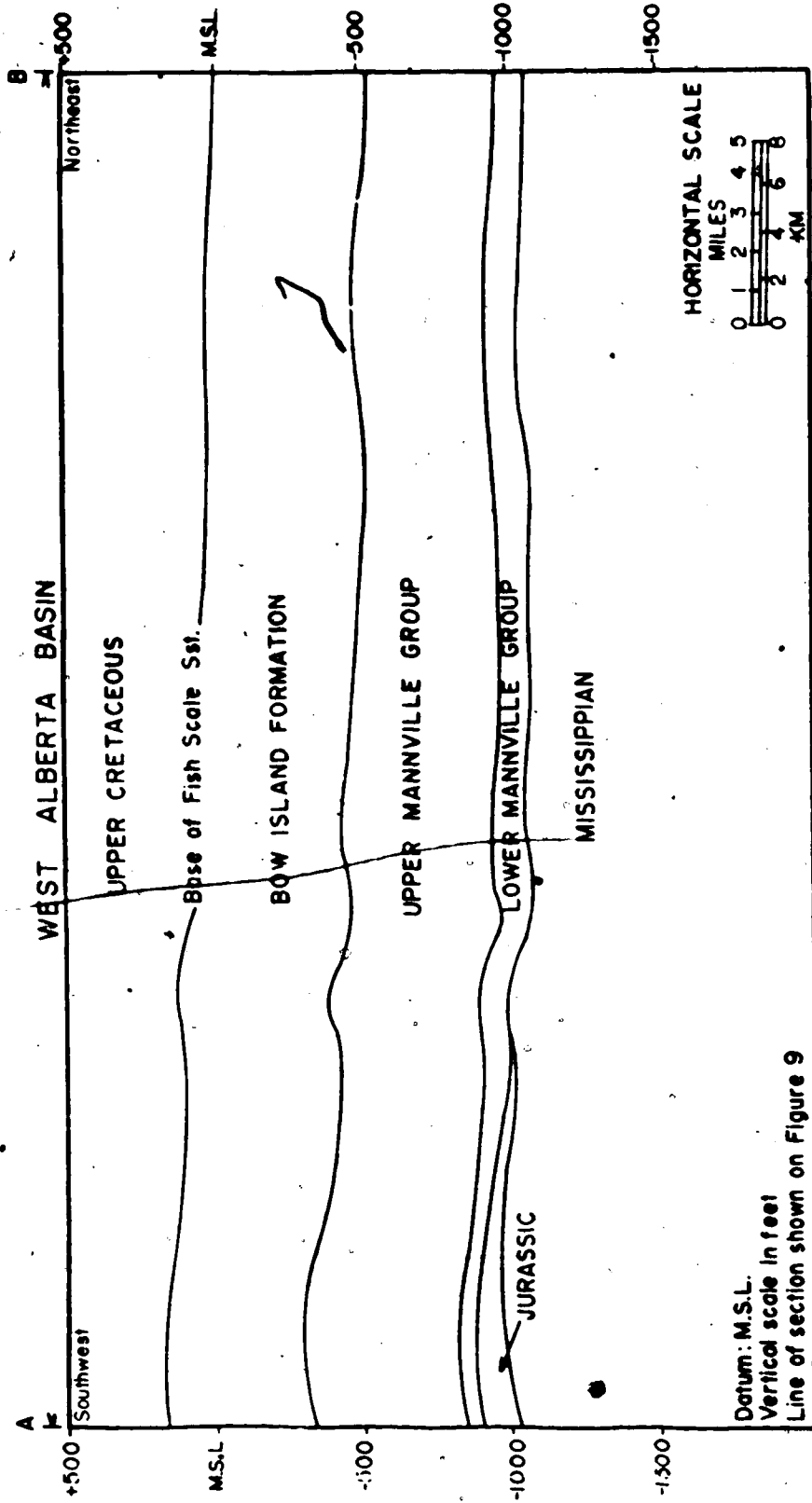
FIGURE 19

The top of the Lower Cretaceous is marked by the base of the Fish Scale Sandstone above the Bow Island Formation. Log correlations (Figures 7 and 8) indicate the uniformity of the Bow Island Formation throughout the Turin area. Structural cross sections drawn parallel to the regional dip and strike (Figures 20 and 21) along the same lines of section as Figures 7 and 8 illustrate the post-Cretaceous northwesterly tilt of the basin, and the major structural elements.



CROSS SECTION X-Y
DIP SECTION ACROSS THE TURIN AREA

FIGURE 20



CROSS SECTION A-B
STRIKE SECTION ACROSS THE TURIN AREA

FIGURE 21

Chapter VI
SAND DISTRIBUTION IN THE MANNVILLE GROUP

A. INTRODUCTION

The Upper Mannville Group is of uniform thickness and averages 460 feet (140 metres) thick in the Turin area. The sequence was divided proportionately into nine intervals, and the thickness of sand in each interval was measured from gamma logs. The percentage of sand in each interval was calculated by computer and contoured sand percentage slice maps were generated. Stacking the nine slice maps produced a "three dimensional" view of the changing distribution and geometry of sand bodies within the Upper Mannville succession. Difficulties in mapping and establishing stratigraphic relations between manually correlated, time transgressive, independent sand systems are largely removed using this numerical approach.

The determination of sand distribution at any given time is simplified in the Turin area, as sediments in each slice may be considered to be isochronous. The base and top of the Upper Mannville Group, as well as a number of intermediate horizons, are subparallel to the base of the Fish Scale Sandstone (see electric log correlations - Figures 7 and 8) which delineates the base of the Upper Cretaceous succession. Hence, within the Upper Mannville sequence, time lines and lithostratigraphic lines are approximately coincident.

The Lower Mannville Group has an average thickness of 100 feet (30 metres), but individual values range between 25 and 200 feet (8 to 64 metres). The pre-Mannville surface is envisaged as consisting of a

series of southwesterly-dipping Mississippian and Jurassic cuestas. The Lower Mannville isopach (Figure 14) indicates that the elevations of these ridges were similar, as were the depths of the intervening valleys. Early Mannville sedimentation was restricted to the valleys, and sand bodies maintained fixed spacial positions throughout Lower Mannville time (confined by the valley walls), more so than the Upper Mannville sands, which were deposited over wide meander belts. Not until late early Mannville time, when topographic relief was negligible, did deposition occur uniformly across the Turin area.

Consequently the age and thickness of the Lower Mannville section encountered in any well depends upon whether drill sites were positioned above pre-Mannville highs or lows. Proportionate subdivision of the Lower Mannville Group therefore produces slices (Intervals 10 and 11) containing sediments which bear only limited depositional relationships, because areas of valley sedimentation are generally older than those areas overlying the pre-Mannville topographic highs.

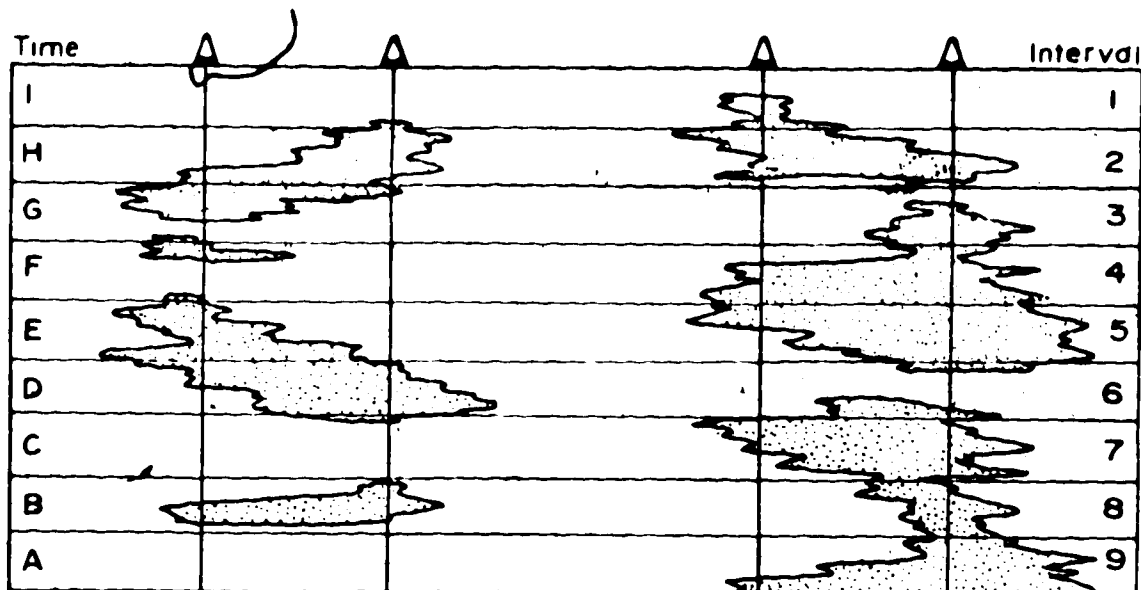
This problem was partially circumvented by subdividing the sequence into four equal 50-foot (15 metre) slices (Intervals 12 to 15). For the lower intervals (14 and 15), barren highs of Mississippian and Jurassic strata occupy a large part of the map area; for these maps sand percentage data were hand contoured, as no provision existed in the computer programs to adequately isolate the "bald zones", and prevent them from influencing the gridding and contouring of the sand. The small, isolated pre-Mannville "bedrock" outcrops in the upper slices (Intervals 12 and 13) were overlooked, and sand data were computer contoured to maintain consistency with the Upper Mannville maps.

Since the pre-Mannville valleys (and ridges) showed some variation, in elevation and shape (valleys had different base levels and gradients, and deposition commenced at different times, with younger streams down-cutting earlier deposits), the fixed thickness subdivision of the Lower Mannville Group did not produce slices containing entirely penecontemporaneous sediments. Both types of slices are required to interpret sand distribution adequately, and to determine time equivalent deposits.

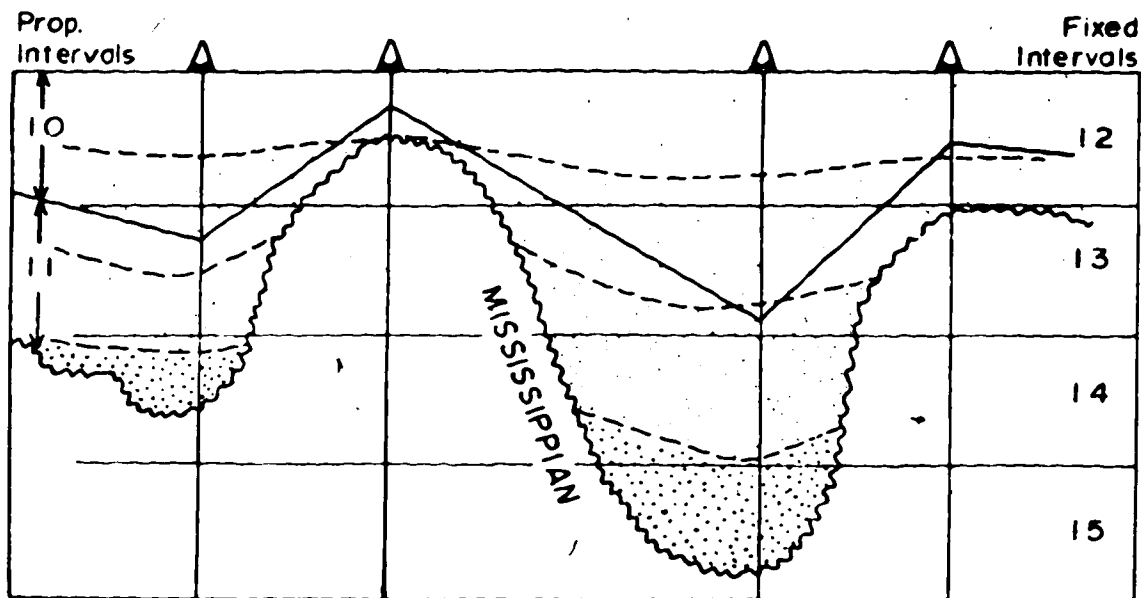
The proportionate subdivisions of the Upper Mannville Group, and both fixed and proportionate subdivisions of the Lower Mannville Group, are illustrated diagrammatically in Figure 22. Figure 23 is an example of a gamma-sonic log subdivided into intervals for sand percentage calculations.

B. LOWER MANNVILLE GROUP

Interval 15 (Figure 24) represents initial Mannville deposition in the deep channels of the Mississippian and Jurassic surface. It occurs in only 13 scattered wells, thereby creating difficulties in defining depositional limits and contouring the sand data. Sedimentation was restricted to three areas - the Turin Valley, where in the south, sands were deposited along two parallel water courses, and in the northwest, where the streams apparently coalesced; a small westerly depression at the base of the dip slope of the Jurassic cuesta; and in a northeasterly directed valley on the northern side of the Enchant Ridge. Sand deposition predominated over fine clastics. Log character at the base of Interval 15 suggests a high proportion of Mississippian limestone debris (Deville Formation equivalent) in a number of wells.



UPPER MANNVILLE GROUP — PROPORTIONATE SUBDIVISION
Two independently deposited sand units illustrated

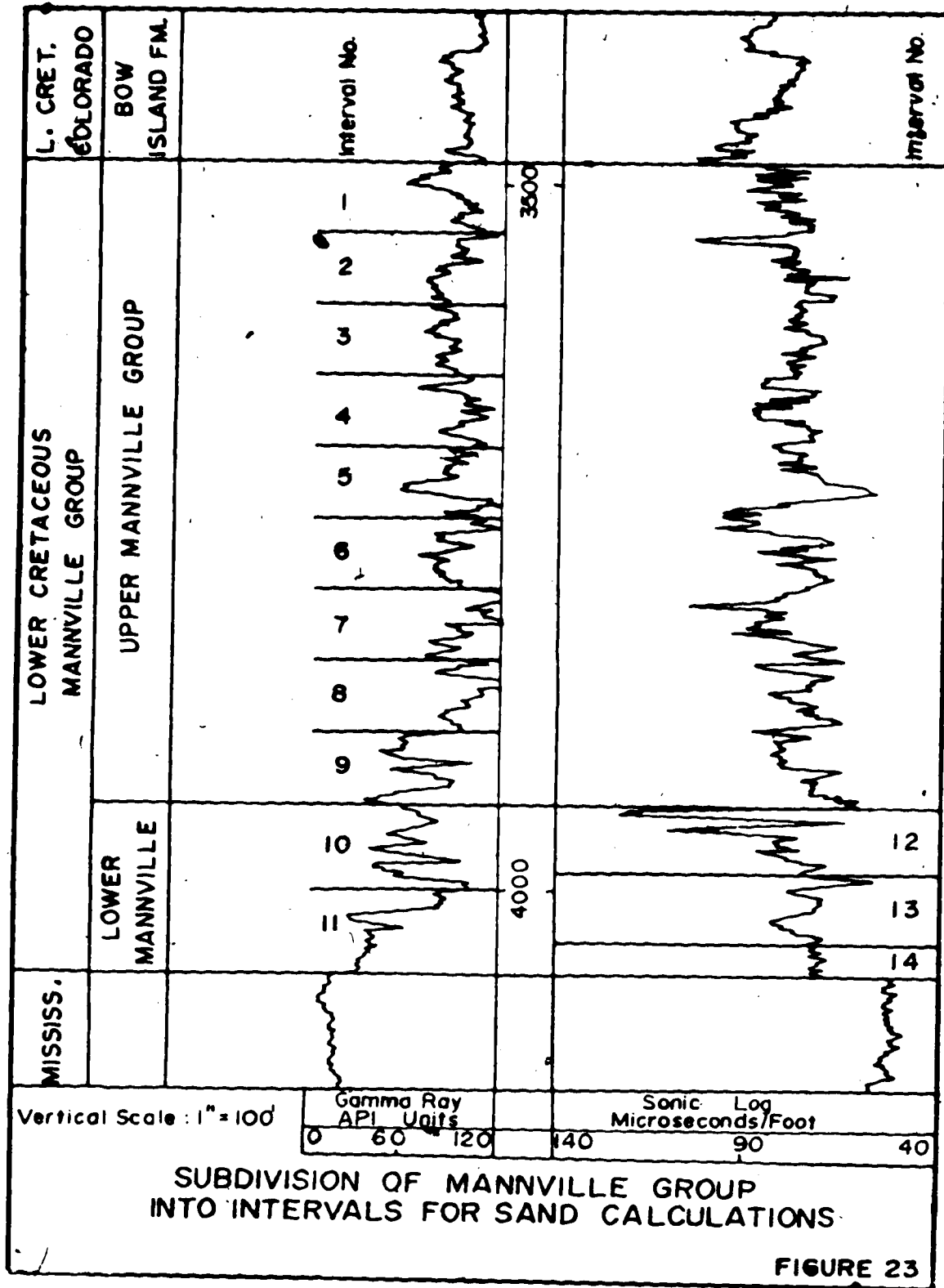


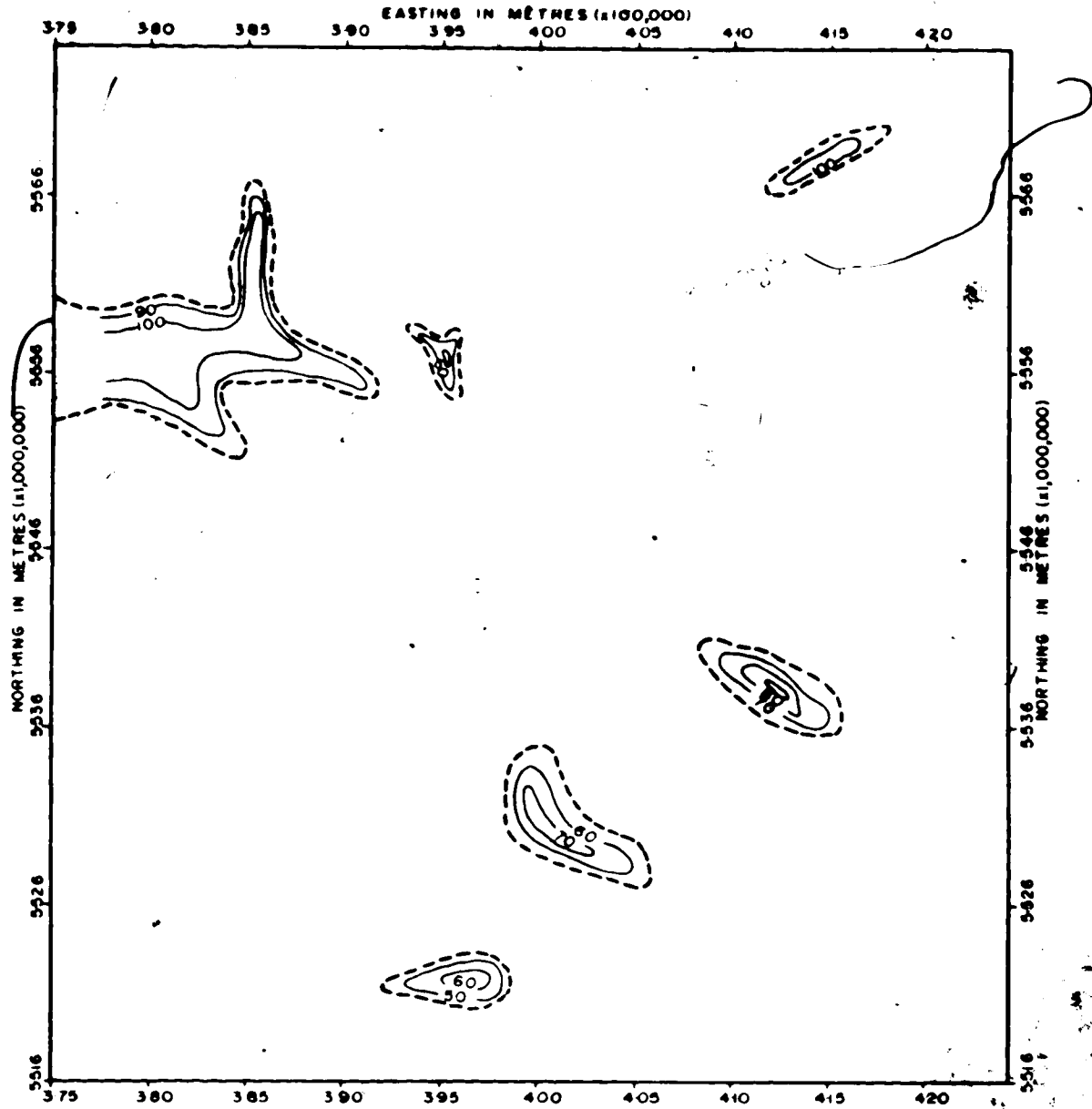
LOWER MANNVILLE GROUP — FIXED & PROPORTIONATE SUBDIVISION
Stippling indicates approximately time equivalent units

NOTE: VERTICAL SCALE DIFFERENT IN EACH DIAGRAM

DIAGRAMMATIC SUBDIVISION OF THE MANNVILLE GROUP

FIGURE 22





SAND PERCENTAGE MAP INTERVAL 15

AREA T10-15, R16-20 W4

CONTOUR INTERVAL 10%

SCALE (KM)



SAND %

□ 40-60

□ 60-80

□ 80-100

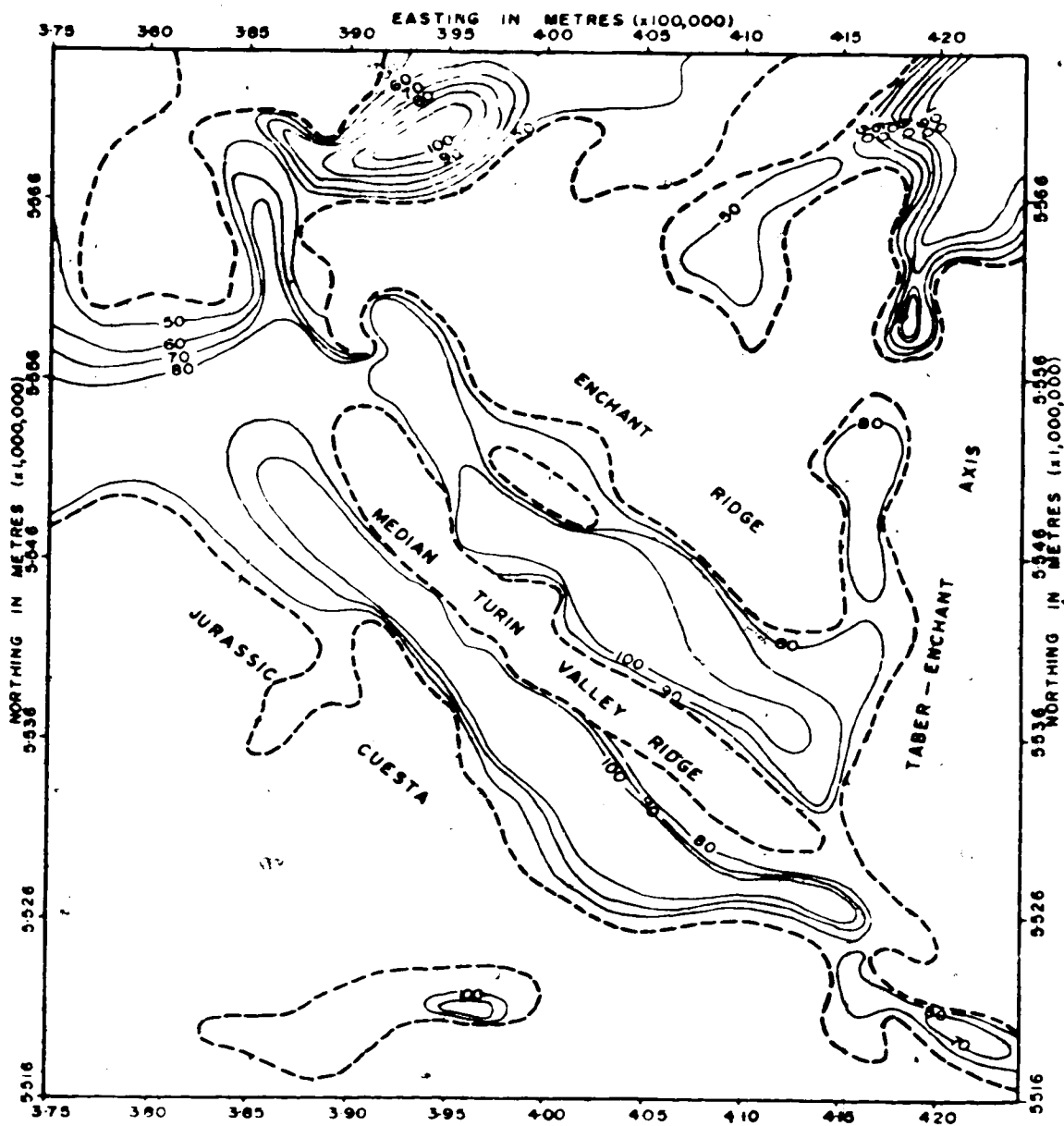
CROPPING PRE-MANNVILLE STRATA

FIGURE 24

The lower Mannville depositional pattern is well defined in Interval 14 (Figure 25). The Turin Valley was the site of thick sand accumulation. A narrow ridge, probably of resistant Mississippian limestone, extended down the length of the valley, separating the two water courses which were apparent on the map of Interval 15. Small tributaries fed the Turin Valley from the southeastern end of the Enchant Ridge, and from the northern face of the Jurassic cuesta.

As shown on the trend surface map of the base of the Mannville Group (Figure 12), the two Turin Valley distributaries joined in the western map area to form a single, broad (6 mile wide) floodplain. Valleys on the northern side of the Enchant Ridge and the southern side of the Jurassic cuesta continued to fill with detritus. The shape and form of these valleys indicate that the sediments accumulating in them were derived mainly from the erosion of the outcropping Jurassic formations, unlike the Turin Valley sediments which were mainly of Cordilleran origin. The paleogeographic maps of Springer et al. (1964) show the Sawtooth and Swift Formations to have been deposited over the southern half of the Turin area. Thin remnants of the Sawtooth now occur along the Jurassic cuesta, but Jurassic strata are absent from the top of Enchant Ridge.

As mentioned above, the computer contoured map of Interval 13 (Figure 26) is somewhat inaccurate because areas of outcropping pre-Mannville strata could not be isolated from areas of sand deposition. Sand values were extrapolated to grid nodes overlying these areas, and contoured accordingly. The zero to forty percent contour interval generally corresponds to regions of pre-Mannville outcrop outlined on the



SAND PERCENTAGE MAP INTERVAL 14

AREA T10-15, R16-20 W4

SCALE (KM)

SAND %

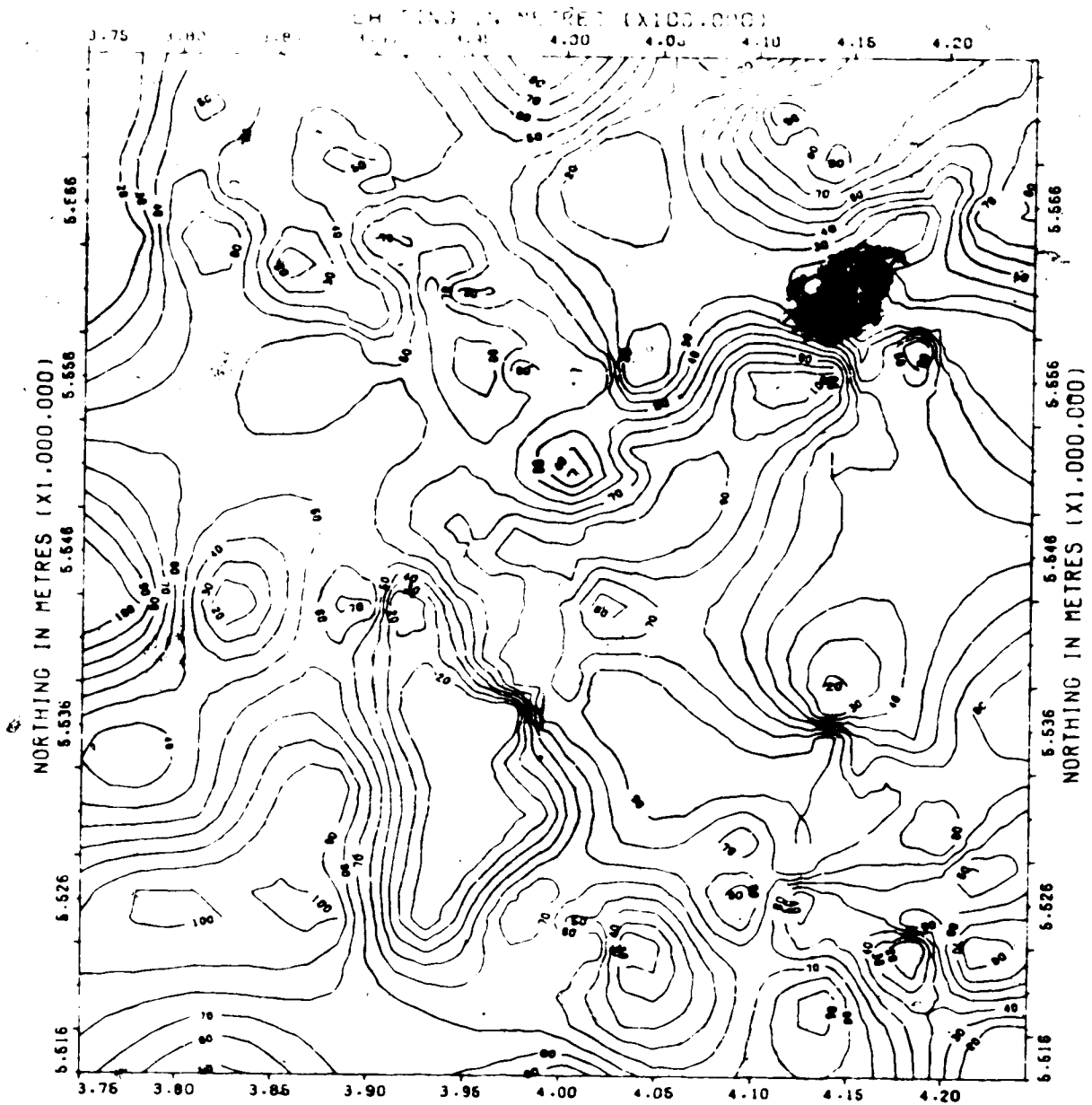
CONTOUR INTERVAL 10%



- 40- 60
- 60- 80
- 80-100

○ OUTCROPPING PRE-MANNVILLE STRATA

FIGURE 25

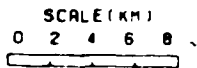


SAND PERCENTAGE MAP : INTERVAL 13

AREA : T10-15.R16-20 W4

CONTOUR INTERVAL : 10%

(0 & 10% CONTOURS DELETED)



- SAND %
- 0- 20
 - 20- 40
 - 40- 60
 - 60- 90
 - 80-100

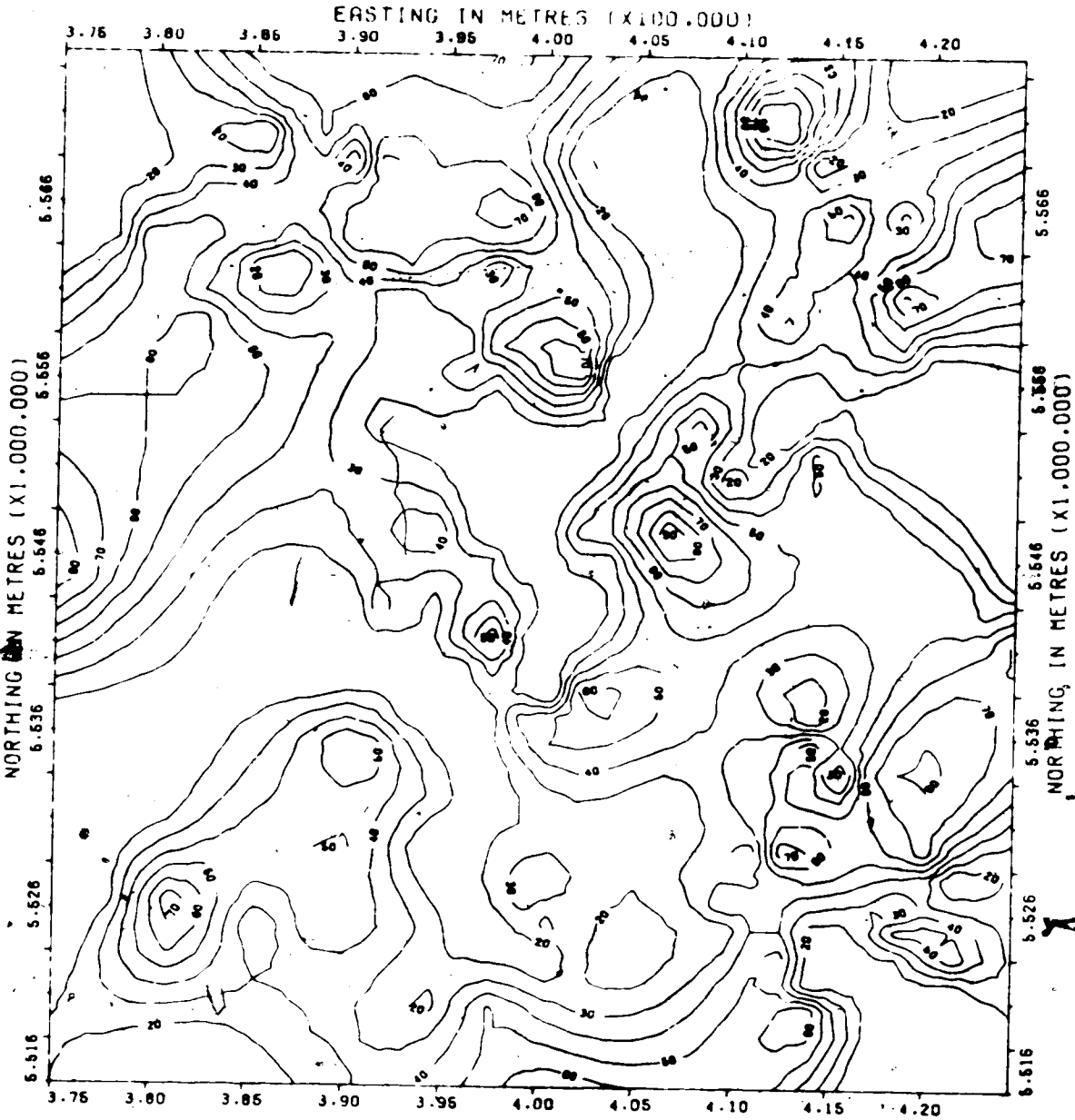
FIGURE 26

Interval 14 map, and does not represent thick argillaceous sequences. Sand deposition was at a maximum in the Turin Valley at this time. The median ridge is not obvious because of interpolation of the high sand values between the two channels. On the western Turin Valley floodplain, increasing volumes of silt and clay were deposited. Sand accumulated on the southwestern edge of the Jurassic cuesta and the northern side of the Enchant Ridge.

Interval 12 (Figure 27) is the uppermost slice of the Lower Mannville Group, and includes the regionally deposited shale of the Ostracode Zone. Scattered pre-Mannville outcrops existed during early Interval 12 time (Enchant Ridge, Jurassic cuesta and southeastern Taber-Enchant Axis), but except for parts of the Taber-Enchant Axis, these areas were covered by late Lower Mannville fine-grained clastics, which were deposited in the lower energy environments away from the main stream channels.

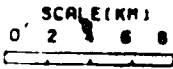
The northern Turin Valley stream was the main water course prior to the deposition of the Ostracode Zone. It eroded the high area in the northwest and established a straight northwesterly course. Mainly fine-grained sediments were deposited in the southern Turin stream, which continued to flow westwards.

An irregular belt of sand occurs in the southwest. This was deposited in a northwesterly-flowing river system entering the Turin area for the first time, from the southeast. The stream captured the early Lower Mannville valley at the foot of the Jurassic cuesta, and joined the southern Turin valley stream during Upper Mannville time.



SAND PERCENTAGE MAP : INTERVAL 12

AREA : T10-15.R16-20 W4
 CONTOUR INTERVAL : 10%
 10&10% CONTOURS DELETED

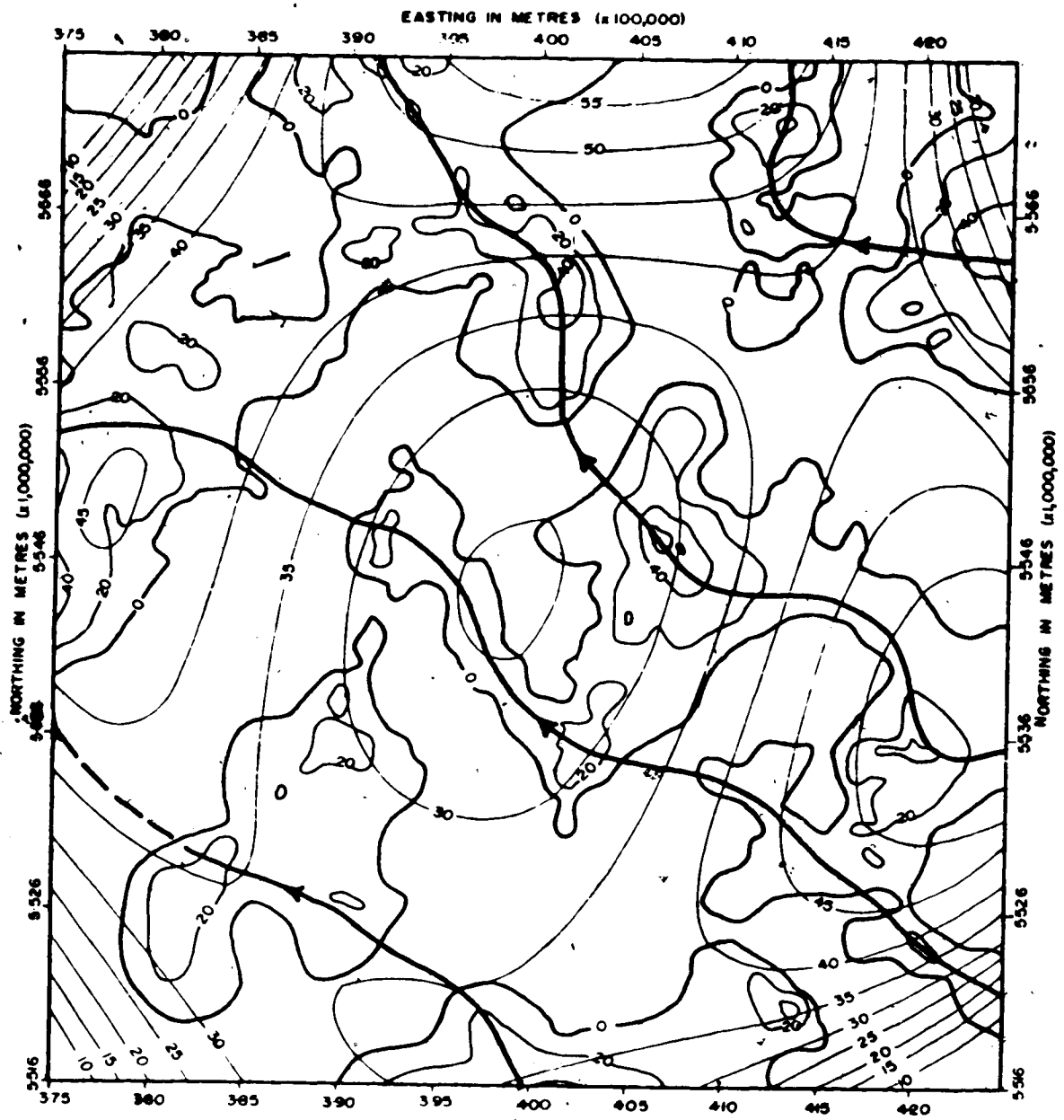


- SAND %
- 0- 20
 - 20- 40
 - 40- 60
 - 60- 80
 - 80-100

FIGURE 27

Trend surface analysis of the Interval 12 sand percentage data (Figure 28) did little to enhance the areas of anomalously thick sand deposition. Thick, clean sand was deposited along the pre-Mannville channels, while silts and clays accumulated in areas removed from active stream flow. Sand deposition occurred in these areas only during times of flooding, and from the intermittent, minor tributaries. Fifty to one hundred percent sand occurs in the main streams and zero to twenty percent in other areas, with little gradation between. Hence, there was no regional or average sand distribution to which a mathematical surface could be applied. The sum of squares of residuals accounted for increases from eight to fifteen percent for first to eighth order surfaces; that is, no matter what the order of surface, the large positive residuals caused by the streams and the lack of negative residuals resulting from the small areas of argillaceous sedimentation prevented fitting a statistically valid surface to the data. The outline of positive residuals approximates the twenty percent contour line of the sand percentage map. In contrast to this situation, Hermund and Jenkins (1970) were able to fit a fourth order surface to the sand isolith of a widespread Pennsylvanian delta in north central Texas, apparently because of the more extensive distribution of sand in such an environment.

Areas of pre-Mannville outcrop are not included in slices produced by the proportionate subdivision of the Lower Mannville Group (Intervals 11 and 10, Figures 29 and 30), thus the computer contoured sand percentage maps of these intervals are free from the limitations of the maps of Intervals 12 and 13. In Interval 11, high sand values occur along



TREND SURFACE MAP : SAND INTERVAL 12

AREA : T10-15, R16-20 W4

TREND SURFACE ORDER 4TH

TREND SURFACE CONTOUR INTERVAL 5%

RESIDUALS CONTOUR INTERVAL 20%

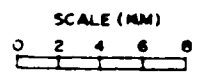
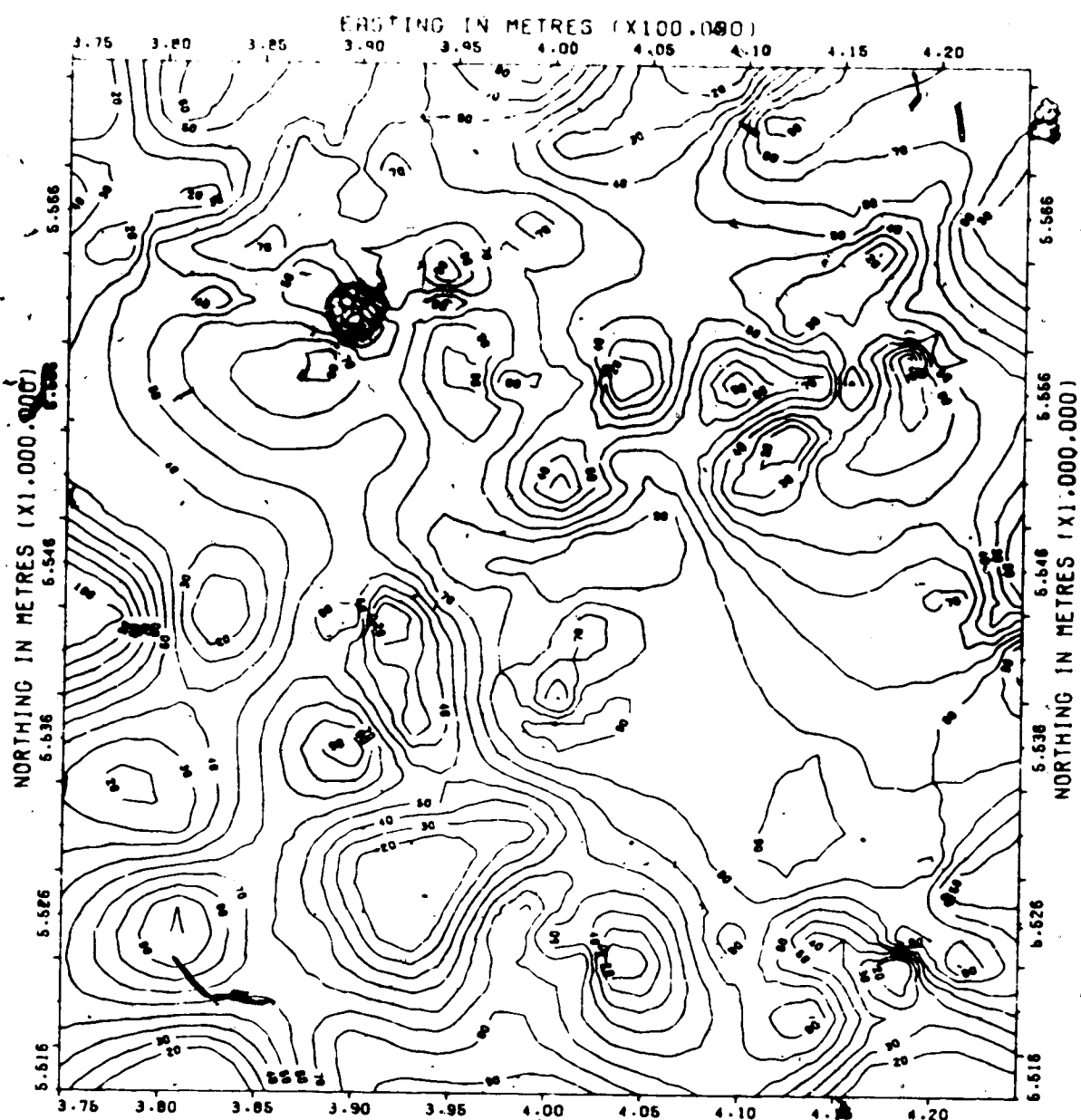
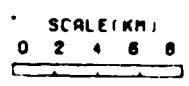


FIGURE 28



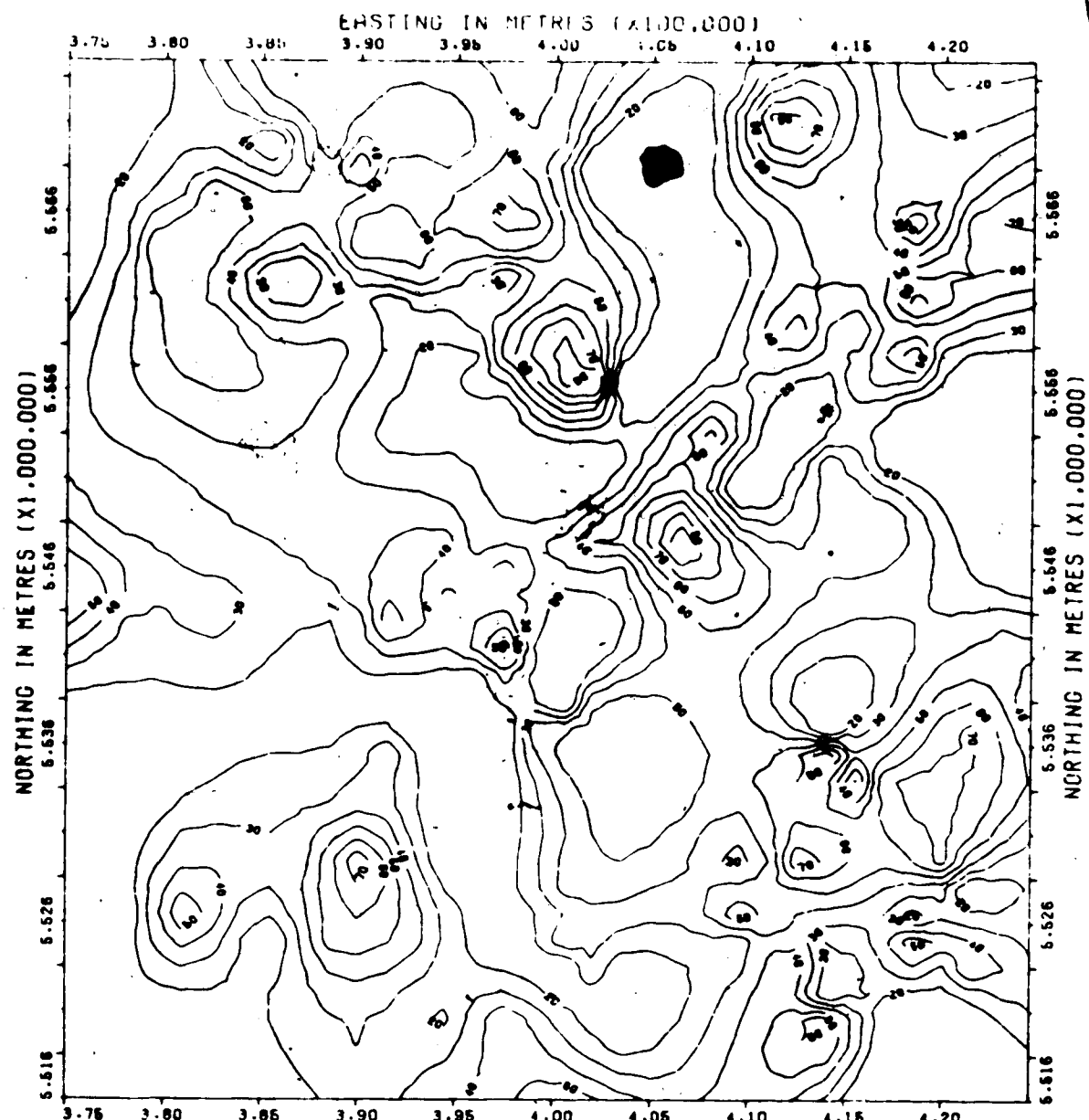
SAND PERCENTAGE MAP : INTERVAL 11

AREA : T10-15.R16-20 M4
CONTOUR INTERVAL : 10%
(0410% CONTOURS DELETED)



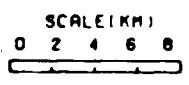
- SAND %
- 0- 20
 - 20- 40
 - 40- 60
 - 60- 80
 - 80-100

FIGURE 29.



SAND PERCENTAGE MAP : INTERVAL 10

AREA : T10-15.R16-20 W4
 CONTOUR INTERVAL : 10%
 (0 & 10% CONTOURS DELETED)



- SAND %
- 0- 20
 - 20- 40
 - 40- 60
 - 60- 80
 - 80-100

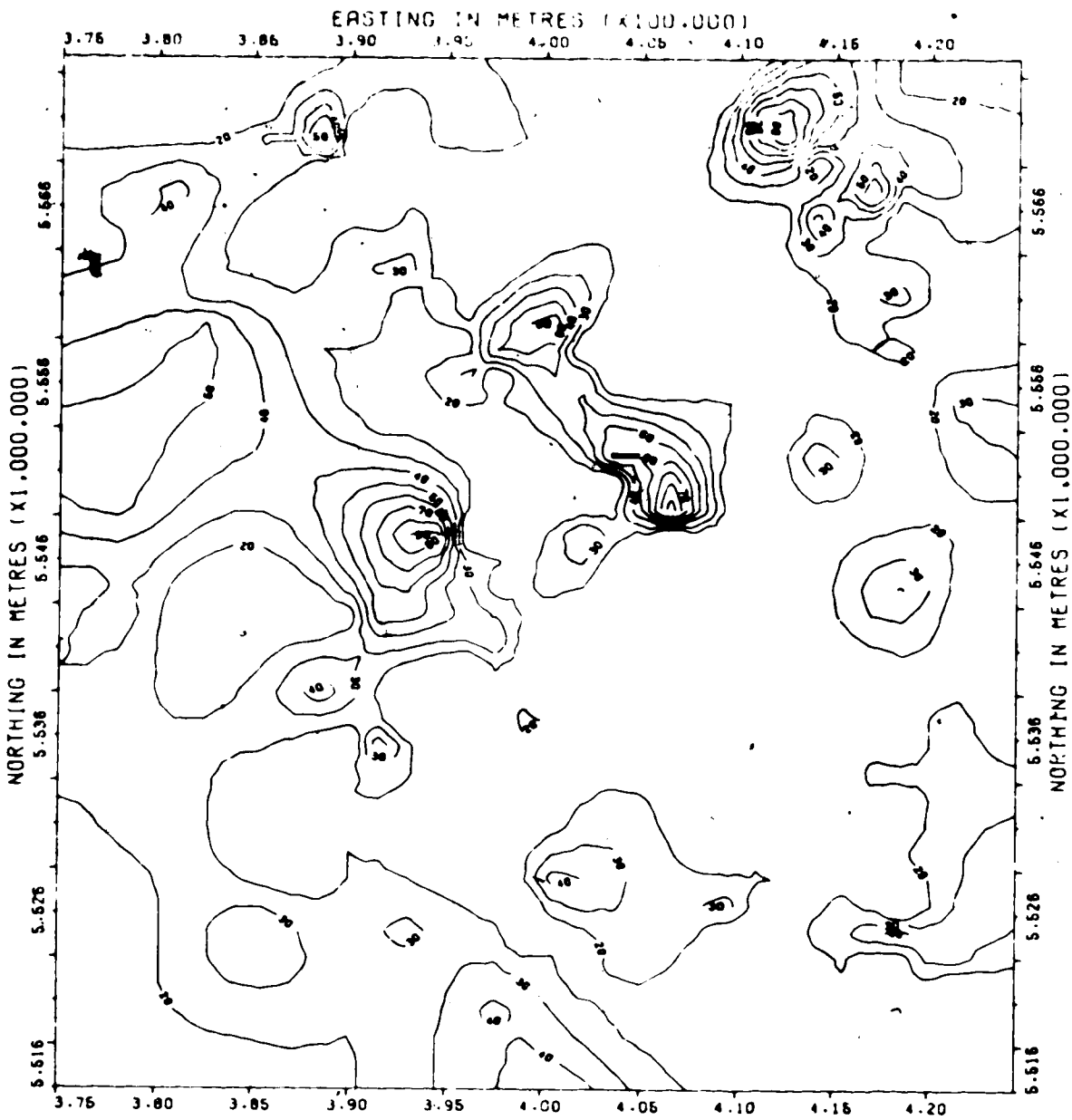
FIGURE 30

the topographic lows on the pre-Mannville surface, and silts and muds occur over the eroded highs. The course of the northern Turin stream is delineated on the Interval 10 map by the line of high sand values. Intervals 11 and 10 illustrate the progressive decrease in the volume of sand deposited throughout Lower Mannville time.

C. UPPER MANNVILLE GROUP

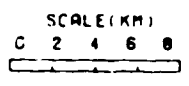
Interval 9 (Figure 31) encompasses most of the Glauconitic Sandstone Equivalent. Differential compaction of Lower Mannville sediments after the deposition of the Ostracode Zone shales produced a topography similar to that which existed in early Mannville time, though much subdued in relief. Streams maintained courses comparable to those of the early Mannville, although the volume of sand entering the Turin area was considerably reduced.

The Turin Valley persisted as the main area of sand deposition. Silts and muds were deposited over pre-Mannville highs and in areas removed from the main streams. A northwesterly-directed stream channel overlying the one cut at the southern edge of the Jurassic cuesta in the southwestern corner of the map area coalesced with the southern Turin Valley stream in the western part of the map area, and increased sand accumulation occurred at the junction. A northwesterly-trending stream is also evident in the northeastern part of the area. The fourth order trend surface residual map of Interval 9 (Figure 32) clearly shows the position of the four northwesterly-flowing streams which drained the Turin area at this time. The trend surface accounted for thirteen percent of the variance within the sand distribution.



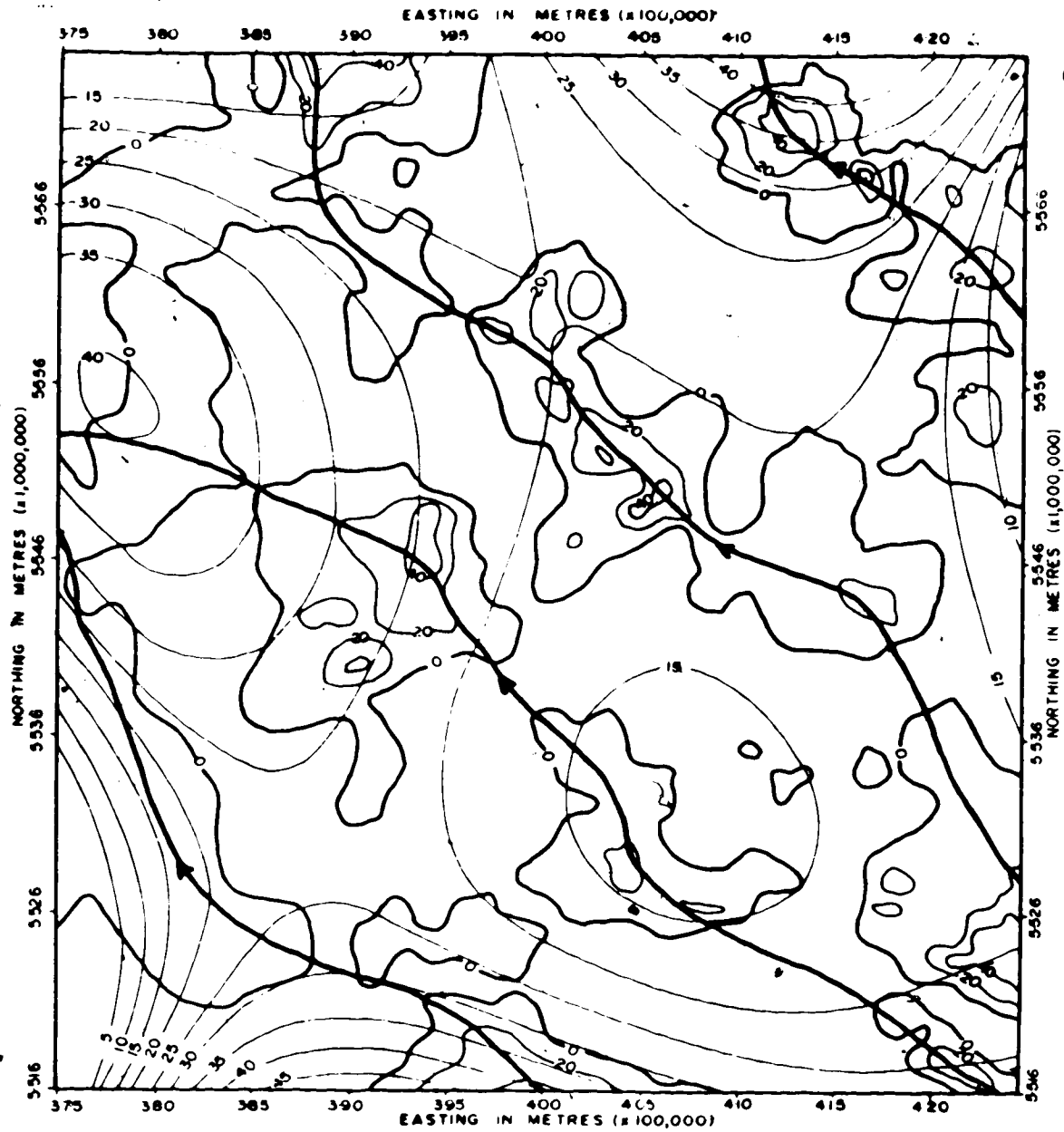
SAND PERCENTAGE MAP : INTERVAL 9

AREA : T10-15.R16-20 W4
 CONTOUR INTERVAL : 9%
 (0 & 10% CONTOURS DELETED)



- SAND %
- 0 - 20
 - 20 - 40
 - 40 - 60
 - 60 - 80
 - 80 - 100

FIGURE 31



TREND SURFACE MAP : SAND INTERVAL 9

AREA T10-15, R16-20 W4

TREND SURFACE ORDER 4TH

TREND SURFACE CONTOUR INTERVAL 5%

RESIDUALS CONTOUR INTERVAL 20%

SCALE (KM)



RESIDUALS

□ POSITIVE

INFERRED
STREAMS

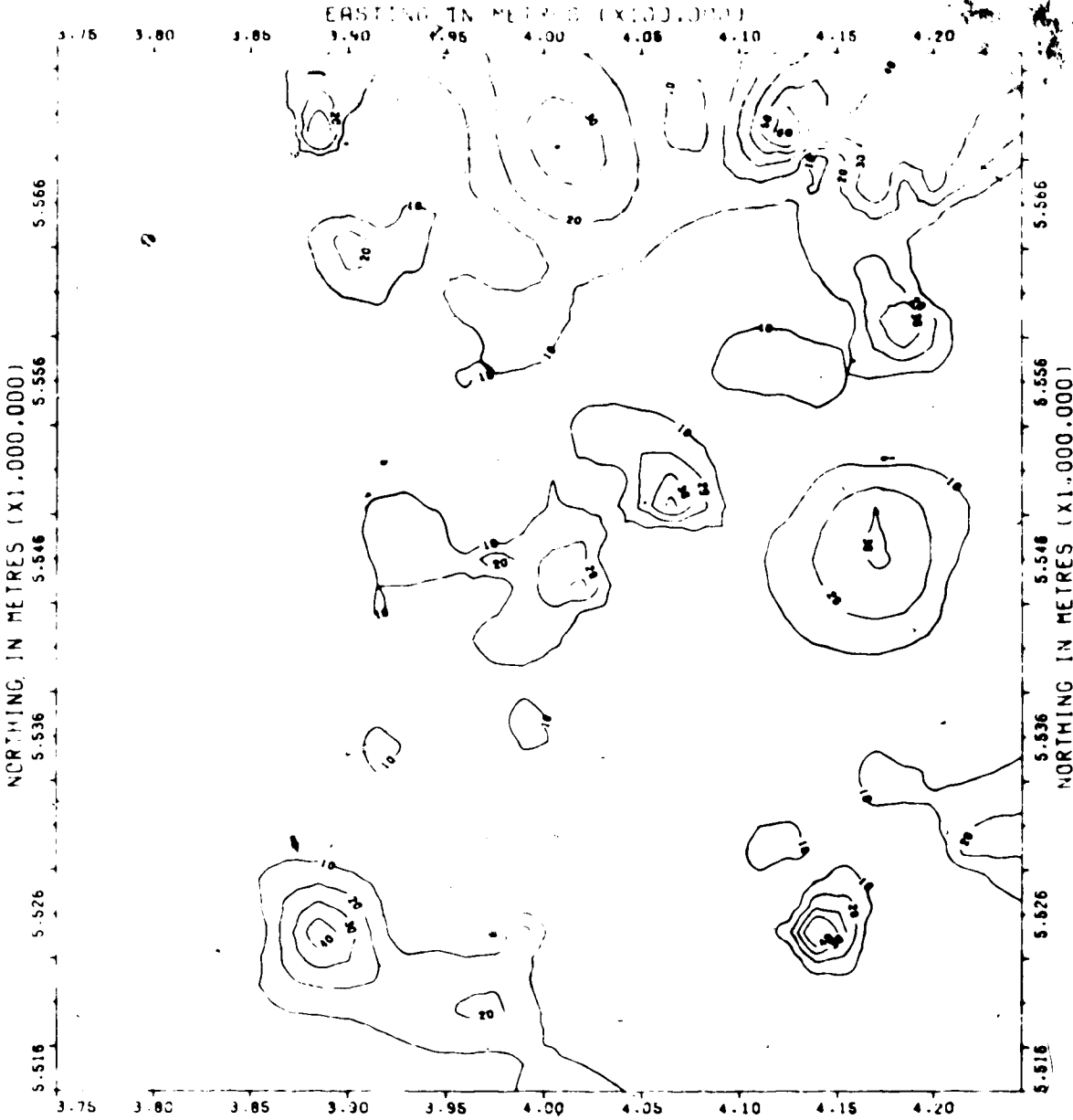
FIGURE 32

Very little sand was deposited within Intervals 8, 7 and 6 (Figures 33, 34 and 35) and the Turin Valley ceased to be the main area of sand deposition. It formed a wide, shallow depression in which approximately 150 feet of silt and mud were deposited, along with small, scattered occurrences of clean sand, the distribution of which suggests point bar deposits of meandering streams. The southwestern and northeastern streams were the main water courses at the time, and unlike the linear streams of Interval 9, mid late Mannville streams show little structural constraint, resulting in the formation of extensive meander belts over a floodplain of low relief.

Interval 5 (Figure 36) marks a period of renewed sand deposition. The four streams are still discernible, although only small volumes of sand were deposited over most of the Turin Valley. A thick sand accumulation occurs in the northeastern corner of the Turin area, but its limited areal extent prevents conclusions being drawn about the river in which it was deposited, the main channel of which apparently lay beyond the map area.

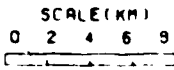
The northeast remained the site of sand deposition in Interval 4 (Figure 37), and little sand was deposited elsewhere. Two chains of low sand values delineate the position of Turin Valley streams at this time.

The largest volume of sand subsequent to the deposition of the Glauconitic Sandstone Equivalent (Interval 9) is present in Interval 3 (Figure 38), with major accumulations occurring in the southwestern and northern regions. Elements of the northern Turin Valley drainage system veered to the northeast and apparently entered the northeastern stream; arcuate trends of high sand values suggest broad, meandering channels.



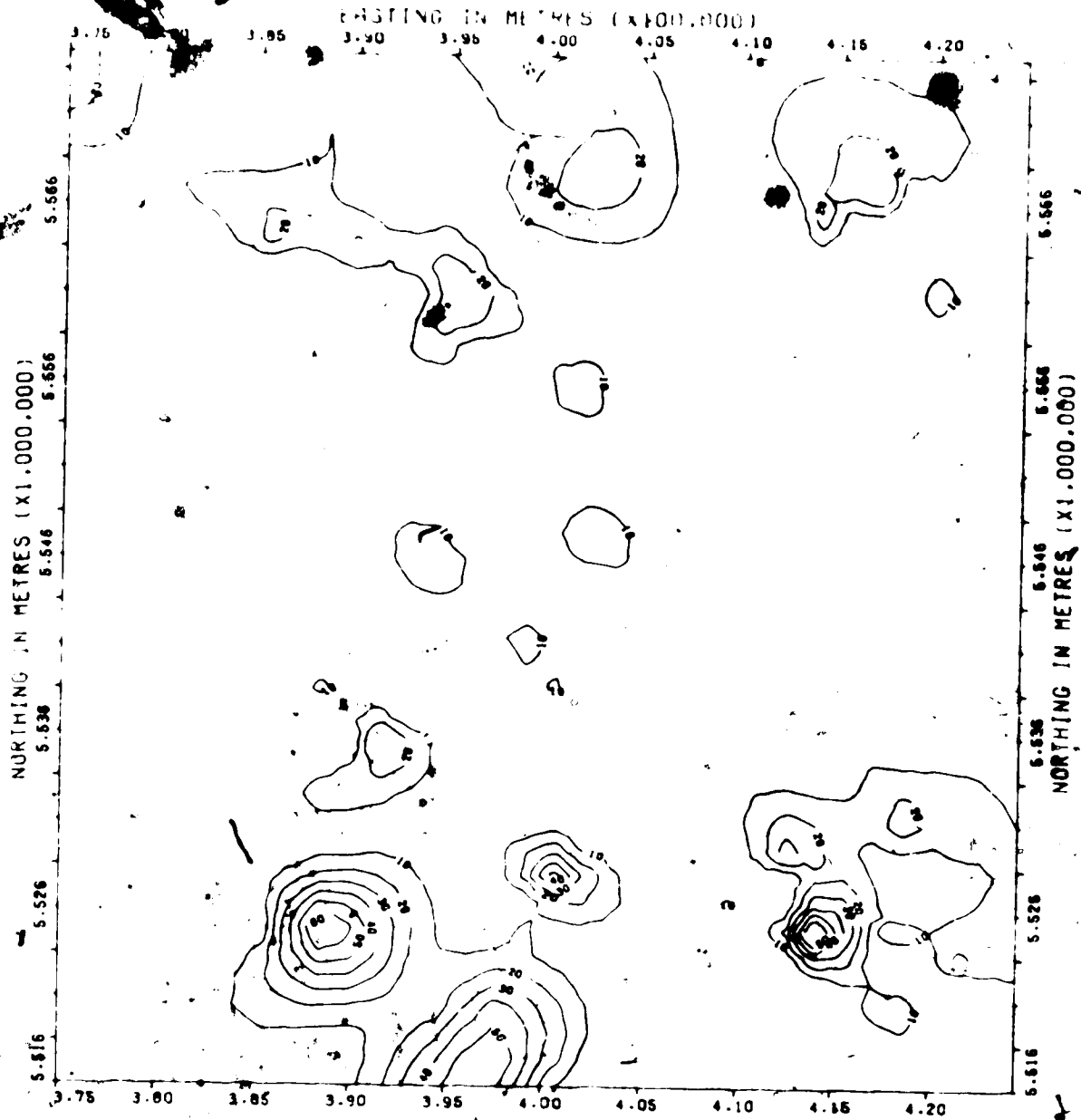
SAND PERCENTAGE MAP : INTERVAL 8

AREA : T10 15.R16-20 W4
 CONTOUR INTERVAL : 10%
 (10% CONTOUR DELETED)



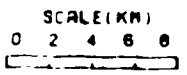
- SAND %
- 0 - 20
 - 20 - 40
 - 40 - 60
 - 60 - 80
 - 80 - 100

FIGURE 33



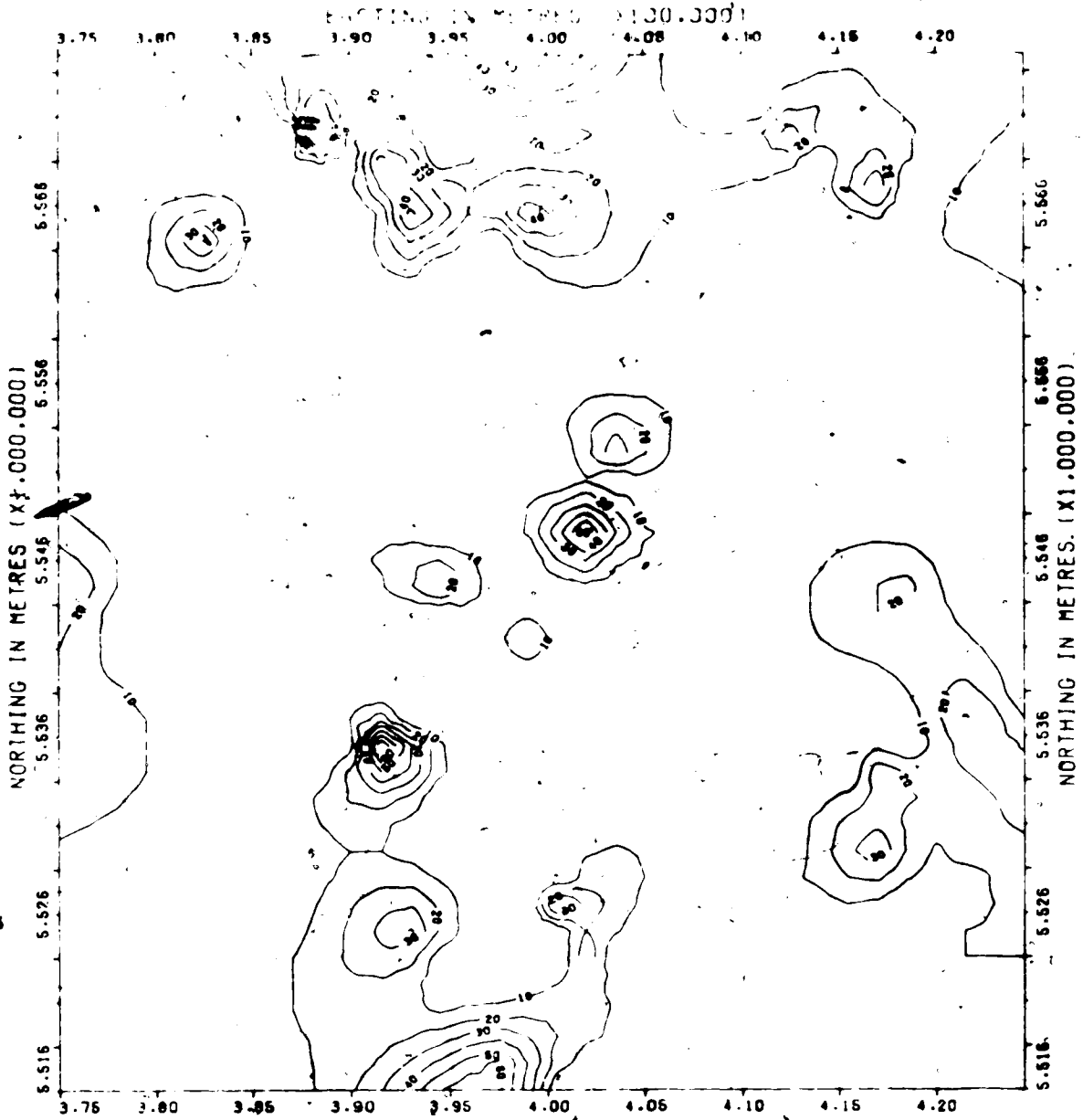
SAND PERCENTAGE MAP : INTERVAL 7

AREA : T10-15:R16-20 M4
 CONTOUR INTERVAL : 10%
 10% CONTOUR DELETED.



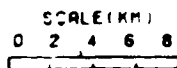
- SAND %
- 0-20
 - 20-40
 - 40-60
 - 60-80
 - 80-100

FIGURE 34



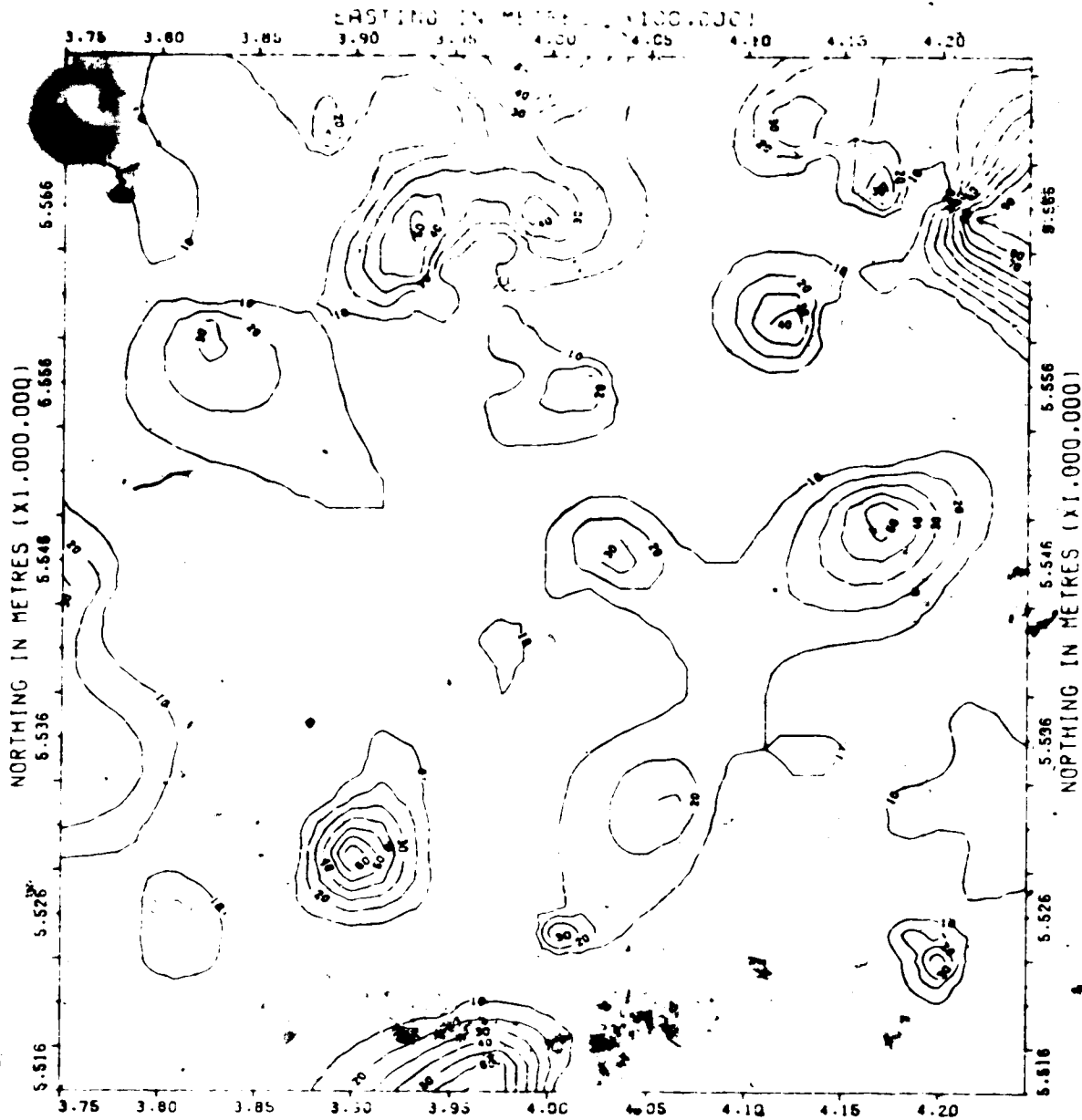
SAND PERCENTAGE MAP : INTERVAL 6

AREA : T10-15.R16-20 W4
 CONTOUR INTERVAL : 10%
 (10% CONTOUR DELETED)



- SAND %
- 0-20
 - 20-40
 - 40-60
 - 60-80
 - 80-100

FIGURE 35

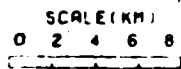


SAND PERCENTAGE MAP : INTERVAL 5

AREA : 1.0-15.R16-20 W4

CONTOUR INTERVAL 5%

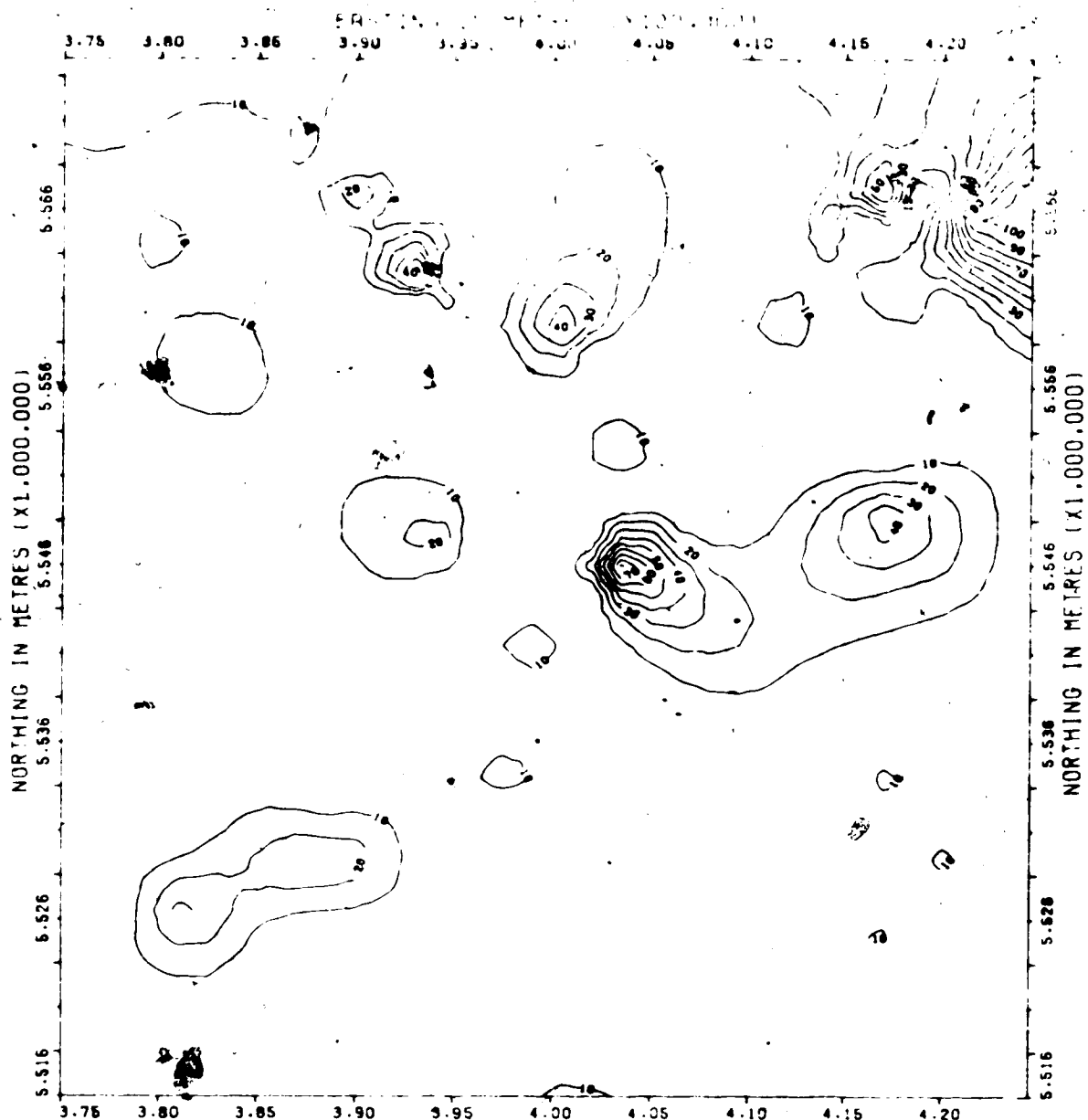
10% CONTOUR DELETED



SAND %

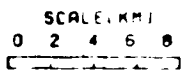
- 0- 20
- 20- 40
- 40- 60
- 60- 80
- 80-100

FIGURE 36



SAND PERCENTAGE MAP : INTERVAL 4

AREA : T10-15.R16-20 W4
 CONTOUR INTERVAL : 10%
 10% CONTOUR DELETED



- SAND %
- 0- 20
 - 20- 40
 - 40- 60
 - 60- 80
 - 80-100

FIGURE 37

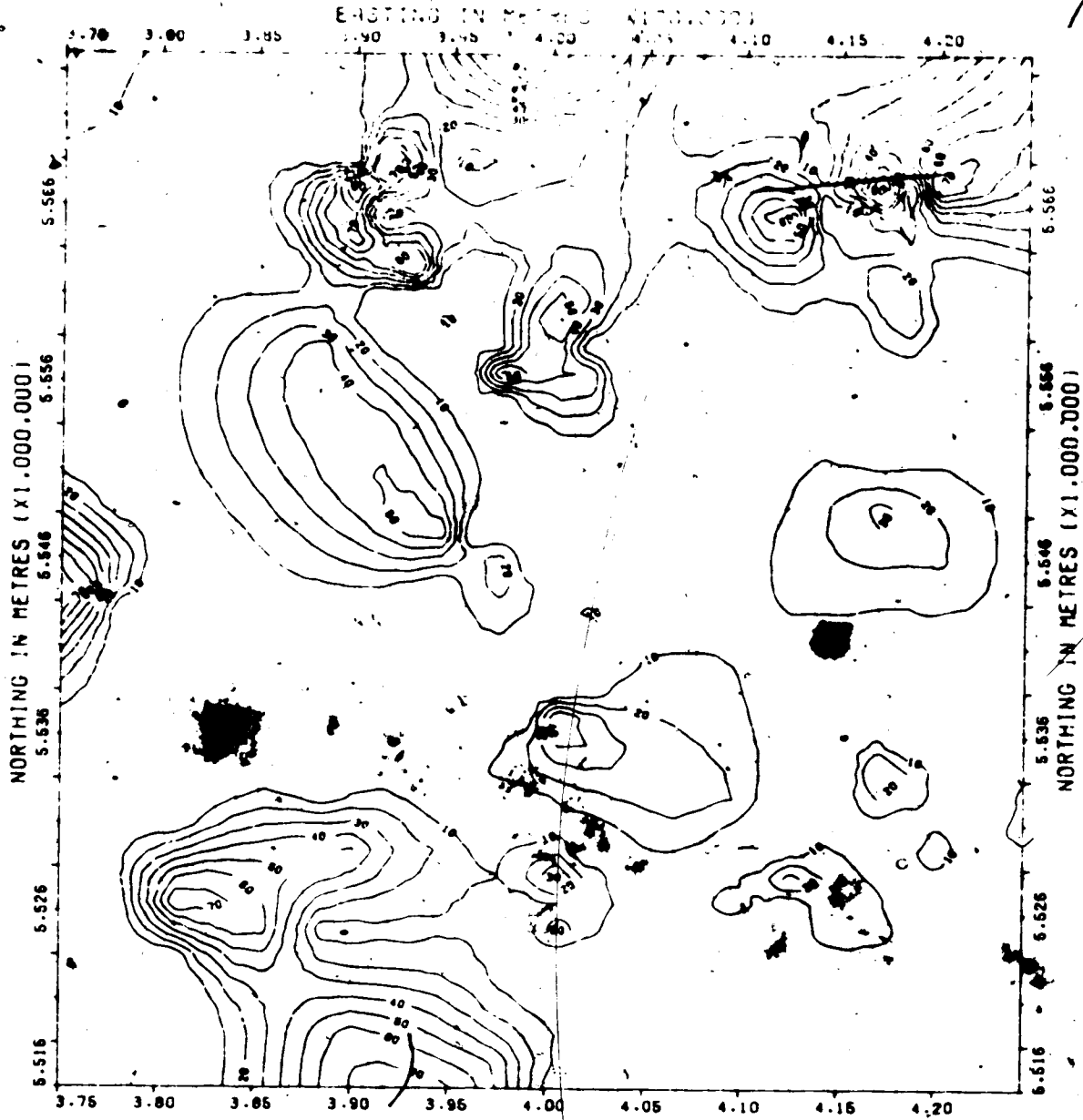
The southern Turin Valley stream maintained a northwesterly course at the time of deposition of Interval 2 (Figure 39). The northeastern stream migrated further into the Turin area, but the volume of sand deposited in the channel decreased. The drainage pattern illustrated in Figure 39 is a composite of the inferred drainage systems of Intervals 3 and 2. The Turin Valley streams formed a single, wide meander belt which, at times, coalesced with the streams in the northeastern and southwestern parts of the map area.

The final phase of Mannville deposition is represented by Interval 1 (Figure 40). Sand distribution is remarkably similar to that of Interval 9, the initial stage of Upper Mannville deposition. The Turin Valley again became the area of greatest sand accumulation, especially within the southern channel.

Inferred drainage patterns are marked on the fourth order trend surface map of Interval 1 (Figure 41). The similarity between the drainage interpretation of this map and that of the second order analysis of the structure on top of the Mannville Group (Figure 17) is obvious.

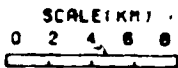
D. QUANTITATIVE ANALYSIS OF SAND DEPOSITION

The application of a gridding program to interval thicknesses measured in each well produced a regular distribution of values from which the average thickness, and hence volume, of each slice was determined. Gridding of interval sand percentage values was used similarly to calculate the volume of sand in each slice. Volumes of the Lower Mannville Group were determined from Intervals 10 and 11. Table 1 shows thickness



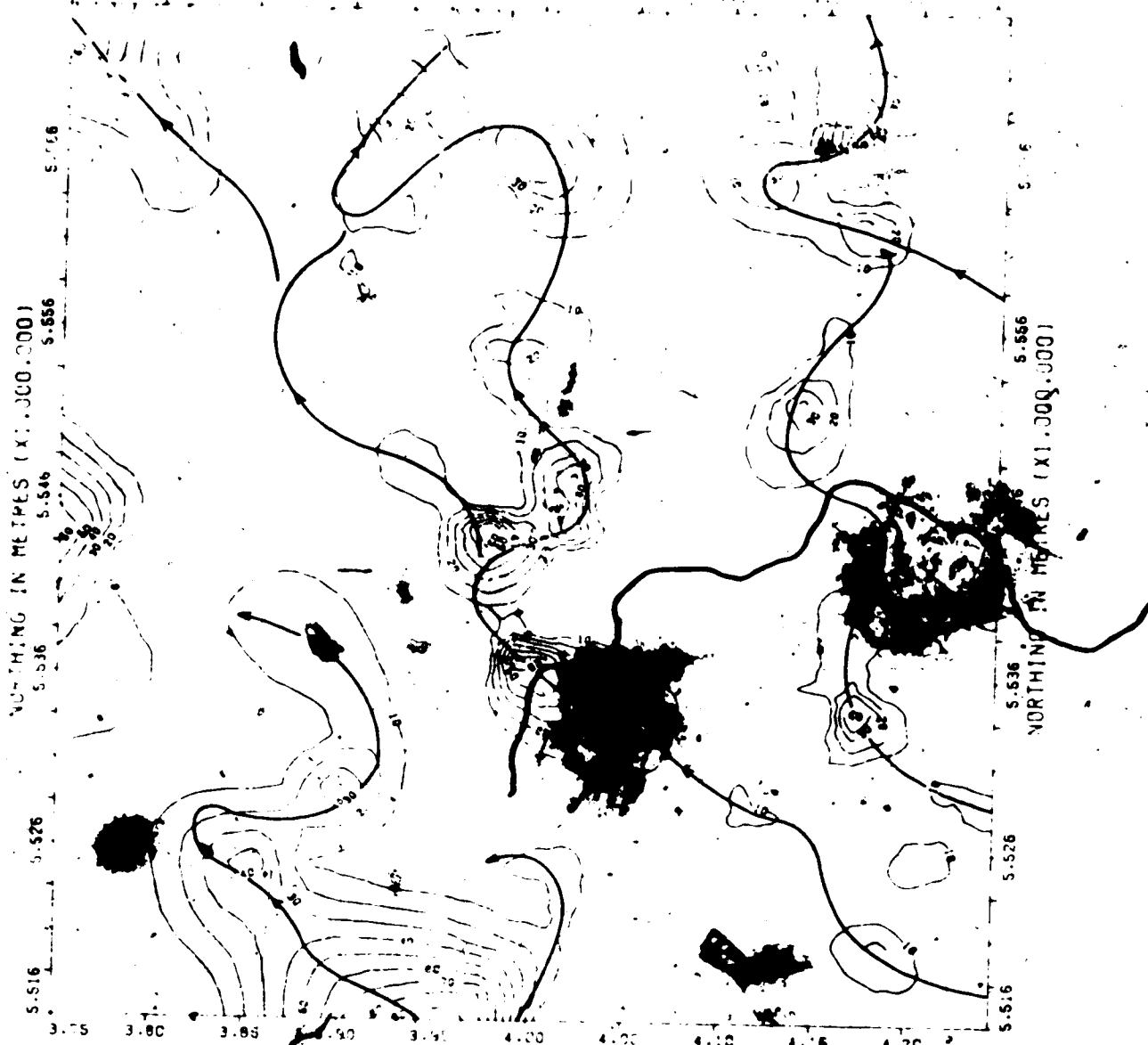
SAND PERCENTAGE MAP : INTERVAL 3

AREA : T10-15-R16-20-44
 CONTOUR INTERVAL : 10%
 (10% CONTOUR DELETED)



- SAND %
- 0- 20
 - 20- 40
 - 40- 60
 - 60- 80
 - 80-100

FIGURE 38



SAND PERCENTAGE MAP : INFERRAL

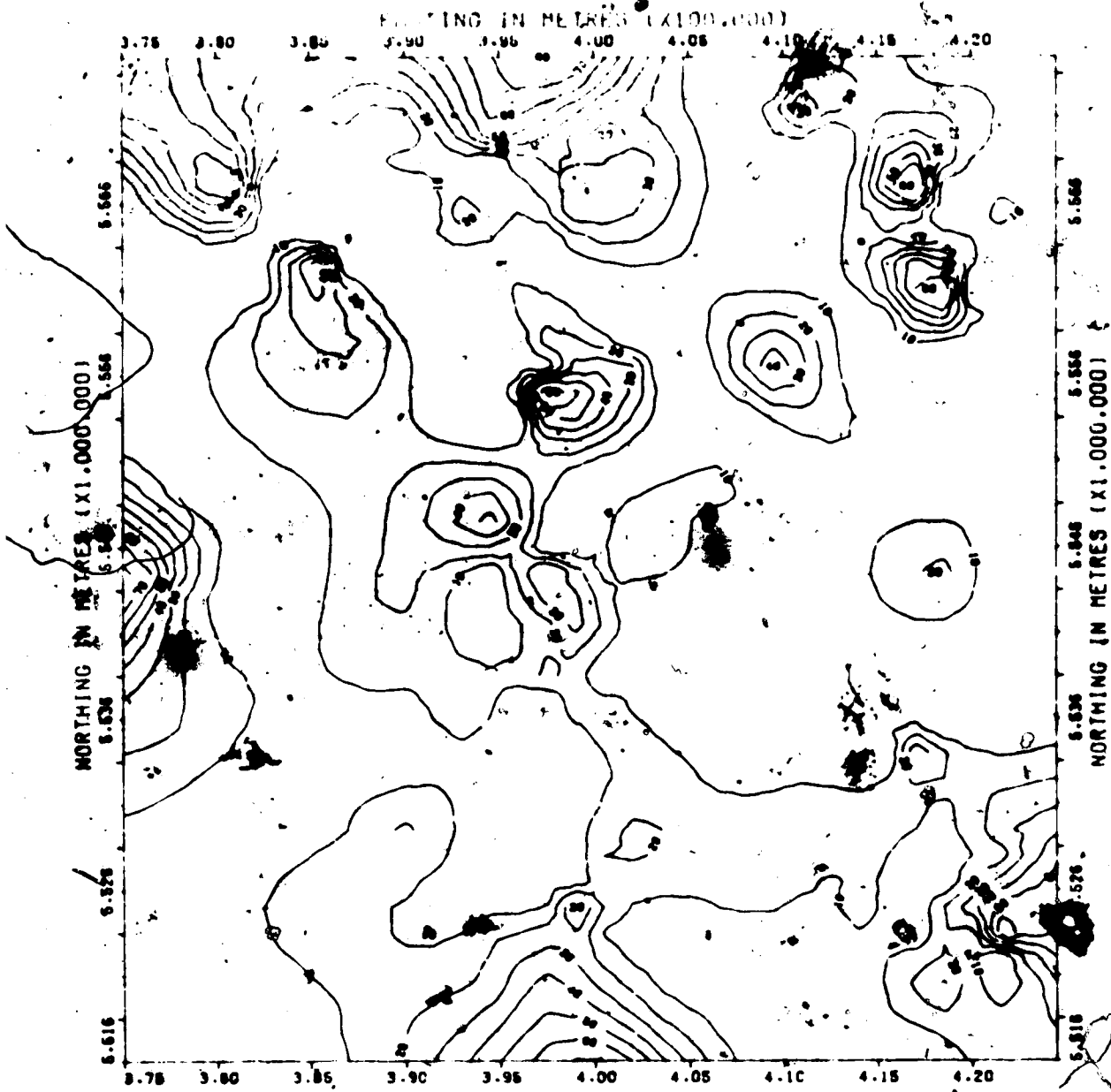
AREA : T10-15, R16-20 W4
 CONTOUR INTERVAL : 10%
 10% CONTOUR DELETED

SCALE : KM
 0 2 4 6 8

- SAND %
- 0-20
 - 20-40
 - 40-60
 - 60-80
 - 80-100

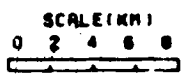
INFERRED STREAMS

FIGURE 39



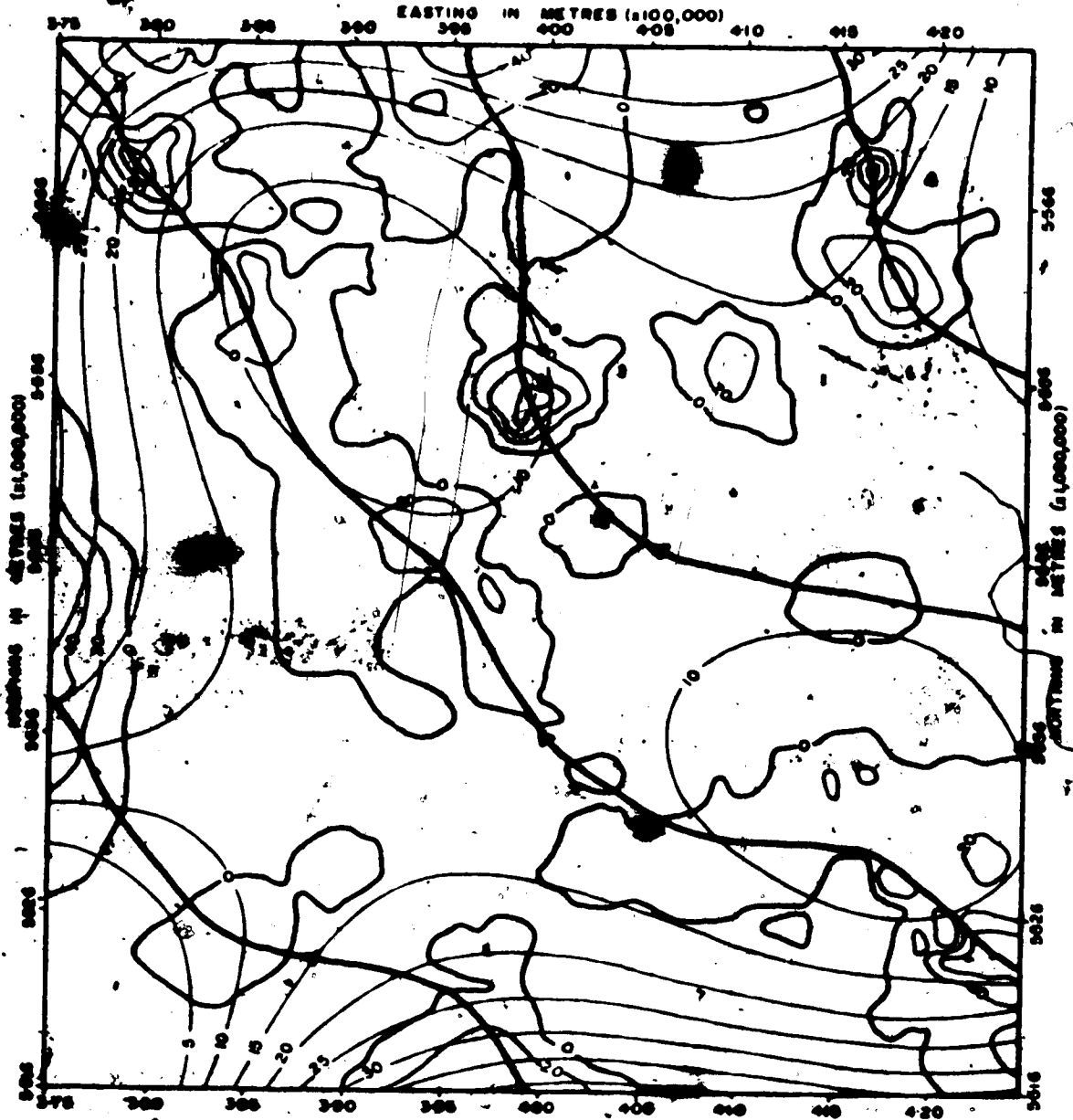
SAND PERCENTAGE MAP : INTERVAL 1

AREA : T10-16.M16-20 M4
 CONTOUR INTERVAL : 10%
 (10% CONTOUR DELETED)



- SAND %
- 0-20
 - 20-40
 - 40-60
 - 60-80
 - 80-100

FIGURE 40



TREND SURFACE MAP : SAND INTERVAL I

AREA : T1Q15, R16-20 W4

SCALE (KM)

TREND SURFACE ORDER : 4TH



TREND SURFACE CONTOUR INTERVAL : 5%

RESIDUALS CONTOUR INTERVAL : 20%

RESIDUALS
□ POSITIVE

INFERRED
STREAMS

FIGURE 41

Interval	Average Interval Thickness		Volume of Interval (x-10 ¹⁰)		Volume of Sand in Interval (x 10 ¹⁰)		Percentage of Interval Occupied by Sand	Volume of Sand (x 10 ⁹ cu. m)
	Metres	Feet	Cu. Metres	Cu. Yds.	Cu. Metres	Cu. Yds.		
1	15.6	51	4.51	5.89	0.59	0.78	13.2	0.38
2	15.6	51	4.52	5.90	0.48	0.62	10.6	0.31
3	15.6	51	4.53	5.91	0.63	0.82	13.9	0.40
4	15.7	52	4.54	5.92	0.30	0.39	6.7	0.19
5	15.7	52	4.55	5.94	0.46	0.60	10.1	0.29
6	15.7	52	4.56	5.96	0.33	0.43	7.2	0.21
7	15.7	52	4.57	5.97	0.29	0.38	6.4	0.19
8	15.7	52	4.58	5.99	0.33	0.44	7.3	0.21
9	15.7	52	4.59	6.01	0.96	1.26	20.9	0.51
10	15.3	50	4.42	5.78	1.49	1.94	33.6	0.97
11	15.3	50	4.40	5.75	2.59	3.38	58.8	1.70

Table 1. Thickness and Volume Parameters of Sand Intervals


and volume parameters for sand intervals. The data presented in Table 2 were derived from Table 1.

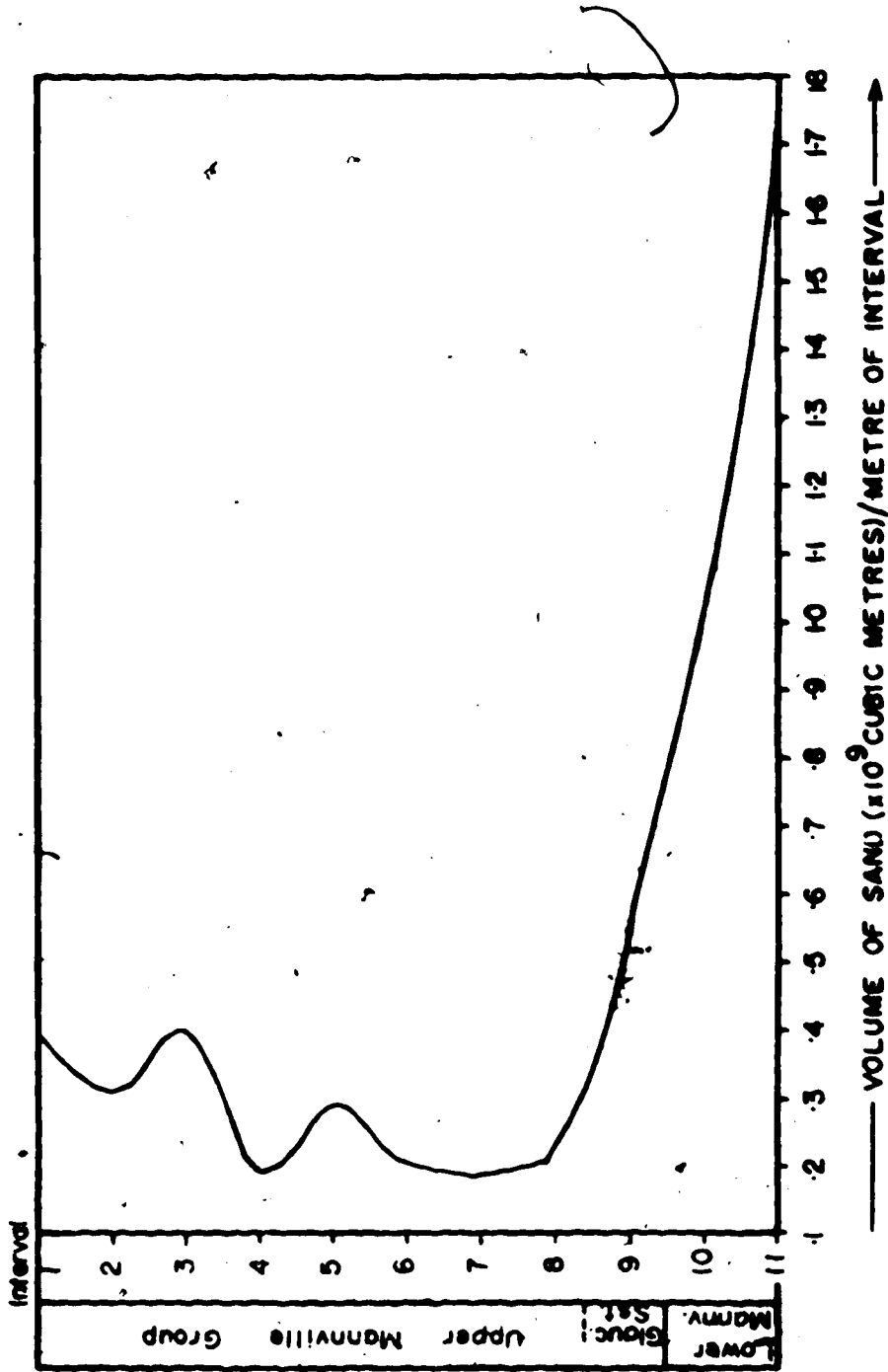
	Cu. Yds.	Cu. Metres
Vol. Mannville Group	6.51×10^{11}	4.98×10^{11}
Vol. Upper Mannville Group	5.36×10^{11}	4.10×10^{11}
Vol. Lower Mannville Group	1.15×10^{11}	0.88×10^{11}
The Upper Mannville constitutes 82.3% and the Lower Mannville 17.7% of the total volume of the group.		
Vol. sand (Mannville Gp.)	11.06×10^{10}	8.46×10^{10}
Vol. sand (U. Mannville Gp.)	5.73×10^{10}	4.38×10^{10}
Vol. sand (L. Mannville Gp.)	5.33×10^{10}	4.08×10^{10}
Seventeen percent of the Mannville Group consists of sand, 52% of which occurs in the Upper Mannville Group and 48% in the Lower Mannville Group.		

Table 2. Volume Parameters for the Mannville Group

Hence, the Lower Mannville Group contains about four and one quarter times the volume of sand per unit thickness compared with the Upper Mannville Group, as derived from $[48 + (\frac{17.7}{82.3} \times 52)]$. This reflects the rapid rate of erosion of the source area during early Mannville time. The volume of sand deposited in the Upper Mannville Group, however, would be greater than indicated because of the marginally higher gamma ray response of late Mannville sandstones caused by high clay content. A more mature landscape and the associated decrease in depositional energy of late Mannville streams would have resulted in larger volumes of clay accumulating within sand bodies, compared with sands deposited during early Mannville time. The volume

of sand per metre of interval thickness for successive intervals is shown in Figure 42. The rate of decrease in the volume of sand deposited is constant between the base of the Mannville Group and the top of the Glauconitic Sandstone Equivalent. This suggests a constant rate of erosion of the Lower Mannville source area until Ostracode Zone time (when no sand was entering the Turin area), followed by minor uplift and erosion during "Glauconite" time. Alternatively, the decrease in the volume of sand deposited may have been due to a raising of base level at this time. The former explanation is favoured, although the data is not conclusive. Herbaly (1974) noted that early Cretaceous sandstones of the Sweetgrass arch had a western origin. In central Alberta, Williams (1963) and Williams *et al.* (1962) inferred an eastern source (Canadian Shield) for the Lower Mannville Group and a western source (Cordilleran region) for the Upper Mannville Group, based on the mineralogy of the sandstones and radiometric ages of detrital minerals. The proximity of the Turin area to the Cordilleran region resulted in it being little affected by the products of erosion of the Shield.

In post-"Glauconite" time the volume of sand deposited  (Figure 42). This was a response to either periodic uplift of the source or intermittent regional variations in drainage pattern. Data presented previously show Mannville streams to be confined to fairly narrow meander belts (of a few miles) due to structural control by the pre-Cretaceous surface. Periodic rejuvenation of a maturing source area was therefore responsible for the pulses of sand deposition during late Mannville time. This is confirmed by studies of the Mannville source area. Potassium-Argon dates determined by Baadsgaard *et al.* (1961) for the time of intrusion of phases of the Nelson, Coast Range and Cassiar-Omineca batholiths



SAND VOLUME DISTRIBUTION, MANNVILLE GROUP

FIGURE 42

of the Cordillera, ranged from 96 million years (m.y.) to 107 m.y. London (1961) dated phases of the intrusion of the Nelson and adjacent batholiths at 101 m.y. and 127 m.y. According to the time scale of Obradovich and Cobban (1975), these periodic igneous intrusions and uplift occurred during the Albian, the time at which the Upper Mannville Group was deposited.

E. CONCLUSION

Clean sands were deposited mainly within the channels of high energy streams throughout Mannville time. The position of Mannville channels was governed by the position of channels in the pre-Mannville surface. Lower Mannville sediments consisted mainly of sand, the volume of which decreased upwards through the section in response to a levelling of the Cordilleran source area. Early Mannville streams maintained relatively narrow courses confined by ridges of Mississippian and Jurassic strata.

Although the basic elements of the early Mannville drainage persisted, the four main drainage systems periodically coalesced during late Mannville time to form extensive floodplains crossed by numerous, small braided and meandering streams. Silt and mud deposition predominated, with periodic influxes of sand resulting from rejuvenation of the source area.

Chapter VII
PETROLEUM DISTRIBUTION

A. INTRODUCTION

Petroleum occurrence was stored on computer file according to well location, type of show (major or minor oil or gas, oil or gas cut, mud, condensate) and stratigraphic position (uppermost Upper Mannville Group, mid Upper Mannville Group, Glauconitic Sandstone Equivalent, sandstones within fifty feet of the Ostracode Zone, and the remainder of the Lower Mannville Group). The distinction between the major and minor oil or gas occurrences was qualitative. Major occurrences were designated as those wells which had been or were presently on production or were capped for future production. Only wells from which structural and sand data were acquired were used in determining petroleum occurrence, thereby precluding a number of development wells in which electric logs were not run.

Maps were generated for each stratigraphic interval showing the distribution of each type of show. For reasons of brevity, only maps of major oil and gas occurrence in the Lower Mannville Group and the Glauconitic Sandstone Equivalent, and all oil and gas occurrences in the Upper Mannville Group (above the Glauconitic Sandstone), are presented.

The outlines of Cretaceous oil and gas pools of the Turin area (Figure 43) were reproduced from the Geological Survey of Canada map of oil and gas pools of western Canada (Map 1316A, 1970). All pools shown have recoverable reserves of greater than one billion cubic feet

27622



National Library
of Canada

Bibliothèque nationale
du Canada

CANADIAN THESES
ON MICROFICHE

THÈSES CANADIENNES
SUR MICROFICHE

NAME OF AUTHOR NOM DE L'AUTEUR RODNEY STUART BROWN

TITLE OF THESIS TITRE DE LA THÈSE COMPUTER ANALYSIS OF SAND AND
PETROLEUM DISTRIBUTION IN THE MANNVILLE
GROUP, TURIN AREA, SOUTHERN ALBERTA

UNIVERSITY UNIVERSITÉ U of ALBERTA

DEGREE FOR WHICH THESIS WAS PRESENTED
GRADE POUR LEQUEL CETTE THÈSE FUT PRÉSENTÉE M SC

YEAR THIS DEGREE CONFERRED ANNÉE D'OBTENTION DE CE GRADE 1976

NAME OF SUPERVISOR NOM DU DIRECTEUR DE THÈSE DR. G. D. WILLIAMS

Permission is hereby granted to the NATIONAL LIBRARY OF CANADA to microfilm this thesis and to lend or sell copies of the film.

L'autorisation est, par la présente, accordée à la BIBLIOTHÈQUE NATIONALE DU CANADA de microfilmer cette thèse et de prêter ou de vendre des exemplaires du film.

The author reserves other publication rights, and neither the thesis nor extensive extracts from it may be printed or otherwise reproduced without the author's written permission.

L'auteur se réserve les autres droits de publication ni la thèse ni de longs extraits de celle-ci ne doivent être imprimés ou autrement reproduits sans l'autorisation écrite de l'auteur.

DATED DATE 26 April 76 SIGNED / SIGNÉ R S Brown

PERMANENT ADDRESS RÉSIDENCE FIXE C/O IMPERIAL OIL LIMITED
500 SIXTH AVE S.W.
CALGARY ALTA T2P 0S1

INFORMATION TO USERS

THIS DISSERTATION HAS BEEN
MICROFILMED EXACTLY AS RECEIVED

This copy was produced from a microfiche copy of the original document. The quality of the copy is heavily dependent upon the quality of the original thesis submitted for microfilming. Every effort has been made to ensure the highest quality of reproduction possible.

PLEASE NOTE: Some pages may have indistinct print. Filmed as received.

Canadian Theses Division
Cataloguing Branch
National Library of Canada
Ottawa, Canada K1A 0N4

AVIS AUX USAGERS

LA THESE A ETE MICROFILMEE
TELLE QUE NOUS L'AVONS RECUE

Cette copie a été faite à partir d'une microfiche du document original. La qualité de la copie dépend grandement de la qualité de la thèse soumise pour le microfilmage. Nous avons tout fait pour assurer une qualité supérieure de reproduction.

NOTA BENE: La qualité d'impression de certaines pages peut laisser à désirer. Microfilmée telle que nous l'avons reçue.

Division des thèses canadiennes
Direction du catalogage
Bibliothèque nationale du Canada
Ottawa, Canada K1A 0N4

THE UNIVERSITY OF ALBERTA

COMPUTER ANALYSIS OF SAND AND PETROLEUM DISTRIBUTION IN THE
MANNVILLE GROUP, TURIN AREA, SOUTHERN ALBERTA

by



RODNEY S. BROWN B.Sc.(Hons.)

A THESIS

SUBMITTED TO THE FACULTY OF GRADUATE STUDIES AND RESEARCH
IN PARTIAL FULFILMENT OF THE REQUIREMENTS FOR THE DEGREE
OF MASTER OF SCIENCE

DEPARTMENT OF GEOLOGY

EDMONTON, ALBERTA

SPRING, 1976

THE UNIVERSITY OF ALBERTA

FACULTY OF GRADUATE STUDIES AND RESEARCH

The undersigned certify that they have read, and recommend to the Faculty of Graduate Studies and Research for acceptance, a thesis entitled "COMPUTER ANALYSIS OF SAND AND PETROLEUM DISTRIBUTION IN THE MANNVILLE GROUP, TURIN AREA, SOUTHERN ALBERTA", submitted by Rodney S. Brown B.Sc. (Hons.), in partial fulfilment of the requirements for the degree of Master of Science.

[Handwritten signature]
.....
Supervisor
[Handwritten signature]
.....
[Handwritten signature]
.....
[Handwritten signature]
.....

DATE 26 April 1976

ABSTRACT

Sand distribution in the Mannville Group in the Turin area was determined using computer generated sand percentage slice maps, structure contour maps and isopach maps. Trend surface analysis was used to separate local anomalies from regional trends within the structural and lithologic data.

Continental Mannville Group sediments were deposited on an eroded surface of southwesterly-dipping Mississippian and Jurassic strata. Initial deposition consisted mainly of sand, and was restricted to stream channels on the pre-Mannville surface, the configuration of which reflected the northwesterly strike of the bedding. Infilling of valleys and the denudation of ridges produced a landscape of low relief by late Lower Mannville time. Maturation of the Cordilleran source area resulted in the progressive decrease in the volume of sand deposited within the Lower Mannville sequence, culminating in the widespread deposition of shales of the Ostracode Zone. Differential compaction of Lower Mannville sediments produced an Upper Mannville topography similar to, yet more subdued than that of the pre-Mannville surface. During late Mannville time, predominantly fine-grained clastics were deposited. Periodic uplift and erosion of the source area resulted in the influx of sand, which was more variably distributed than in the Lower Mannville Group. Drainage channels frequently coalesced to form wide valleys and floodplains of meandering and braided streams. Mannville sedimentation was halted by the transgression of the Colorado Sea.

Petroleum distribution is a function of pre-Mannville topography, sand distribution and post-depositional northwesterly-tilting of the basin. Traps are predominantly stratigraphic, formed by shaling out of channel sands. Oil and gas pools occur in the updip portion of sands

which accumulated along the flanks and crests of structural highs corresponding to topographic highs in the pre-Mannville surface. Production occurs mainly from the Lower Mannville Group and the Glauconitic Sandstone Equivalent.

ACKNOWLEDGEMENTS

The author wishes to thank Dr. G.D. Williams, project supervisor, for advice and financial support given during the preparation of the thesis. Messrs. D. Flint, T. Lam, and D. Proudfoot of the Western Canada Coal Resource Data Base, and Mr. K. McDonell of the Computing Science Department, University of Alberta, assisted in the application and creation of computer programs used in the study. Their help is greatly appreciated.

The Alberta Research Council made available microfilm facilities for the examination of electric well logs.

Special thanks go to Linda for assistance rendered throughout the year and for typing the manuscript.

Financial assistance was provided by a University of Alberta Graduate Teaching Assistantship and a Province of Alberta Graduate Studies Scholarship.

TABLE OF CONTENTS

	PAGE
ABSTRACT	iv
ACKNOWLEDGEMENTS	vi
LIST OF TABLES	ix
LIST OF FIGURES	ix
CHAPTER	
I. INTRODUCTION	1
A. PURPOSE AND LOCATION OF STUDY	1
B. PREVIOUS WORK	1
II. METHOD OF STUDY	7
A. COMPILATION OF GEOLOGIC DATA	7
B. COMPUTER TECHNIQUES	8
(1) Gridding and Contouring	8
(2) Trend Surface Analysis	11
III. REGIONAL GEOLOGY	15
IV. GEOLOGY OF THE MANNVILLE GROUP	19
V. GEOLOGY OF THE TURIN AREA	28
A. PRE-MANNVILLE GEOLOGY	28
B. LOWER MANNVILLE GEOLOGY	36
C. UPPER MANNVILLE GEOLOGY	42
D. POST-MANNVILLE GEOLOGY	45
VI. SAND DISTRIBUTION IN THE MANNVILLE GROUP	51
A. INTRODUCTION	51
B. LOWER MANNVILLE GROUP	53

TABLE OF CONTENTS (cont'd)

CHAPTER	PAGE
C. UPPER MANNVILLE GROUP	66
D. QUANTITATIVE ANALYSIS OF SAND DEPOSITION	75
E. CONCLUSION	84
VII. PETROLEUM DISTRIBUTION	85
A. INTRODUCTION	85
B. LOWER MANNVILLE GROUP	87
C. GLAUCONITIC SANDSTONE EQUIVALENT	91
D. UPPER MANNVILLE GROUP (POST-GLAUCONITIC SANDSTONE EQUIVALENT)	92
E. POST-MANNVILLE GROUP	95
VIII. SUMMARY AND CONCLUSIONS	97
IX. REFERENCES	100

LIST OF TABLES

TABLE		PAGE
1.	Thickness and Volume Parameters of Sand Intervals	80
2.	Volume Parameters for the Mannville Group	81

LIST OF FIGURES

FIGURE		PAGE
1.	Location Map	2
2.	Location Map - Turin area (showing location of wells)	3
3.	Regional Geology Map - Western Canada Sedimentary Basin	16
4.	Neocomian (Pre-Mannville) Paleogeography	21
5.	Early Upper Mannville Paleogeography	22
6.	Lower Cretaceous Correlation Chart - Western Canada and Montana	23
7.	IES Log Correlation; cross section X-Y	29
8.	IES Log Correlation; cross section A-B	30
9.	Structure Map: Top of Mississippian	31
10.	Isopach Map: Jurassic	33
11.	Structure Map: Base of Mannville Group	35
12.	Trend Surface Map: Base of Mannville Group	37
13.	Structure Map: Top of Lower Mannville Group	38
14.	Isopach Map: Lower Mannville Group	39
15.	Diagrammatic Cross sections - Turin Area	41
16.	Structure Map: Top of Mannville Group	43
17.	Trend Surface Map: Top of Mannville Group	44

LIST OF FIGURES (cont'd)

FIGURE		PAGE
18.	Isopach Map: Upper Mannville Group	46
19.	Isopach Map: Mannville Group	47
20.	Dip section across the Turin Area; cross section X-Y	49
21.	Strike section across the Turin Area; cross section A-B	50
22.	Diagrammatic subdivision of the Mannville Group	54
23.	Subdivision of Mannville Group into intervals for Sand Calculations	55
24.	Sand Percentage Map: Interval 15	56
25.	Sand Percentage Map: Interval 14	58
26.	Sand Percentage Map: Interval 13	59
27.	Sand Percentage Map: Interval 12	61
28.	Trend Surface Map: Interval 12	63
29.	Sand Percentage Map: Interval 11	64
30.	Sand Percentage Map: Interval 10	65
31.	Sand Percentage Map: Interval 9	67
32.	Trend Surface Map: Interval 9	68
33.	Sand Percentage Map: Interval 8	70
34.	Sand Percentage Map: Interval 7	71
35.	Sand Percentage Map: Interval 6	72
36.	Sand Percentage Map: Interval 5	73
37.	Sand Percentage Map: Interval 4	74
38.	Sand Percentage Map: Interval 3	76
39.	Sand Percentage Map: Interval 2	77
40.	Sand Percentage Map: Interval 1	78

LIST OF FIGURES (cont'd)

FIGURE		PAGE
41.	Trend Surface Map: Interval 1	79
42.	Sand Volume Distribution, Mannville Group	83
43.	Petroleum Distribution: Lower Cretaceous	86
44.	Petroleum Distribution: Lower Mannville Group	88
45.	Petroleum Distribution: Glauconitic Sandstone Equiv.	93
46.	Petroleum Distribution: Upper Mannville Group	94
47.	Petroleum Distribution: Bow Island Formation	96

LIST OF APPENDICES

Computer printout of structural and lithologic data used in this study is held by the Geology Department library, University of Alberta.

Chapter I
INTRODUCTION

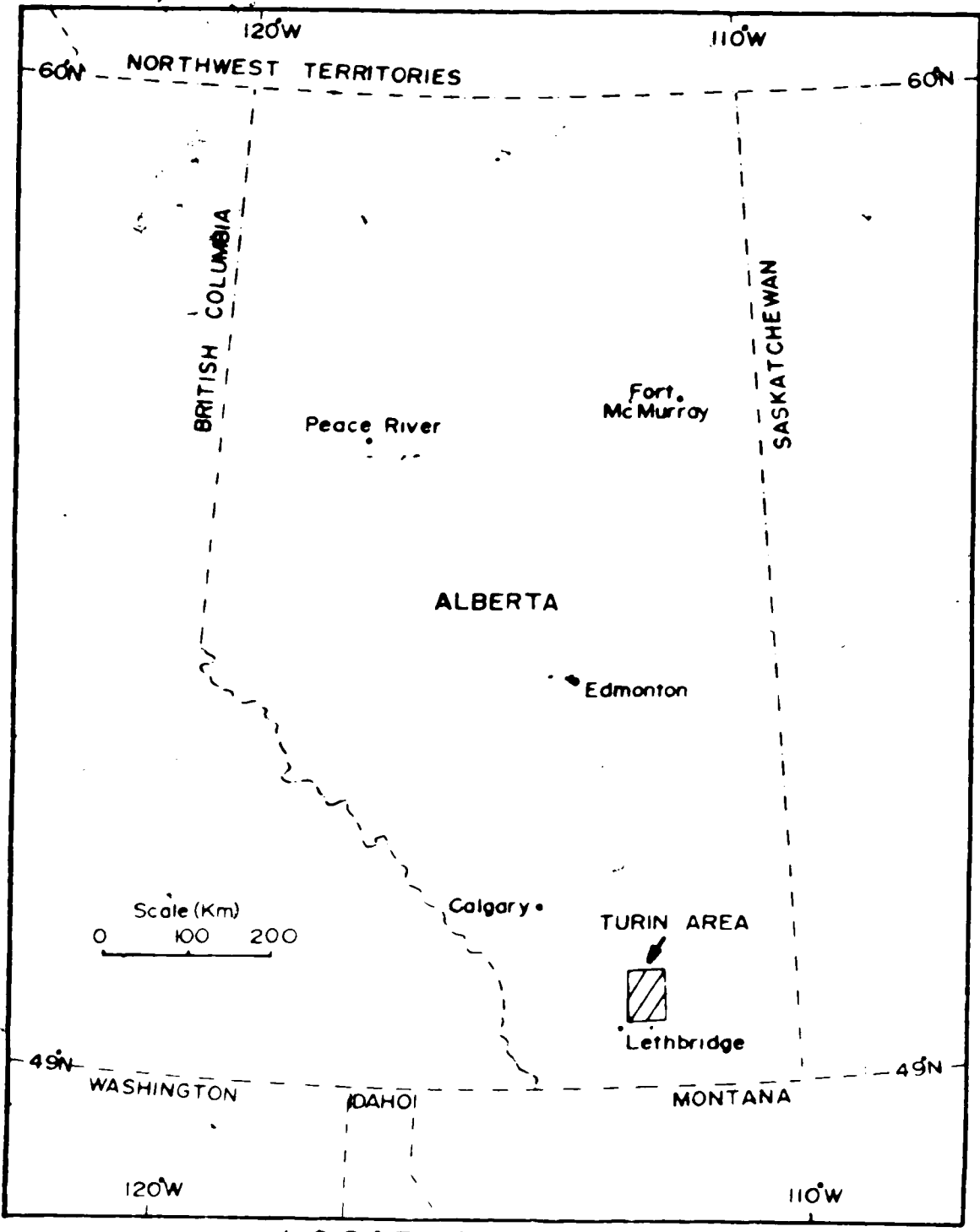
A. PURPOSE AND LOCATION OF STUDY

The purpose of the study was threefold:

1. To map the distribution of sandstones in the Mannville Group using numerical techniques. This method was seen as a viable alternative to conventional interpretive log correlation, particularly within a continental sequence where sandstones are laterally discontinuous and exhibit considerable variation in log response.
2. To find reasons for the distribution of sandstones in the succession.
3. To determine the factors controlling the occurrence of oil and gas in the sandstones.

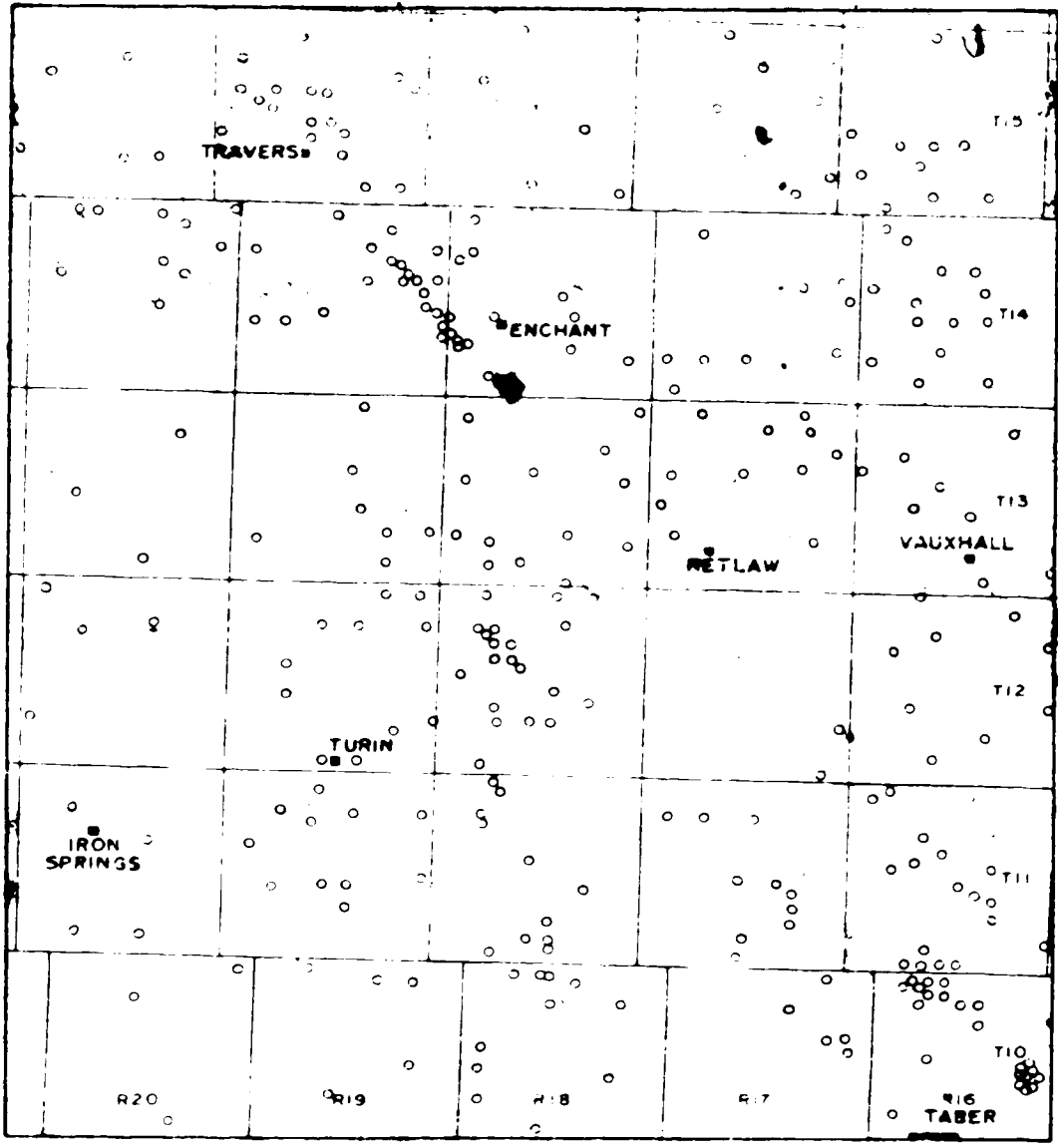
The Turin area is located in the southern Alberta plains (Fig. 1) within Townships 10 to 15, Ranges 16 to 20 west of the Fourth Meridian (Fig. 2), and covering approximately 1,100 square miles (2,850 square kilometres).

This area was chosen because the Mannville Group is entirely continental, and has oil and gas production from a number of sandstones within the sequence (the Little Bow, Enchant, Retlaw, Turin and Taber North fields). The shape and distribution of these fields suggested a fluvial origin for the reservoirs. Well density and distribution was sufficient to enable detailed lithologic analysis.



LOCATION MAP

FIGURE 1



LOCATION MAP - TURIN AREA

(SHOWING WELL DISTRIBUTION)

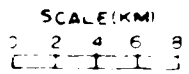


FIGURE 2

Poor Copy

B. PREVIOUS WORK

A chronological review of publications on the Mannville Group and its equivalents in Alberta, from McLearn's (1932, 1944) initial attempts at a regional correlation of the Lower Cretaceous, to the definitive, localized, sedimentological studies of the 1960's, is given in Acham (1971). Supplemental to this is Mellon's (1967) geographic subdivision of previous work, and a listing of important paleontological and sedimentological studies. The Lower Cretaceous correlations of Rudkin (1964) for western Canada and north central United States remain generally accepted to this date.

The Mannville Group and its equivalents in southwestern Saskatchewan were described by Maycock (1967) and Christopher (1975), and in southeastern Saskatchewan by Price (1963). Stelck (1975) discussed basement control of Cretaceous sand sequences in western Canada.

Correlations between Cretaceous formations of Montana and sequences in the western interior of the United States were presented by Cobban and Reeside (1952) and Gill and Cobban (1966), and a synthesis of the Cretaceous of central western United States was given by McGookey (1972). A recent attempt at reconstructing the Cretaceous palaeogeography of North America was made by Williams and Stelck (1975).

The Jurassic succession in Alberta and Saskatchewan was described by Weir (1954), Milner and Thomas (1954), Thompson and Crookford (1958) and Milner and Blaklee (1958). An overview and collation of previous work occurs in Springer *et al.* (1964). Peterson (1972) described the Jurassic of Montana and its correlatives in the central western United States. The Mississippian stratigraphy of western Canada is presented in Macauley *et al.* (1964), and in Craig (1972) for Montana.

Petroleum occurrences in the Lower Cretaceous of southern Alberta are documented in White (1960), Century (1966), and Larson (1969). Berry (1974) described the geology and development of the Grand Forks oil field, 15 miles (25 kilometres) east of the Turin area which produces from sandstones of the Mannville Group. The petroleum geology of the Alberta portion of the Sweetgrass arch is discussed in Herbaly (1974), and Cox (1966) described Jurassic and Cretaceous stratigraphic traps associated with the structure.

The composition, form, and depositional environments of fluvial sandstone bodies were described by Allen (1965), Potter (1967), Visher (1972) and Schumm (1972).

Computer application to geology during the decade following the pioneering work of the late 1950's was briefly outlined by Krumbein (1969). Krumbein's (1956) study into the separation of regional and local components in facies maps was the forerunner to his use of trend surface analysis of contour maps (Krumbein, 1959). Merriam and Harbaugh (1963) applied trend surface analysis to structural data in several areas of the central United States, and showed the relationship between trend anomalies and the distribution of oil and gas fields. Whitten (1969) described the use of computers in handling directional variables measured in structural geology.

Statistical analysis of data and computer modelling of sedimentary and stratigraphic features were discussed by Harbaugh and Bonham-Carter (1970). Davis (1973) contains useful sections on contouring and trend surface analysis, and Chayes (1970) discussed the significance of higher order trend surfaces.

Robinson et al. (1969) used spatial filtering to analyse stratigraphic horizons in southeastern Alberta, and defined structural trends in the Turin area similar to those mapped by trend surface analysis in the present study. A comparable investigation to that of the author was conducted by Wermund and Jenkins (1970), in which trend surface analysis was used to recognize deltaic sand bodies in the Upper Pennsylvanian of north central Texas.

Chapter II METHOD OF STUDY

A. COMPILATION OF GEOLOGIC DATA

Stratigraphic correlations were established between the base of the Fish Scale Sandstone and top of the Mississippian, using IES, gamma-sonic and density logs from one well in each of the thirty townships in the study area. The tops of the Upper Mannville Group, Lower Mannville Group, Jurassic and Mississippian were then picked in 302 wells. Elevations relative to mean sea level were used in the generation of computer-contoured structure and isopach maps. Trend surface analysis was applied to the top and base of the Mannville Group to separate anomalous structural and depositional features from regional trends. These maps formed the basis for determining the degree of structural control on the distribution of sandstone in the Mannville Group.

For mapping purposes the Upper Mannville Group was proportionately subdivided into nine slices, each approximately fifty feet (fifteen metres) thick, and the Lower Mannville Group into slices of constant thickness (fifty feet), the total number of slices depending on the total isopach of the group. Sandstone thickness in each slice was picked from gamma logs. The gamma radiation response of sandstone ranges from 35 to 160+ API units, depending upon clay content (Wood et al., 1974), with an "average" response of 85 API units. In this study, a 60 API unit cutoff was used to indicate clean fluvial sands within the Mannville sequence.

Computer-contoured sandstone percentage maps were produced for each slice, and stacking of these maps showed the changing depositional pattern during Mannville time. Trend surface analysis of the sand isolith maps was used to separate regional sand distribution from anomalously thick accumulations, and thereby to enhance the outline of individual sandstone bodies. Changes in the influx of sand during deposition were ascertained by calculating the volume of sandstone per unit of thickness in each slice, and these data were used to make inferences regarding erosion of the source area and regional sedimentation.

Petroleum occurrences in the Turin area were plotted according to type and stratigraphic position, and comparison of these plots with the lithologic and structural maps led to the formulation of an hypothesis regarding the entrapment of petroleum in the Mannville Group.

B. COMPUTER TECHNIQUES

1. Gridding and Contouring

Uniformity of distribution and the density of data points determine the reliability of contour maps. The type of distribution of wells in the Turin area was checked according to the procedure of Davis (1973, pp. 301-307) — a chi-square method to test for uniformity and a Poisson distribution to test for randomness. A uniform distribution of points is one in which the density of points in one subarea is equal to the density of points in another of the same size. Such a distribution may be random (where any subarea is as likely to receive a point as any other subarea, with the placement of a point having no influence on the position of any other) or regular (where points occur at the nodes of a grid). A minimum of five data points in each subarea were required for the chi-square method used to be valid.

The Turin area was divided into 30 subareas of equal size, with the expected number of data points (wells) in each subarea being:

$$E = \frac{\text{total number of data points}}{\text{number of subareas}} = \frac{302}{30} = 10$$

A chi-square test of goodness-of-fit of the expected (uniform) distribution to the observed distribution is given by:

$$\chi^2 = \sum \frac{(O-E)^2}{E}$$

where O is the observed number of data points in a subarea. The test has $(m-2)$ degrees of freedom, where m is the number of subareas. The computed chi-square value exceeded the critical value of chi-square at the 5% significance level and so the data were not uniformly distributed.

The non-random distribution of points in the Turin area was verified by the Poisson distribution test. For n points to be randomly distributed within an area consisting of m subareas of equal size, the probability, Pr , that r points will fall into a subarea is:

$$Pr = \frac{e^{-\gamma} \gamma^r}{r!}$$

where γ is the expected number of points per subarea and e is the base of natural logarithms. The expected number of subareas that contain r points is:

$$E(r) = Pr \cdot m$$

The expected number of subareas that contained from zero to the maximum number of points in any subarea was calculated, and the observed number of subareas containing r points was determined. The observed and expected values were compared by a chi-square test, and the computed chi-square value was found to exceed the critical value of chi-square at the 5% significance level.

The high density of wells at producing fields resulted in an overall distribution intermediate between random and clustered. Because clustered data exert greater influence on contouring programs than those that are widely spaced, a gridding routine was used to produce a regular distribution of data points. The University of Alberta Computing Services' gridding program CGRID1 and contouring program CONTUR were used in the generation of structure and isopach maps. CGRID1 computes data values at the nodes of a grid superimposed on Z scattered points, and uses either Laplacian or Spline interpolation or varying degrees of both, depending on the value of C in the equation:

$$[D^2x + D^2y - C(D^4x + D^4y)]Z = 0$$

$$(D = \text{delta})$$

If $C = 0.0$, Laplacian interpolation takes place, and the computed surface has sharp peaks and dips at the data points, with no chance of spurious peaks occurring in areas devoid of data (Fox, 1962). By increasing C , Spline interpolation predominates over Laplacian and the surface passes

more smoothly through the data points; however, the possibility of spurious peaks and steep extrapolation in areas lacking data increase. A value of $C^2 = 5.0$ was used in the present study.

In performing the interpolation, the program initially moved data points to the nearest grid points, and then shifted them back to their proper positions as the shape of the surface became evident. Values were computed at the nodes of a 40×34 grid, thereby producing a grid cell to data point ratio of 5:1, with each grid cell approximately equivalent in size to one township section. Reducing the grid cell size produced a smoother, more aesthetically pleasing contour map; however, such a reduction increased the number of gridded values to be calculated and hence the cost of the operation. Isopach map grids were created by subtracting the gridded elevations of the intervals' upper and lower structural surfaces.

The contouring method used in CONTUR is a modified version of the one described by Dayhoff (1963). The program interpolates between the gridded data points since a required contour line will usually not pass through the corners of the grid cells. All grid cells are searched for each contour value required and the points of intersection with the grid are written on a scratch file prior to contouring.

2. Trend Surface Analysis

The structural configuration of a stratigraphic horizon may be thought of in terms of a regional component, such as the depositional or structural dip within a sedimentary basin, and a local component caused by subsequent phases of deformation or localized sedimentologic variations (Krumbein, 1956). Similarly, regionally distributed

lithologic facies may show local thickness or compositional variations which are distinguishable from, or superimposed upon, the regional trend. Trend surface analysis was used to separate local and regional elements in structural and lithologic data in the Turin area. This method, described by Krumbein (1959), Merriam and Harbaugh (1963) and Whitten (1969), involves the simulation of the regional trend by fitting a polynomial surface to the data. A first order polynomial fit is a plane, and the complexity of the surface increases with increasing order. The observed value at each data point is expressed in terms of its predicted value (on the surface) and an error component. Points lying above the predicted surface are considered positive residuals and those below negative. A best fit of the surface to the data is achieved using the least squares method, that is, the sum of the squares of the residuals is a minimum.

Trend surfaces are expressed algebraically as:

$$z = c_0 + \sum_{i=1}^n (c_i x^i + c_{i+n} y^i) + \sum_{i=1}^n (c_{2n+i} x^{n-i} y^i) + c_{3n} xy$$

where x and y are the map coordinates, z is the mapping parameter (e.g., structural elevation), n is the order of the surface fitted, and $i = 0, 1, 2, \dots, n$ (modified after Wernund and Jenkins (1970, p. 260)).


Once the coefficients c , that satisfy the least squares criterion for the specified order of polynomial, are determined, the predicted values of z can be calculated. The error term or residual equals the difference between the predicted and observed values. For the purpose

of contouring the trend surface and the residuals, a gridding routine was applied to ensure regular data distribution. As the grid cell size approximated that of one township section, residuals smaller than this could not be resolved.

First to eighth order surfaces were calculated for each set of data, and plots were generated for surfaces showing high statistical fit (indicated by the percent sum of squares accounted for) and good separation of regional and local components. A shortcoming of trend surface analysis was the subjectivity involved in deciding which order of polynomial gave the best resolution of meaningful anomalies. For progressively higher order polynomials, goodness of fit increased, resulting in progressively smaller deviations of the observed surface from the fitted surface. For the structural data, the observed surfaces so closely corresponded to the fifth to eighth order predicted surfaces, that few residuals existed, and the purpose of the exercise was defeated. The significance of progressively higher order surfaces was discussed by Chayes (1970), with reference to petrographic data.

Merriam and Harbaugh (1963) fitted trend surfaces of varying order to structural data from sedimentary basins of the central United States. Residuals were shown to correspond to areas of known petroleum occurrence; however, the trend surface chosen was done so by direct comparison of the various residual maps with the petroleum distribution plots, and not according to whether it showed the best statistical fit to the data. Without subjectively determining which order of surface produces the most meaningful anomalies for a given area, the residuals alone are of limited interpretative value.

For the uniformly dipping structural surfaces of the Turin area, second order polynomials were used (with 94% sum of squares accounted for) to enhance local topographic variations and hence determine the position of channels within the surfaces. Sand percentage data did not exhibit a regional distribution to which a valid mathematical surface could be applied (15% sum of squares accounted for with eighth order surfaces). Positive residuals (which corresponded to thick sand accumulations) resembled the raw data plot of sand distribution; however, the use of fourth order surfaces (with 13% sum of squares accounted for) led to a more accurate interpretation of the position of the distributaries in which most of the sand was deposited.

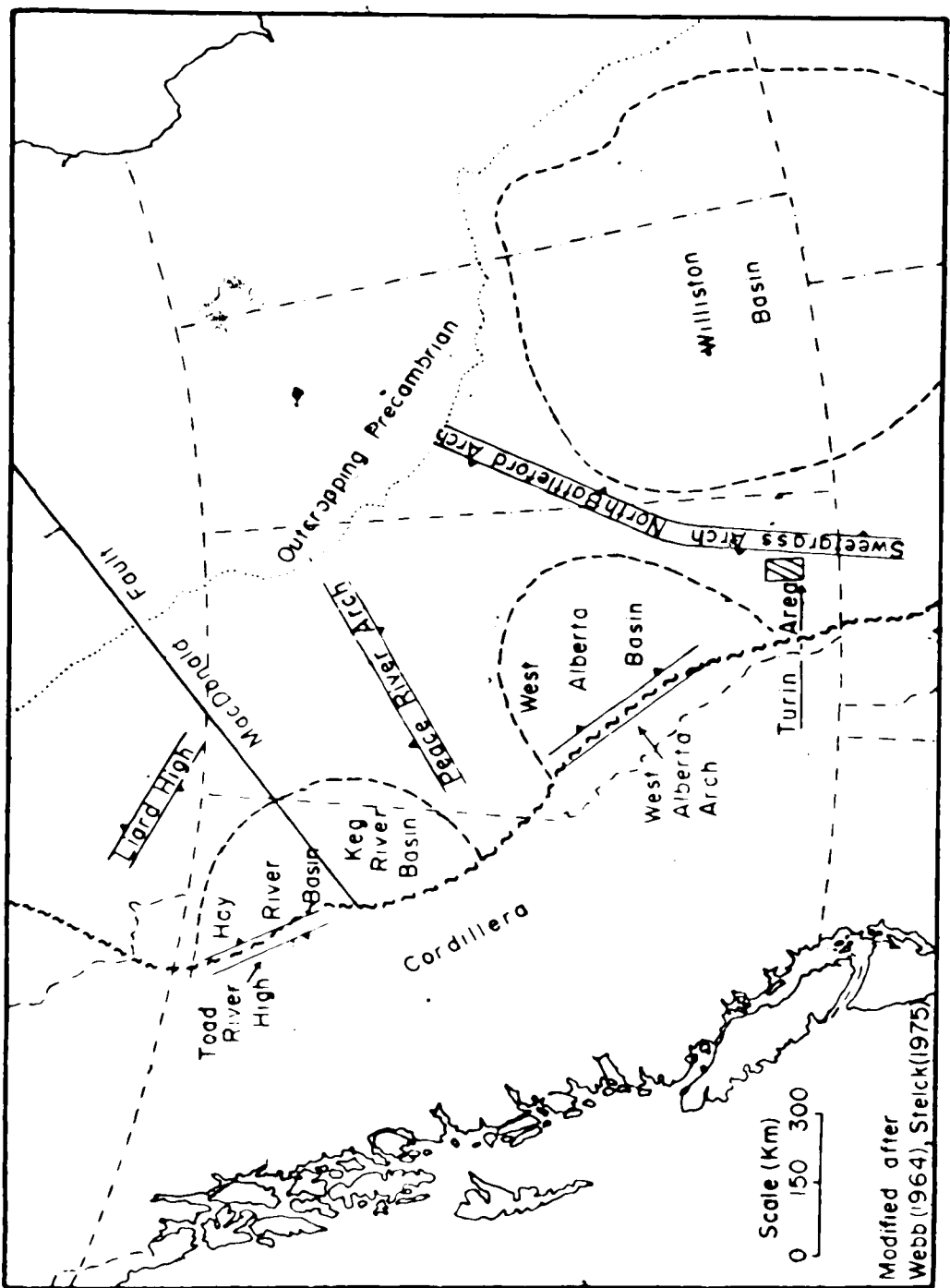


Chapter III
REGIONAL GEOLOGY

The Turin area lies in the southwestern part of the western Canada sedimentary basin, a northwesterly-trending Phanerozoic feature, flanked to the northeast by the Precambrian Canadian Shield (Fig. 3). The western margin is structural, and corresponds to the eastern edge of the Cordillera. The Palaeozoic and Mesozoic depositional basin extended farther west, but was subject to severe deformation during Mesozoic and Tertiary orogenies. Sediments thicken towards the Cordillera and attain a maximum thickness of approximately 16,000 feet (4,900 metres).

The Precambrian basement extends beneath the sedimentary cover and has had a profound effect upon the distribution and type of overlying sediments. Burwash *et al.* (1964, p. 14) stated that "... since the beginning of Palaeozoic time, movements in the basement have been epeirogenic, with localized vertical displacements subordinate to broad regional arching and subsidence". The arches are thought by Burwash and Krupicka (1969, 1970), Burwash *et al.*, (1973) to be the loci of potassium metasomatism of basement gneisses. The associated decrease in specific gravity has caused regional, periodic, isostatic readjustments to occur, forming a number of depositional sub-basins between the arches.

The Peace River arch forms the northern limit, and the West Alberta arch the western limit of the West Alberta basin (Stelck, 1975). In the southern part of the basin, the Sweetgrass arch extends northwards from Montana, across southeastern Alberta and meets the southward-plunging North Battleford arch extending from the Shield. This composite feature



REGIONAL GEOLOGY MAP — WESTERN CANADA SEDIMENTARY BASIN

FIGURE 3

separates the West Alberta basin from the Williston basin of Saskatchewan and Montana.

A summary of the depositional history of the western Canada sedimentary basin was given by Webb (1964). Early Palaeozoic deposition was confined to the Cordilleran miogeosyncline along the subsiding western margin of the craton. Periodic transgressions of the craton, followed by epeirogenic uplift and erosion, occurred during middle Cambrian to late Jurassic time. Cratonic sediments were predominantly shallow marine, and their eroded subcrop edges in Alberta subparallel the margin of the Shield.

Carbonate, evaporite and clastic sequences were deposited over the Williston basin, western plains and Rocky Mountain region during the Devonian and Mississippian. Regional uplift occurred in the Pennsylvanian, and Middle Palaeozoic formations were erosionally truncated in a northeasterly direction (Webb, 1964). The interior cratonic region remained uplifted during the Permian and Triassic while miogeosynclinal sedimentation occurred along the craton's western margin.

Thin Jurassic marine shelf deposits occur over the western plains and thicken westwards, grading to deep water shales in the eastern Cordilleran region (Springer *et al.*, 1964). Marine transgressions extended into the West Alberta basin from the west and south, resulting in the accumulation of shales and localized beach sands. Red beds were initially deposited in the Williston basin, followed by a shallow marine sequence in the middle Jurassic. Epeirogenic uplift and withdrawal of the sea in the late Jurassic is marked by a basinwide depositional hiatus.

Cretaceous beds overlie eroded Jurassic, Mississippian and Devonian strata with slight angular unconformity, overlapping progressively older beds in a northeasterly direction across the western plains (Rudkin, 1964). Incursions of the northern Boreal Sea and the southern Gulfian Sea onto the central North American continent occurred during the Lower Cretaceous (Williams and Stelck, 1975), and coalesced in the late Early Cretaceous to form a continuous seaway. The source of clastics was mainly from the central Cordilleran region, where granitic intrusion and vulcanism occurred throughout the Cretaceous. Upper Cretaceous rocks of the plains and Rocky Mountain foothills are mainly marine shales at the base, and become sandy and continental upwards (Williams and Burk, 1964).

Tertiary sedimentation in the western Canada sedimentary basin was continental. Uplift and deformation of the Rocky Mountains culminated in the Eocene (Taylor et al., 1964), following which the mountains and the region to the east underwent intense erosion, and coarse fluvial sands and gravels were deposited over the western plains. The western basin remained uplifted during the Quaternary and was the site of Pleistocene glaciation.

Chapter IV
GEOLOGY OF THE MANNVILLE GROUP

The Mannville Group represents the initial Cretaceous sedimentation on an uplifted erosional surface of Devonian, Carboniferous and Jurassic strata in the central and southern plains of the western Canada sedimentary basin. Deposition commenced in the Aptian and continued until early Late Albian, at which time the northern Boreal ocean and the Gulfian sea in the south transgressed, resulting in widespread deposition of Colorado Group marine sediments (Williams and Stelck, 1975).

Nauss (1945) named the Mannville Formation in the Vermilion area of east-central Alberta, and correlated it with the McMurray, Clearwater and Grand Rapids Formations of the lower Athabasca River. The unit was raised to group status by Badgley (1952), and subdivided by Glaister (1959) into two parts, with the boundary placed at the top of the Ostracode Zone of Loranger (1951). The Lower Mannville Group of central Alberta was defined by Williams (1963) as being equivalent to the McMurray Formation, comprising a basal Deville Member or "Detrital Zone" which was mainly restricted to topographic lows on the sub-Mannville surface; the Eilerslie Member or "Basal Quartz", a thick quartz sandstone and siltstone unit; and an upper "Calcareous" Member or "Ostracode Zone". Williams (1963) also divided the Upper Mannville Group into a basal Clearwater Formation (containing the Glauconitic Sandstone or Wabiskaw Member), and an upper Grand Rapids Formation. These formations overlie the McMurray Formation in the lower Athabasca River area. The Clearwater Formation was deposited during a southerly transgression of

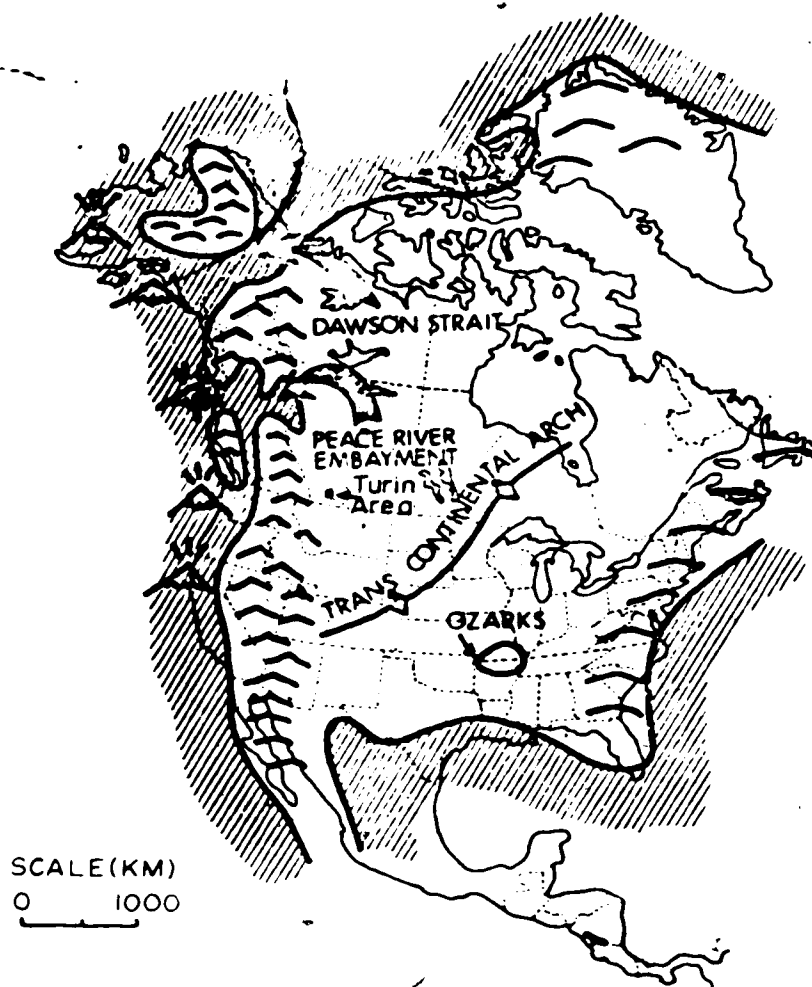
the Boreal sea. It grades laterally and vertically into the continental Grand Rapids Formation. The contact between the two is diachronous. Mellon (1967) did not consider the lithologies of the two formations sufficiently diverse in central Alberta, and renamed the correlative sequence the Fort Augustus Formation. At the end of Mannville time, the Clearwater sea retreated northwards and established a strand line on the northern side of the Peace River arch.

North American palaeogeography prior to Mannville deposition, and during early Upper Mannville time is shown in Figures 4 and 5 (after Williams and Stelck, 1975).

Lower Cretaceous strata thicken westward, and are called the Blairmore Group in the Alberta foothills (Fig. 6). Sedimentation in this area predated that in the plains, with deposition of the Cadomin Formation, a conglomerate averaging ten feet in thickness. The Blairmore Group in the southern foothills was divided by Mellon and Wall (1963) and Mellon (1967) into three units, the lower two of which were equivalent to the Mannville Group and an upper unit equivalent to the Bow Island Formation of the Colorado Group.

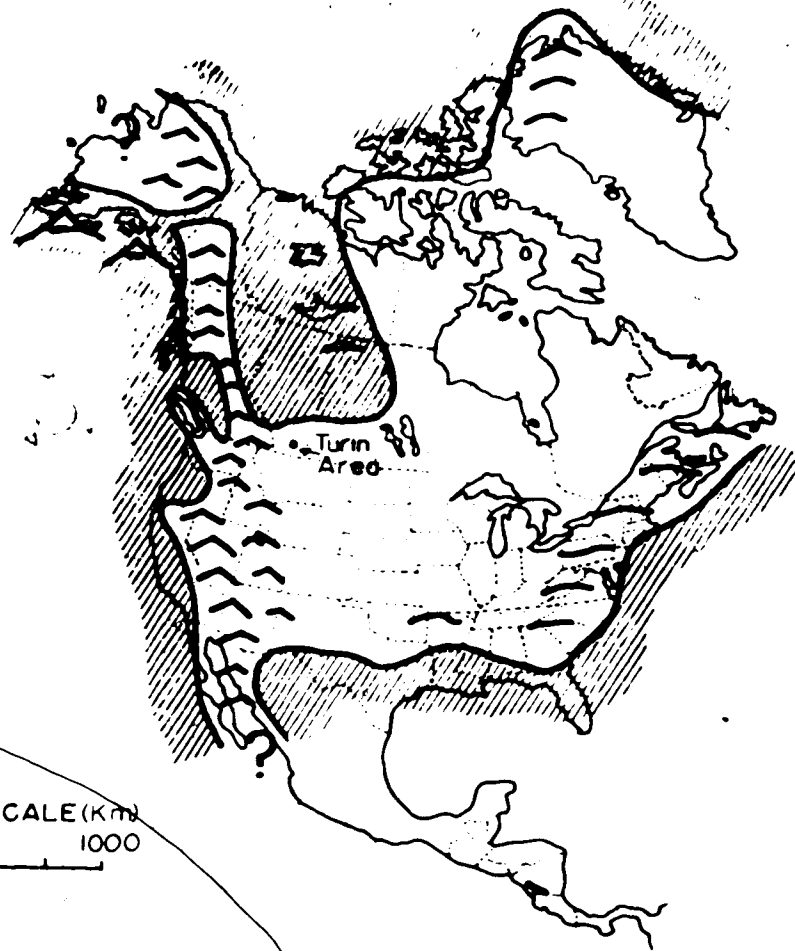
The Gladstone Formation (Mellon, 1967) constitutes the lower Blairmore Group, and consists of a basal conglomerate, equivalent to the Cadomin Formation in the north, a middle sequence of siltstone, shale and fine sandstone, and an upper "Calcareous" member of silty freshwater limestone and calcareous shale. The formation is correlated with the Lower Mannville Group.

Mellon (1967) proposed the name Beaver Mines Formation for the middle Blairmore Group, and correlated it with the Upper Mannville of



NEOCOMIAN (PRE-MANNVILLE) PALAEOGEOGRAPHY
After Williams and Stelck (1975)

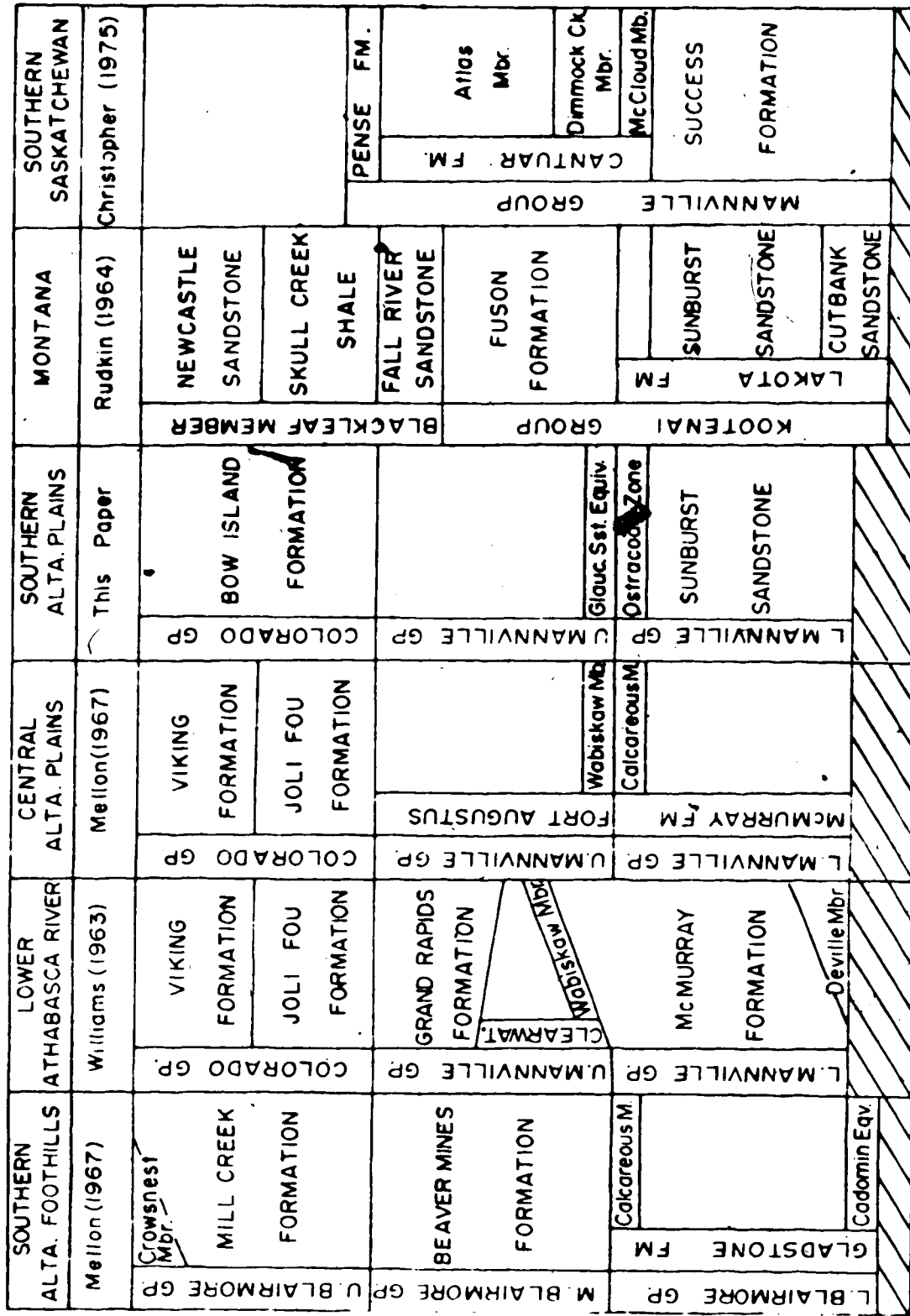
FIGURE 4



SCALE (km)
0 1000

EARLY UPPER MANNVILLE PALAEOGEOGRAPHY
After Williams and Stelck (1975)

FIGURE 5



LOWER CRETACEOUS CORRELATION CHART - WESTERN CANADA AND MONTANA
 FIGURE 6

the plains. It consists of a lower shaly unit and an upper sandy section, and is conformable with the underlying Gladstone Formation. The succession is continental, and represents sedimentation on a western landmass during the transgression and regression of the Clearwater sea.

A widespread depositional hiatus occurred within the western Canada sedimentary basin following the regression of the Clearwater sea. Subsequent inundation of the basin by the southern and northern seas resulted in the deposition of the marine Colorado Group sediments. The Rocky Mountain foothills area initially remained the site of continental sedimentation, but was gradually overlapped by the Colorado sea. The Mill Creek Formation constitutes the continental Upper Blairmore sequence of the foothills. It consists mainly of argillites and thin interbeds of quartzose sandstone, in contrast to the feldspathic sandstones of the Beaver Mines Formation. Tuff beds and bentonite partings occur in the upper 300 feet of the Mill Creek Formation. In the southernmost area, the formation is overlain by, and possibly correlative in part with, the Crowsnest Volcanics. The Upper Blairmore Group of the foothills interfingers eastwards with the Bow Island Formation of the plains. During latest Lower Cretaceous time, the foothills area was finally transgressed by the Colorado sea and the Blairmore Group was overlain by shales of the Blackstone Formation, in part equivalent to the Upper Colorado Group.

The composition and depositional history of the Mannville Group in southern Saskatchewan has been recently revised by Christopher (1975). This area lay to the east of the Sweetgrass-North Battleford Arch, the drainage system of which initially flowed southward through the Williston

basin. Christopher (1975) showed a threefold subdivision of the group. The lowest unit is the Success Formation, a quartz sandstone succession of possible Neocomian age, equivalent to the Deville and part of the Ellerslie Members of the Lower Mannville Group of central Alberta. The Success Formation is divisible into two depositional units, resulting from two phases of uplift and erosion of the Shield source area. The basal coarse textured unit with interbedded mudstones and siltstones occurs in the deeper channels and is overlain by channel sandstones which were the products of meandering streams which periodically underwent braiding.

Uplift of the Swift Current region to the south resulted in the termination of Success sedimentation and a change in the direction of streams towards the west-northwest, to join the Mannville drainage pattern of Alberta. The Cantuar Formation (equivalent to the Upper Mannville Group) was deposited at this time, with early Cantuar streams channelling through the Success Formation into the underlying Devonian and Mississippian strata in some areas. The McCloud Member represents these initial deposits. The overlying Dimmock Creek Member was deposited under swampy, estuarine and marine conditions during the southern transgression of the Boreal sea (Clearwater time). Christopher (1975) stated that the sea extended into the Dakotas, apparently conflicting with Williams and Stelck (1975) who showed the southeastern extent of the Clearwater sea limited by the North Battleford arch. Christopher's Dimmock Creek Member may represent a subsequent transgression across Saskatchewan as the North Battleford arch ceased to act as a barrier.

During the final phase of Upper Mannville deposition (Atlas Member of the Cantuar Formation), southern Saskatchewan was a low-relief plain,

and the site of predominantly argillaceous deposition with periodic influxes of sand from the rising Rocky Mountain region. The Pense Formation was deposited during the inundation of the Colorado sea, which brought Mannville continental sedimentation to an end. Christopher (1975) has chosen to include this lower Colorado Group equivalent within the Mannville Group.

In Montana, the Kootenai Group is equivalent to the Mannville Group, with the Lakota Formation correlative with the Lower Mannville and the Fuson Formation and Fall River Sandstone with the Upper Mannville Group (Rudkin, 1964). The Lower Kootenai Group is divisible into a lower Cutbank Sandstone, an overlying Sunburst Sandstone, and an upper shale, equivalent to the Ostracode Zone. The Cutbank Sandstone is about 50 feet thick and thins northwards into Alberta. It consists of coarse sandstones and conglomerates and is depositonally continuous with the Sunburst Sandstone. It is either absent, or indistinguishable from the Sunburst Sandstone over most of southern Alberta. Its upper part is equivalent to the Deville and Ellerslie Members of central Alberta, while the lower conglomerate is correlated with the Cadomin Formation of the foothills. The Sunburst Sandstone consists of medium-grained sandstones, becoming finer at the top, and grading upwards into shales equivalent to the Ostracode Zone. These in turn are overlain by fluvial sandstones and shales of the Fuson Formation and Fall River Sandstone. Fall River continental sedimentation was followed by the deposition of the Skull Creek Shale (basal Colorado equivalent).

The southern Alberta plains lie at the centre of the five above-mentioned areas. Lithologically, the sequence resembles more closely that of the Mannville Group of the central Alberta plains.

In the Turin area, the Lower Mannville is continental, and consists of a lower sandy member (Sunburst Sandstone) and an overlying, thin (ten to thirty feet), shaly Ostracode Zone. A basal detrital unit equivalent to the Deville Member, or thin remnants of the Cutbank Sandstone, are not readily discernible.

Williams and Stelck (1975) show the southern limit of the Clearwater sea at the latitude of Calgary (Fig. 5). This is substantiated by the uniformity of the Upper Mannville section in the Turin area, and the absence of Grand Rapids and Clearwater components on well logs.

The author was reluctant to extend the term Fort Augustus Formation from central Alberta into the southern plains (no comparative study was attempted), and has used the term Upper Mannville Group for the beds above the Ostracode Zone. A high resistivity sandstone at the base of the Upper Mannville appears to be correlative with the Glauconitic Sandstone in the north, and is referred to as Glauconitic Sandstone Equivalent.

The marine Colorado Group overlies the Mannville in the southern plains. A thin sandstone at the base is generally included in the Basal Colorado Sandstone; however, the distinction drawn between it and sandstones at the top of the Mannville Group is highly subjective.

Chapter V

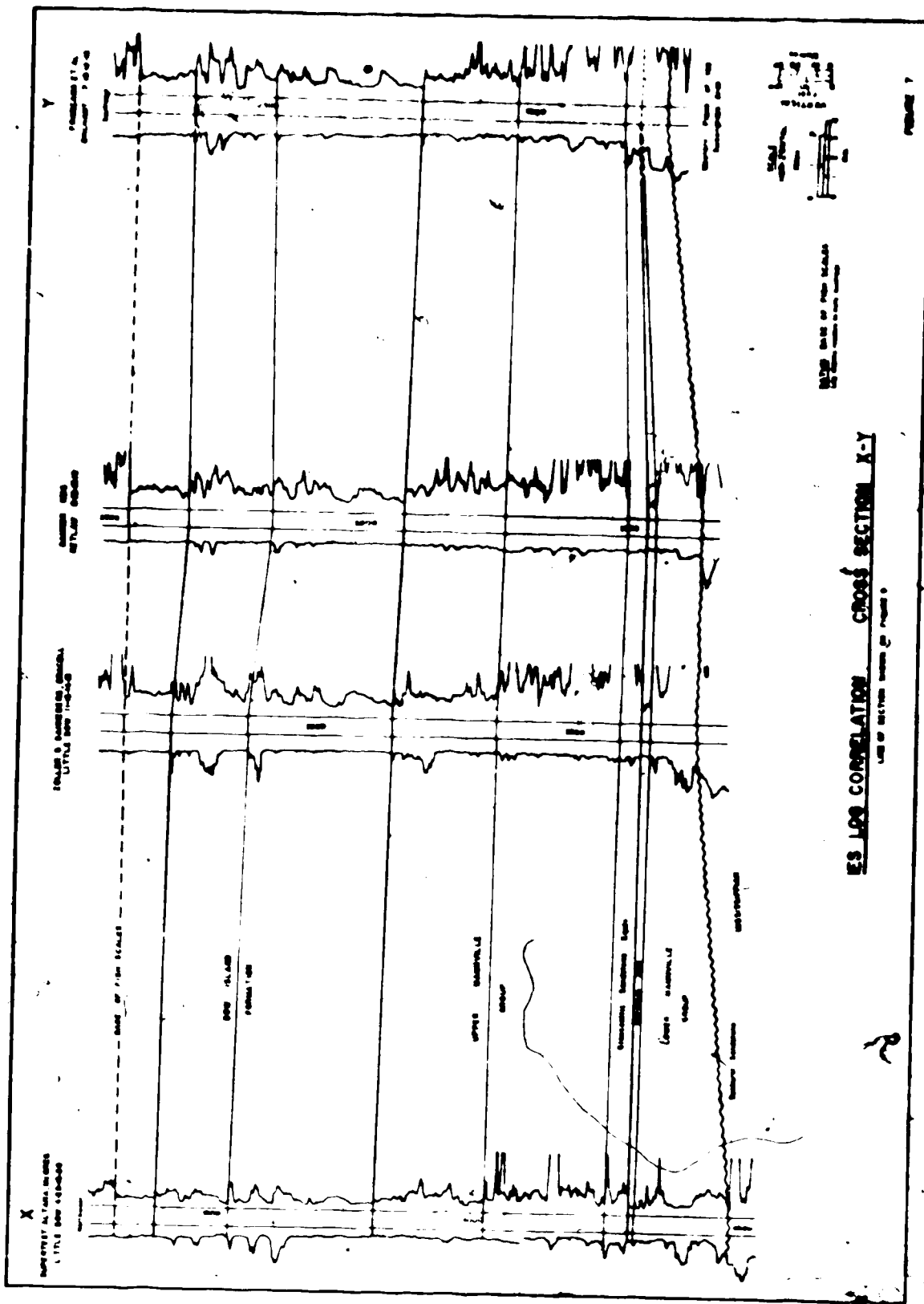
GEOLOGY OF THE TURIN AREA

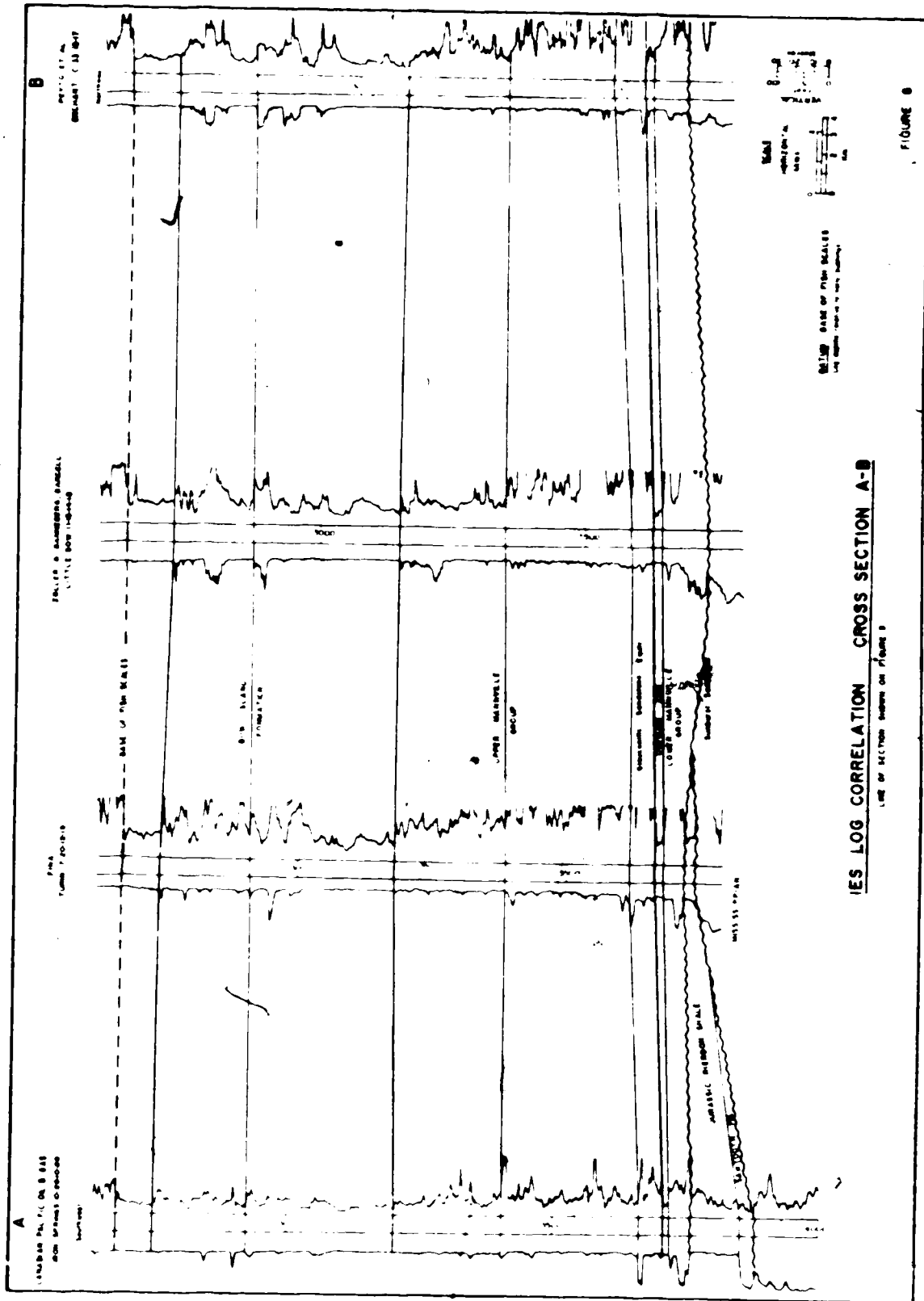
The Turin area lies on the margin of the West Alberta basin and the Sweetgrass arch. As shown by Herbaly (1974), the arch in southern Alberta may be divided into four northerly-plunging axes, the westernmost of which, the Taber-Enchant Axis, passes through the Turin area.

Strata dip gently from the arch towards the northwest, having attained the present structural configuration as a result of tilting associated with the Cordilleran Laramide orogeny. Electric log correlations (Figs. 7 and 8) of the interval from the top of the Mississippian to base of the Upper Cretaceous (base of Fish Scales) illustrate the pre-Tertiary southwesterly dip of the Mississippian and Jurassic strata and a northwesterly component of dip away from the Sweetgrass arch. The Lower Cretaceous succession is of fairly uniform thickness which is influenced mainly by pre-Cretaceous surface topography.

A. PRE-MANNVILLE GEOLOGY

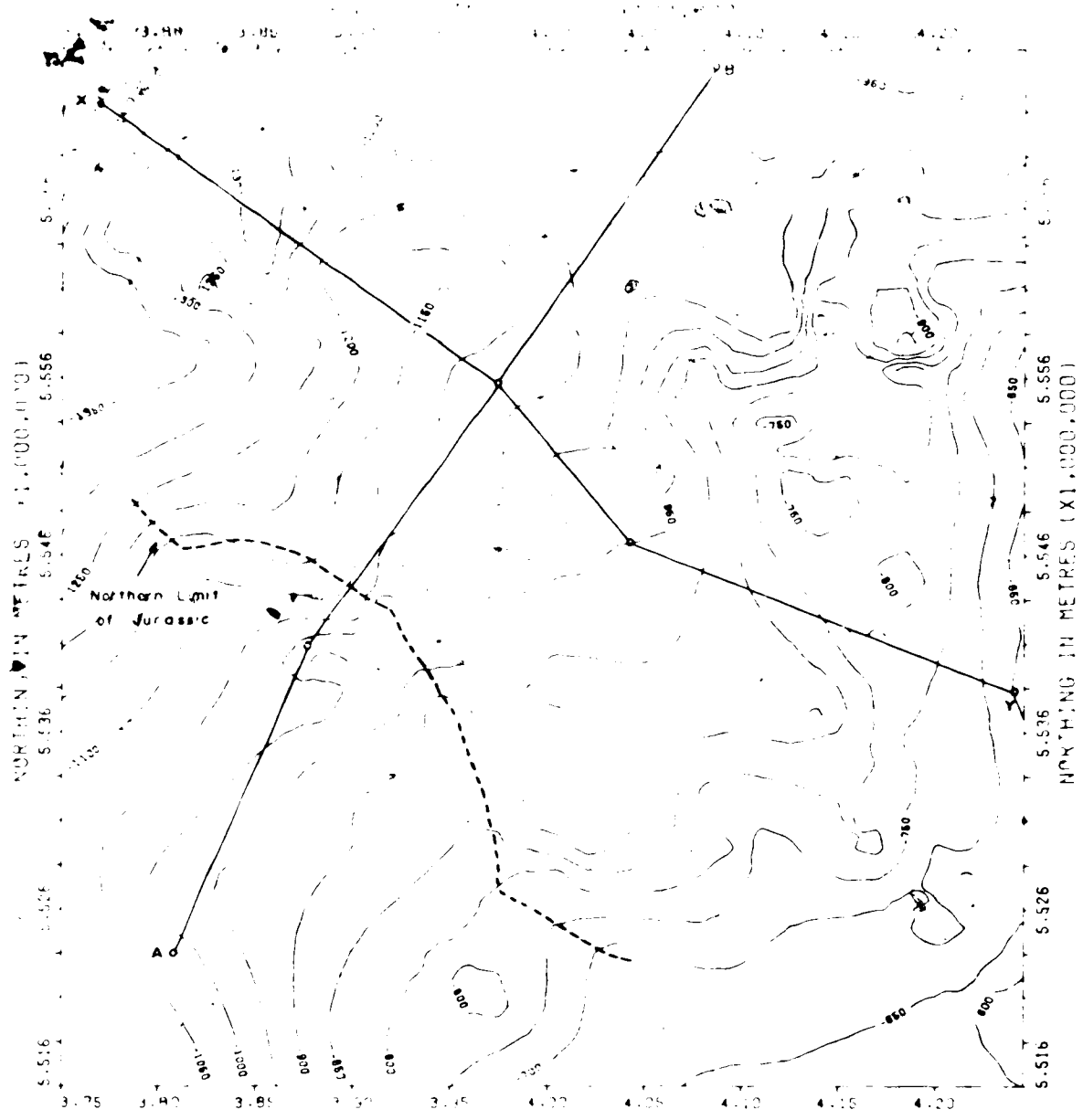
The top of the Mississippian (Fig. 9) is homoclinal, dipping at approximately $0^{\circ}15'$ to the northwest. Mississippian sediments were deposited on a shallow cratonic shelf, thickening towards the southwest (Macauley et al., 1964). Uplift, and the northeasterly truncation of the sequence during Pennsylvanian to Triassic time is evidenced in the Turin area by the subcrop of progressively older formations towards the northeast - from the Turner Valley and Shunda Formations in the southwest to the Pekisko Formation in the northeast.





IES LOG CORRELATION CROSS SECTION A-B

FIGURE 8



STRUCTURE LINE: TOP OF MISSISSIPPIAN

AREA: 110-15-R:16-20-W4

CONTOUR INTERVAL: 50 FT

UNIT: MSL

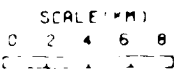
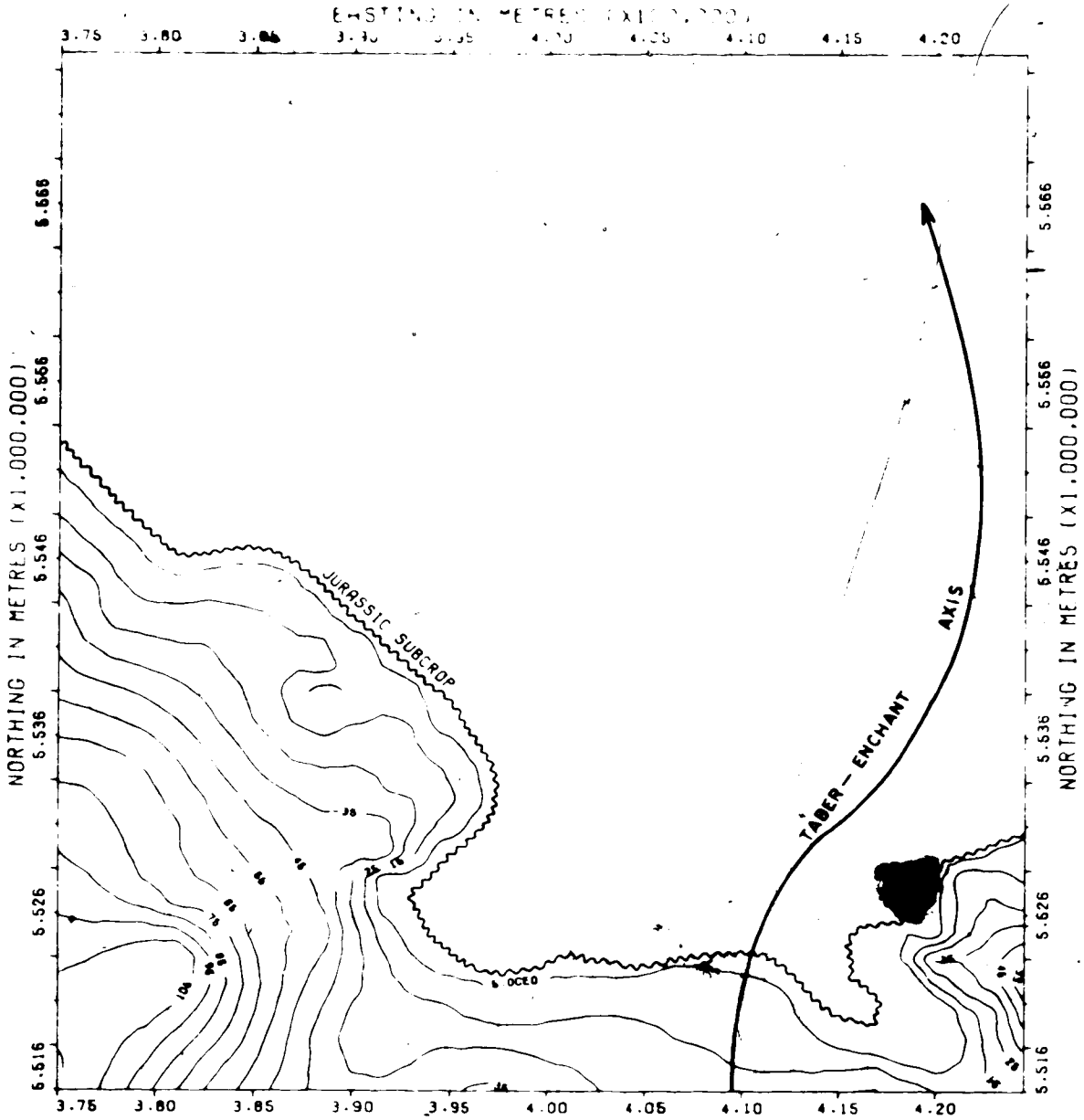


FIGURE 3

The Mississippian surface was overlapped by a southern sea in Middle Jurassic time. The Sweetgrass arch was undergoing uplift at this time (Springer *et al.*, 1964), and was the source of beach sands (Sawtooth Formation) deposited along its western margin, including the Turin area. The sea retreated to the south in late Middle Jurassic time. The Arch subsided in the early Late Jurassic and was covered by marine Rierdon shales. Subsequent uplift and erosion of the central and northern plains area resulted in the deposition of marine shales and sandstones of the Swift Formation across southern Alberta and Montana. The sea again retreated from the Turin area in latest Jurassic time and erosion of Jurassic and Mississippian strata continued until the onset of Mannville deposition.

The Jurassic subcrop edge (Fig. 10) is therefore erosional, although the Jurassic palaeogeographic maps of Springer *et al.* (1964) show the depositional limits to be approximately coincident with the erosional edge mapped in the Turin area. Rierdon shales constitute most of the Jurassic section in the map area, with only scattered remnants of Sawtooth and Swift Formations.

The Taber-Enchant Axis (Herbaly, 1974) probably extended northwards through the Jurassic subcrop embayment in Rierdon time (see Jurassic isopach map - Fig. 10). Sediments thicken rapidly to the southwest and southeast, while a more gradual increase occurs along the axis to the south. Jurassic sediments are restricted to the southern side of a broad, northwest-trending Mississippian ridge, indicated on Fig. 9. This southwesterly-dipping cuesta dominated the physiography of the southwest part of the Turin area in pre- and only Mannville times.



ISOPACH MAP : JURASSIC

AREA : T10-15.R16-20 W4

ISOPACH INTERVAL : 10FT.

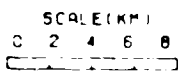


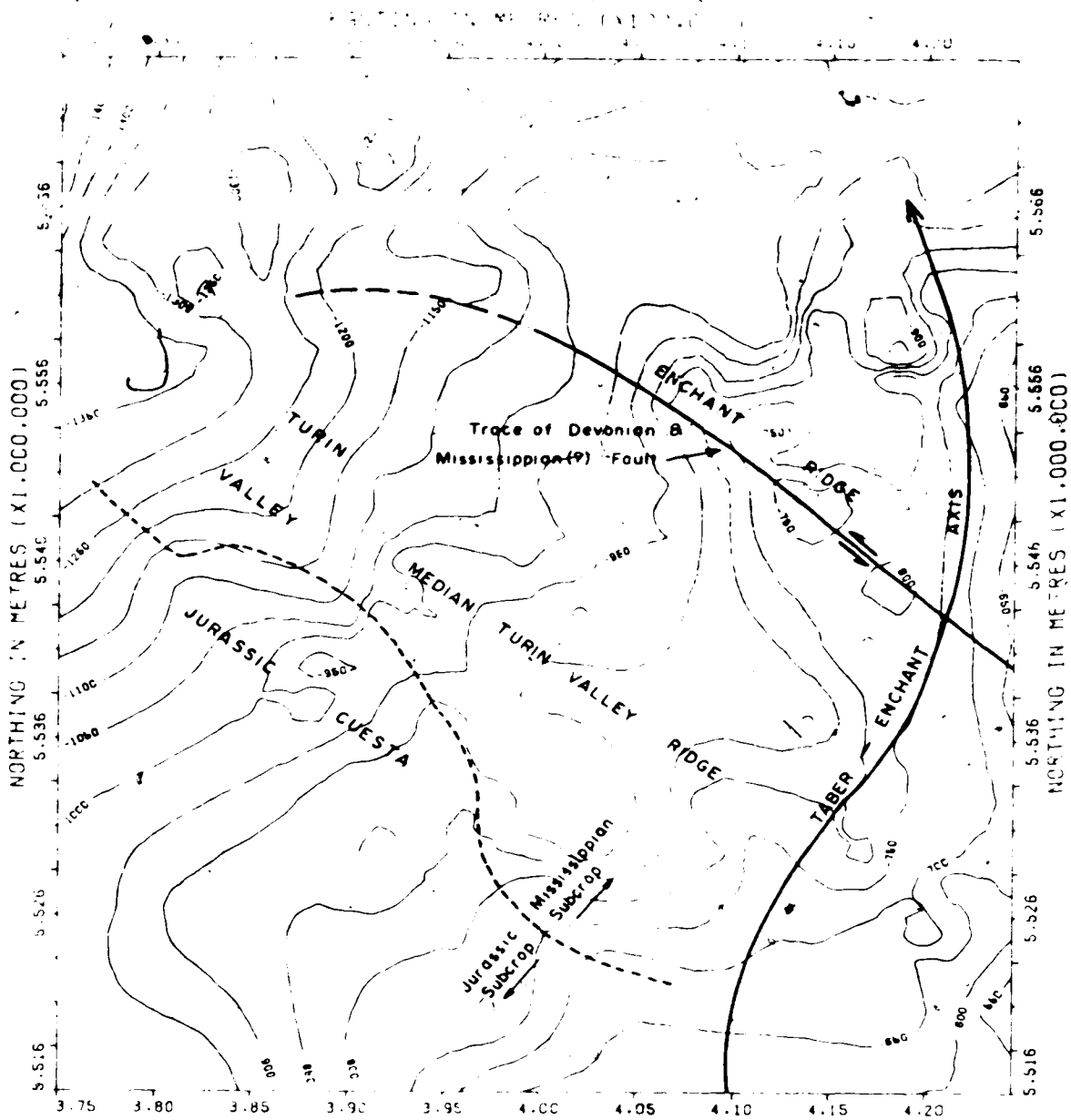
FIGURE 10

The structure map on the base of the Mannville Group (Fig. 11) represents the composite Jurassic and Mississippian surface onto which Mannville sediments were deposited. Surface relief, deduced from the Lower Mannville isopach map (Fig. 14), is of the order of 175 feet (53 metres). The inferred drainage pattern is northwesterly following the depositional strike of the bedding.

Herbaly (1974) shows a northwesterly-striking, sinistral transcurrent fault on the Devonian structure map of the Sweetgrass arch. This dislocation is present at the top of the Mississippian in the eastern Turin area, but whether structure at this level was due to post-Mississippian movement or control of Mississippian sedimentation by the underlying faulted Devonian surface was not determined.

The drainage pattern of the pre-Mannville surface was influenced significantly by the fault described above. The offset Taber-Enchant Axis forms a prominent ridge (here named the Enchant Ridge) on the northern side of the fault while a large, northwesterly-trending valley (the Turin Valley) developed to the south. The southwestern margin of the valley was formed by a cuesta of Mississippian limestone overlain by Jurassic strata. The valley is 11 miles (18 kilometres) wide in the central Turin area, and narrows towards the arch in the southeast. A low ridge (the median Turin Valley Ridge) divides the valley into two parallel channels which coalesce in the western part of the map area.

In the northeastern corner of the map area, north of the Enchant Ridge, two northerly-directed channels developed, separated by a small ridge. In the south, a shallow, westerly-trending valley formed at the base of the dip slope of the Jurassic cuesta.



STRUCTURE MAP : BASE OF MANNVILLE GROUP

AREA : T10 15.R.0 20 W4
 CONTOUR INTERVAL : 50 FT.
 DATUM : MSL

SCALE : 1" = 1/4 MI.
 0 2 4 5 9

FIGURE 11

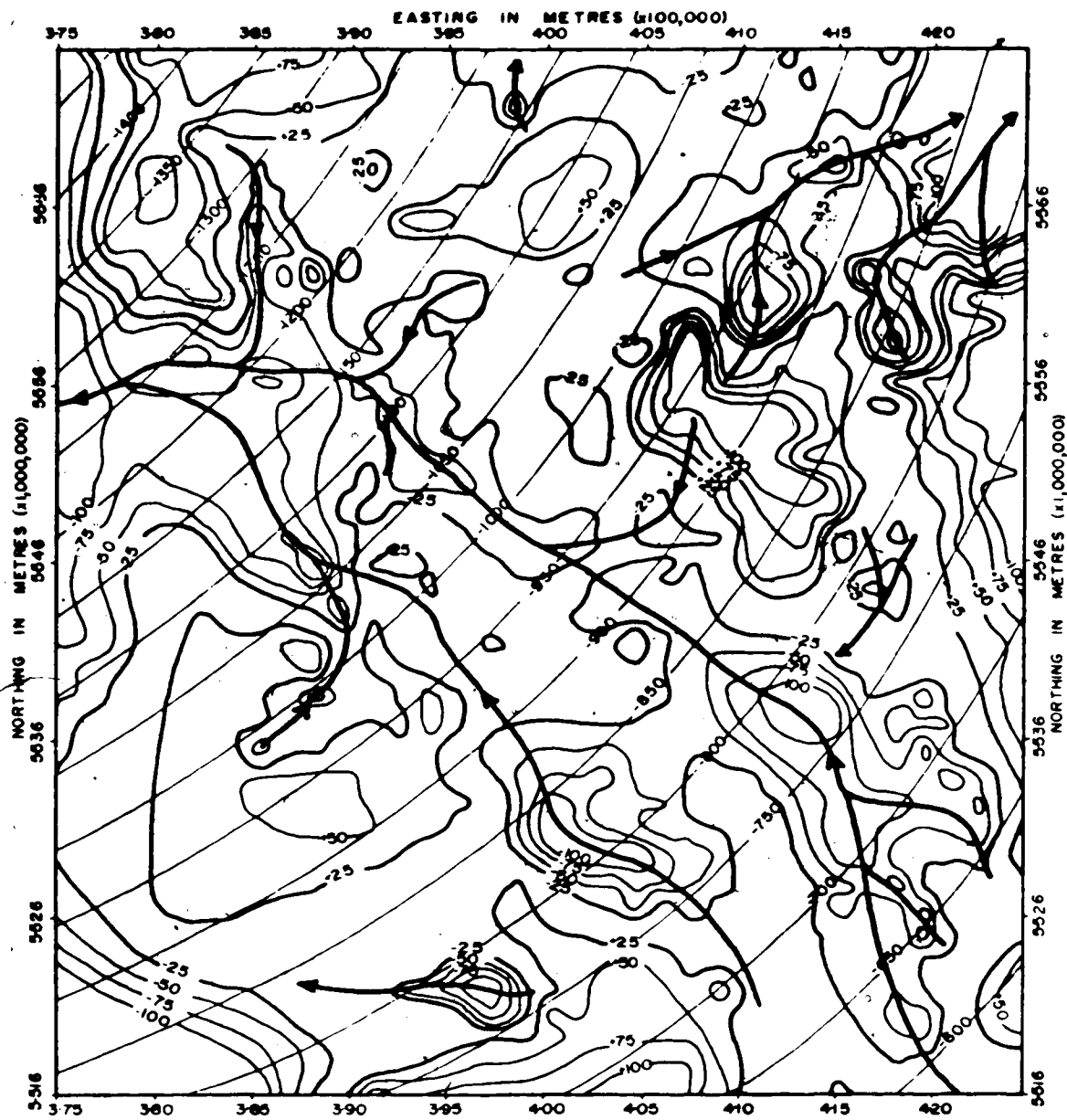
The above-mentioned topographic features were enhanced by fitting a second-order trend surface to the structure on the base of the Mannville Group (Fig. 12). The trend surface is a uniform northwesterly-dipping homocline showing a slight "spoon effect". This surface accounted for 94 percent of the variance in the original surface.

The Jurassic cuesta, Enchant Ridge and the Taber-Enchant Axis are represented as positive residuals. Relief on the Enchant Ridge becomes more subdued to the northwest, beyond the limit of the transcurrent Devonian fault.

B. LOWER MANNVILLE GEOLOGY

The dip on top of the Lower Mannville Group (Fig. 13) is similar to that on the pre-Mannville surface, but irregularities are less pronounced. The isopach map of the Lower Mannville strata (Fig. 14) reflects the topographic features discussed previously. Thickest Lower Mannville sections occur in pre-Mannville channels and lows, and isopach thins overlie topographic highs. Sediments thin towards the Sweetgrass Arch.

It is assumed that relief on the pre-Mannville surface, as presently mapped, was accentuated by the downcutting of pre-Mannville water courses by Lower Mannville streams. Unlike the pre-Mannville streams, the rate of deposition of Lower Mannville streams exceeded the rate of erosion, due to the abundant sediment supply from the uplifted Corilleran area, and preservation of deposits through regional subsidence. Channels were progressively filled with detritus.

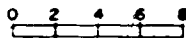


TREND SURFACE MAP : BASE OF MANNVILLE GROUP

AREA : T10-15, R16-20 W4

SCALE (KM)

TREND SURFACE ORDER 2ND



TREND SURFACE CONTOUR INTERVAL 50 FT

RESIDUALS CONTOUR INTERVAL 25 FT

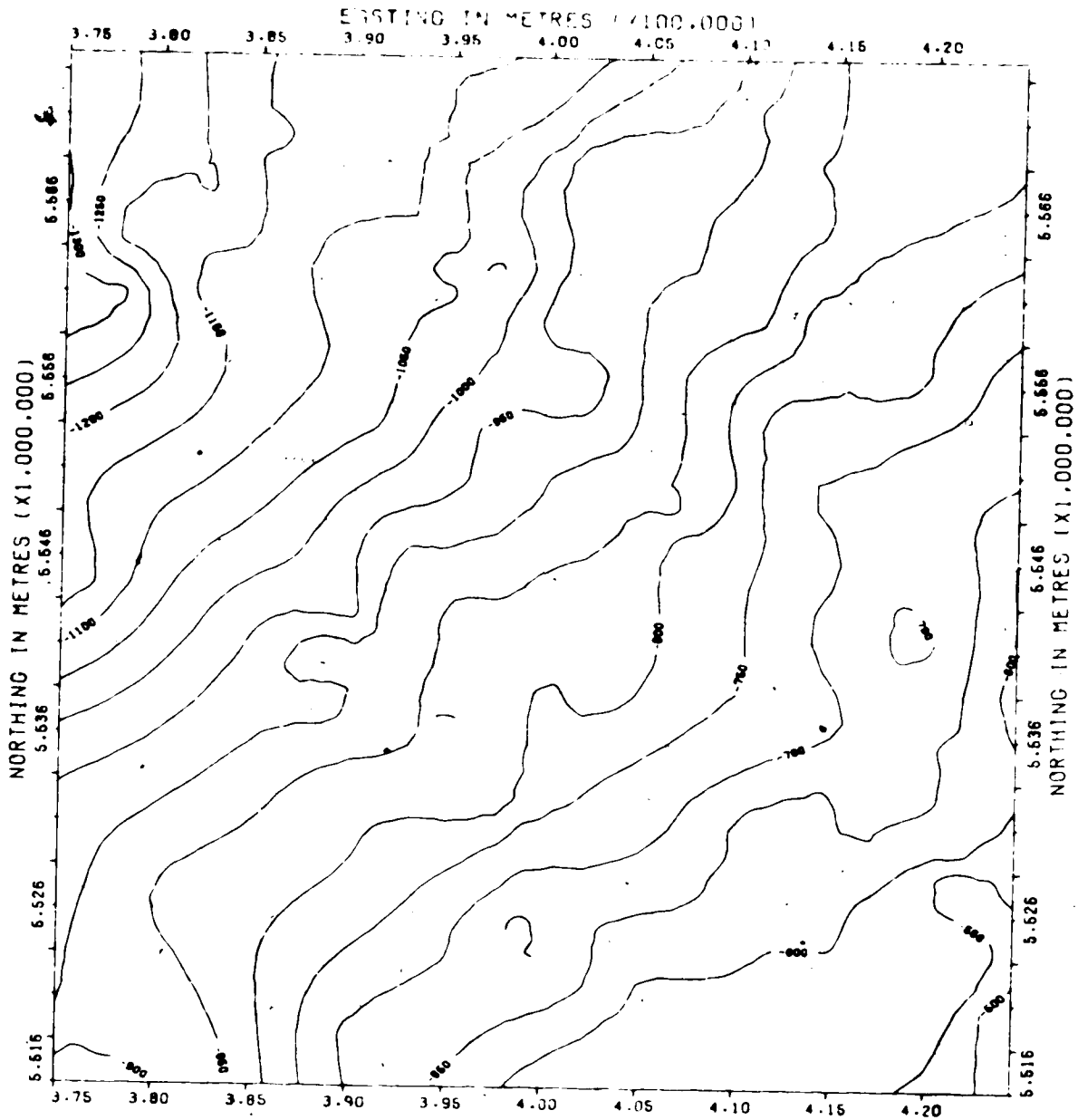
RESIDUALS

□ POSITIVE

□ NEGATIVE

INFERRED STREAMS

FIGURE 12



STRUCTURE MAP : TOP OF LOWER MANNVILLE GP.

AREA : T10-15.R16-20 W4

CONTOUR INTERVAL : 50 FT.

DATUM : MSL

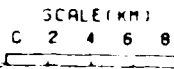
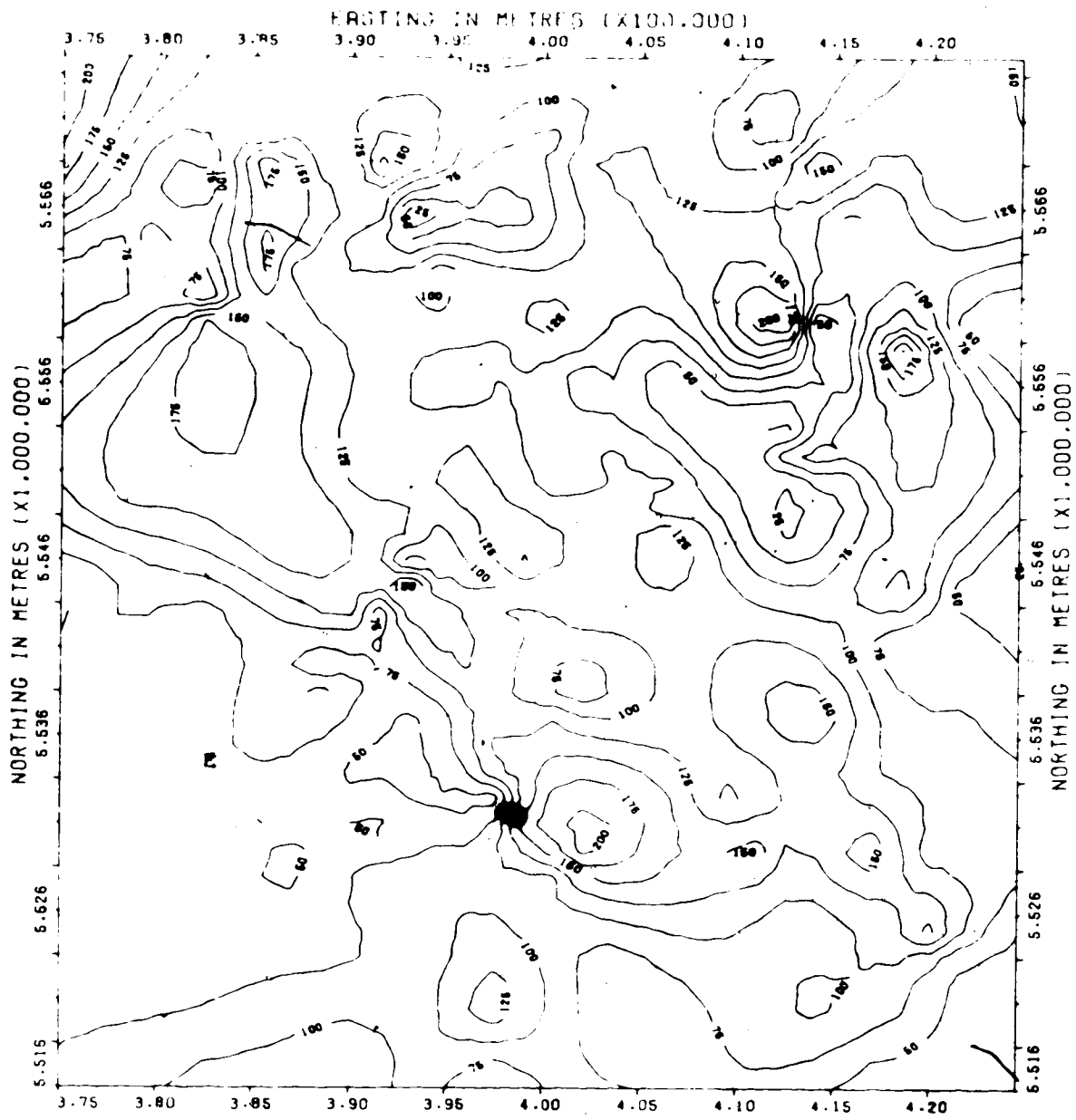


FIGURE 13

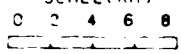


ISOPACH MAP : LOWER MANNVILLE GROUP

AREA : T10-15.R16-20 W4

ISOPACH INTERVAL : 25FT.

SCALE (KM)



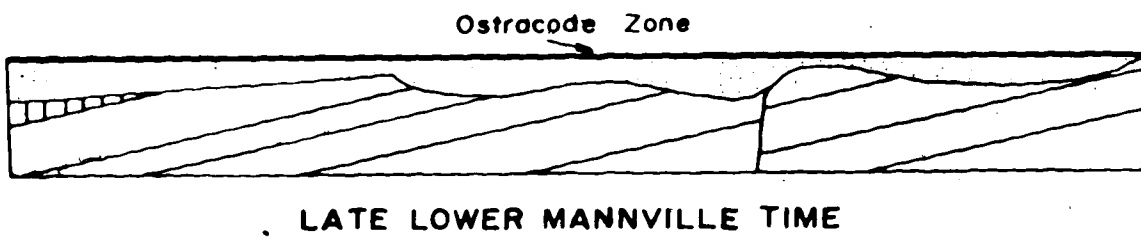
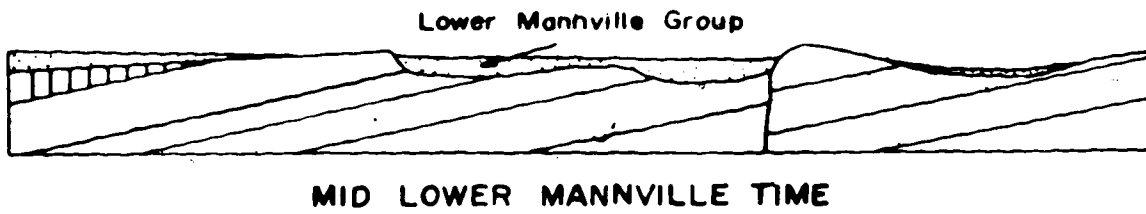
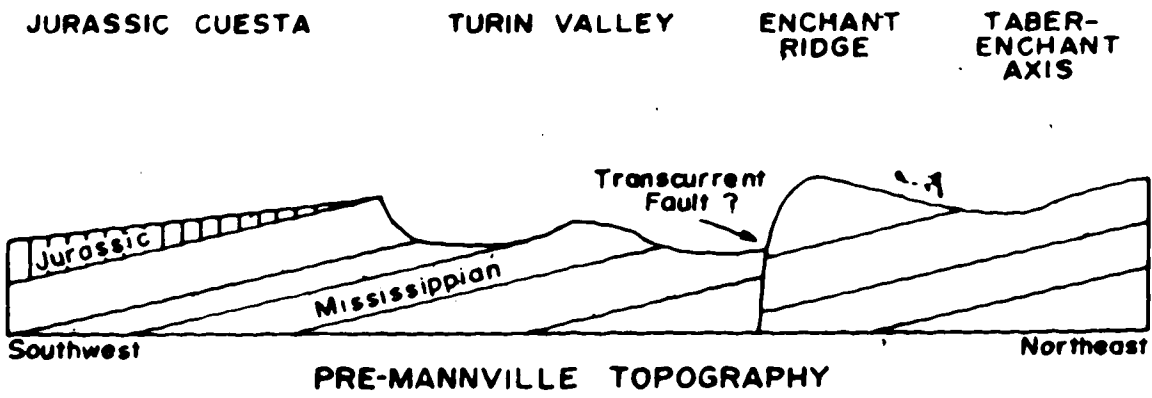
THICK
 THIN

FIGURE 14

Towards the end of early Mannville time, the denudation of Jurassic and Mississippian highs, plus the infilling of channels with clastic material, had resulted in the formation of an extensive plain across the Turin area. Highs were eventually covered with sediment (25 to 50 feet of Lower Mannville strata occur over the highest parts of the Sweetgrass arch in the map area), until little expression remained of the pre-Mannville topography. Lakes and swamps developed, in which muds were deposited as a result of waning sediment supply from a maturing western source area. These muds constitute the Ostracode Zone and vary in thickness from 10 to 30 feet, with the thickest sections occurring above lows on the pre-Mannville surface. A thin limestone (two feet) occurs at the top of the Ostracode Zone in several places.

The Sweetgrass arch remained high, as evidenced by the easterly thinning of the Ostracode Zone towards the arch, and its absence from the top of the arch in the southeastern corner of the map area (Fig. 7). A diagrammatic representation of the changing topography and depositional pattern throughout early Mannville time is shown on Figure 15.

Relief on the top of the Lower Mannville Group is similar to, yet more subdued than that of the pre-Mannville surface. The relief is a function of "remnant" relief from the pre-Mannville (as shown by the absence of the Ostracode Zone on the Sweetgrass arch) and more importantly, differential compaction of Lower Mannville sediments. Minor variations in thickness of the Ostracode Zone over most of the Turin area indicate negligible relief at that time. A period of exposure and non-deposition occurred prior to the onset of Upper Mannville sedimentation, during which time compaction of Lower Mannville sediments took



DIAGRAMMATIC CROSS SECTIONS - TURIN AREA

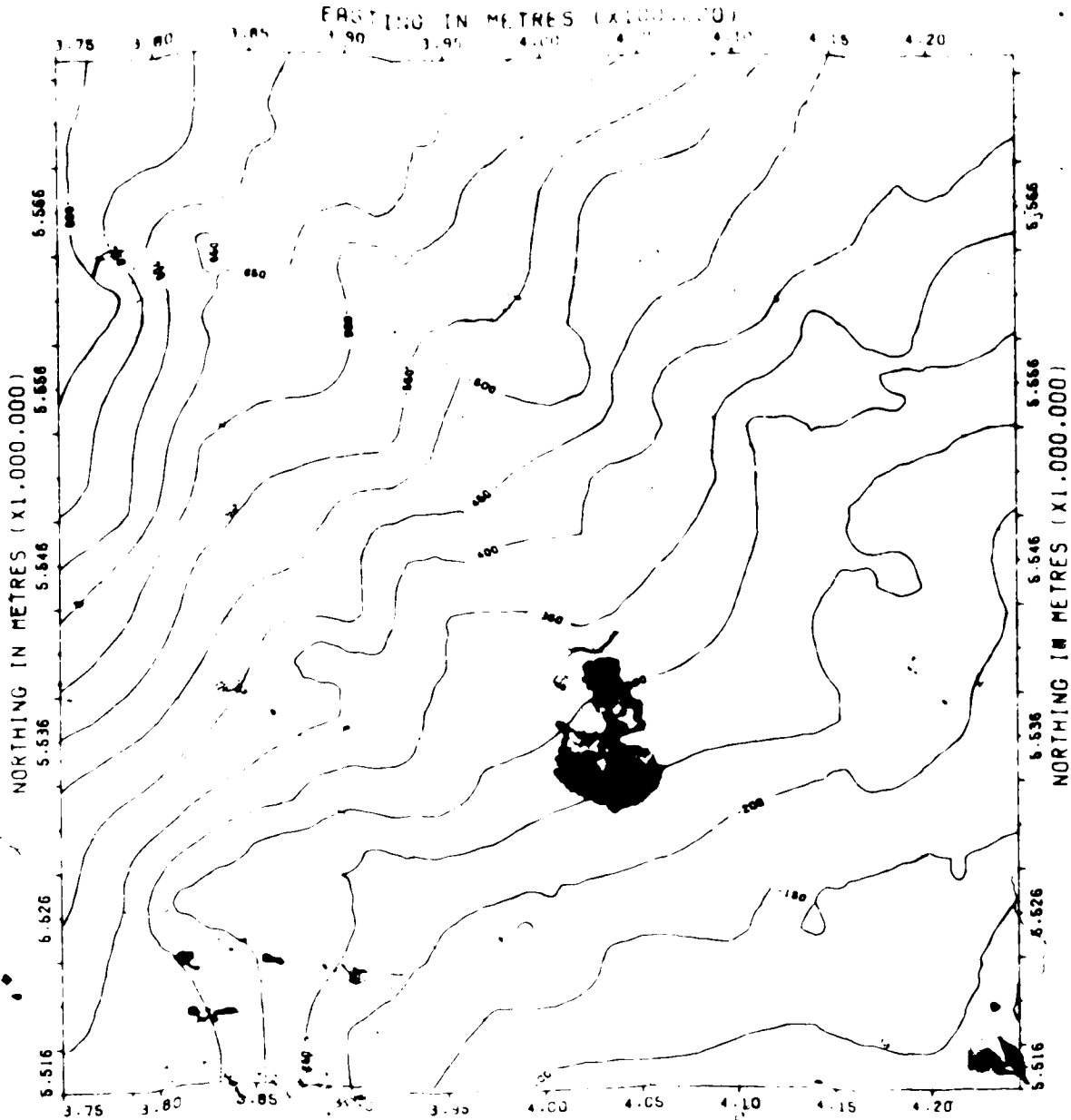
FIGURE 15

plate, producing a topographic surface comparable to that of early Mannville time (as discussed later in Chapter VII, the early late Mannville streams maintained courses similar to those of the early Mannville).

C. UPPER MANNVILLE GEOLOGY

The structure contour map on the top of the Mannville Group (Figure 16) is virtually identical to that on the top of the Lower Mannville (Figure 13), with the surface dipping at $0^{\circ}15'$ to the northwest. A second order trend surface accounted for 98 percent of the variance in elevations on the top of the Mannville. This surface dips towards the northwest (Figure 17), with positive residuals lying above the Taber-Enchant Axis, the Enchant Ridge and the Jurassic cuesta. Small, scattered negative residuals mark the position of the Turin Valley and a broad depression north of the Enchant Ridge. The structure map on the top of the Mannville was overlain by the trend surface map in plotting the courses of Upper Mannville streams shown on Figure 17.

The Turin Valley was wider during late Mannville time than it was during the deposition of the Lower Mannville Group. The position of channels is indefinite, suggestive of a floodplain traversed by braided and meandering streams. The high area to the northwest of the Enchant Ridge was breached by the northern Turin Valley stream, which cut a broad meander belt across the northern map area. The position of the southern Turin Valley stream is imprecise, and the structural maps fail to indicate whether the stream maintained its western course, or veered towards the northern valley.



STRUCTURE MAP : TOP OF MANVILLE GROUP

AREA : T10-15-R-6-20-W4

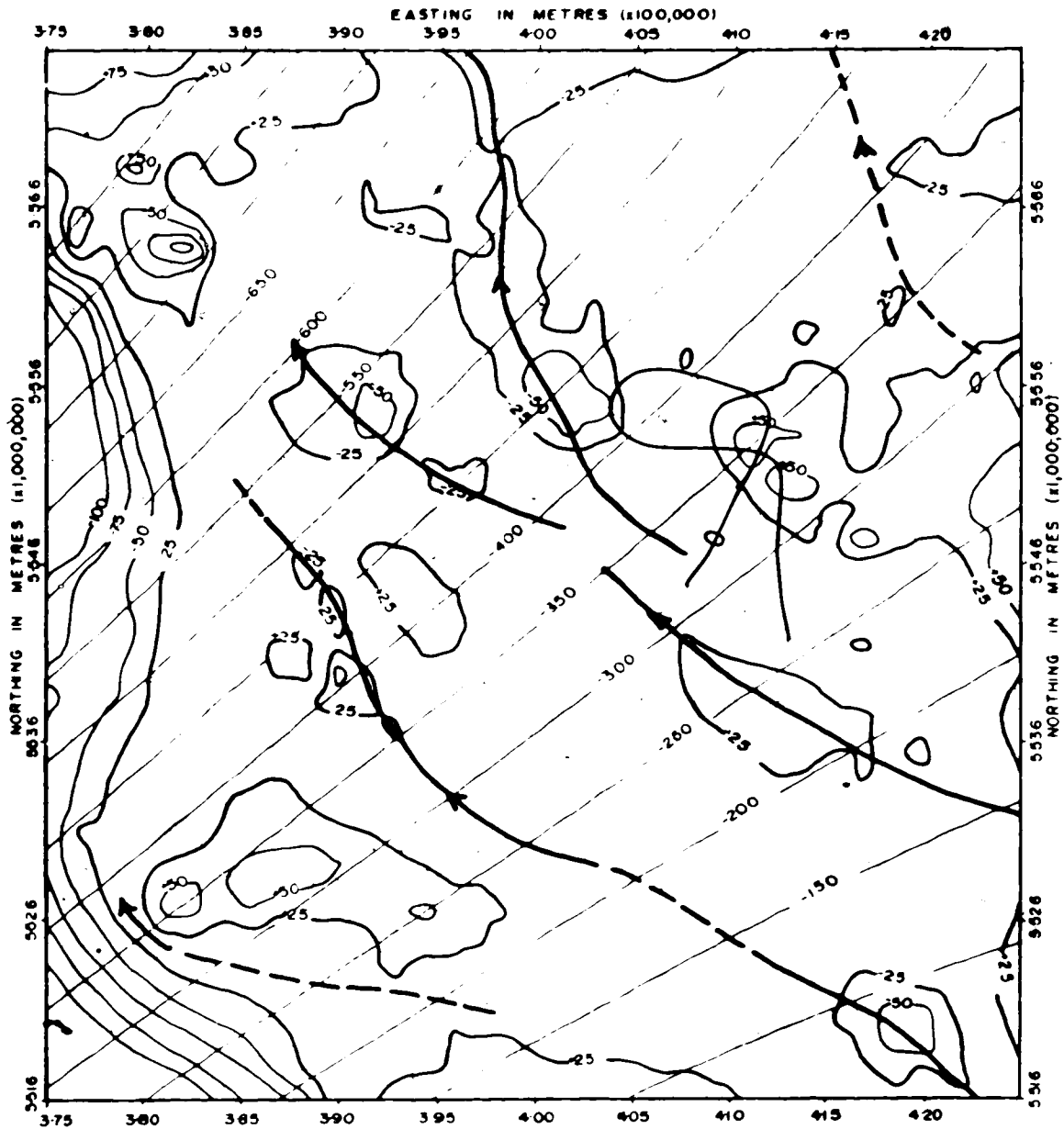
CONTOUR INTERVAL : 20 FEET

DATUM : MSL

SCALE (KM.)



FIGURE 16



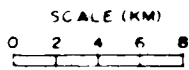
TREND SURFACE MAP : TOP OF MANNVILLE GROUP

AREA T10-15, R16-20 W4

TREND SURFACE ORDER 2ND

TREND SURFACE CONTOUR INTERVAL 50 FT

RESIDUALS CONTOUR INTERVAL 25 FT



RESIDUALS
 □ POSITIVE
 □ NEGATIVE

INFERRED STREAMS

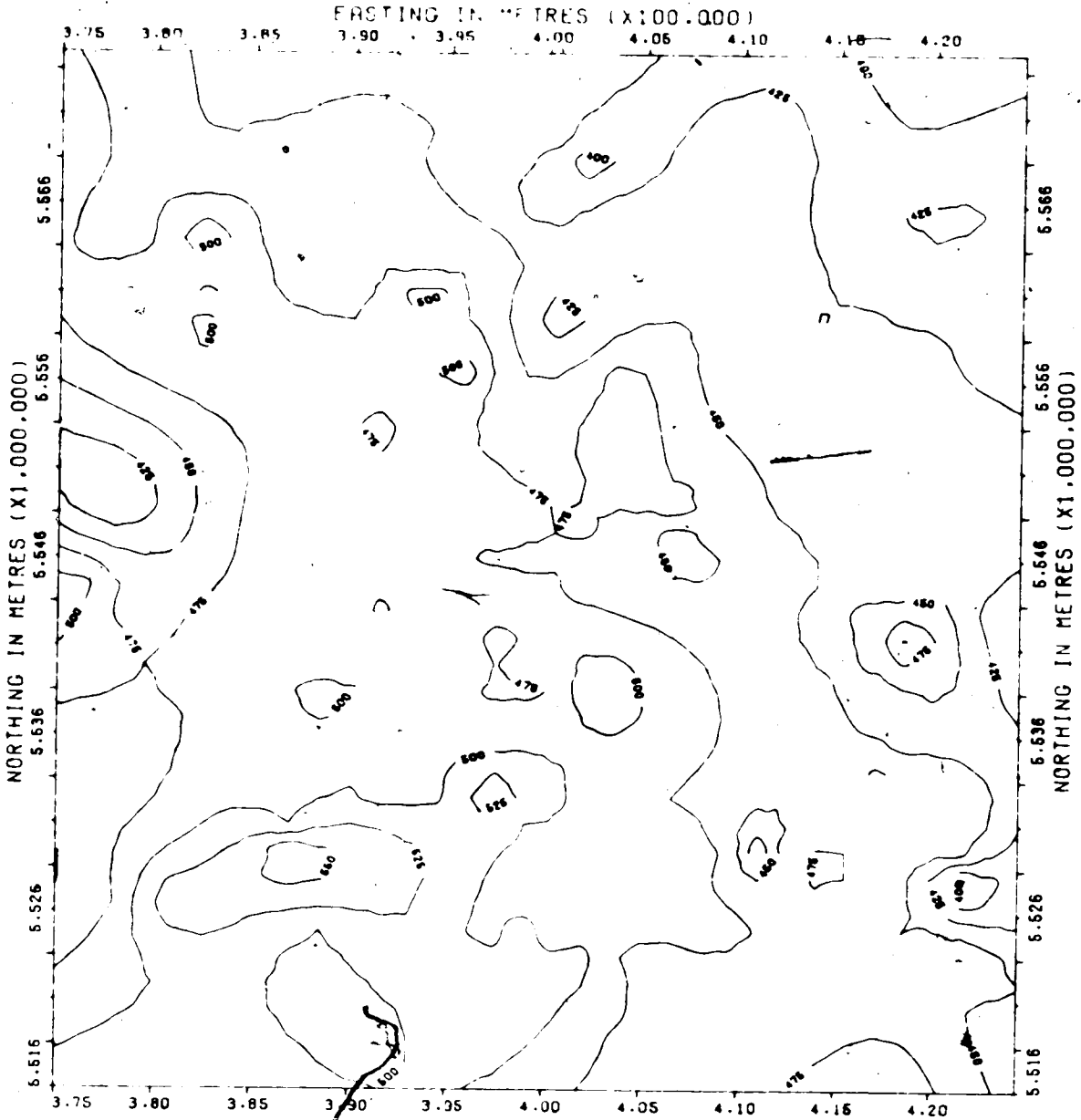
FIGURE 17

A fundamental depositional change occurred during late Mannville time. The Upper Mannville isopach (Figure 18) shows little resemblance to that of the Lower Mannville, as it thickens uniformly to the southwest, with depositional trends less influenced by pre-Mannville topography.

The isopach of the total Mannville Group (Figure 19) shows a regional southwesterly thickening, with areas of anomalously thick sediments along the Turin Valley and other smaller pre-Mannville channels. Thinning is evident over the Sweetgrass arch and pre-Mannville highs. Local variations in thickness are caused primarily by changes in thickness of the Lower Mannville Group.

D. POST-MANNVILLE GEOLOGY

Continental sedimentation in the Turin area terminated with deposition of marine shales and interbedded sandstone (Bow Island Formation) associated with the transgression of the Colorado sea in the late Early Albian. A thin sand occurs locally at the top of the Mannville Group, and has been variously identified in well files as Basal Colorado Sand, or included in the Upper Mannville Group. It is generally interpreted (G.D. Williams, personal communication) as a beach deposit derived from the reworking of Upper Mannville sandstones by the overlapping Colorado sea. Other than showing a high resistivity peak on electric logs, the sand appears to differ little from underlying sandstones; the interval was not cored in the Turin area. The sand is usually less than three feet thick, and has been included in the Colorado Group in the present study.

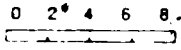


ISOPACH MAP : UPPER MANNVILLE GROUP

AREA : T10-15.R:6-20 W4

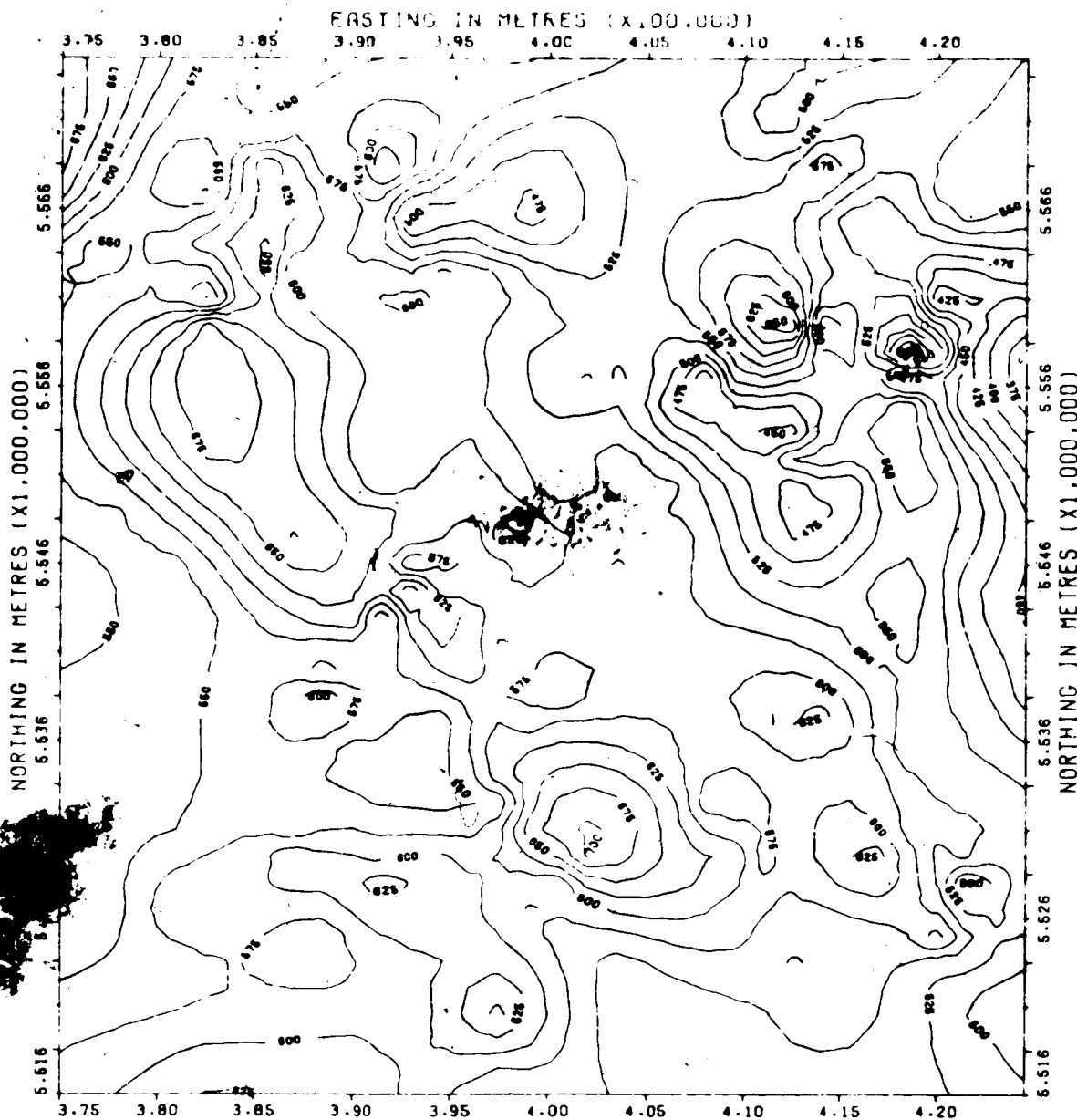
ISOPACH INTERVAL : 25FT.

SCALE (KM)



THICK
 THIN

FIGURE 18

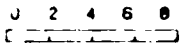


ISOPACH MAP : MANNVILLE GROUP

AREA : T10-15.R:16-20 W4

ISOPACH INTERVAL : 25FT.

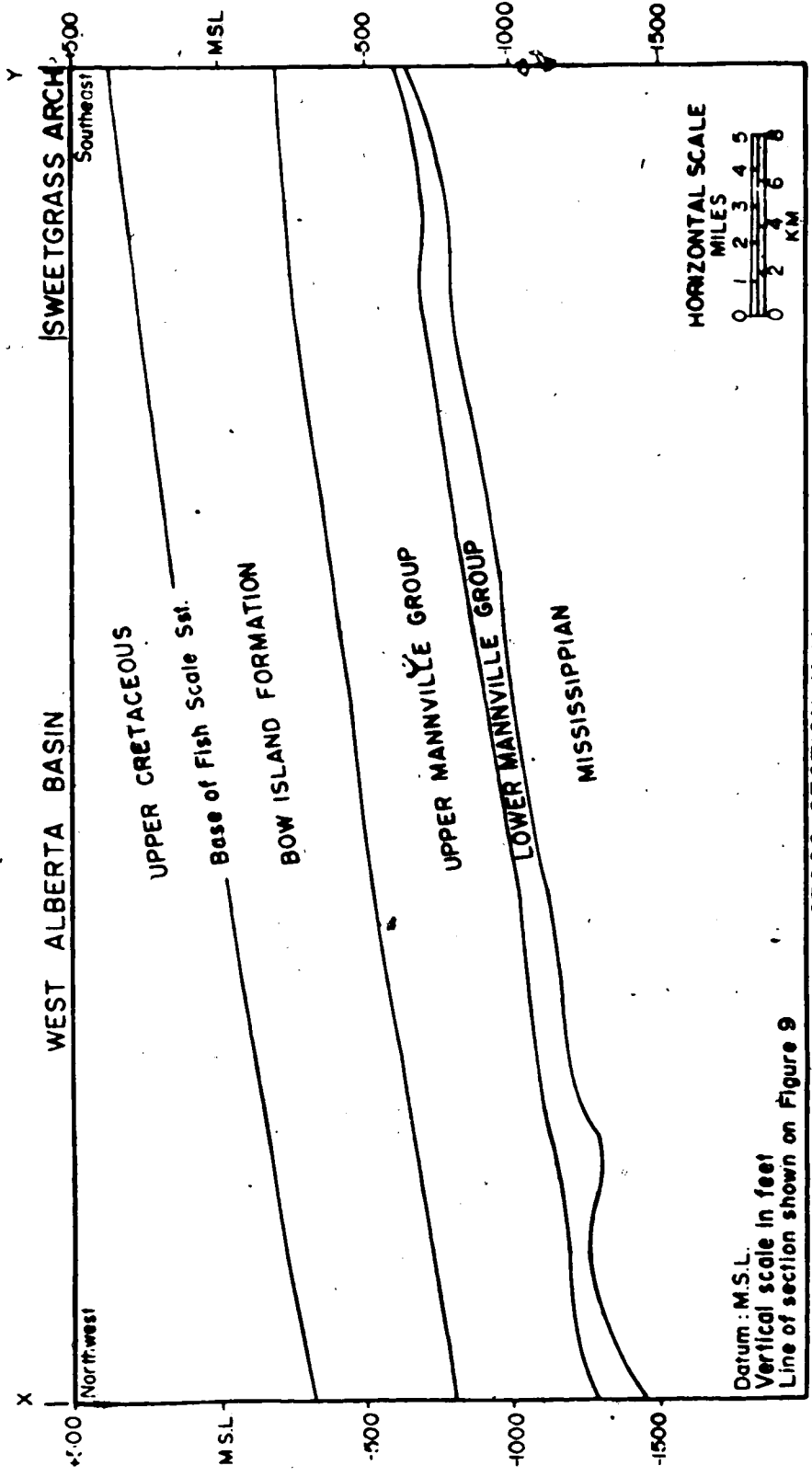
SCALE (KM)



THICK
 THIN

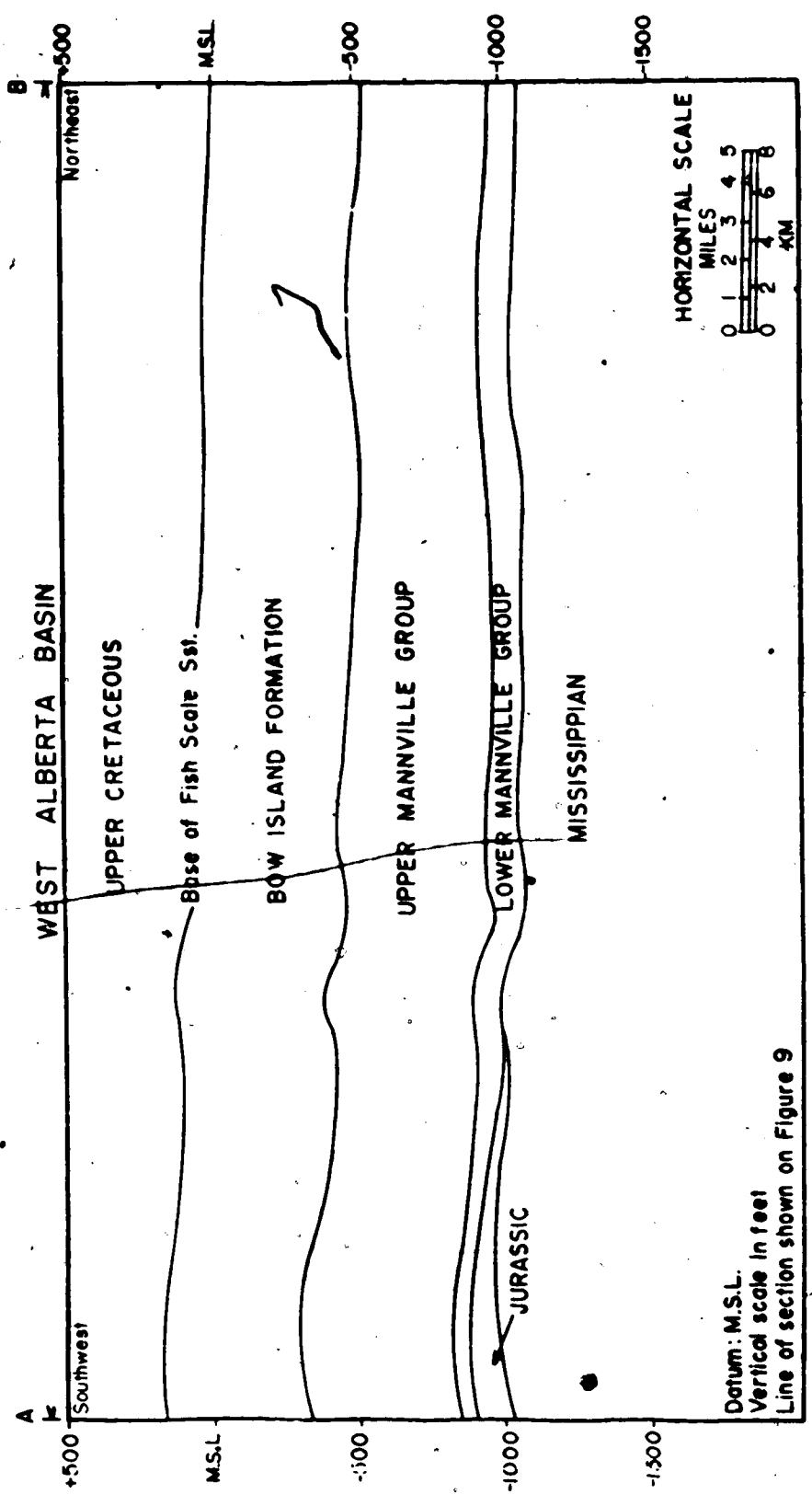
FIGURE 19

The top of the Lower Cretaceous is marked by the base of the Fish Scale Sandstone above the Bow Island Formation. Log correlations (Figures 7 and 8) indicate the uniformity of the Bow Island Formation throughout the Turin area. Structural cross sections drawn parallel to the regional dip and strike (Figures 20 and 21) along the same lines of section as Figures 7 and 8 illustrate the post-Cretaceous northwesterly tilt of the basin, and the major structural elements.



CROSS SECTION X-Y
DIP SECTION ACROSS THE TURIN AREA

FIGURE 20



CROSS SECTION A-B
STRIKE SECTION ACROSS THE TURIN AREA.

FIGURE 21

Chapter VI

SAND DISTRIBUTION IN THE MANNVILLE GROUP

A. INTRODUCTION

The Upper Mannville Group is of uniform thickness and averages 460 feet (140 metres) thick in the Turin area. The sequence was divided proportionately into nine intervals, and the thickness of sand in each interval was measured from gamma logs. The percentage of sand in each interval was calculated by computer and contoured sand percentage slice maps were generated. Stacking the nine slice maps produced a "three dimensional" view of the changing distribution and geometry of sand bodies within the Upper Mannville succession. Difficulties in mapping and establishing stratigraphic relations between manually correlated, time transgressive, independent sand systems are largely removed using this numerical approach.

The determination of sand distribution at any given time is simplified in the Turin area, as sediments in each slice may be considered to be isochronous. The base and top of the Upper Mannville Group, as well as a number of intermediate horizons, are subparallel to the base of the Fish Scale Sandstone (see electric log correlations - Figures 7 and 8) which delineates the base of the Upper Cretaceous succession. Hence, within the Upper Mannville sequence, time lines and lithostratigraphic lines are approximately coincident.

The Lower Mannville Group has an average thickness of 100 feet (30 metres), but individual values range between 25 and 200 feet (8 to 64 metres). The pre-Mannville surface is envisaged as consisting of a

series of southwesterly-dipping Mississippian and Jurassic cuestas. The Lower Mannville isopach (Figure 14) indicates that the elevations of these ridges were similar, as were the depths of the intervening valleys. Early Mannville sedimentation was restricted to the valleys, and sand bodies maintained fixed spacial positions throughout Lower Mannville time (confined by the valley walls), more so than the Upper Mannville sands, which were deposited over wide meander belts. Not until late early Mannville time, when topographic relief was negligible, did deposition occur uniformly across the Turin area.

Consequently the age and thickness of the Lower Mannville section encountered in any well depends upon whether drill sites were positioned above pre-Mannville highs or lows. Proportionate subdivision of the Lower Mannville Group therefore produces slices (Intervals 10 and 11) containing sediments which bear only limited depositional relationships, because areas of valley sedimentation are generally older than those areas overlying the pre-Mannville topographic highs.

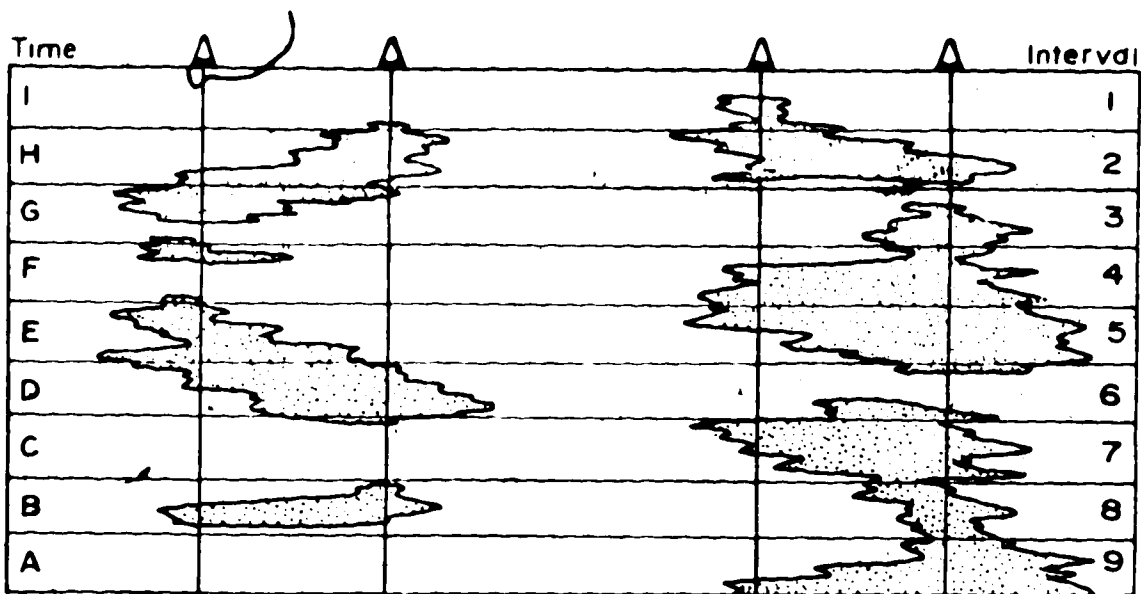
This problem was partially circumvented by subdividing the sequence into four equal 50-foot (15 metre) slices (Intervals 12 to 15). For the lower intervals (14 and 15), barren highs of Mississippian and Jurassic strata occupy a large part of the map area; for these maps sand percentage data were hand contoured, as no provision existed in the computer programs to adequately isolate the "bald zones", and prevent them from influencing the gridding and contouring of the sand. The small, isolated pre-Mannville "bedrock" outcrops in the upper slices (Intervals 12 and 13) were overlooked, and sand data were computer contoured to maintain consistency with the Upper Mannville maps.

Since the pre-Mannville valleys (and ridges) showed some variation, in elevation and shape (valleys had different base levels and gradients, and deposition commenced at different times, with younger streams down-cutting earlier deposits), the fixed thickness subdivision of the Lower Mannville Group did not produce slices containing entirely penecontemporaneous sediments. Both types of slices are required to interpret sand distribution adequately, and to determine time equivalent deposits.

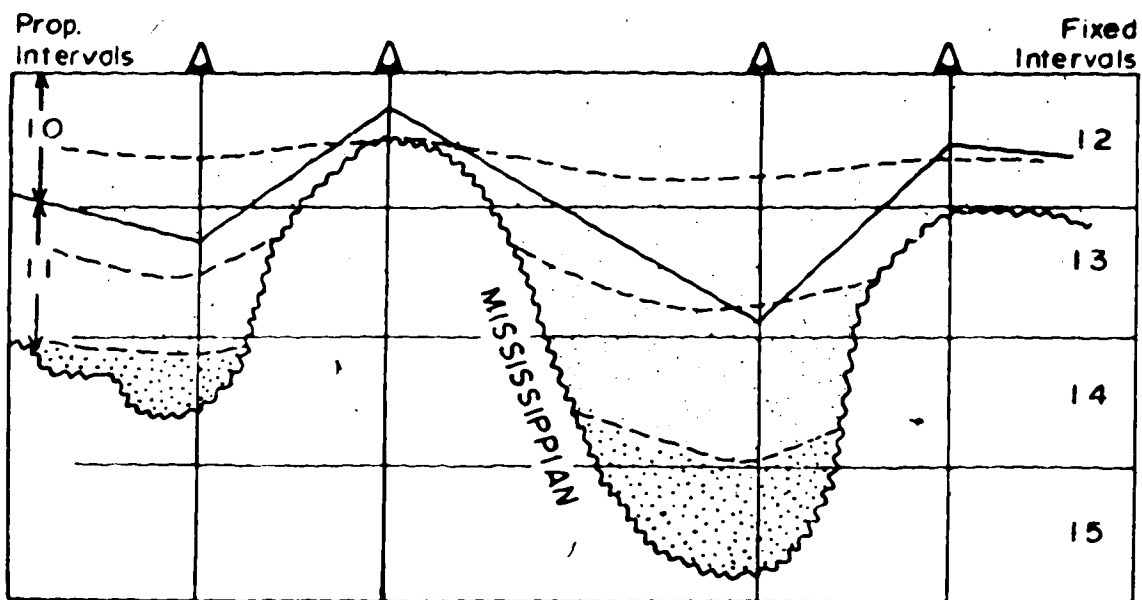
The proportionate subdivisions of the Upper Mannville Group, and both fixed and proportionate subdivisions of the Lower Mannville Group, are illustrated diagrammatically in Figure 22. Figure 23 is an example of a gamma-sonic log subdivided into intervals for sand percentage calculations.

B. LOWER MANNVILLE GROUP

Interval 15 (Figure 24) represents initial Mannville deposition in the deep channels of the Mississippian and Jurassic surface. It occurs in only 13 scattered wells, thereby creating difficulties in defining depositional limits and contouring the sand data. Sedimentation was restricted to three areas - the Turin Valley, where in the south, sands were deposited along two parallel water courses, and in the northwest, where the streams apparently coalesced; a small westerly depression at the base of the dip slope of the Jurassic cuesta; and in a northeasterly directed valley on the northern side of the Enchant Ridge. Sand deposition predominated over fine clastics. Log character at the base of Interval 15 suggests a high proportion of Mississippian limestone debris (Deville Formation equivalent) in a number of wells.



UPPER MANNVILLE GROUP — PROPORTIONATE SUBDIVISION
Two independently deposited sand units illustrated

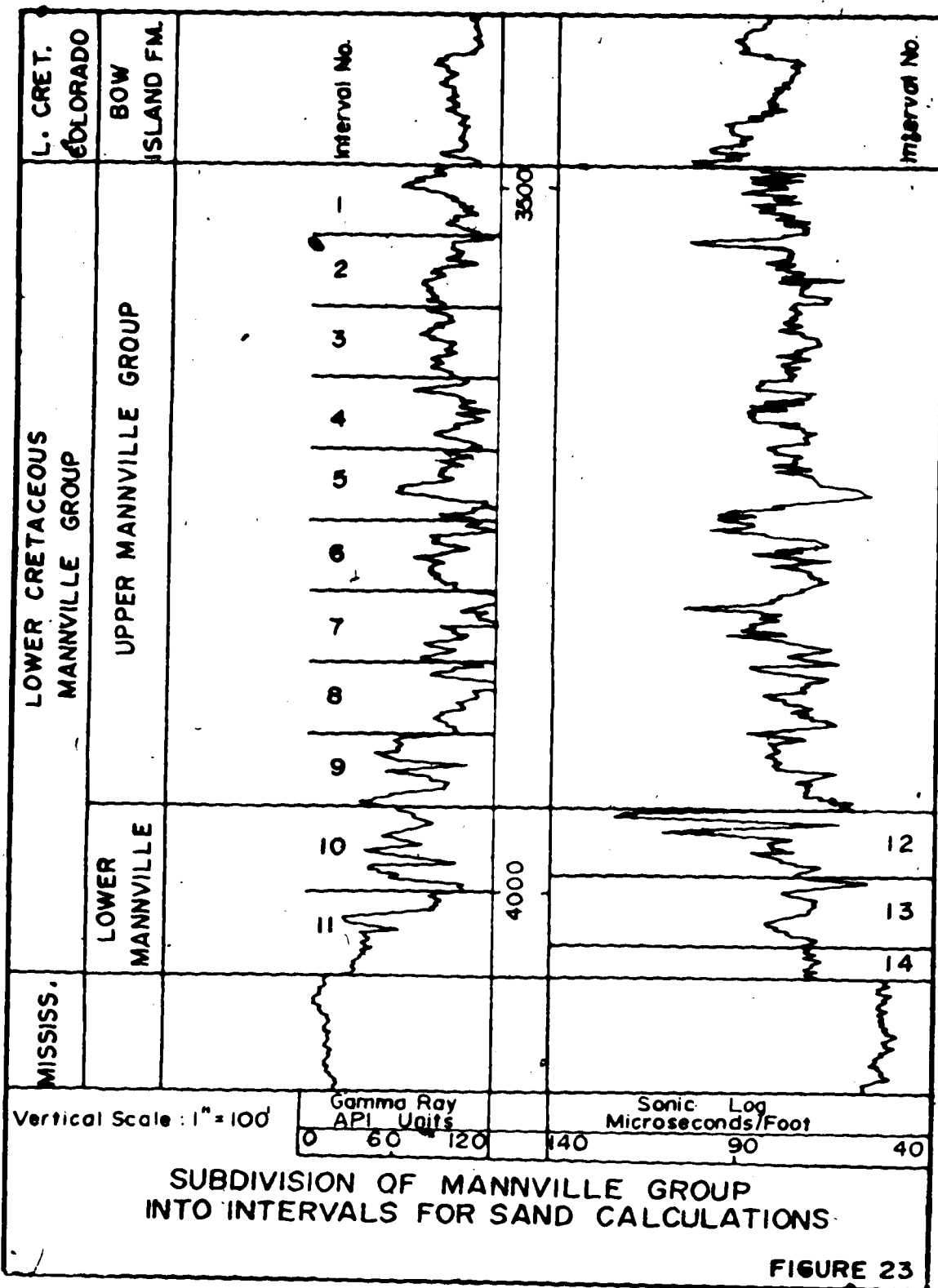


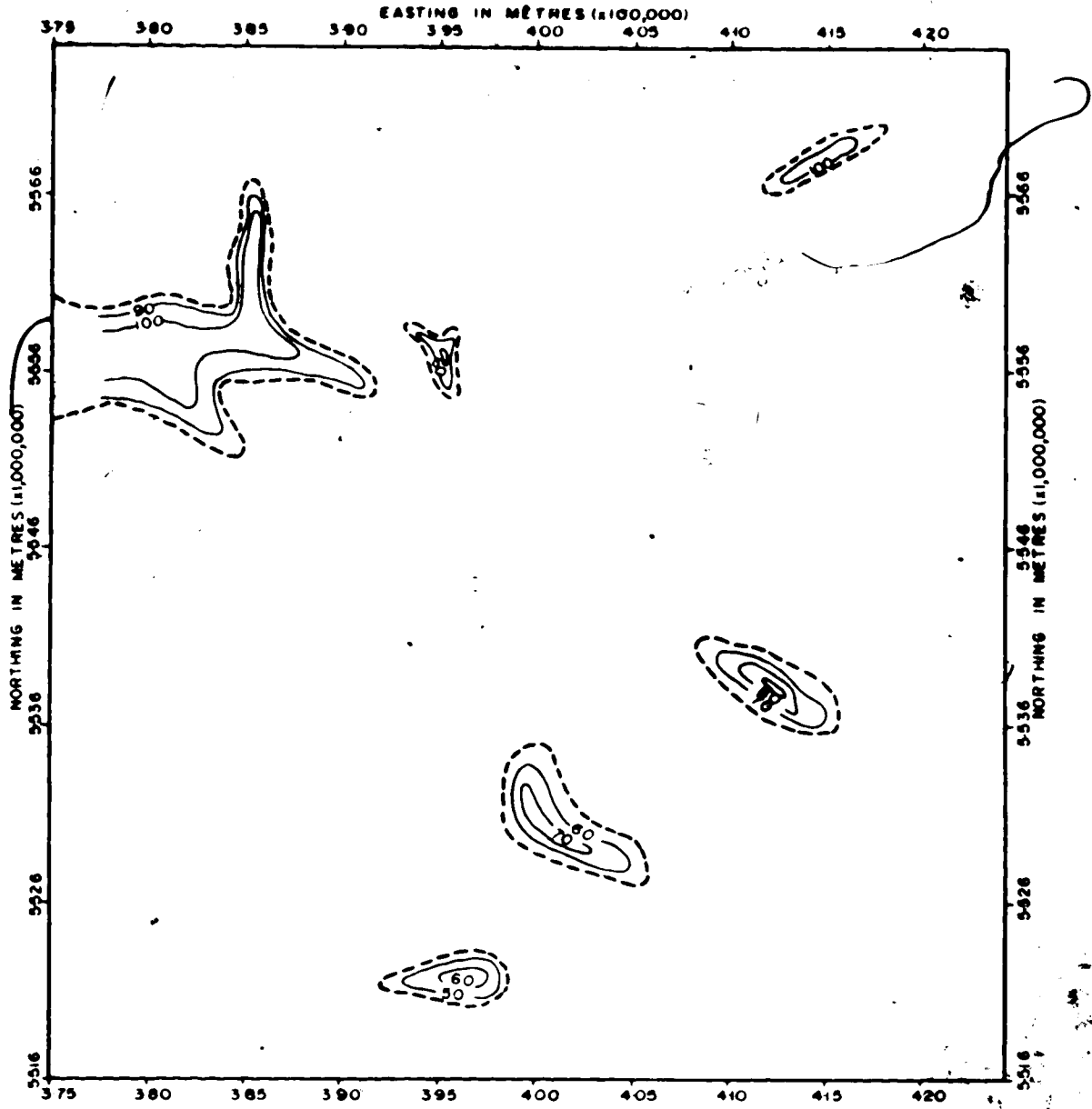
LOWER MANNVILLE GROUP—FIXED & PROPORTIONATE SUBDIVISION
Stippling indicates approximately time equivalent units

NOTE: VERTICAL SCALE DIFFERENT IN EACH DIAGRAM

DIAGRAMMATIC SUBDIVISION OF THE MANNVILLE GROUP

FIGURE 22

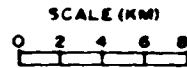




SAND PERCENTAGE MAP INTERVAL 15

AREA T10-15, R16-20 W4

CONTOUR INTERVAL 10%



- SAND %
- 40-60
- 60-80
- 80-100

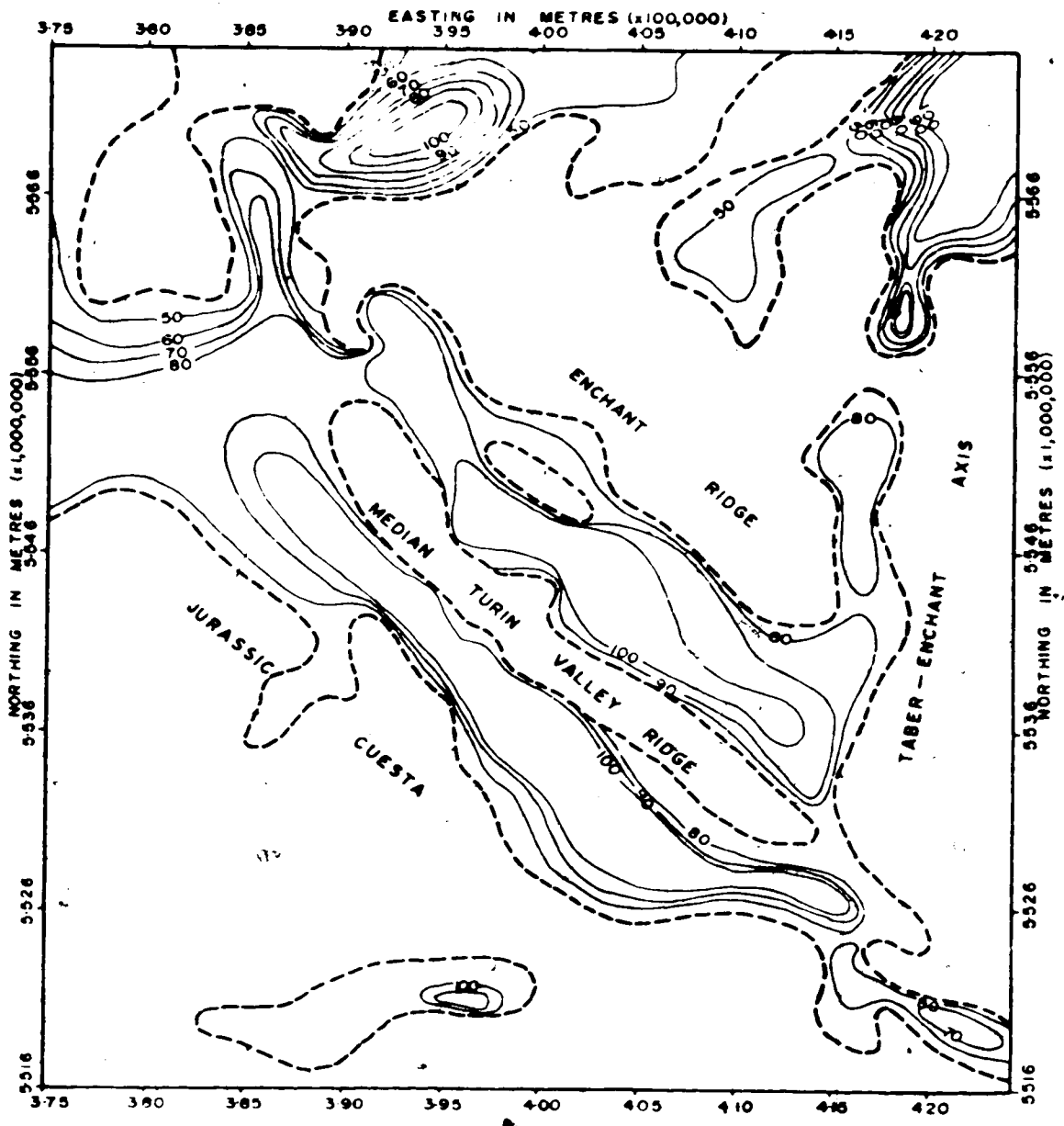
○/○ CROPPING PRE-MANNVILLE STRATA

FIGURE 24

The lower Mannville depositional pattern is well defined in Interval 14 (Figure 25). The Turin Valley was the site of thick sand accumulation. A narrow ridge, probably of resistant Mississippian limestone, extended down the length of the valley, separating the two water courses which were apparent on the map of Interval 15. Small tributaries fed the Turin Valley from the southeastern end of the Enchant Ridge, and from the northern face of the Jurassic cuesta.

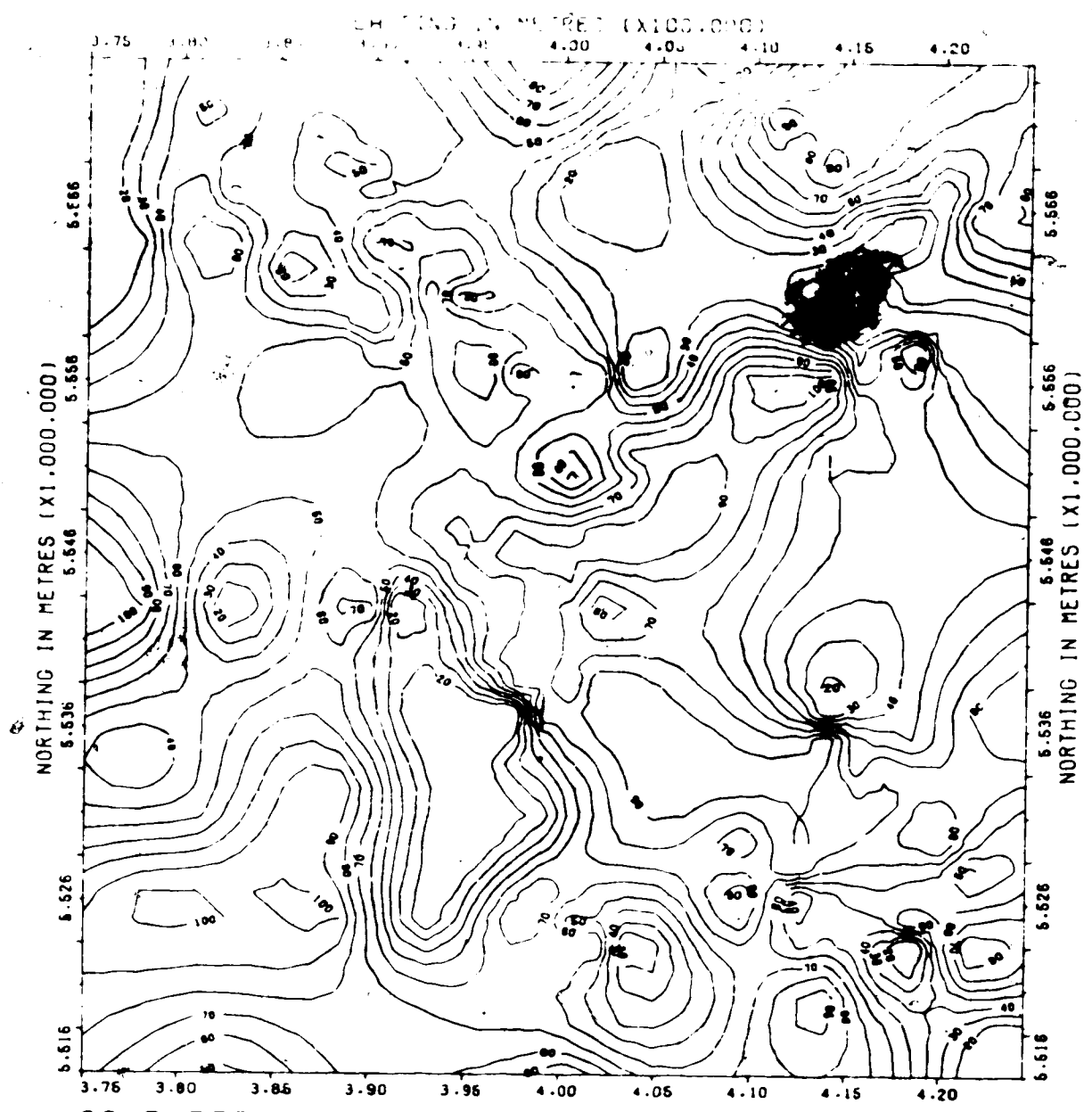
As shown on the trend surface map of the base of the Mannville Group (Figure 12), the two Turin Valley distributaries joined in the western map area to form a single, broad (6 mile wide) floodplain. Valleys on the northern side of the Enchant Ridge and the southern side of the Jurassic cuesta continued to fill with detritus. The shape and form of these valleys indicate that the sediments accumulating in them were derived mainly from the erosion of the outcropping Jurassic formations, unlike the Turin Valley sediments which were mainly of Cordilleran origin. The paleogeographic maps of Springer et al. (1964) show the Sawtooth and Swift Formations to have been deposited over the southern half of the Turin area. Thin remnants of the Sawtooth now occur along the Jurassic cuesta, but Jurassic strata are absent from the top of Enchant Ridge.

As mentioned above, the computer contoured map of Interval 13 (Figure 26) is somewhat inaccurate because areas of outcropping pre-Mannville strata could not be isolated from areas of sand deposition. Sand values were extrapolated to grid nodes overlying these areas, and contoured accordingly. The zero to forty percent contour interval generally corresponds to regions of pre-Mannville outcrop outlined on the



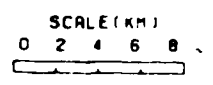
SAND PERCENTAGE MAP INTERVAL 14
AREA T10-15, R16-20 W4
CONTOUR INTERVAL 10%
SCALE (KM)
0 2 4 6 8
SAND %
□ 40- 60
□ 60- 80
□ 80-100
OUTCROPPING PRE-MANNVILLE STRATA

FIGURE 25



SAND PERCENTAGE MAP : INTERVAL 13

AREA : T10-15-R16-20 W4
CONTOUR INTERVAL : 10%
(0410% CONTOURS DELETED)



- SAND %
- 0- 20
 - 20- 40
 - 40- 60
 - 60- 90
 - 80-100

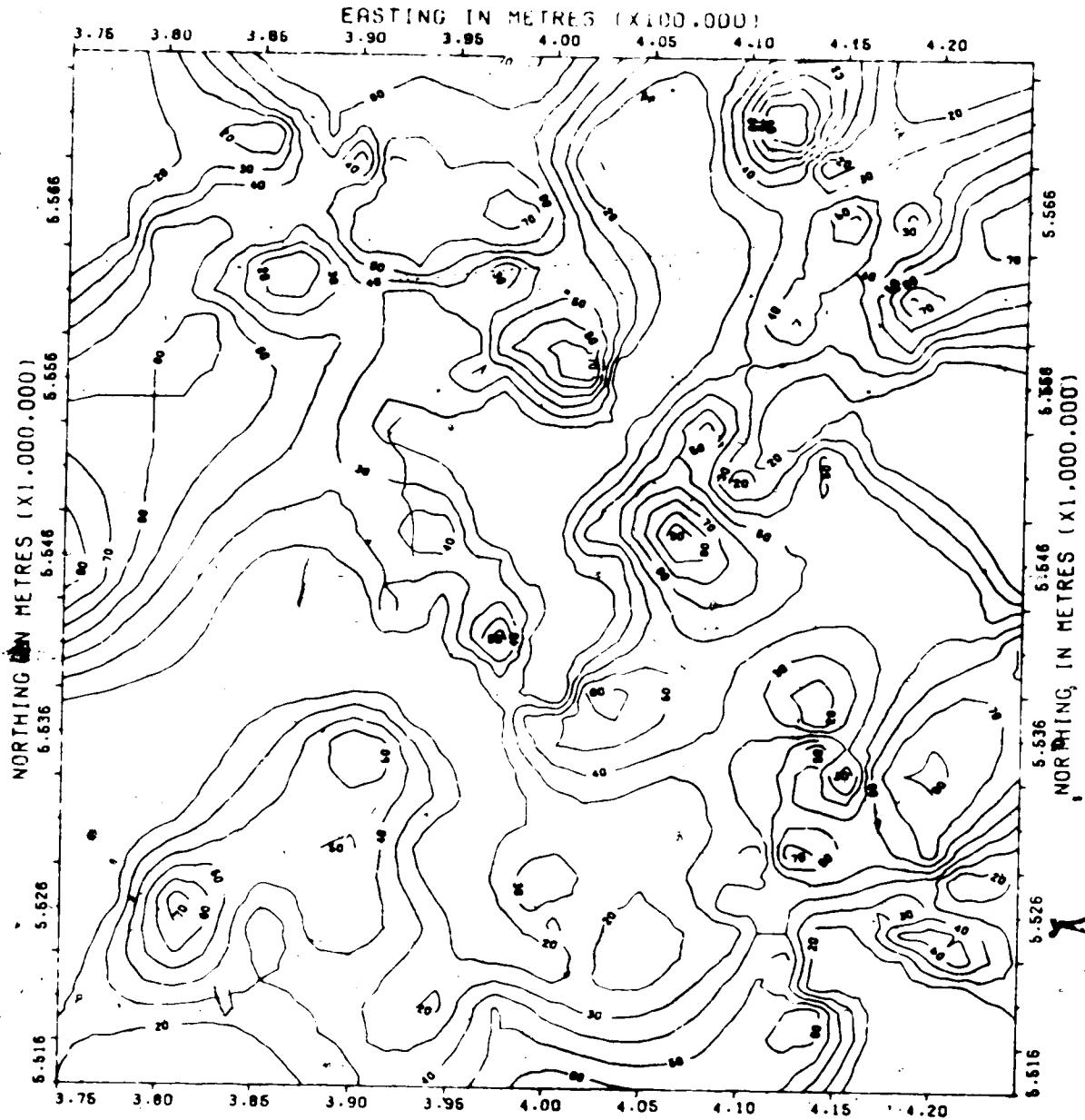
FIGURE 26

Interval 14 map, and does not represent thick argillaceous sequences. Sand deposition was at a maximum in the Turin Valley at this time. The median ridge is not obvious because of interpolation of the high sand values between the two channels. On the western Turin Valley floodplain, increasing volumes of silt and clay were deposited. Sand accumulated on the southwestern edge of the Jurassic cuesta and the northern side of the Enchant Ridge.

Interval 12 (Figure 27) is the uppermost slice of the Lower Mannville Group, and includes the regionally deposited shale of the Ostracode Zone. Scattered pre-Mannville outcrops existed during early Interval 12 time (Enchant Ridge, Jurassic cuesta and southeastern Taber-Enchant Axis), but except for parts of the Taber-Enchant Axis, these areas were covered by late Lower Mannville fine-grained clastics, which were deposited in the lower energy environments away from the main stream channels.

The northern Turin Valley stream was the main water course prior to the deposition of the Ostracode Zone. It eroded the high area in the northwest and established a straight northwesterly course. Mainly fine-grained sediments were deposited in the southern Turin stream, which continued to flow westwards.

An irregular belt of sand occurs in the southwest. This was deposited in a northwesterly-flowing river system entering the Turin area for the first time, from the southeast. The stream captured the early Lower Mannville valley at the foot of the Jurassic cuesta, and joined the southern Turin valley stream during Upper Mannville time.

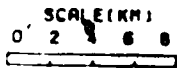


SAND PERCENTAGE MAP : INTERVAL 12

AREA : T10-15.R16-20 W4

CONTOUR INTERVAL : 10%

10&10% CONTOURS DELETED



SAND %

□ 0- 20

□ 20- 40

□ 40- 60

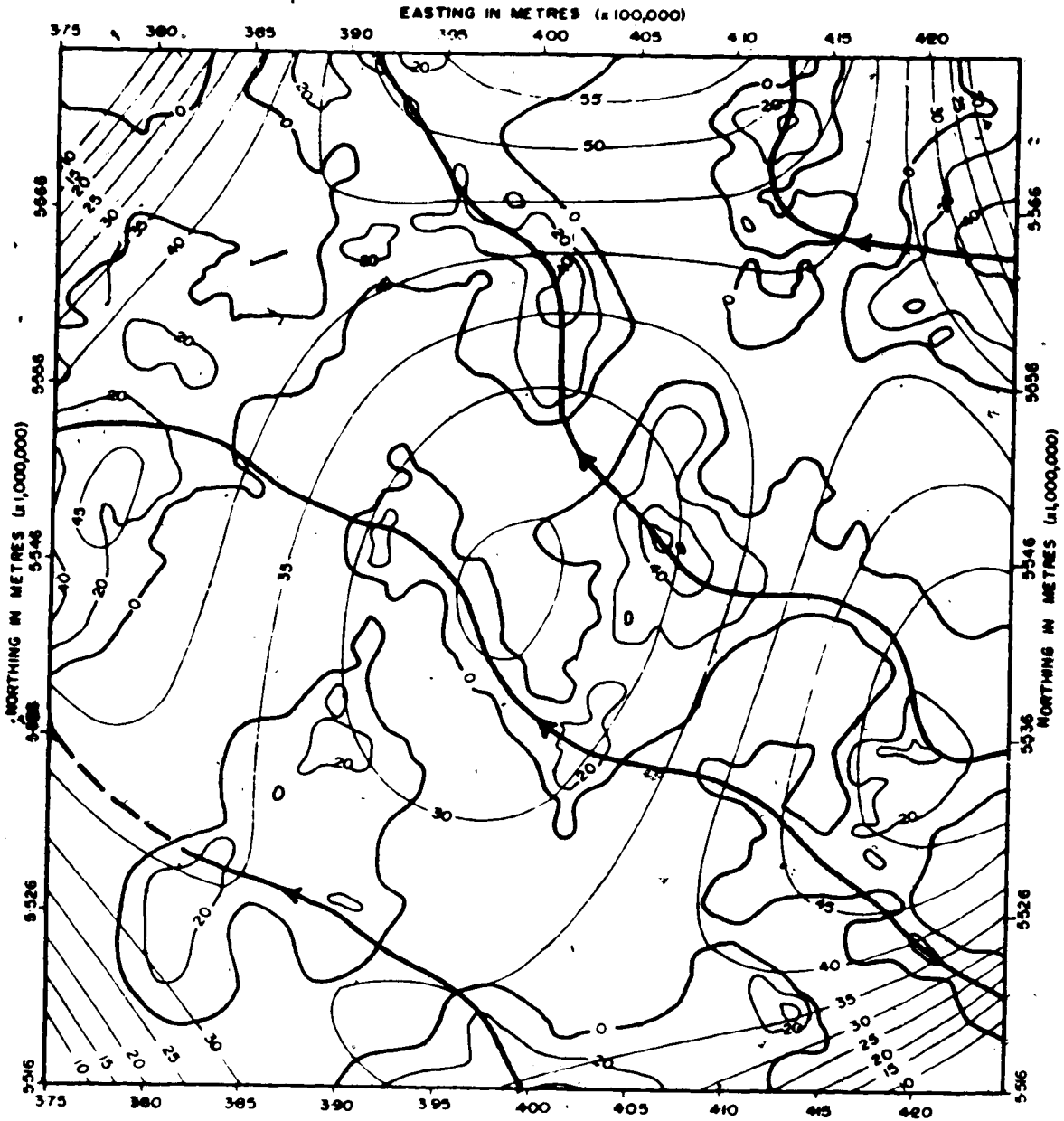
□ 60- 80

□ 80-100

FIGURE 27

Trend surface analysis of the Interval 12 sand percentage data (Figure 28) did little to enhance the areas of anomalously thick sand deposition. Thick, clean sand was deposited along the pre-Mannville channels, while silts and clays accumulated in areas removed from active stream flow. Sand deposition occurred in these areas only during times of flooding, and from the intermittent, minor tributaries. Fifty to one hundred percent sand occurs in the main streams and zero to twenty percent in other areas, with little gradation between. Hence, there was no regional or average sand distribution to which a mathematical surface could be applied. The sum of squares of residuals accounted for increases from eight to fifteen percent for first to eighth order surfaces; that is, no matter what the order of surface, the large positive residuals caused by the streams and the lack of negative residuals resulting from the small areas of argillaceous sedimentation prevented fitting a statistically valid surface to the data. The outline of positive residuals approximates the twenty percent contour line of the sand percentage map. In contrast to this situation, Wermund and Jenkins (1970) were able to fit a fourth order surface to the sand isolith of a widespread Pennsylvanian delta in north central Texas, apparently because of the more extensive distribution of sand in such an environment.

Areas of pre-Mannville outcrop are not included in slices produced by the proportionate subdivision of the Lower Mannville Group (Intervals 11 and 10, Figures 29 and 30), thus the computer contoured sand percentage maps of these intervals are free from the limitations of the maps of Intervals 12 and 13. In Interval 11, high sand values occur along



TREND SURFACE MAP : SAND INTERVAL I2

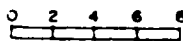
AREA : T10-B, R16-20 W4

TREND SURFACE ORDER 4TH

TREND SURFACE CONTOUR INTERVAL 5%

RESIDUALS CONTOUR INTERVAL 20%

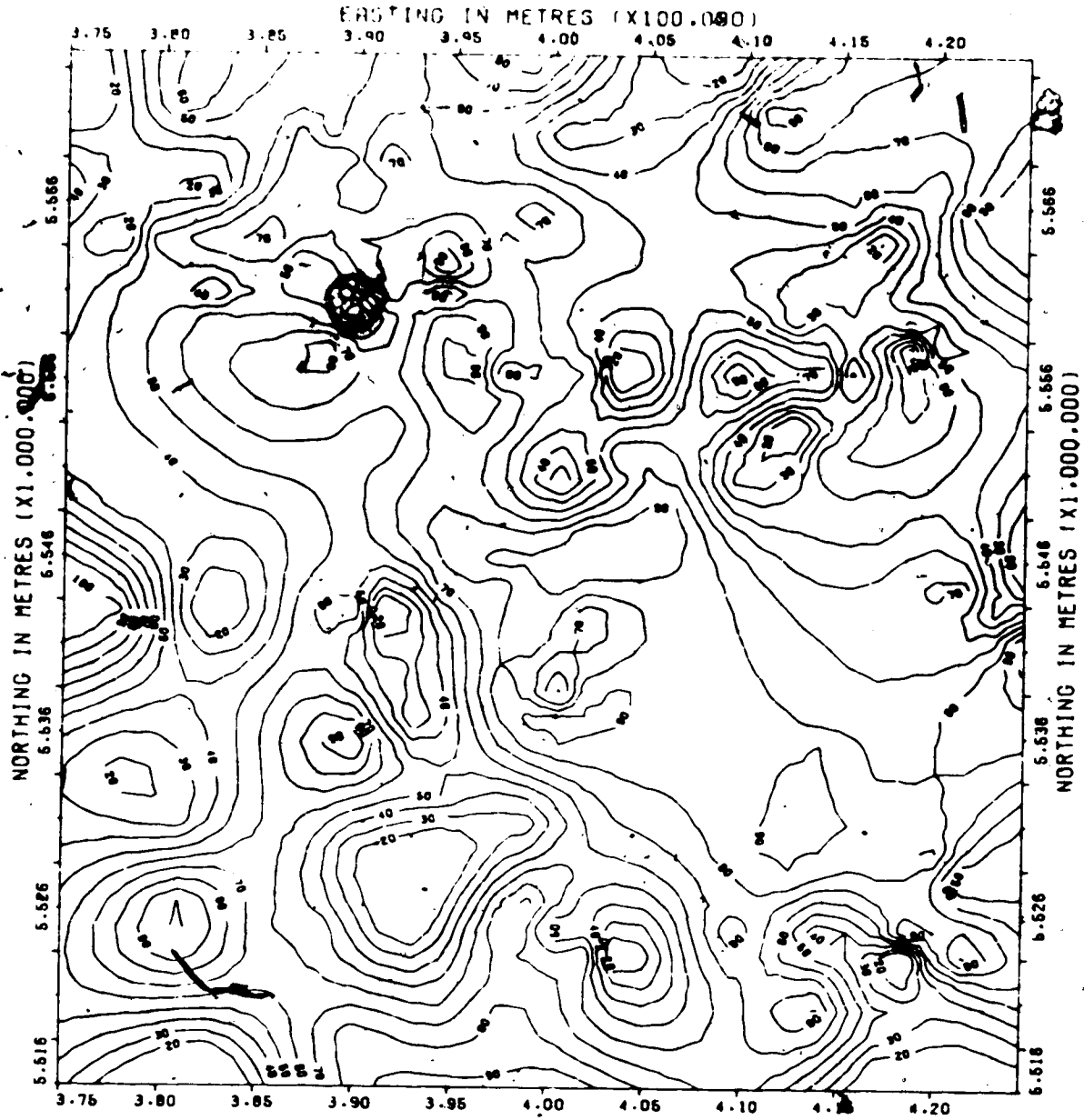
SCALE (MM)



RESIDUALS
□ POSITIVE

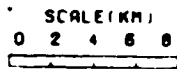
INFERRED
STREAMS

FIGURE 28



SAND PERCENTAGE MAP : INTERVAL 11

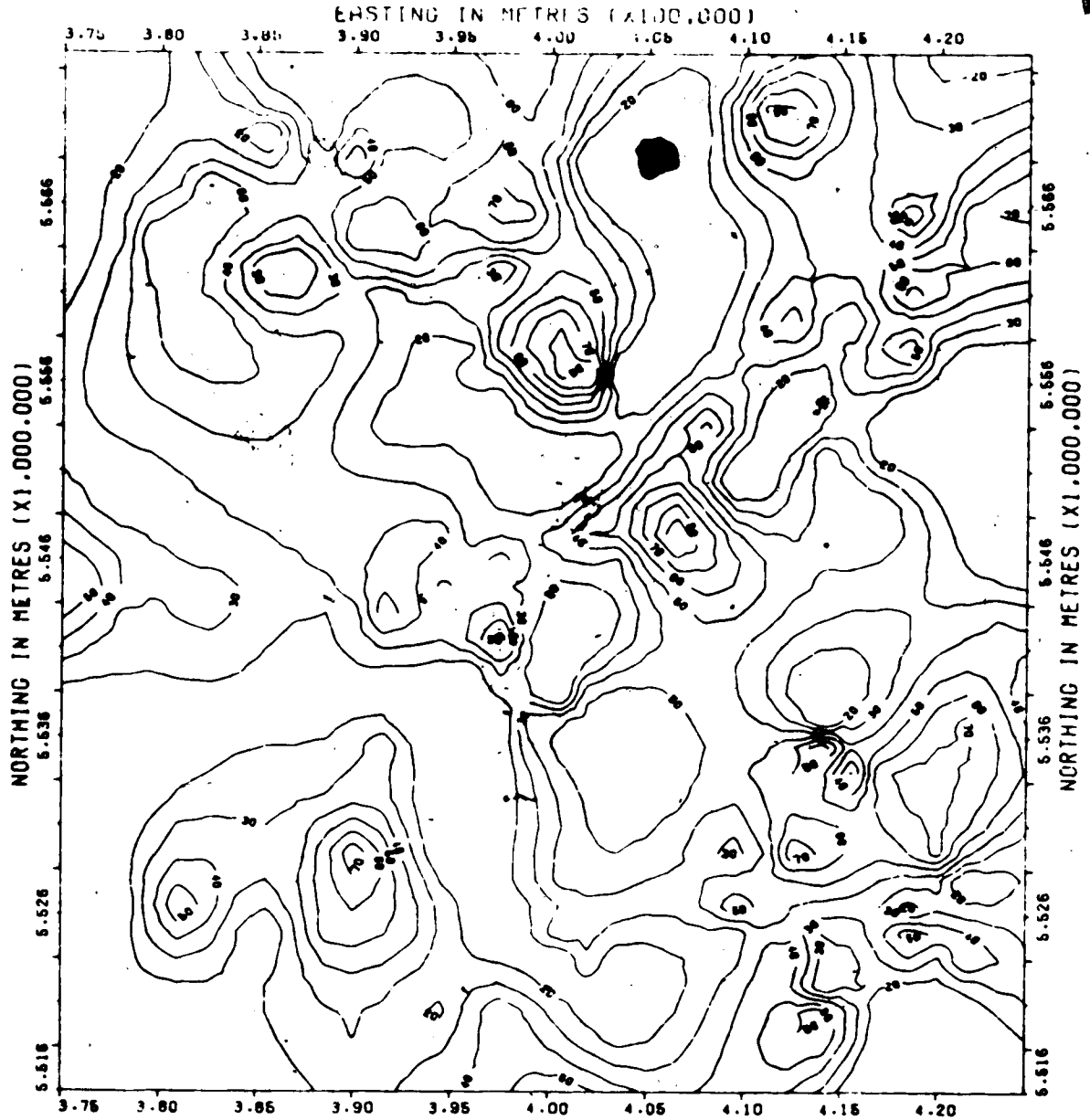
AREA : T10-15.R16-20 M4
 CONTOUR INTERVAL : 10%
 (0 & 10% CONTOURS DELETED)



SAND %

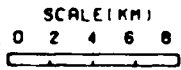
- 0- 20
- 20- 40
- 40- 60
- 60- 80
- 80-100

FIGURE 29.



SAND PERCENTAGE MAP : INTERVAL 10

AREA : T10-15.R16-20 W4
 CONTOUR INTERVAL : 10%
 (0 & 10% CONTOURS DELETED)



- SAND %
- 0 - 20
 - 20 - 40
 - 40 - 60
 - 60 - 80
 - 80 - 100

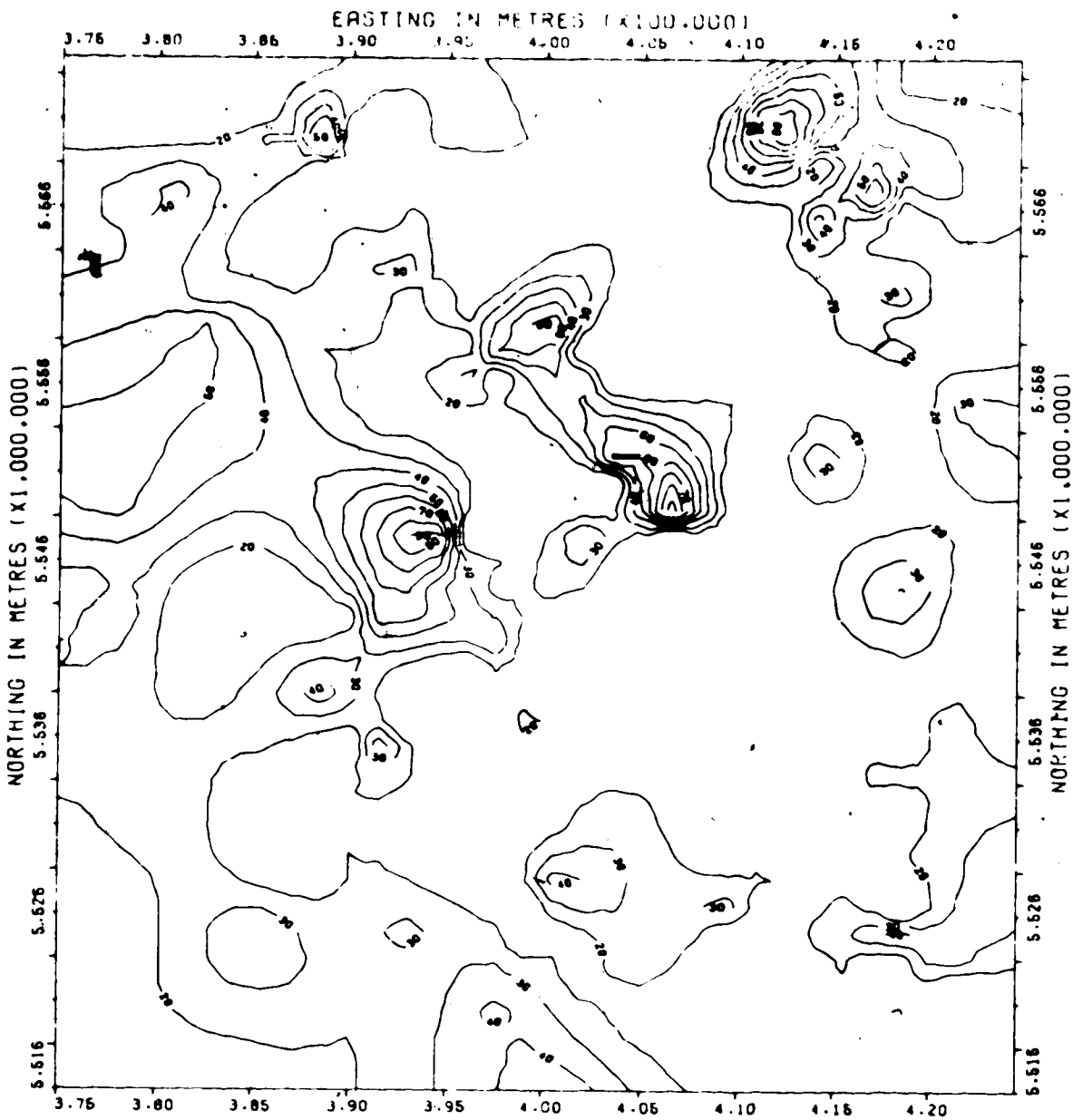
FIGURE 30

the topographic lows on the pre-Mannville surface, and silts and muds occur over the eroded highs. The course of the northern Turin stream is delineated on the Interval 10 map by the line of high sand values. Intervals 11 and 10 illustrate the progressive decrease in the volume of sand deposited throughout Lower Mannville time.

C. UPPER MANNVILLE GROUP

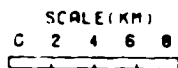
Interval 9 (Figure 31) encompasses most of the Glauconitic Sandstone Equivalent. Differential compaction of Lower Mannville sediments after the deposition of the Ostracode Zone shales produced a topography similar to that which existed in early Mannville time, though much subdued in relief. Streams maintained courses comparable to those of the early Mannville, although the volume of sand entering the Turin area was considerably reduced.

The Turin Valley persisted as the main area of sand deposition. Silts and muds were deposited over pre-Mannville highs and in areas removed from the main streams. A northwesterly-directed stream channel overlying the one cut at the southern edge of the Jurassic cuesta in the southwestern corner of the map area coalesced with the southern Turin Valley stream in the western part of the map area, and increased sand accumulation occurred at the junction. A northwesterly-trending stream is also evident in the northeastern part of the area. The fourth order trend surface residual map of Interval 9 (Figure 32) clearly shows the position of the four northwesterly-flowing streams which drained the Turin area at this time. The trend surface accounted for thirteen percent of the variance within the sand distribution.



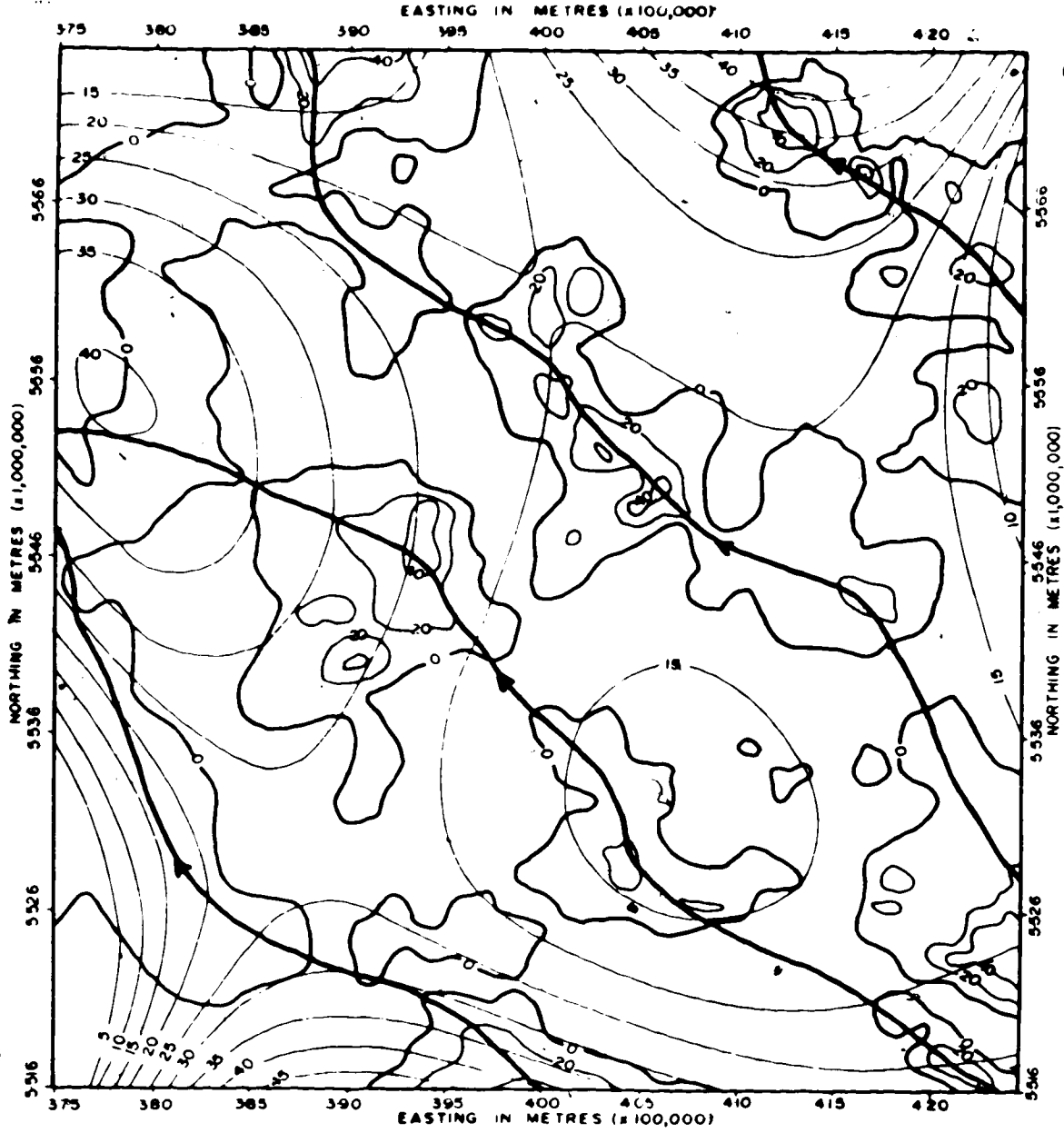
SAND PERCENTAGE MAP : INTERVAL 9

AREA : T10-15.R16-20 W4
 CONTOUR INTERVAL : 10%
 (0 & 10% CONTOURS DELETED)



- SAND %
- 0- 20
 - 20- 40
 - 40- 60
 - 60- 80
 - 80-100

FIGURE 31



TREND SURFACE MAP : SAND INTERVAL 9

AREA T10-15, R16-20 W4

SCALE (KM)

RESIDUALS

INFERRED
STREAMS

TREND SURFACE ORDER 4TH



□ POSITIVE

TREND SURFACE CONTOUR INTERVAL 5%

RESIDUALS CONTOUR INTERVAL 20%

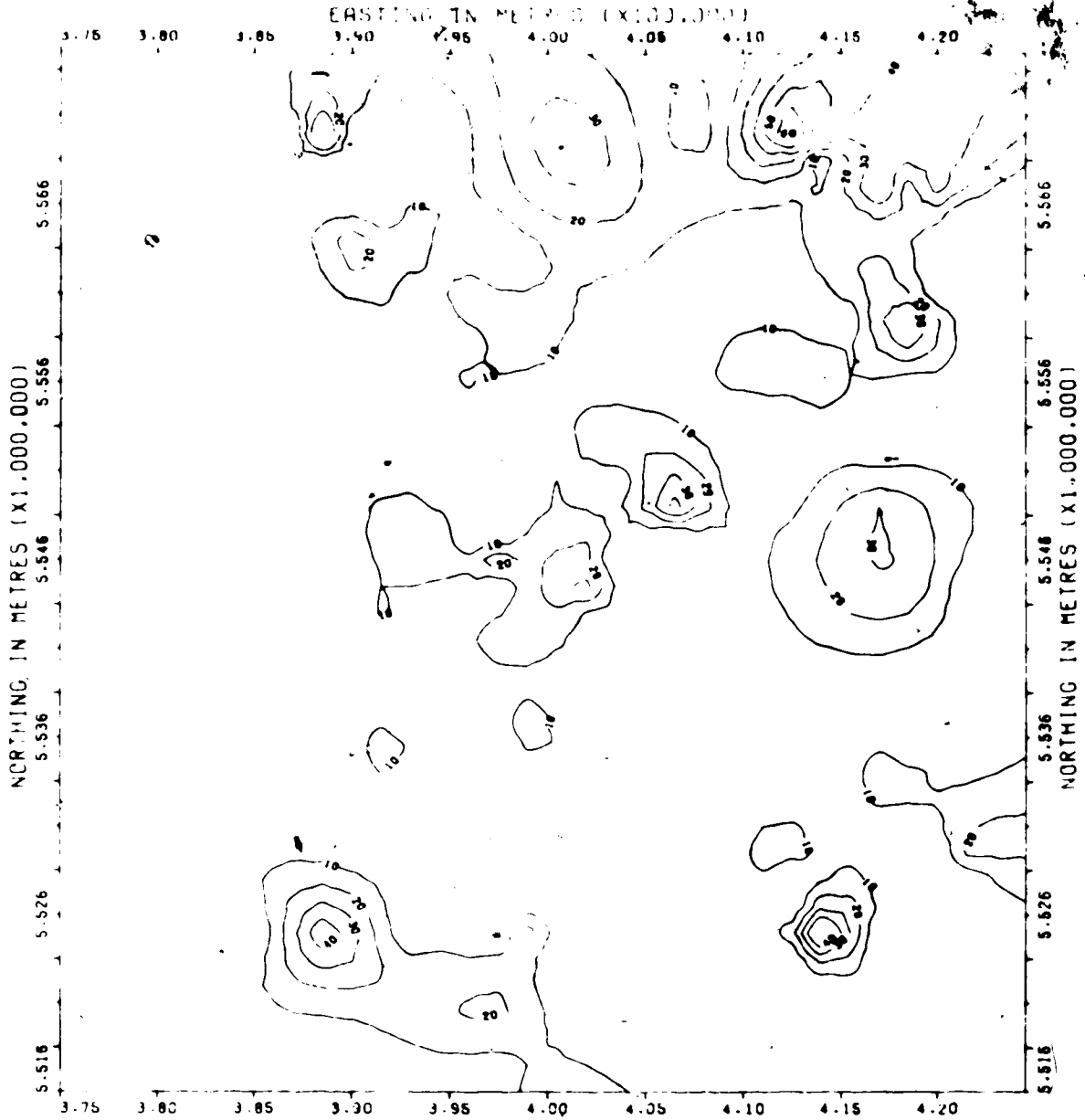
FIGURE 32

Very little sand was deposited within Intervals 8, 7 and 6 (Figures 33, 34 and 35) and the Turin Valley ceased to be the main area of sand deposition. It formed a wide, shallow depression in which approximately 150 feet of silt and mud were deposited, along with small, scattered occurrences of clean sand, the distribution of which suggests point bar deposits of meandering streams. The southwestern and northeastern streams were the main water courses at the time, and unlike the linear streams of Interval 9, mid late Mannville streams show little structural constraint, resulting in the formation of extensive meander belts over a floodplain of low relief.

Interval 5 (Figure 36) marks a period of renewed sand deposition. The four streams are still discernible, although only small volumes of sand were deposited over most of the Turin Valley. A thick sand accumulation occurs in the northeastern corner of the Turin area, but its limited areal extent prevents conclusions being drawn about the river in which it was deposited, the main channel of which apparently lay beyond the map area.

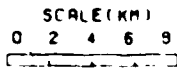
The northeast remained the site of sand deposition in Interval 4 (Figure 37), and little sand was deposited elsewhere. Two chains of low sand values delineate the position of Turin Valley streams at this time.

The largest volume of sand subsequent to the deposition of the Glauconitic Sandstone Equivalent (Interval 9) is present in Interval 3 (Figure 38), with major accumulations occurring in the southwestern and northern regions. Elements of the northern Turin Valley drainage system veered to the northeast and apparently entered the northeastern stream; arcuate trends of high sand values suggest broad, meandering channels.



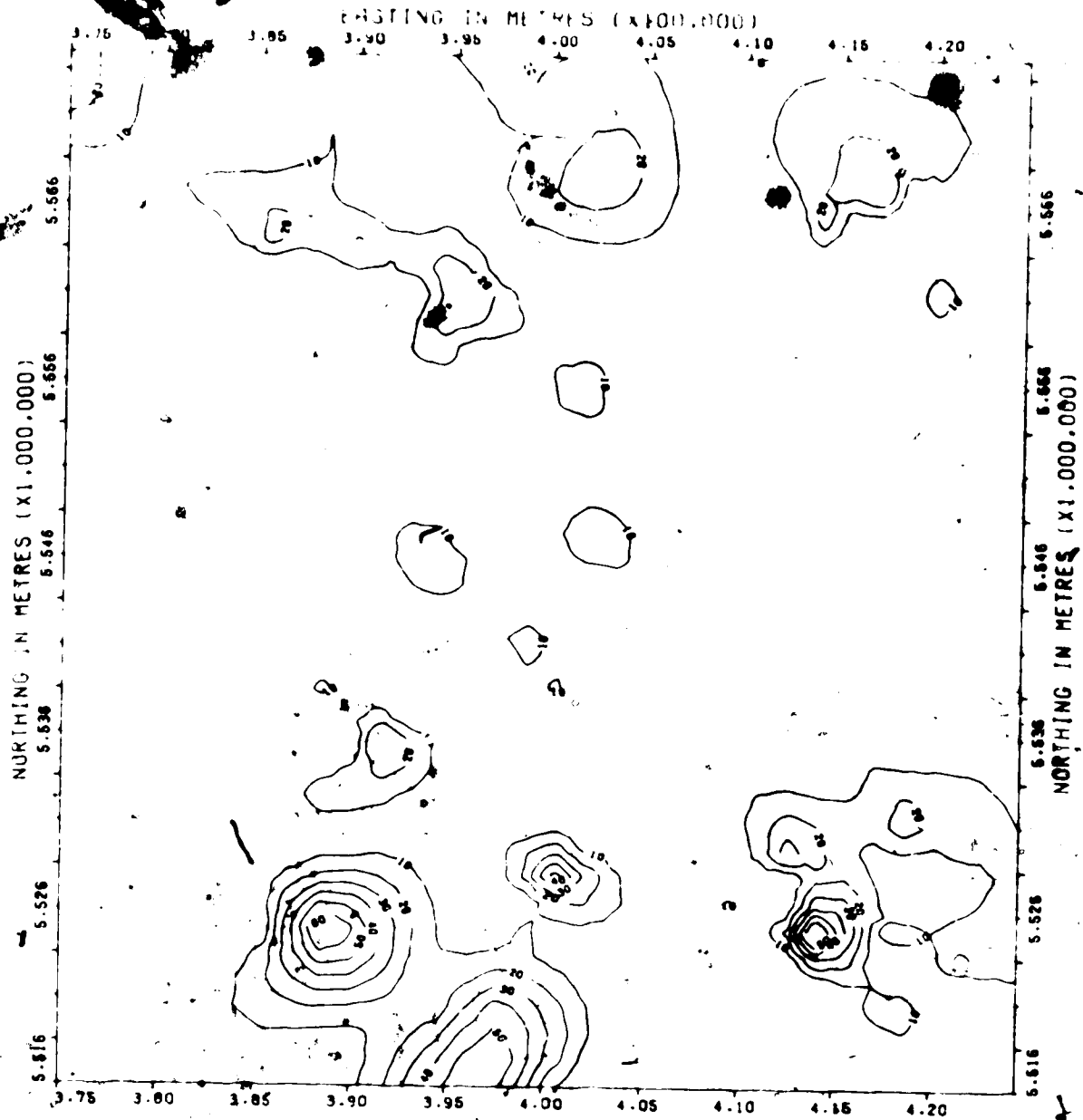
SAND PERCENTAGE MAP : INTERVAL 8

AREA : T10 15. R16-20 W4
 CONTOUR INTERVAL : 10%
 10% CONTOUR DELETED :



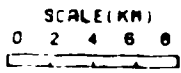
- SAND %
- 0- 20
 - 20- 40
 - 40- 60
 - 60- 80
 - 80-100

FIGURE 33



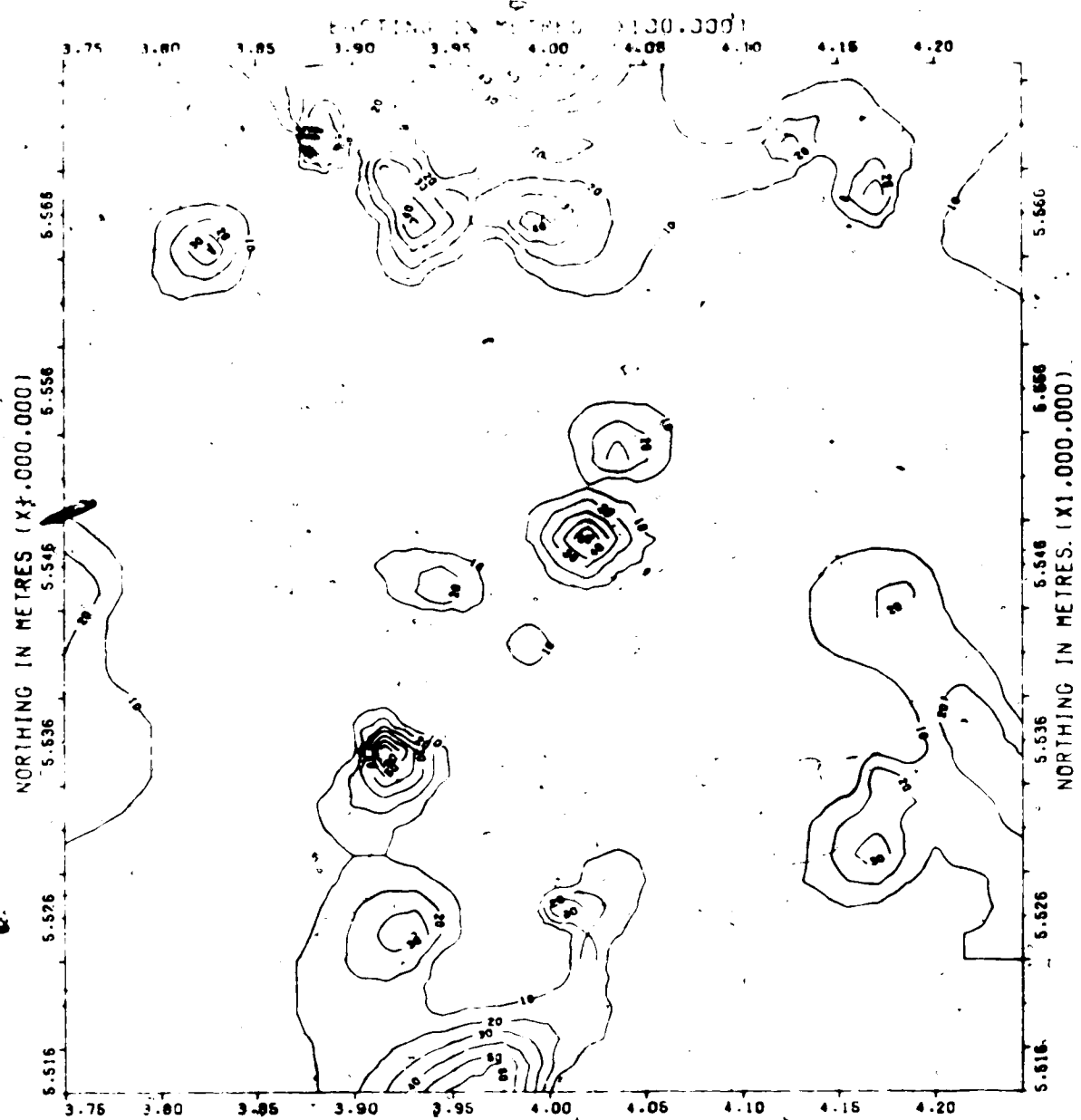
SAND PERCENTAGE MAP : INTERVAL 7

AREA : T10-15/R16-20 W4
 CONTOUR INTERVAL : 10%
 10% CONTOUR DELETED



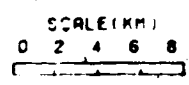
- SAND %
- 0- 20
 - 20- 40
 - 40- 60
 - 60- 80
 - 80-100

FIGURE 34



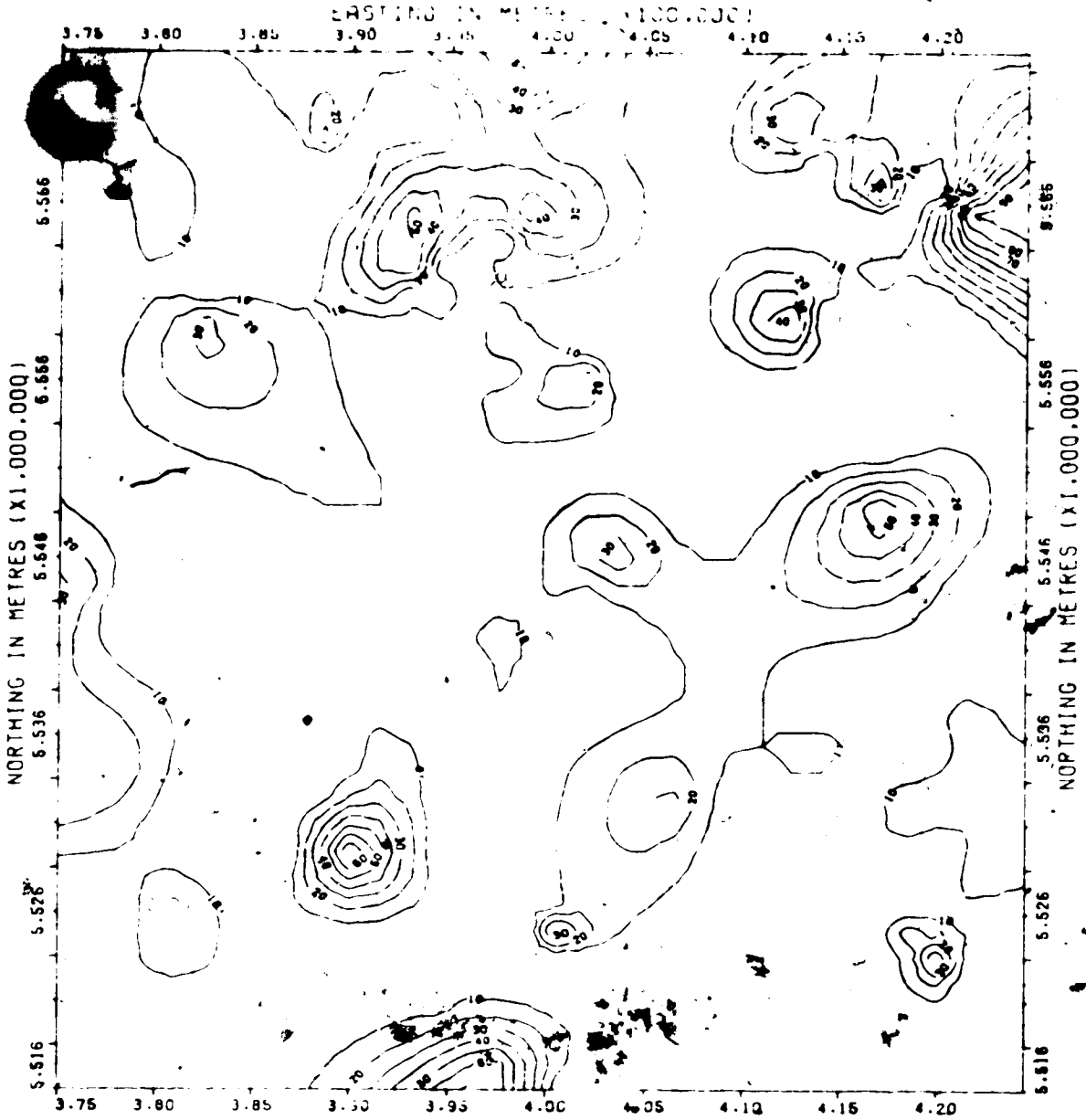
SAND PERCENTAGE MAP : INTERVAL 6

AREA : T10-15.R16-20 M4
 CONTOUR INTERVAL : 10%
 (10% CONTOUR DELETED)



- SAND %
- 0-20
 - 20-40
 - 40-60
 - 60-80
 - 80-100

FIGURE 35

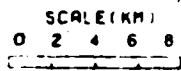


SAND PERCENTAGE MAP : INTERVAL 5

AREA : 1.0-15.R16-20 W4

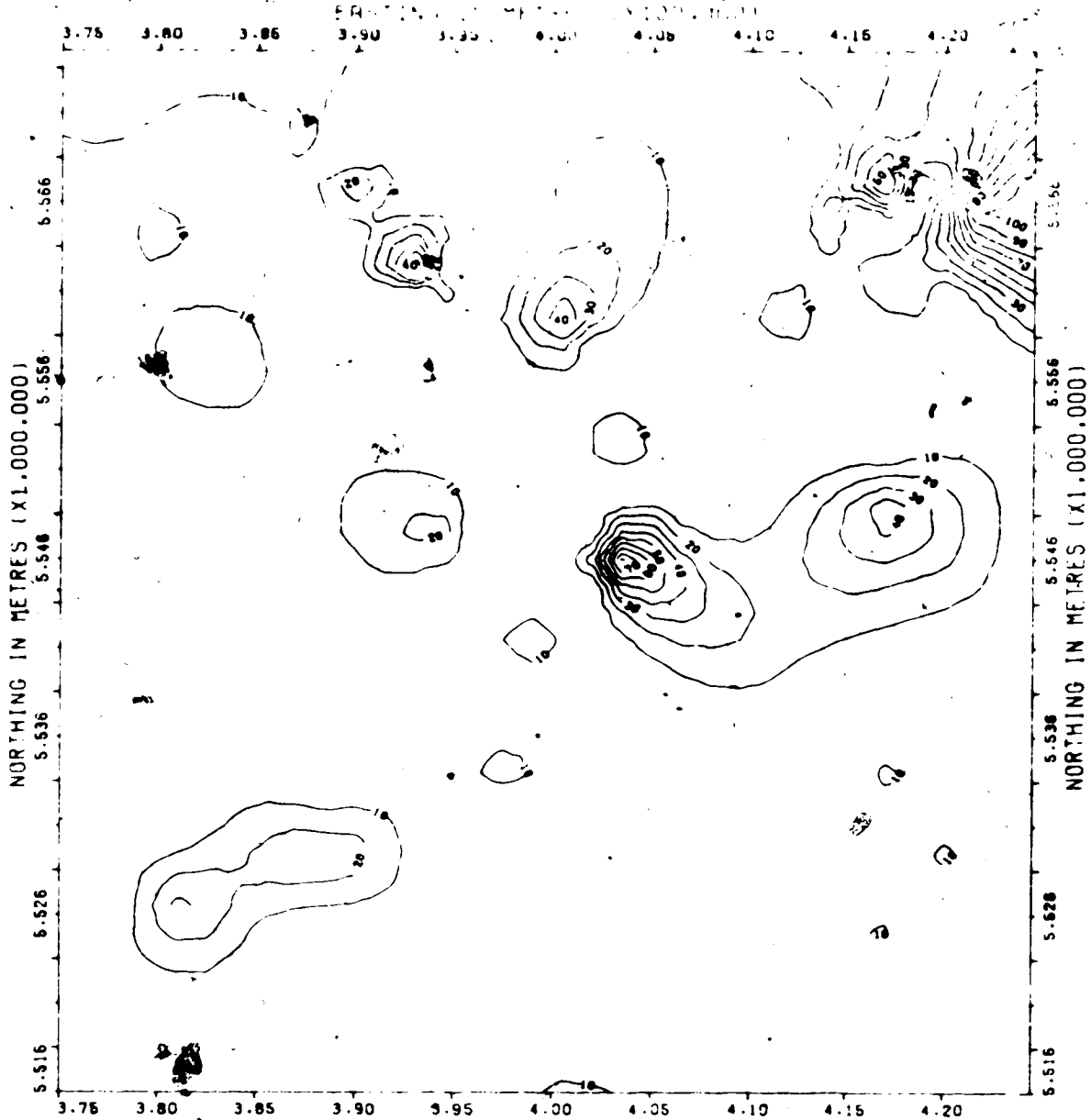
CONTOUR INTERVAL 5%

10% CONTOUR DELETED



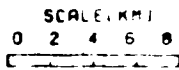
- SCALE (KM)
- | SAND % |
|--------|
| 0-20 |
| 20-40 |
| 40-60 |
| 60-80 |
| 80-100 |

FIGURE 36



SAND PERCENTAGE MAP : INTERVAL 4

AREA : T10-15.R16-20 W4
 CONTOUR INTERVAL : 10%
 10% CONTOUR DELETED



- SAND %
- 0- 20
 - 20- 40
 - 40- 60
 - 60- 80
 - 80-100

FIGURE 37

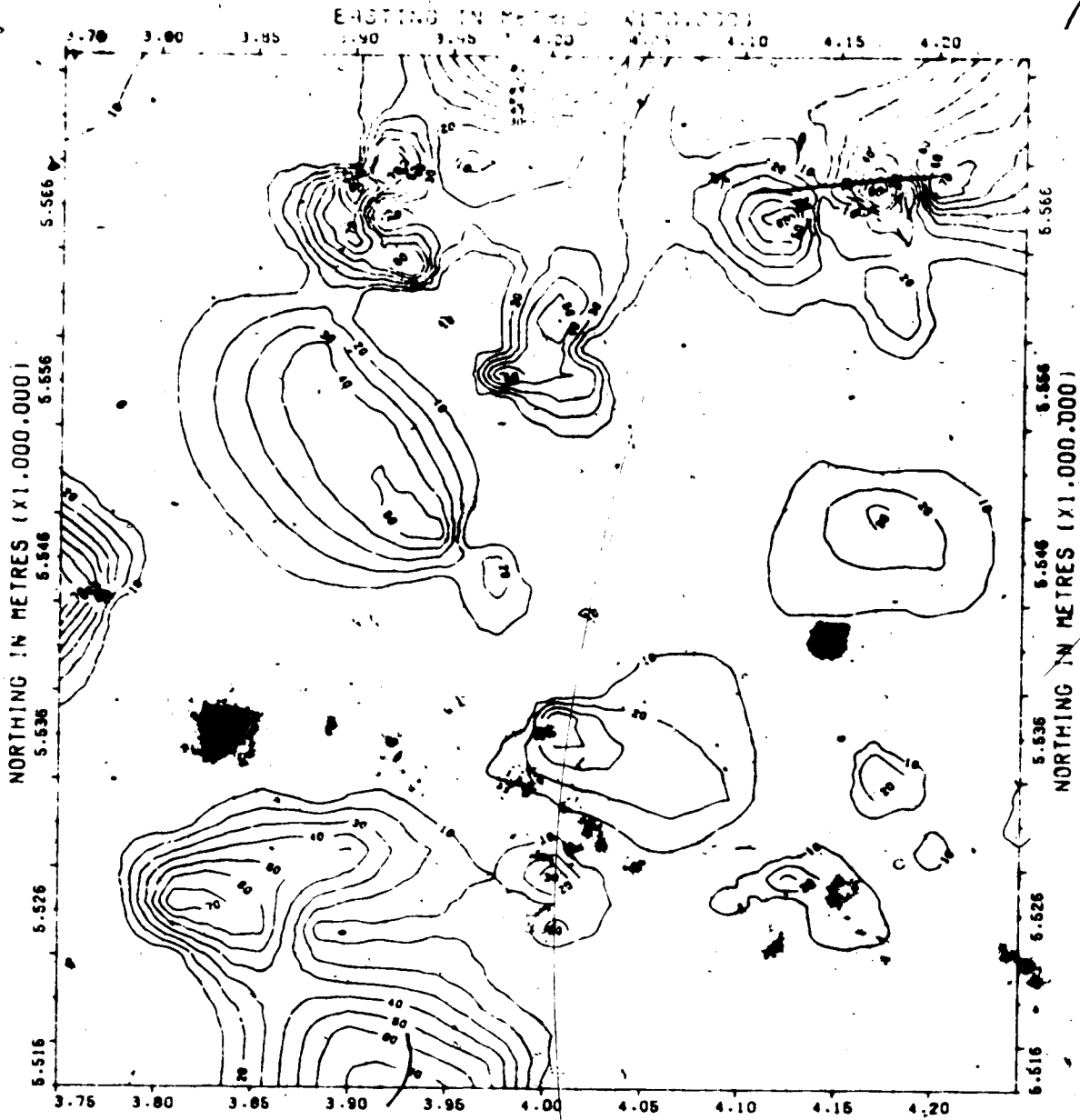
The southern Turin Valley stream maintained a northwesterly course at the time of deposition of Interval 2 (Figure 39). The northeastern stream migrated further into the Turin area, but the volume of sand deposited in the channel decreased. The drainage pattern illustrated in Figure 39 is a composite of the inferred drainage systems of Intervals 3 and 2. The Turin Valley streams formed a single, wide meander belt which, at times, coalesced with the streams in the northeastern and southwestern parts of the map area.

The final phase of Mannville deposition is represented by Interval 1 (Figure 40). Sand distribution is remarkably similar to that of Interval 9, the initial stage of Upper Mannville deposition. The Turin Valley again became the area of greatest sand accumulation, especially within the southern channel.

Inferred drainage patterns are marked on the fourth order trend surface map of Interval 1 (Figure 41). The similarity between the drainage interpretation of this map and that of the second order analysis of the structure on top of the Mannville Group (Figure 17) is obvious.

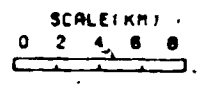
D. QUANTITATIVE ANALYSIS OF SAND DEPOSITION

The application of a gridding program to interval thicknesses measured in each well produced a regular distribution of values from which the average thickness, and hence volume, of each slice was determined. Gridding of interval sand percentage values was used similarly to calculate the volume of sand in each slice. Volumes of the Lower Mannville Group were determined from Intervals 10 and 11. Table 1 shows thickness



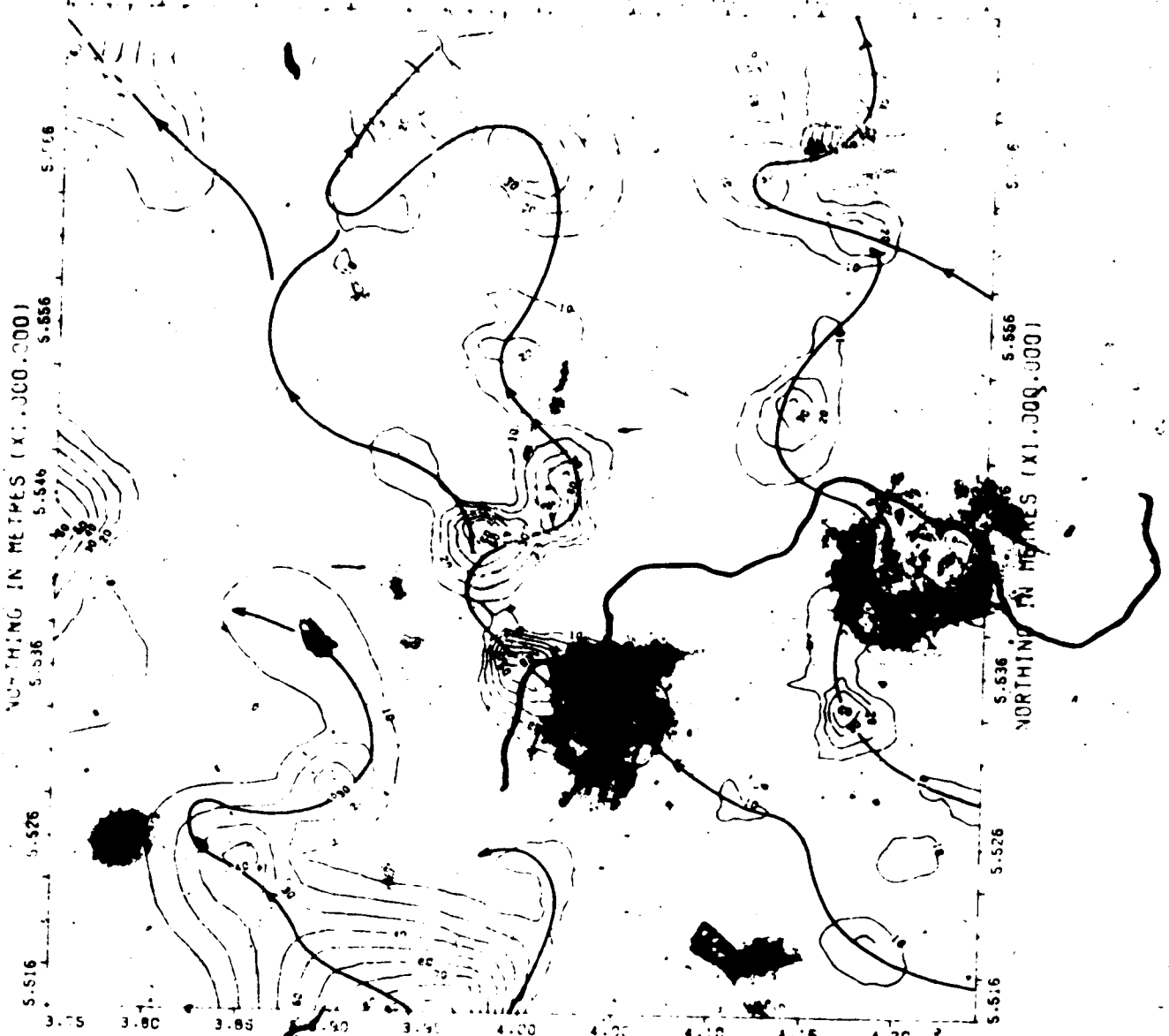
SAND PERCENTAGE MAP : INTERVAL 3

AREA : T10-15-R16-20-44
 CONTOUR INTERVAL : 10%
 (10% CONTOUR DELETED)



- SAND %
- 0 - 20
 - 20 - 40
 - 40 - 60
 - 60 - 80
 - 80 - 100

FIGURE 38



NORTHING IN METRES (X1,000,000)
5.536
5.546
5.556

NORTHING IN METRES (X1,000,000)
5.536
5.546
5.556

5.516

3.75 3.80 3.85 3.90 4.00 4.05 4.10 4.15 4.20

5.516

SAND PERCENTAGE MAP : INFERRAL

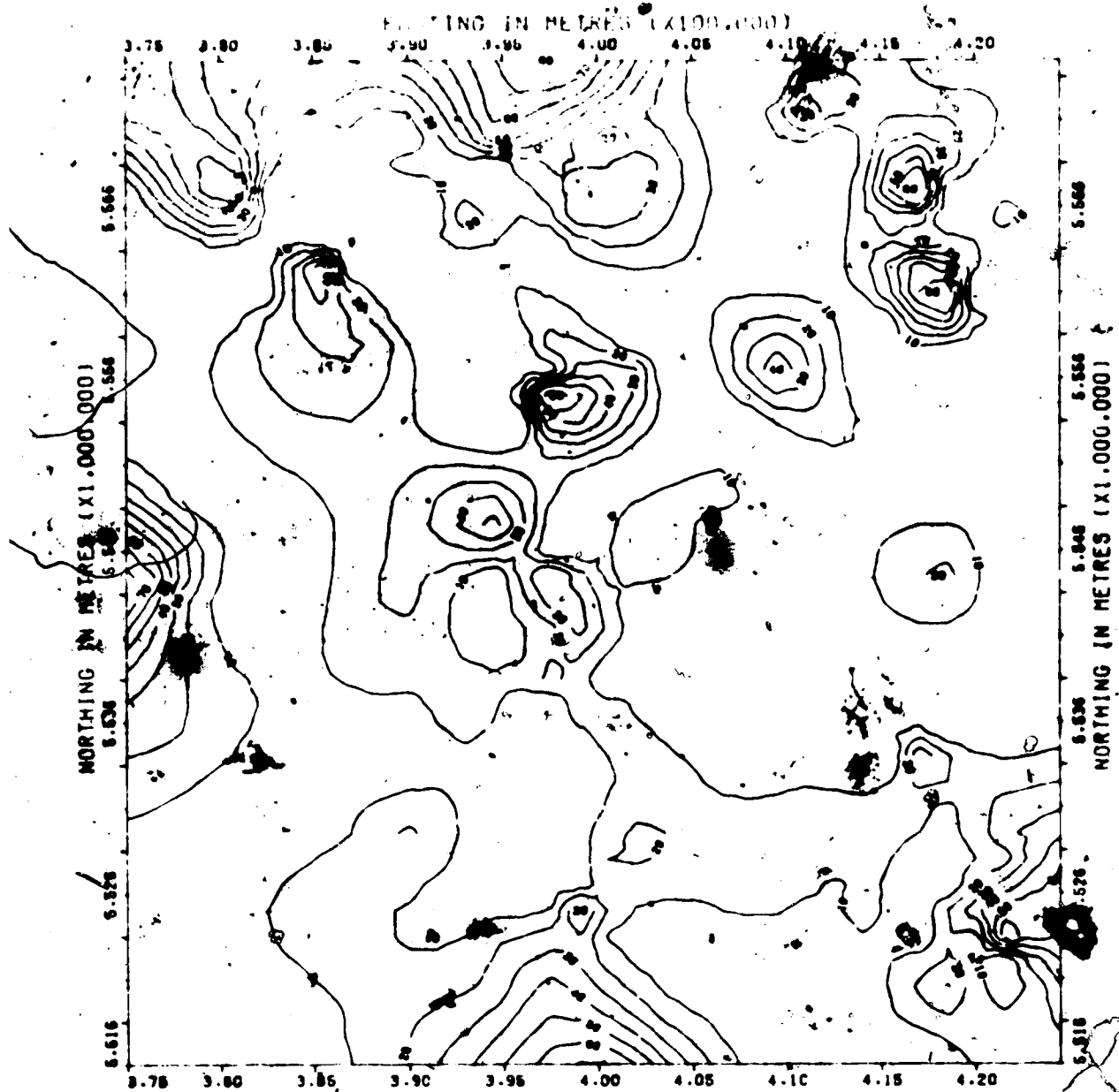
AREA : T10-15.R16-20 W4
CONTOUR INTERVAL : 10%
10% CONTOUR DELETED

SCALE 1:100,000
0 1 2 3 4 5 6 7 8

SAND %
0-10
10-20
20-30
30-40
40-50
50-60
60-70
70-80
80-100

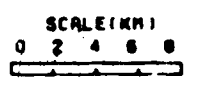
INFERRED STREAMS

FIGURE 39



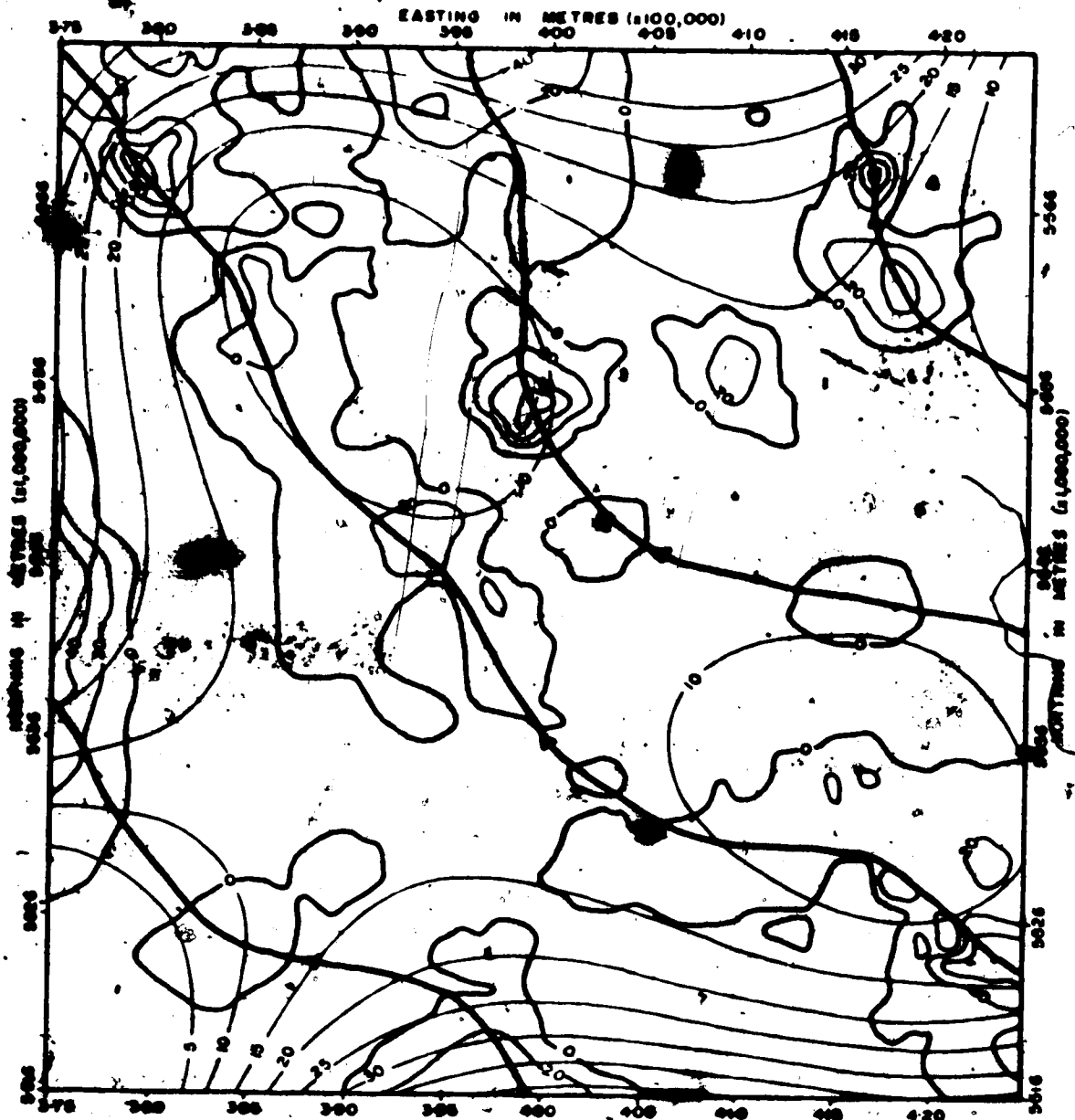
SAND PERCENTAGE MAP : INTERVAL 1

AREA : T10-15, R16-20 M4
 CONTOUR INTERVAL : 10%
 (0% CONTOUR DELETED)



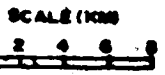
- SAND %
- 0- 20
 - 20- 40
 - 40- 60
 - 60- 80
 - 80-100

FIGURE 40



TREND SURFACE MAP : SAND INTERVAL I

AREA : T10-15, R16-20 W4



TREND SURFACE ORDER : 4TH

TREND SURFACE CONTOUR INTERVAL : 5%

RESIDUALS CONTOUR INTERVAL : 20%

RESIDUALS
 □ POSITIVE

INFERRED
 STREAMS

FIGURE 41

Interval	Average Interval Thickness		Volume of Interval (x-10 ¹⁰)		Volume of Sand in Interval (x-10 ¹⁰)		Percentage of Interval Occupied by Sand	Volume of Sand (x 10 ⁹ cu. m) per metre of Interval
	Metres	Feet	Cu. Metres	Cu. Yds.	Cu. Metres	Cu. Yds.		
1	15.6	51	4.51	5.89	0.59	0.78	13.2	0.38
2	15.6	51	4.52	5.90	0.48	0.62	10.6	0.31
3	15.6	51	4.53	5.91	0.63	0.82	13.9	0.40
4	15.7	52	4.54	5.92	0.30	0.39	6.7	0.19
5	15.7	52	4.55	5.94	0.46	0.60	10.1	0.29
6	15.7	52	4.56	5.96	0.33	0.43	7.2	0.21
7	15.7	52	4.57	5.97	0.29	0.38	6.4	0.19
8	15.7	52	4.58	5.99	0.33	0.44	7.3	0.21
9	15.7	52	4.59	6.01	0.96	1.26	20.9	0.51
10	15.3	50	4.42	5.78	1.49	1.94	33.6	0.97
11	15.3	50	4.40	5.75	2.59	3.38	58.8	1.70

Table 1. Thickness and Volume Parameters of Sand Intervals

and volume parameters for sand intervals. The data presented in Table 2 were derived from Table 1.

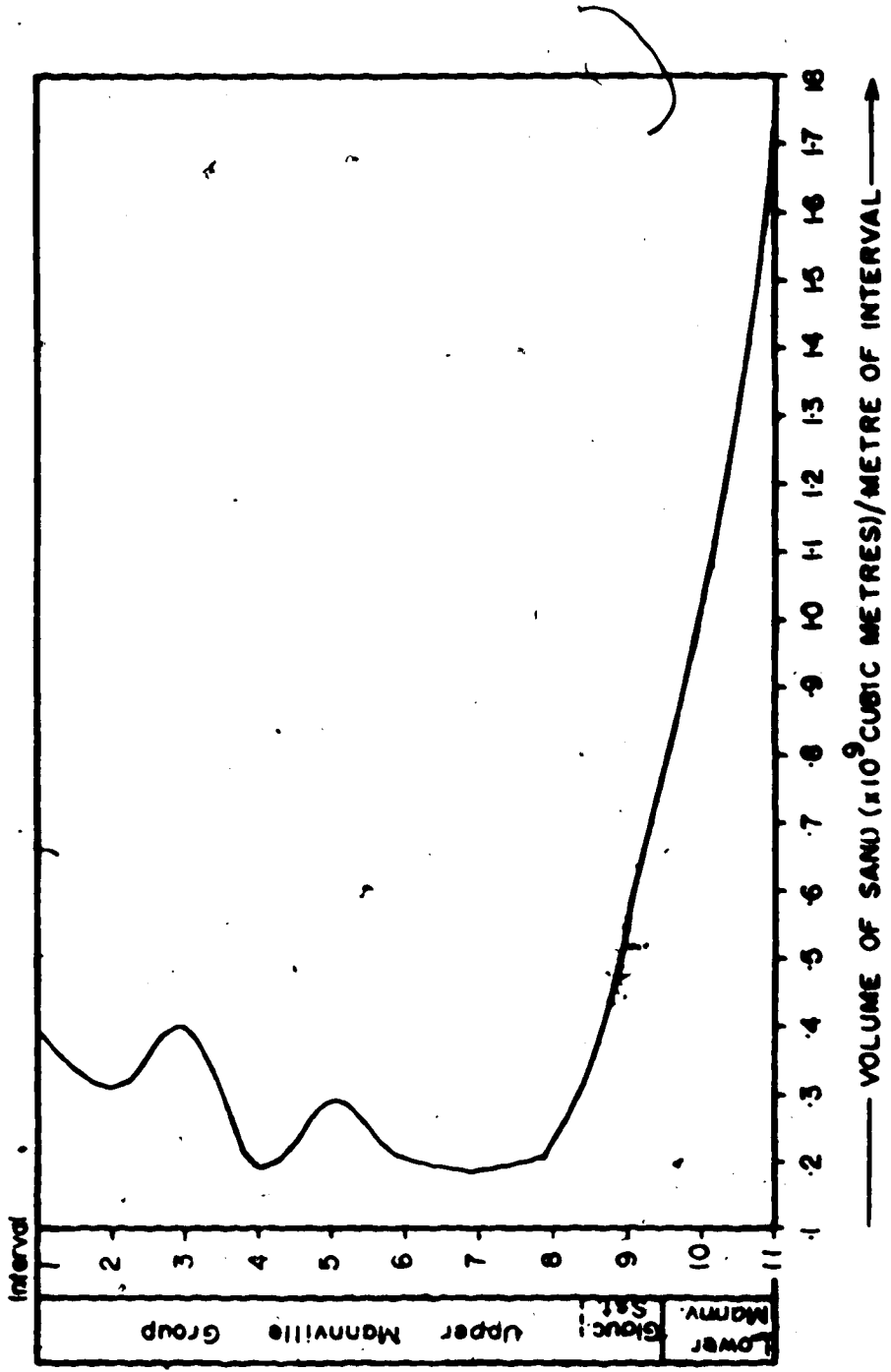
	Cu. Yds.	Cu. Metres
Vol. Mannville Group	6.51×10^{11}	4.98×10^{11}
Vol. Upper Mannville Group	5.36×10^{11}	4.10×10^{11}
Vol. Lower Mannville Group	1.15×10^{11}	0.88×10^{11}
The Upper Mannville constitutes 82.3% and the Lower Mannville 17.7% of the total volume of the group.		
Vol. sand (Mannville Gp.)	11.06×10^{10}	8.46×10^{10}
Vol. sand (U. Mannville Gp.)	5.73×10^{10}	4.38×10^{10}
Vol. sand (L. Mannville Gp.)	5.33×10^{10}	4.08×10^{10}
Seventeen percent of the Mannville Group consists of sand, 52% of which occurs in the Upper Mannville Group and 48% in the Lower Mannville Group.		

Table 2. Volume Parameters for the Mannville Group

Hence, the Lower Mannville Group contains about four and one quarter times the volume of sand per unit thickness compared with the Upper Mannville Group, as derived from $[48 + (\frac{17.7}{82.3} \times 52)]$. This reflects the rapid rate of erosion of the source area during early Mannville time. The volume of sand deposited in the Upper Mannville Group, however, would be greater than indicated because of the marginally higher gamma ray response of late Mannville sandstones caused by high clay content. A more mature landscape and the associated decrease in depositional energy of late Mannville streams would have resulted in larger volumes of clay accumulating within sand bodies, compared with sands deposited during early Mannville time. The volume

of sand per metre of interval thickness for successive intervals is shown in Figure 42. The rate of decrease in the volume of sand deposited is constant between the base of the Mannville Group and the top of the Glauconitic Sandstone Equivalent. This suggests a constant rate of erosion of the Lower Mannville source area until Ostracode Zone time (when no sand was entering the Turin area), followed by minor uplift and erosion during "Glauconite" time. Alternatively, the decrease in the volume of sand deposited may have been due to a raising of base level at this time. The former explanation is favoured, although the data is not conclusive. Herbaly (1974) noted that early Cretaceous sandstones of the Sweetgrass arch had a western origin. In central Alberta, Williams (1963) and Williams et al. (1962) inferred an eastern source (Canadian Shield) for the Lower Mannville Group and a western source (Cordilleran region) for the Upper Mannville Group, based on the mineralogy of the sandstones and radiometric ages of detrital minerals. The proximity of the Turin area to the Cordilleran region resulted in it being little affected by the products of erosion of the Shield.

In post-"Glauconite" time the volume of sand deposited (Figure 42). This was a response to either periodic uplift of the source or intermittent regional variations in drainage pattern. Data presented previously show Mannville streams to be confined to fairly narrow meander belts (of a few miles) due to structural control by the pre-Cretaceous surface. Periodic rejuvenation of a maturing source area was therefore responsible for the pulses of sand deposition during late Mannville time. This is confirmed by studies of the Mannville source area. Potassium-Argon dates determined by Baadsgaard et al. (1961) for the time of intrusion of phases of the Nelson, Coast Range and Cassiar-Omineca batholiths



SAND VOLUME DISTRIBUTION, MANNVILLE GROUP

FIGURE 42

of the Cordillera, ranged from 96 million years (m.y.) to 107 m.y. London (1961) dated phases of the intrusion of the Nelson and adjacent batholiths at 101 m.y. and 127 m.y. According to the time scale of Obradovich and Cobban (1975), these periodic igneous intrusions and uplift occurred during the Albian, the time at which the Upper Mannville Group was deposited.

E. CONCLUSION

Clean sands were deposited mainly within the channels of high energy streams throughout Mannville time. The position of Mannville channels was governed by the position of channels in the pre-Mannville surface. Lower Mannville sediments consisted mainly of sand, the volume of which decreased upwards through the section in response to a levelling of the Cordilleran source area. Early Mannville streams maintained relatively narrow courses confined by ridges of Mississippian and Jurassic strata.

Although the basic elements of the early Mannville drainage persisted, the four main drainage systems periodically coalesced during late Mannville time to form extensive floodplains crossed by numerous, small braided and meandering streams. Silt and mud deposition predominated, with periodic influxes of sand resulting from rejuvenation of the source area.

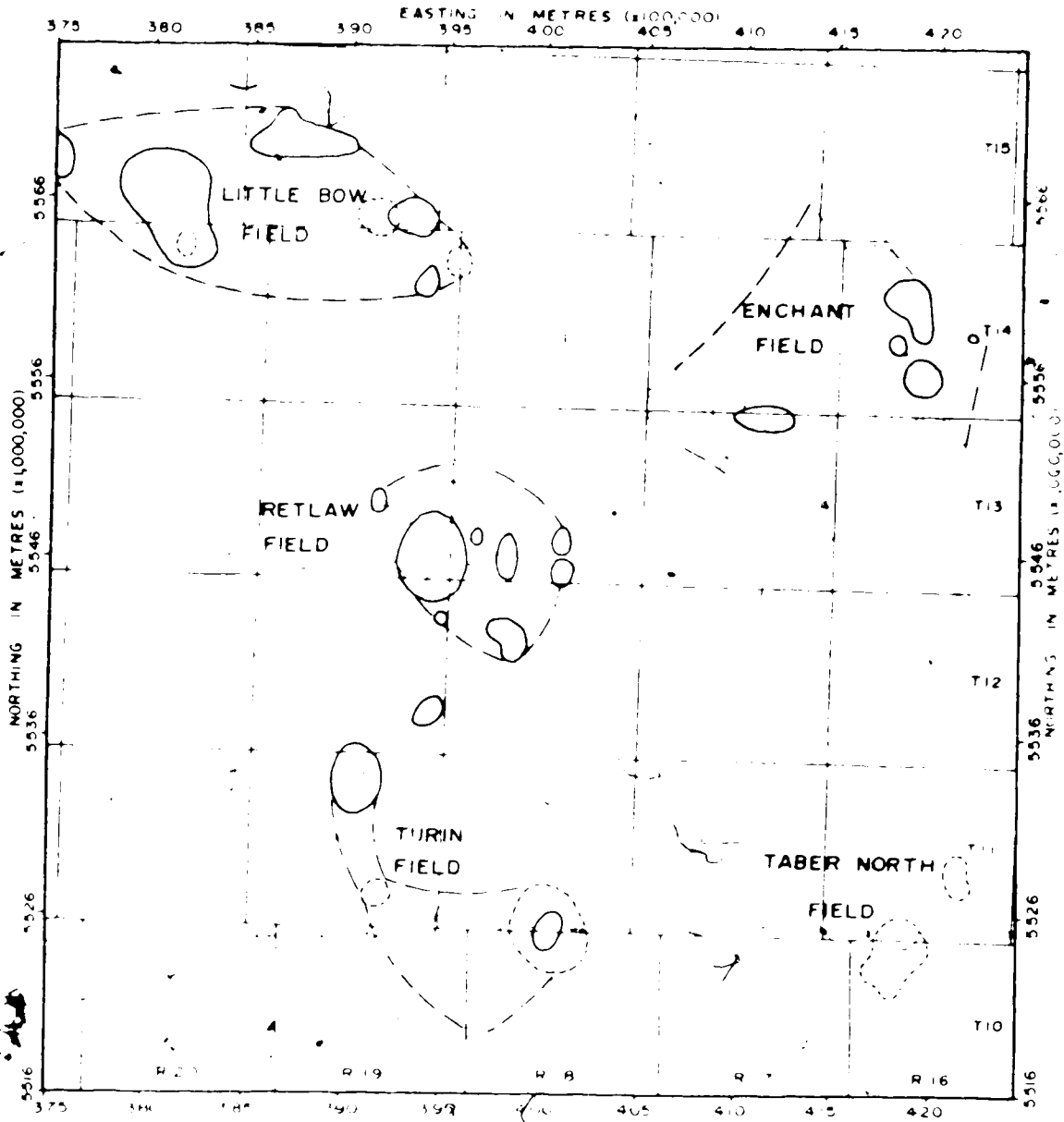
Chapter VII
PETROLEUM DISTRIBUTION

A. INTRODUCTION

Petroleum occurrence was stored on computer file according to well location, type of show (major or minor oil or gas, oil or gas cut mud, condensate) and stratigraphic position (uppermost Upper Mannville Group, mid Upper Mannville Group, Glauconitic Sandstone Equivalent, sandstones within fifty feet of the Ostracode Zone, and the remainder of the Lower Mannville Group). The distinction between the major and minor oil or gas occurrences was qualitative. Major occurrences were designated as those wells which had been or were presently on production or were capped for future production. Only wells from which structural and sand data were acquired were used in determining petroleum occurrence, thereby precluding a number of development wells in which electric logs were not run.

Maps were generated for each stratigraphic interval showing the distribution of each type of show. For reasons of brevity, only maps of major oil and gas occurrence in the Lower Mannville Group and the Glauconitic Sandstone Equivalent, and all oil and gas occurrences in the Upper Mannville Group (above the Glauconitic Sandstone), are presented.

The outlines of Cretaceous oil and gas pools of the Turin area (Figure 43) were reproduced from the Geological Survey of Canada map of oil and gas pools of western Canada (Map 1316A, 1970). All pools shown have recoverable reserves of greater than one billion cubic feet



PETROLEUM DISTRIBUTION - LOWER CRETACEOUS

- UPPER MANNING FORMATION
- LOWER MANNING FORMATION
- BOWLAND FORMATION
- ...

FIGURE 43

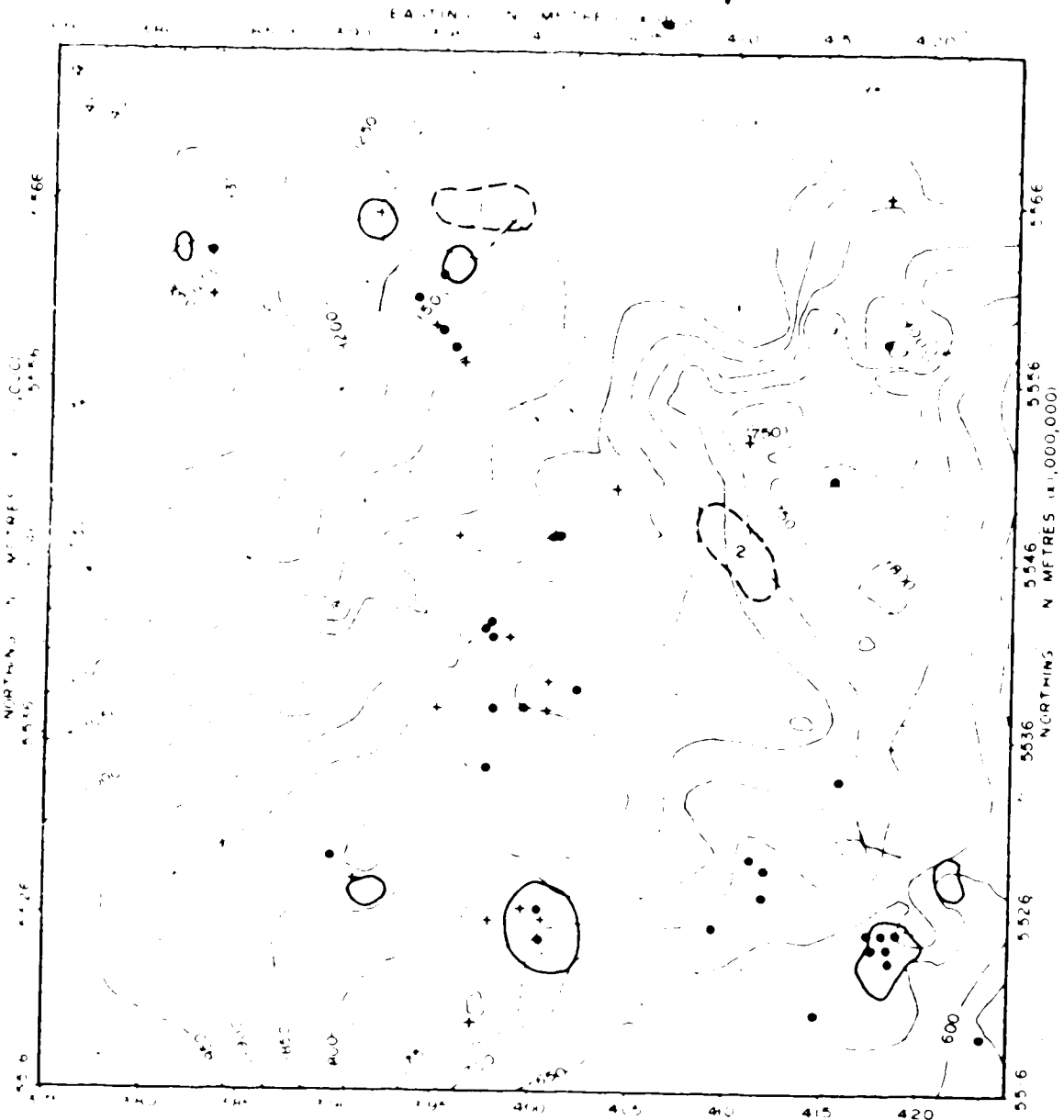
of gas or one thousand barrels of oil. The extension of some fields subsequent to the publication of the map in 1970 accounts for the occurrence of computer plotted production wells beyond the indicated field limits shown in Figures 44 to 46.

B. LOWER MANNVILLE GROUP

Oil and gas production from the Lower Mannville is obtained from the Sunburst Sandstone. Traps are stratigraphic, and related exclusively to topographic highs in the pre-Mannville surface. Petroleum distribution has been superimposed upon the structure contour map of the base of the Mannville Group to illustrate structural control (Figure 44). Pre-Mannville highs correspond to Lower Mannville isopach thins (Figure 14). Southeastward oil and gas migration probably occurred in the Tertiary due to regional tilting.

The Taber, North field lies at the southeastern end of the Turin Valley, on the western flank of the Sweetgrass arch. Sandstones lense out into shales in an updip (southeasterly) direction. The two main pools are located on ridges flanking the northern Turin Valley stream. The southern ridge is more prominent and extends the length of the Turin Valley (this feature was discussed in previous chapters). Drilling of the ridge in the last six years has resulted in the discovery of a number of major oil pools. One small pool was defined on the northern ridge.

Mainly gas production is obtained from the Turin field which is located along the southwestern side of the crest of the Jurassic cuesta. The field occurs at the structurally higher southeastern end of the cuesta.



PETROLEUM DISTRIBUTION : LOWER MANNVILLE GROUP
 SHOWN BY BASE OF MANNVILLE GROUP STR. (SEE INTER. MAP (ATUM MSL))

- MAJOR OIL FIELD
- OIL FIELD (M.S.L. AFTER 1975)
- ⊕ MAJOR GAS FIELD
- ⊕ MEDIUM GAS FIELD
- ⊕ SMALL GAS FIELD
- ⊕ GAS AT M.S.L.
- ⊕ WELLS

FIGURE 44

The Little Bow field is located over a broad Mississippian high extending northwest from the Enchant Ridge fault trend. Oil and gas pools overlie localized highs and structural noses within the field. Since 1970, small pools have been discovered to the southeast of the Little Bow field, along the northeastern side of the Turin Valley.

Lower Mannville oil and gas production is also a function of sand distribution, occurring only where highs are capped or flanked by sequences of moderate to high sand content (greater than 40%). This accounts for the lack of production from Enchant Ridge and the northwestern end of the Jurassic cuesta. The Lower Mannville isopach in these areas varies from 20 to 50 feet, the upper 15 to 20 feet of which consists of shales of the Ostracode Zone, which overlie late Lower Mannville silts and muds. Interval sand percentage values range from 0 to 20 (Figure 27). Three small pools occur in local depressions on the Enchant Ridge where sand content increases to 50%. The zone of no production at the centre of the median Turin Valley Ridge also corresponds to sand percentage values less than 20%.

Using the criteria of high sand percentage values coincident with pre-Mannville highs and Tertiary southeastward migration of fluids as the main factors determining the accumulation of Lower Mannville petroleum, two potential undrilled areas occur within the Turin area (undrilled according to Alberta Research Council's well file and Carter Mapping's one mile well maps of the area).

An area three and one half miles long by two miles wide in the southwestern part of Township 15, Range 18, extending from the eastern limit of the Little Bow field, holds definite gas potential (Area 1, Figure

44). It overlies the northwestern extension of Inchant Ridge, and has sand values of 60 to 70 percent indicated on the sand percentage map of Interval 12 (Figure 27), the uppermost slice of the Lower Mannville Group. Sand content decreases towards the east (updip), and the zone occurs within a closed isopach thin, in which Lower Mannville thickness ranges from 25 to 100 feet. The structure on top of the Lower Mannville (Figure 13) shows closure in three directions on the Ostracode Zone shale. Closure to the east is provided by shaling out of the sands in Interval 12. The prospect consists of 5 to 40 feet of clean sand capped by 20+ feet of shale with closure in four directions. Gas production occurs at the limits of closure (between the 75 and 100 foot isopach contours) in the northwest (Township 15, Range 19), and beyond the limit of closure in the southeast (Township 14, Ranges 18 and 19). A suspended gas well is located in the north in Township 15, Range 18, at the 60 foot isopach contour. Consequently the crest of the feature remains undrilled. This may be due to its east-west orientation, contrary to the northwesterly trend of the majority of pools in the Turin area, including the Lower Mannville pool of the adjoining Little Bow field.

Reserve calculations for gas above the 60 foot isopach contour indicate:

Volume of pool = 1.673×10^9 cubic feet (assuming 10 foot average net pay over 6 square miles)

Average porosity = 20% (average porosity of Lower Mannville pools in Little Bow field = 19.8%)

Water saturation = 30% (as in Little Bow field)

Assumed expansion factor = 115 (based on a reservoir top at -1,100 feet subsea, temperature change from 105°F to 60°F and an associated pressure change from 1,675 psia to 14.65 psia)

Therefore the potential gas in place is $1.673 \times 10^9 \times .2 \times .7 \times 115 = 27$ billion cubic feet.

For this and other potential areas, closures and volumes were derived from computer contoured maps. Verification of reserves, or for that matter the validity of the existence of pools, by hand contouring and detailed log examination, was not attempted. The above description and calculation is designed to show that rapidly generated regional computer maps are useful exploration tools for a "first look" at a region, limiting the number of areas requiring time consuming, detailed hand analysis.

A four mile by two mile, northwesterly-trending undrilled area between the town of Retlaw and the southwestern margin of the Enchant field (Bow Island production, has moderate potential (Area 2, Figure 44). The area lies between the northern Tyrin Valley channel and Enchant Ridge. Sand values in Interval 12 decrease from 80% to 50% towards the southeast and southwest, and decrease to zero towards the top of Enchant Ridge. Sands are capped by shales of Interval 9 (0 to 10% sand). If the decrease in sand is partly due to lensing, a trap exists in the southeast of the area because of the regional northwesterly dip.

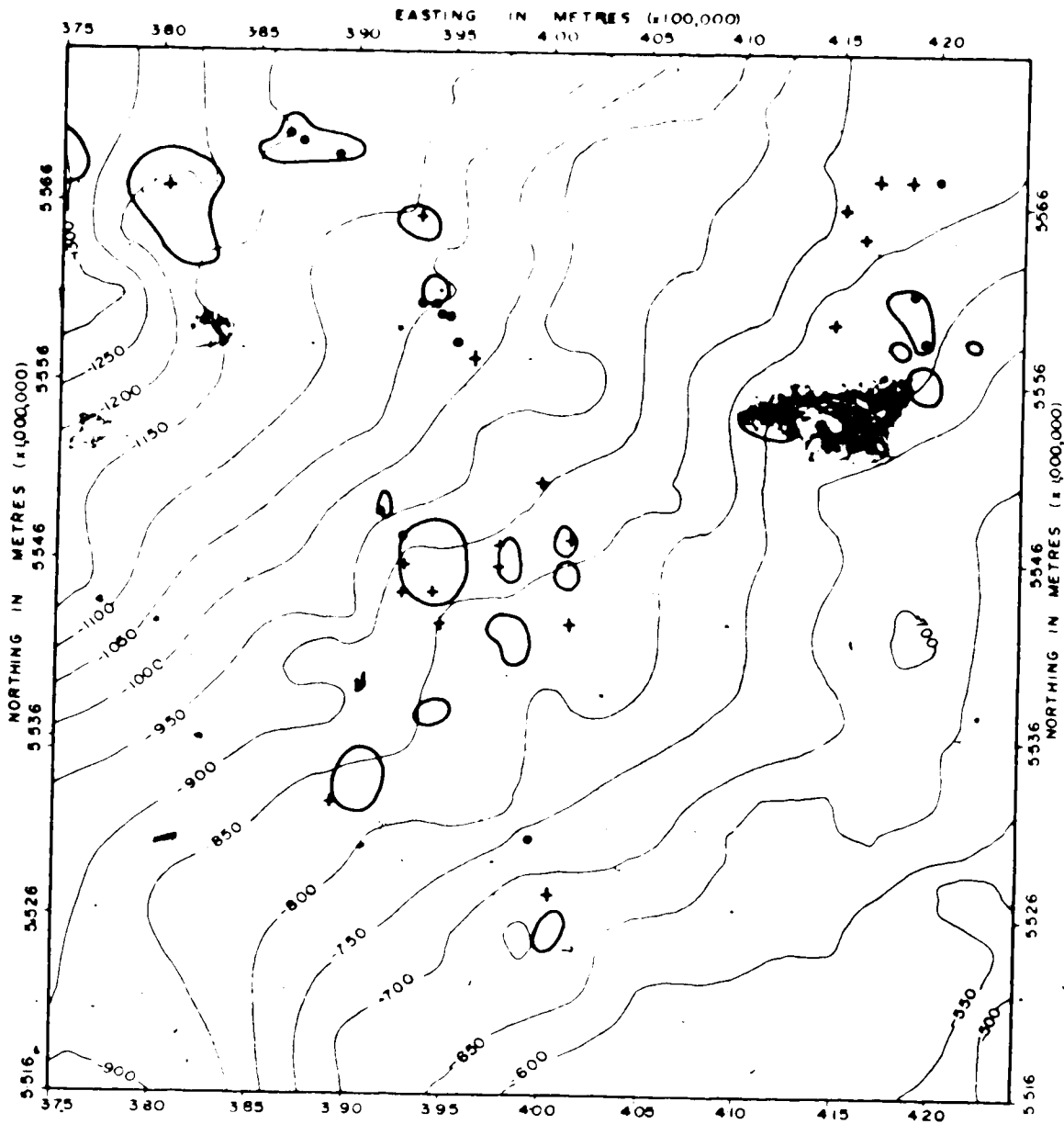
C. GLAUCONITIC SANDSTONE EQUIVALENT

Petroleum distribution in the Glauconitic Sandstone Equivalent, and factors controlling its occurrence are similar to those in the Lower Mannville Group. The outlines of oil and gas fields have been superimposed on the structure map on the top of the Lower Mannville to illus-

trate structural control (Figure 45). The Glauconitic Sandstone Equivalent is approximately coincident with Interval 9 (Figure 31). Oil and gas production is obtained from the Little Bow and Turin fields, and from the Retlaw field at the northwestern end of the median Turin Valley Ridge. The main Retlaw pool overlies part of a local sand concentration (with up to 90% sand) deposited around the end of the ridge by the southern Turin Valley stream. The absence of a comparable sand buildup during early Mannville time explains the limited Lower Mannville Retlaw production. The main Little Bow and Turin pools occur within local sand concentrations. Minor shows only are found in the Taber North area because of a lack of reservoir sandstone. Oil production in the Enchant field occurs from a depression containing up to 30% sand on the northern side of the Enchant Ridge. Oil and gas fields in the Glauconitic Sandstone Equivalent are capped by shales of Intervals 8 and 9 and underlain by the impervious Ostragode Zone. Decreased sand deposition in Interval 9 restricted the distribution of reservoirs and for this reason, the two potential Lower Mannville occurrences are not overlain by pools within the Glauconitic Sandstone Equivalent. No undrilled prospects are apparent in the Glauconitic Sandstone Equivalent.

D. UPPER MANNVILLE GROUP (POST-GLAUCONITIC SANDSTONE EQUIV.)

Production and shows in the Upper Mannville Group are negligible (Figure 46); small amounts of oil are produced from the Retlaw field, and gas is obtained from the Enchant field. Thick shales have prevented the upward migration of petroleum into the irregularly distributed Upper Mannville sand lenses. In the Enchant field, production is obtained



PETROLEUM DISTRIBUTION : GLAUCONITIC SANDSTONE EQUIV.

SHOWN ON TOP OF LOWER MANNVILLE GROUP STRUCTURE CONTOUR MAP (DATUM MSL)

- MAJOR OIL + MAJOR GAS
- POOL LIMITS, AFTER G.S.C. (1970)

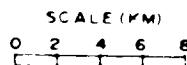
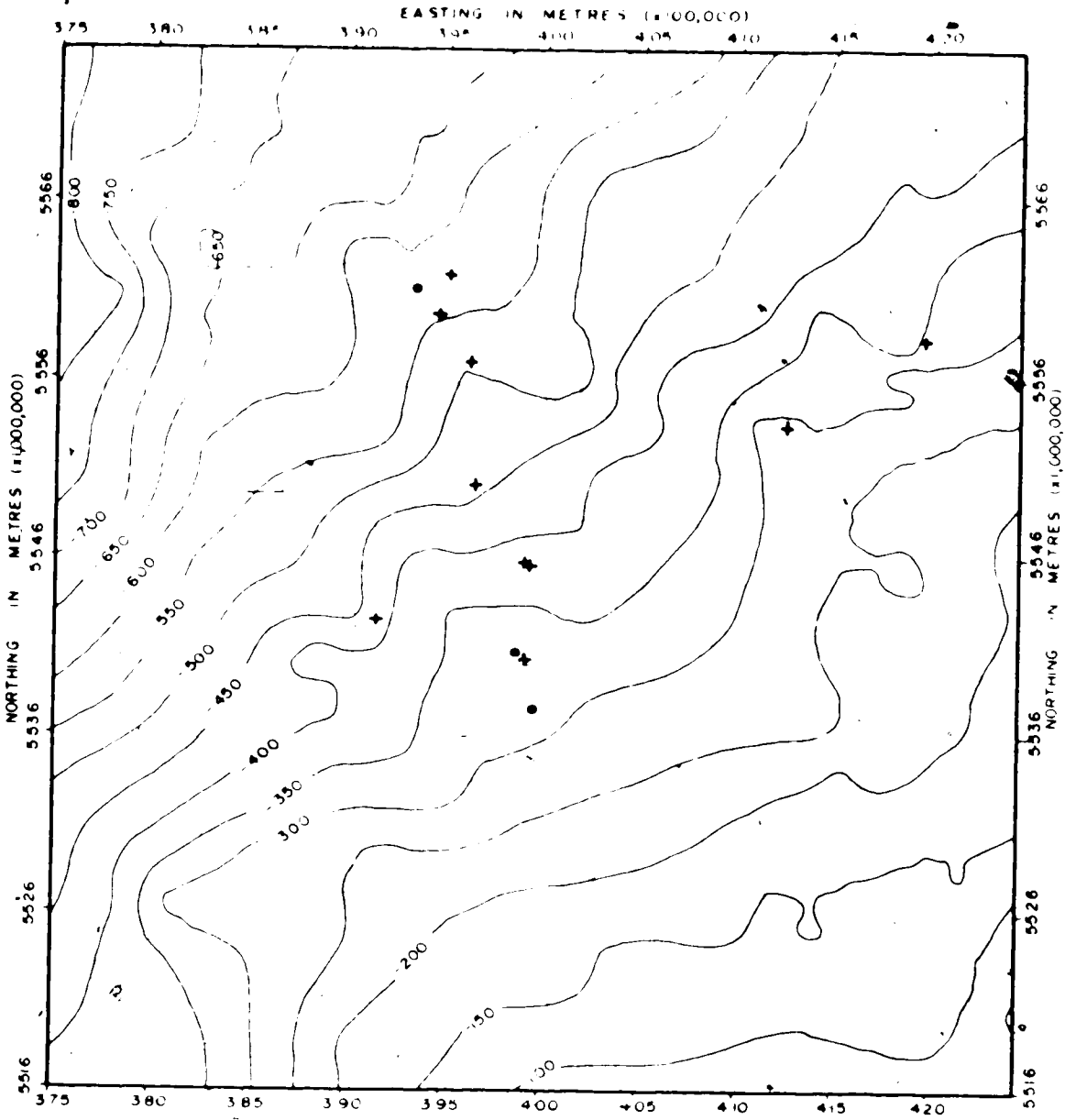


FIGURE 45



PETROLEUM DISTRIBUTION : UPPER MANNVILLE GP.

SHOWN ON TOP OF MANNVILLE GROUP STRUCTURE CONTOUR MAP (DATUM M.S.L.)

● OIL SHOW + GAS SHOW

SCALE (KM)

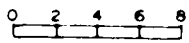


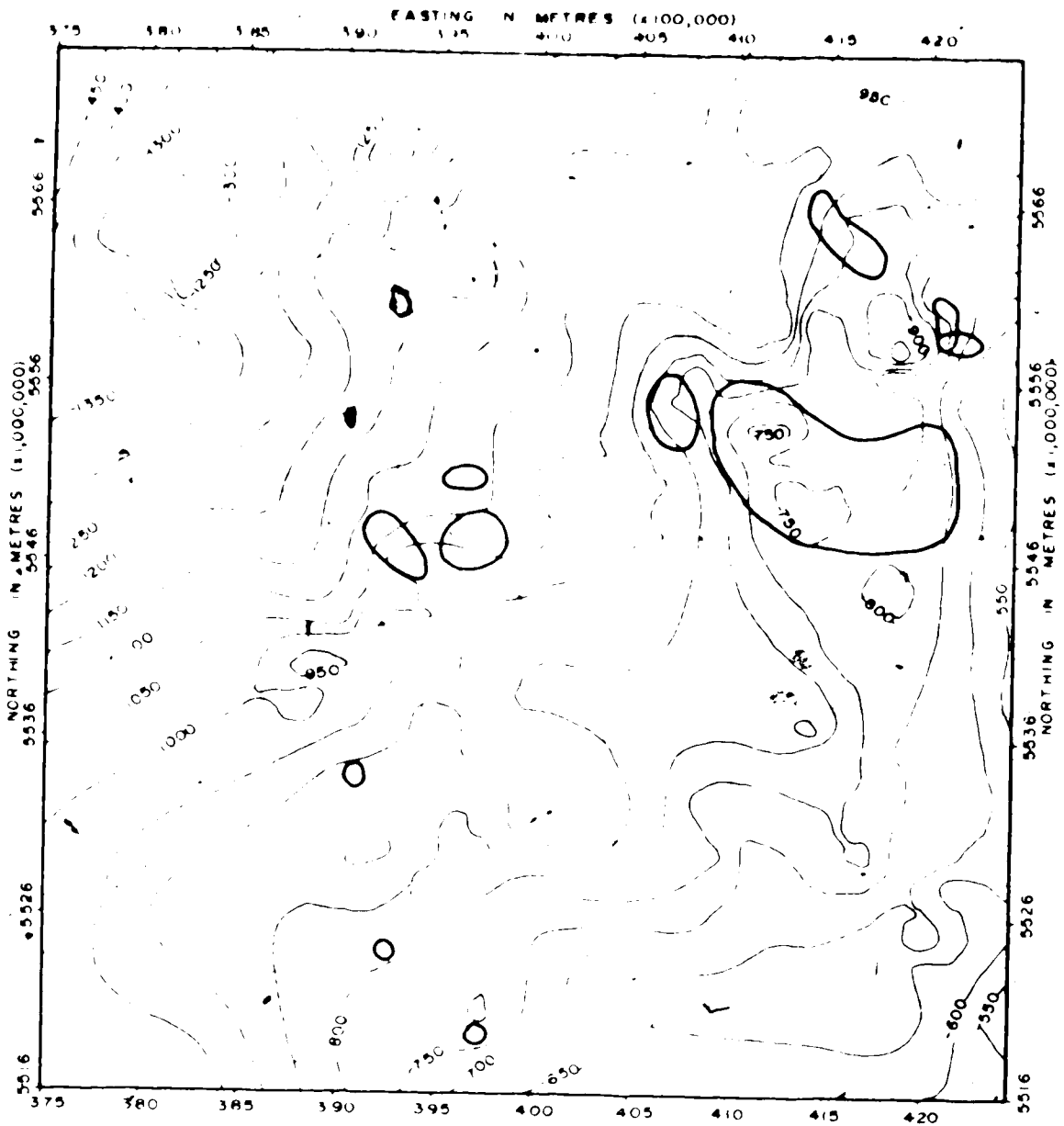
FIGURE 46

from the sandstones at the top of the Mannville Group, suggesting that marine Colorado shales may have been the source of the gas. The absence of sands in Interval 1 (Figure 40) over the Jurassic cuesta prevented comparable pools developing in the southwestern map area.

POST-MANNVILLE GROUP

Data on post-Mannville petroleum occurrences were not collected; however, inferences may be made from the distribution of gas in the Bow Island Formation as mapped by the Geological Survey of Canada (1970). Gas fields, when superimposed on the base of Mannville structure contour map (Figure 47), are seen to occur above pre-Mannville topographic highs of greatest relief. Differential compaction of Bow Island and underlying strata over the highs appears to have formed the traps. The largest occurrence is the Enchant field, which overlies Enchant Ridge; gas also occurs over the median Turin Valley Ridge (Retlaw field) and at the southeastern end of the Jurassic cuesta (Turin field).

Bow Island gas fields are also coincident with positive residuals on the base of the Mannville Group trend surface map (Figure 12). The Little Bow field (Mannville production) overlies the large northwestern residual, and the absence of Bow Island gas in this field is probably due to lack of an updip seal, permitting migration towards the Enchant field. The residual between the Little Bow field and the Enchant Ridge which is apparent on Figure 12, is absent on the trend surface map on the top of the Mannville Group (Figure 17), because of erosion of the high during late Mannville time. As a consequence, no structure is present at the Bow Island stratigraphic level, and no gas accumulation occurs.



PETROLEUM DISTRIBUTION : BOW ISLAND FORMATION

SHOWN ON BASE OF MANNVILLE GROUP STRUCTURE CONTOUR MAP (DATUM M.S.L.)

○ GAS POOLS, AFTER G.S.C. (1970)

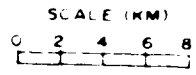


FIGURE 47

Chapter VIII

SUMMARY AND CONCLUSIONS

1) The Turin area lies at the margin of the Sweetgrass arch and the West Alberta basin. Continental sediments of the Mannville Group were deposited on an eroded surface of southwesterly-dipping Mississippian and Jurassic strata. The drainage pattern developed on this surface reflected the northwesterly strike of the bedding. The physiography was dominated by a Jurassic-capped Mississippian cuesta in the southwest and a fault-controlled Mississippian ridge in the northeast (Enchant Ridge), separated by the Turin Valley.

2) Sediments were derived from the Cordilleran region, which was subject to batholithic intrusion and uplift during the early Cretaceous. Sand deposition predominated initially, confined to pre-Mannville channels. Consequently, sand bodies are linear in form. Infilling of valleys and denudation of the ridges produced a land surface of low relief by late early Mannville time. Sand continued to be deposited along the axes of pre-Mannville valleys, while fine-grained sediments accumulated in lower energy depositional environments removed from active stream flow. Maturation of the source area is reflected in the progressive decrease in the volume of sand deposited, culminating in the widespread deposition of Ostracode Zone shales.

3) Differential compaction of Lower Mannville sediments produced an Upper Mannville depositional surface similar to, yet more subdued in form than that which existed during early Mannville time. Silts and muds were the main sediments deposited, but periodic uplift and erosion of the source area resulted in the influx of sand, the distribution of which was more variable than that of the underlying sequence. Drainage channels frequently coalesced to form wide valleys and floodplains of meandering streams. The section thickens regionally towards the southwest.

4) Mannville sedimentation was halted by the onset of the Colorado sea. The present structural configuration of the basin is the result of northwesterly tilting during the Tertiary.

5) Distribution of petroleum in the Mannville Group is a function of pre-Mannville topography, sand distribution, and Tertiary tilting. Traps are stratigraphic, and are formed by channeling out of channel sands to an axial (southerly) direction. Fields are confined to the tops and flanks of structural highs, which correspond to ridges in the pre-Mannville surface. Production occurs mainly from the sandstone and the siliceous sandstone Equivalent, capped by thin shales, which have prevented the upward migration of petroleum into higher reservoirs. Gas in the uppermost sands of the Mannville was probably derived from marine shales of the Colorado Group. Gas in the Bow Island formation occurs in traps formed by differential compaction over upper Mannville highs, where closure exceeded the degree of Tertiary tilting.

6) Computer-generated structure and trap maps were of a satisfactory standard for regional interpretation. Some of the subjectivity inherent in hand-contouring data was eliminated by the mechanical gridding and contouring algorithms used in the computer programs. Even though these mechanical techniques have a degree of "subjectivity" (e.g., the methods used to choose control points and interpolate to grid nodes), mapping is performed in exactly the same way each time. Trends were mapped which otherwise may have been overlooked due to geologic prejudice of the area. Sand percentage analysis, using proportionate and fixed slices through the Mannville Group, was an effective means of mapping gross sand distribution and the geometry of sand bodies. Trend surface analysis was useful in enhancing local features on structure contour maps, permitting a

more accurate interpretation of the Mannville drainage pattern. The irregular regional sand distribution prevented statistically valid surfaces being fitted to sand percentage data. The resulting residuals showed little that was not already apparent on raw data contour maps.

REFERENCES

- Acham, P.A., 1971, The Mannville Group (Lower Cretaceous) of the Hussar area, southern Alberta. Unpubl. M.Sc. Thesis, Univ. of Alberta, Edmonton.
- Allen, J.R.L., 1965, A Review of the Origin and Characteristics of Recent Alluvial Sediments. *Sedimentology* 5(2), 89-191.
- Baadsgaard, H., Folinsbee, R.E. and Lipson, J., 1961, Potassium - Argon Dates of Biotites from Cordilleran Granites. *Geol. Soc. Amer. Bull.*, 72(5), 689-701.
- Baars, D.L., 1972, Devonian System, In: Mallory, W.W. (Ed.), *Geologic Atlas of the Rocky Mountain Region*. Rocky Mountain Assoc. Geol., Denver, 90-99.
- Badgley, P.C., 1952, Notes on the Subsurface Stratigraphy and Oil and Gas Geology of the Lower Cretaceous Series in Central Alberta. *Geol. Surv. Canada*, Paper 52-11.
- Burwash, R.A., 1974, A Note on the Discovery and Development of the Grand Forks Cretaceous Oil Field, Southern Alberta. *Bull. Can. Petrol. Geol.* 2(3), 325-339.
- Burwash, R.A., Baadsgaard, H., Peterman, Z.E. and Hunt, G.H., 1964, Precambrian, In: McCrossan, R.G. and Glaister, R.P. (Eds.), *Geological History of Western Canada*. Alberta Soc. Petrol. Geol., Calgary, 14-19.
- Burwash, R.A. and Krupicka, J., 1969, Cratonic Reactivation in the Precambrian Basement of Western Canada. I. Deformation and Chemistry. *Can. J. Earth Sci.* 6, 1381-1396.
- Burwash, R.A. and Krupicka, J., 1970, Cratonic Reactivation in the Precambrian Basement of Western Canada. II. Metasomatism and Isostasy. *Can. J. Earth Sci.* 7, 1275-1294.
- Burwash, R.A., Krupicka, J. and Culbert, R.R., 1973, Cratonic Reactivation in the Precambrian Basement of Western Canada. III. Crustal Evolution. *Can. J. Earth Sci.* 10, 283-291.
- Century, J.R., 1967, Oil Fields of Alberta Supplement. Alberta Soc. Petrol. Geol., Calgary, 136 pp.
- Chayes, F., 1970, On Deciding Whether Trend Surfaces of Progressively Higher Order are Meaningful. *Geol. Soc. Amer. Bull.*, 81, 1273-1278.
- Christopher, J.E., 1975, The Depositional Setting of the Mannville Group (Lower Cretaceous) in Southwestern Saskatchewan, In: Caldwell, W.G.E. (Ed.), *The Cretaceous System in the Western Interior of North America*. Geol. Assoc. Canada, Spec. Paper 13, 523-552.

- Cobban, W.A. and Reeside, J.R., Jr., 1952, Correlation of the Cretaceous Formations of the Western Interior of the United States. Geol. Soc. Amer. Bull., 63, 1011-1044.
- Cox, J.E. (Ed.), 1966, 17th Ann. Field Conf. Guidebook, Jurassic and Cretaceous Stratigraphic Traps, Sweetgrass Arch, Billings Geological Society, Great Falls, 227 pp.
- Craig, L.C., 1972, Mississippian System, In: Mallory, W.W. (Ed.), Geologic Atlas of the Rocky Mountain Region. Rocky Mountain Assoc. Geol., Denver, 100-110.
- Davis, J.C., 1973, Statistics and Data Analysis in Geology. John Wiley and Sons Inc., New York, 550 pp.
- Dayhoff, M.O., 1963, A Contour Map Program for X-ray Crystallography, C. ACM., 7, 620-622.
- Fox, L., 1962, Numerical Solution of Ordinary and Partial Differential Equations, Pergamon, Oxford, 509 pp.
- Geological Survey of Canada, 1970, Oil and Gas Pools of Western Canada (Southern Alberta), Map 1316A.
- Gill, J.R. and Cobban, W.A., 1966, The Red Bird Section of the Upper Cretaceous Pierre Shale in Wyoming. U.S. Geol. Surv., Prof. Paper 393A, 1-73.
- Glaister, R.P., 1959, Lower Cretaceous of Southern Alberta and Adjoining Areas. Bull. Amer. Assoc. Petrol. Geol., 34(9), 1795-1801.
- Harbaugh, J.W. and Bonham-Carter, G., 1970, Computer Simulation in Geology. John Wiley and Sons Inc., New York, 575 pp.
- Herbaly, E.L., 1974, Petroleum Geology of the Sweetgrass Arch, Alberta. Bull. Amer. Assoc. Petrol. Geol., 58(11), Pt. 1, 2227-2244.
- Krumbein, W.C., 1956, Regional and Local Components in Facies Maps. Bull. Amer. Assoc. Petrol. Geol., 40(9), 2163-2194.
- Krumbein, W.C., 1959, Trend Surface Analysis of Contour Type Maps with Irregular Control Point Spacing. J. Geophys. Res., 64(7), 823-834.
- Krumbein, W.C., 1969, The Computer in Geological Perspective, In: Merriam, D.F. (Ed.), Computer Applications in the Earth Sciences. Plenum Press, New York, 251-276.
- Larson, L.H. (Ed.), 1969, Gas Fields of Alberta. Alberta Soc. Petrol. Geol., Calgary, 407 pp.
- Loranger, D.M., 1951, Useful Blairmore Microfossil Zone in Central and Southern Alberta, Canada. Bull. Amer. Assoc. Petrol. Geol., 35(11), 2348-2367.

- Lowdon, J.A., 1980, Age Determinations by the Geological Survey of Canada, Rept. 1, Isotopic Ages. Geol. Surv. Can., Paper 60-17.
- Macauley, G., Penner, D.G., Procter, R.M. and Tisdall, W.H., 1964, Carboniferous, In: McCrossan, R.G. and Glaister, R.P. (Eds.), Geological History of Western Canada. Alberta Soc. Petrol. Geol., Calgary, 89-102.
- Maycock, I.D., 1967, Mannville Group and Associated Lower Cretaceous Clastic Rocks in Southwestern Saskatchewan. Sask. Dept. Min. Res., Rept. 96, 108 pp.
- McGookey, D.P., 1972, Cretaceous System, In: Mallory, W.W. (Ed.), Geologic Atlas of the Rocky Mountain Region. Rocky Mountain Assoc. Geol., Denver, 190-228.
- McLearn, F.H., 1932, Problems of the Lower Cretaceous of the Canadian Interior. Trans. Roy. Soc. Canada, 3rd Ser., Sec. 4, 26, 157-175.
- McLearn, F.H., 1944, Revision of the Palaeogeography of the Lower Cretaceous of the Western Interior of Canada. Geol. Surv. Can., Paper 44-17, 14 pp.
- Mellon, G.B., 1967, Stratigraphy and Petrology of the Lower Cretaceous Blairmore and Mannville Groups, Alberta Foothills and Plains. Res. Council Alberta, Bull. 21, 270 pp.
- Mellon, G.B. and Wall, J.H., 1961, Correlation of the Blairmore Group and Equivalent Strata. Edmonton Geol. Soc. Quart., 5(1).
- Merriam, D.F. and Harbaugh, J.W., 1963, Computer Helps Map Oil Structures. Oil and Gas J., 61(47), 158-163.
- Milner, R.L. and Thomas, G.E., 1954, Jurassic System in Saskatchewan, In: Clark, L.M. (Ed.), Western Canada Sedimentary Basin. Amer. Assoc. Petrol. Geol., Tulsa, 250-267.
- Milner, R.L. and Blaklee, G.W., 1958, Notes on the Jurassic of Southwestern Saskatchewan, In: Goodman, A.J. (Ed.), Jurassic and Carboniferous of Western Canada. Amer. Assoc. Petrol. Geol., Tulsa, 65-84.
- Nauss, A.W., 1945, Cretaceous Stratigraphy of Vermilion Area, Alberta, Canada. Bull. Amer. Assoc. Petrol. Geol., 29(11), 1605-1629.
- Obradovich, J.D. and Cobban, W.A., 1975, A Time Scale for the Late Cretaceous of the Western Interior of North America, In: Caldwell, W.G.E. (Ed.), The Cretaceous System in Western Interior of North America. Geol. Assoc. Can., Spec. Paper 13, 31-54.
- Peterson, J.A., 1972, Jurassic System, In: Mallory, W.W. (Ed.), Geologic Atlas of the Rocky Mountain Region. Rocky Mountain Assoc. Geol., Denver, 177-189.

- Potter, P.E., 1967, Sand Bodies and Sedimentary Environments: A Review. Bull. Amer. Assoc. Petrol. Geol., 51(3), 337-365.
- Price, L.L., 1963, Lower Cretaceous Rocks of Southeastern Saskatchewan. Geol. Surv. Can., Paper 62-69.
- Robinson, J.E., Charlesworth, H.A.K. and Ellis, M.J., 1969, Structural Analysis using Spacial Filtering in Interior Plains of Southeastern Alberta. Bull. Amer. Assoc. Petrol. Geol., 53, 2341-2367.
- Rudkin, R.A., 1964, Lower Cretaceous, In: McCrossan, R.G. and Glaister, R.P. (Eds.), Geological History of Western Canada. Alberta Soc. Petrol. Geol., Calgary, 156-168.
- Schumm, S.A., 1972, Fluvial Palaeochannels, In: Rigby, J.K. and Hamblin, W.K. (Eds.), Recognition of Ancient Sedimentary Environments. Soc. Econ. Paleontologists and Mineralogists, Spec. Publ. 16, 98-107.
- Springer, G.D., MacDonald, W.D. and Crockford, M.B.B., 1964, Jurassic, In: McCrossan, R.G. and Glaister, R.P. (Eds.), Geological History of Western Canada. Alberta Soc. Petrol. Geol., Calgary, 137-155.
- Stelck, C.R., 1975, Basement Control of Cretaceous Sand Sequences in Western Canada, In: Caldwell, W.G.E. (Ed.), The Cretaceous System in the Western Interior of North America. Geol. Assoc. Can., Spec. Paper 13, 427-440.
- Taylor, R.S., Mathews, W.H. and Kupsch, W.O., 1964, Tertiary, In: McCrossan, R.G. and Glaister, R.P. (Eds.), Geological History of Western Canada. Alberta Soc. Petrol. Geol., Calgary, 190-194.
- Thompson, R.L. and Crockford, M.B.B., 1958, The Jurassic Subsurface in Southern Saskatchewan, In: Goodman, A.J. (Ed.), Jurassic and Carboniferous of Western Canada. Amer. Assoc. Petrol. Geol., Tulsa, 52-64.
- Visher, G.S., 1972, Physical Characteristics of Fluvial Deposits, In: Rigby, J.K. and Hamblin, W.K. (Eds.), Recognition of Ancient Sedimentary Environments. Soc. Econ. Paleontologists and Mineralogists, Spec. Publ. 16, 84-97.
- Webb, J.B., 1964, Historical Summary, In: McCrossan, R.G. and Glaister, R.P. (Eds.), Geological History of Western Canada. Alberta Soc. Petrol. Geol., Calgary, 218-232.
- Weir, J.D., 1954, Marine Jurassic Formations of Southern Alberta Plains, In: Clark, L.M. (Ed.), Western Canada Sedimentary Basin. Amer. Assoc. Petrol. Geol., Tulsa, 233-249.
- Wermund, E.G. and Jenkins, W.A., Jr., 1970, Recognition of Deltas by Fitting Trend Surfaces to Upper Pennsylvanian Sandstones in North Central Texas, In: Morgan, J.P. (Ed.), Deltaic Sedimentation Modern and Ancient. Soc. Econ. Paleontologists and Mineralogists, Spec. Publ. 15, 256-269.

Whitten, E.H.T., 1969, Trends in Computer Application in Structural Geology, In Merriam, D.F. (Ed.), Computer Applications in the Earth Sciences. Plenum Press, New York, 223-250.

Williams, G.D., 1963, The Mannville Group (Lower Cretaceous) of Central Alberta. Bull. Can. Petrol. Geol., 11, 350-368.

Williams, G.D., Baadsgaard, H. and Steen, G., 1962, Mineral Dates from the Mannville Group. J. Alberta Soc. Petrol. Geol., 10(6), 320-325.

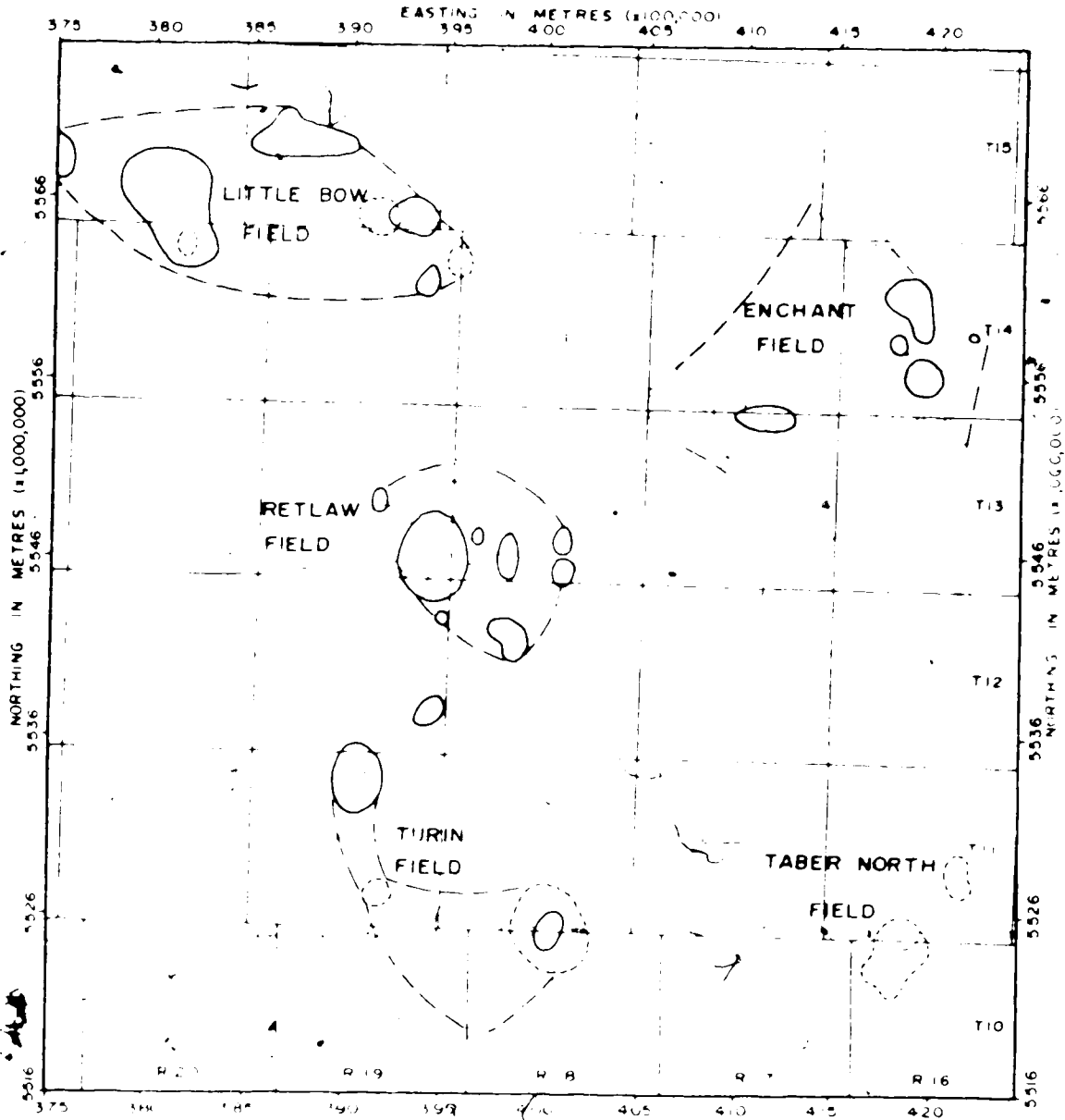
Williams, G.D. and Burk, C.F., Jr., 1964, Upper Cretaceous Geology of Western Canada. Alberta Soc. Petrol. Geol., Calgary, 169-189.

Williams, G.D. and Stelck, C.R., 1975, Speculations on Palaeogeography of North America, In: Caldwell, J.G. (Ed.), The Cretaceous System in the Western Interior of North America. Geol. Assoc. Can., Spec. Paper 13, 1-20.

White, R.J. (Ed.), 1960, Oil Fields of Alberta. Alberta Soc. Petrol. Geol., Calgary, 272 pp.

Wood, R.D., Wichmann, P.A. and Watt, H.B., 1974, Gamma Ray Neutron Log. Dresser Atlas Log Review 1, Sect. 8, 1-20.

Handwritten notes and scribbles on the right side of the page, including phrases like "Structural Geology", "Cretaceous", "Argon", "Geology", "Petrol.", "169-189", "Cretaceous", "Geol.", "petrol.", and "Neutron Log".



PETROLEUM DISTRIBUTION - LOWER CRETACEOUS

○ UPPER MEMBER OF ... BOW ... LAKE ...
 ○ LOWER MEMBER OF ...
 ○ ...
 ○ ...

FIGURE 43

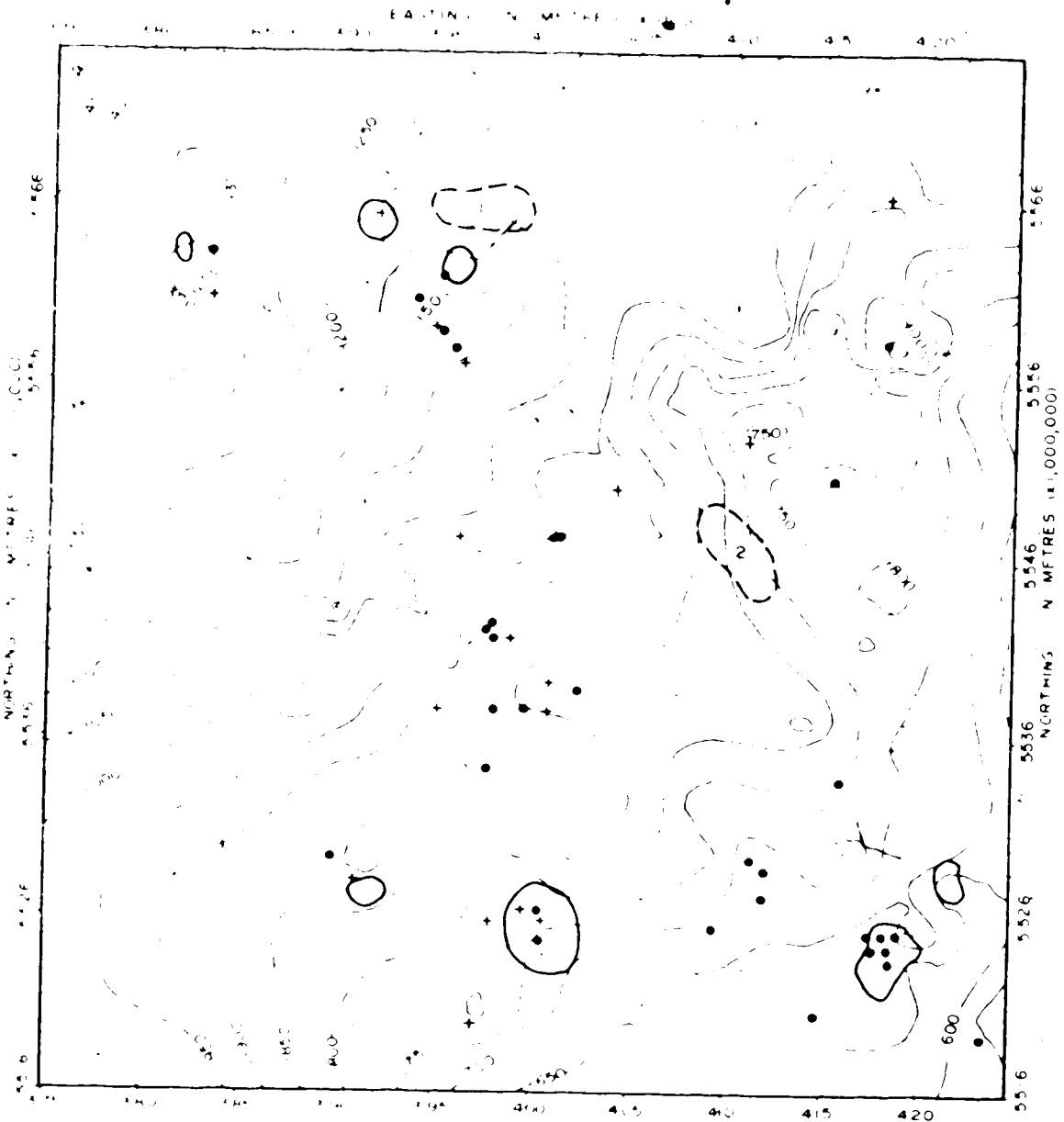
of gas or one thousand barrels of oil. The extension of some fields subsequent to the publication of the map in 1970 accounts for the occurrence of computer plotted production wells beyond the indicated field limits shown in Figures 44 to 46.

B. LOWER MANNVILLE GROUP

Oil and gas production from the Lower Mannville is obtained from the Sunburst Sandstone. Traps are stratigraphic, and related exclusively to topographic highs in the pre-Mannville surface. Petroleum distribution has been superimposed upon the structure contour map of the base of the Mannville Group to illustrate structural control (Figure 44). Pre-Mannville highs correspond to Lower Mannville isopach thins (Figure 14). Southeastward oil and gas migration probably occurred in the Tertiary due to regional tilting.

The Taber, North field lies at the southeastern end of the Turin Valley, on the western flank of the Sweetgrass arch. Sandstones lense out into shales in an updip (southeasterly) direction. The two main pools are located on ridges flanking the northern Turin Valley stream. The southern ridge is more prominent and extends the length of the Turin Valley (this feature was discussed in previous chapters). Drilling of the ridge in the last six years has resulted in the discovery of a number of major oil pools. One small pool was defined on the northern ridge.

Mainly gas production is obtained from the Turin field which is located along the southwestern side of the crest of the Jurassic cuesta. The field occurs at the structurally higher southeastern end of the cuesta.



PETROLEUM DISTRIBUTION - LOWER MANNVILLE GROUP

SHOWN BY BASE OF MANNVILLE GROUP STR. (SEE STR. MAP (ATUM M.S.L.))

- MAJOR OIL WELLS
- + MINOR GAS WELLS
- OIL WELLS, AFTER 1970
- OIL WELLS, BEFORE 1970

FIGURE 44

The Little Bow field is located over a broad Mississippian high extending northwest from the Enchant Ridge fault trend. Oil and gas pools overlie localized highs and structural noses within the field. Since 1970, small pools have been discovered to the southeast of the Little Bow field, along the northeastern side of the Turin Valley.

Lower Mannville oil and gas production is also a function of sand distribution, occurring only where highs are capped or flanked by sequences of moderate to high sand content (greater than 40%). This accounts for the lack of production from Enchant Ridge and the northwestern end of the Jurassic cuesta. The Lower Mannville isopach in these areas varies from 20 to 50 feet, the upper 15 to 20 feet of which consists of shales of the Ostracode Zone, which overlie late Lower Mannville silts and muds. Interval sand percentage values range from 0 to 20 (Figure 27). Three small pools occur in local depressions on the Enchant Ridge where sand content increases to 50%. The zone of no production at the centre of the median Turin Valley Ridge also corresponds to sand percentage values less than 20%.

Using the criteria of high sand percentage values coincident with pre-Mannville highs and Tertiary southeastward migration of fluids as the main factors determining the accumulation of Lower Mannville petroleum, two potential undrilled areas occur within the Turin area (undrilled according to Alberta Research Council's well file and Carter Mapping's one mile well maps of the area).

An area three and one half miles long by two miles wide in the southwestern part of Township 15, Range 18, extending from the eastern limit of the Little Bow field, holds definite gas potential (Area 1, Figure

44). It overlies the northwestern extension of Inchant Ridge, and has sand values of 60 to 70 percent indicated on the sand percentage map of Interval 12 (Figure 27), the uppermost slice of the Lower Mannville Group. Sand content decreases towards the east (updip), and the zone occurs within a closed isopach thin, in which Lower Mannville thickness ranges from 25 to 100 feet. The structure on top of the Lower Mannville (Figure 13) shows closure in three directions on the Ostracode Zone shale. Closure to the east is provided by shaling out of the sands in Interval 12. The prospect consists of 5 to 40 feet of clean sand capped by 20+ feet of shale with closure in four directions. Gas production occurs at the limits of closure (between the 75 and 100 foot isopach contours) in the northwest (Township 15, Range 19), and beyond the limit of closure in the southeast (Township 14, Ranges 18 and 19). A suspended gas well is located in the north in Township 15, Range 18, at the 60 foot isopach contour. Consequently the crest of the feature remains undrilled. This may be due to its east-west orientation, contrary to the northwesterly trend of the majority of pools in the Turin area, including the Lower Mannville pool of the adjoining Little Bow field.

Reserve calculations for gas above the 60 foot isopach contour indicate:

Volume of pool = 1.673×10^9 cubic feet (assuming 10 foot average net pay over 6 square miles)

Average porosity = 20% (average porosity of Lower Mannville pools in Little Bow field = 19.8%)

Water saturation = 30% (as in Little Bow field)

Assumed expansion factor = 115 (based on a reservoir top at -1,100 feet subsea, temperature change from 105°F to 60°F and an associated pressure change from 1,675 psia to 14.65 psia)

Therefore the potential gas in place is $1.673 \times 10^9 \times .2 \times .7 \times 115 =$
27 billion cubic feet.

For this and other potential areas, closures and volumes were derived from computer contoured maps. Verification of reserves, or for that matter the validity of the existence of pools, by hand contouring and detailed log examination, was not attempted. The above description and calculation is designed to show that rapidly generated regional computer maps are useful exploration tools for a "first look" at a region, limiting the number of areas requiring time consuming, detailed hand analysis.

A four mile by two mile, northwesterly-trending undrilled area between the town of Retlaw and the southwestern margin of the Enchant field (Bow Island production), has moderate potential (Area 2, Figure 44). The area lies between the northern Tyrin Valley channel and Enchant Ridge. Sand values in Interval 12 decrease from 80% to 50% towards the southeast and southwest, and decrease to zero towards the top of Enchant Ridge. Sands are capped by shales of Interval 9 (0 to 10% sand). If the decrease in sand is partly due to lensing, a trap exists in the southeast of the area because of the regional northwesterly dip.

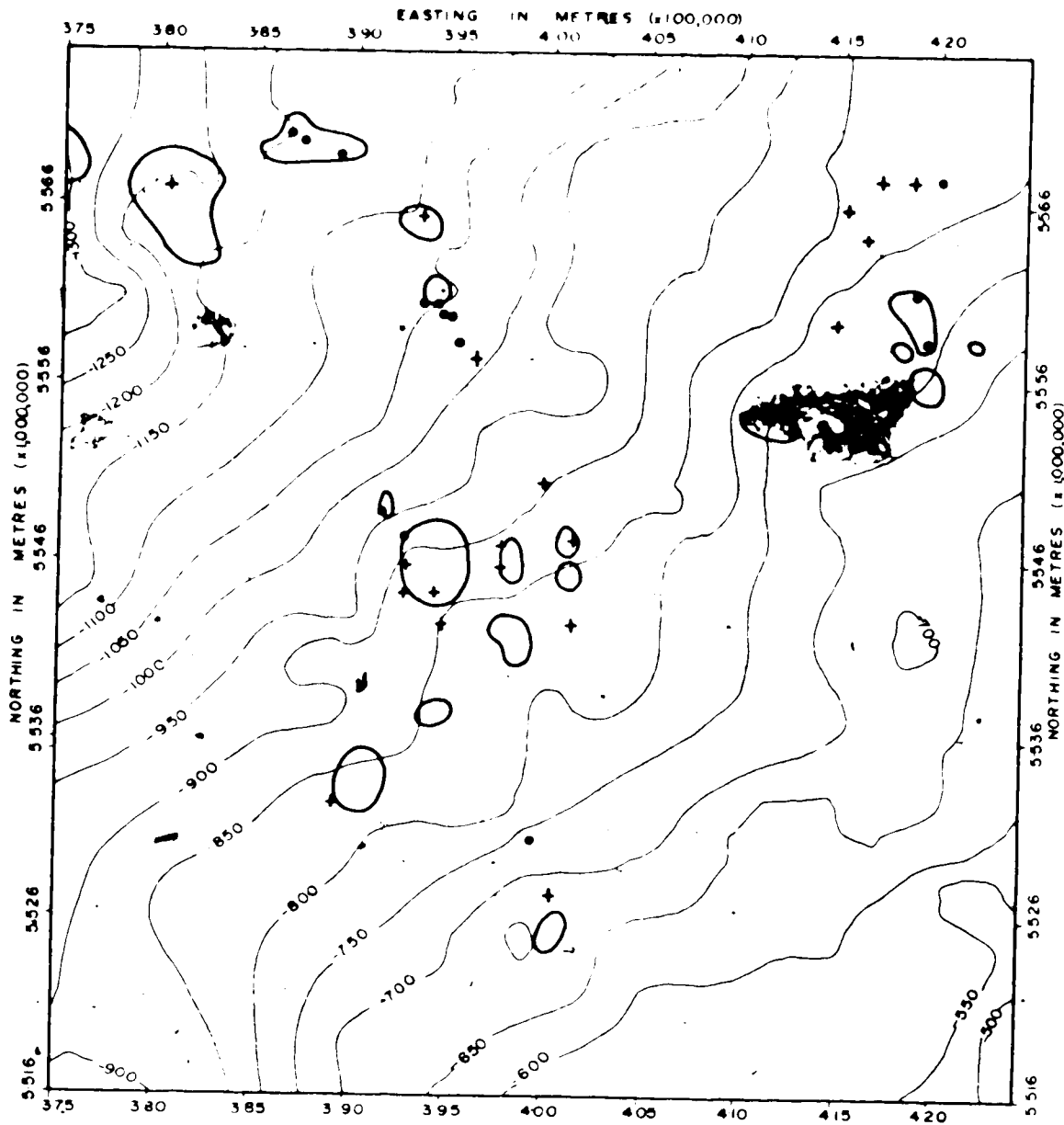
C. GLAUCONITIC SANDSTONE EQUIVALENT

Petroleum distribution in the Glauconitic Sandstone Equivalent, and factors controlling its occurrence are similar to those in the Lower Mannville Group. The outlines of oil and gas fields have been superimposed on the structure map on the top of the Lower Mannville to illus-

trate structural control (Figure 45). The Glauconitic Sandstone Equivalent is approximately coincident with Interval 9 (Figure 31). Oil and gas production is obtained from the Little Bow and Turin fields, and from the Retlaw field at the northwestern end of the median Turin Valley Ridge. The main Retlaw pool overlies part of a local sand concentration (with up to 90% sand) deposited around the end of the ridge by the southern Turin Valley stream. The absence of a comparable sand buildup during early Mannville time explains the limited Lower Mannville Retlaw production. The main Little Bow and Turin pools occur within local sand concentrations. Minor shows only are found in the Taber North area because of a lack of reservoir sandstone. Oil production in the Enchant field occurs from a depression containing up to 30% sand on the northern side of the Enchant Ridge. Oil and gas fields in the Glauconitic Sandstone Equivalent are capped by shales of Intervals 8 and 9 and underlain by the impervious Ostracode Zone. Decreased sand deposition in Interval 9 restricted the distribution of reservoirs and for this reason, the two potential Lower Mannville occurrences are not overlain by pools within the Glauconitic Sandstone Equivalent. No undrilled prospects are apparent in the Glauconitic Sandstone Equivalent.

D. UPPER MANNVILLE GROUP (POST-GLAUCONITIC SANDSTONE EQUIV.)

Production and shows in the Upper Mannville Group are negligible (Figure 46); small amounts of oil are produced from the Retlaw field, and gas is obtained from the Enchant field. Thick shales have prevented the upward migration of petroleum into the irregularly distributed Upper Mannville sand lenses. In the Enchant field, production is obtained



PETROLEUM DISTRIBUTION : GLAUCONITIC SANDSTONE EQUIV.
 SHOWN ON TOP OF LOWER MANNVILLE GROUP STRUCTURE CONTOUR MAP (DATUM M.S.L.)

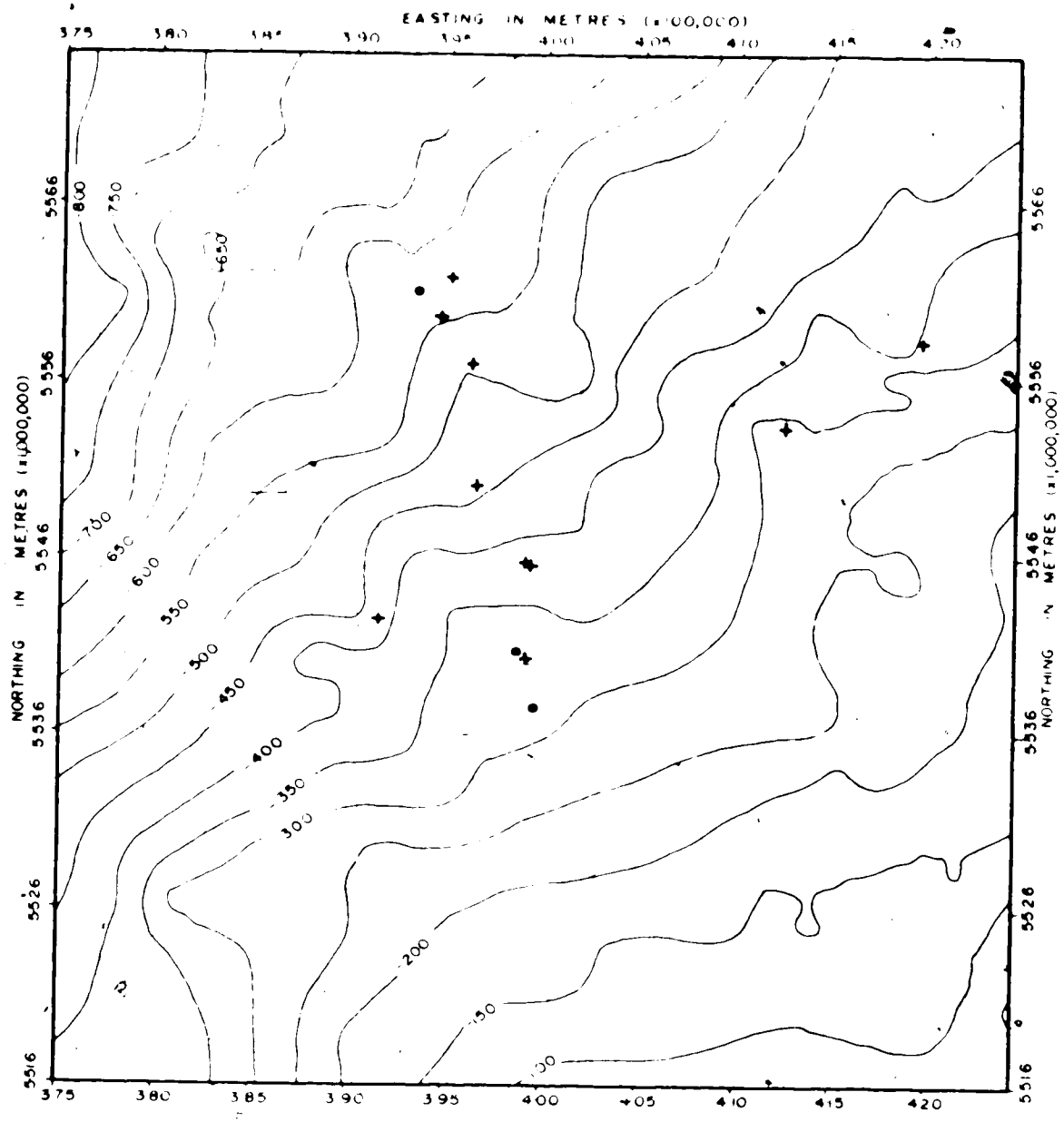
● MAJOR OIL + MAJOR GAS

○ POOL LIMITS, AFTER G.S.C. (1970)

SCALE (KM)



FIGURE 45



PETROLEUM DISTRIBUTION : UPPER MANNVILLE GP.

SHOWN ON TOP OF MANNVILLE GROUP STRUCTURE CONTOUR MAP (DATUM M.S.L.)

● OIL SHOW + GAS SHOW

SCALE (KM)

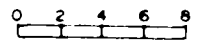


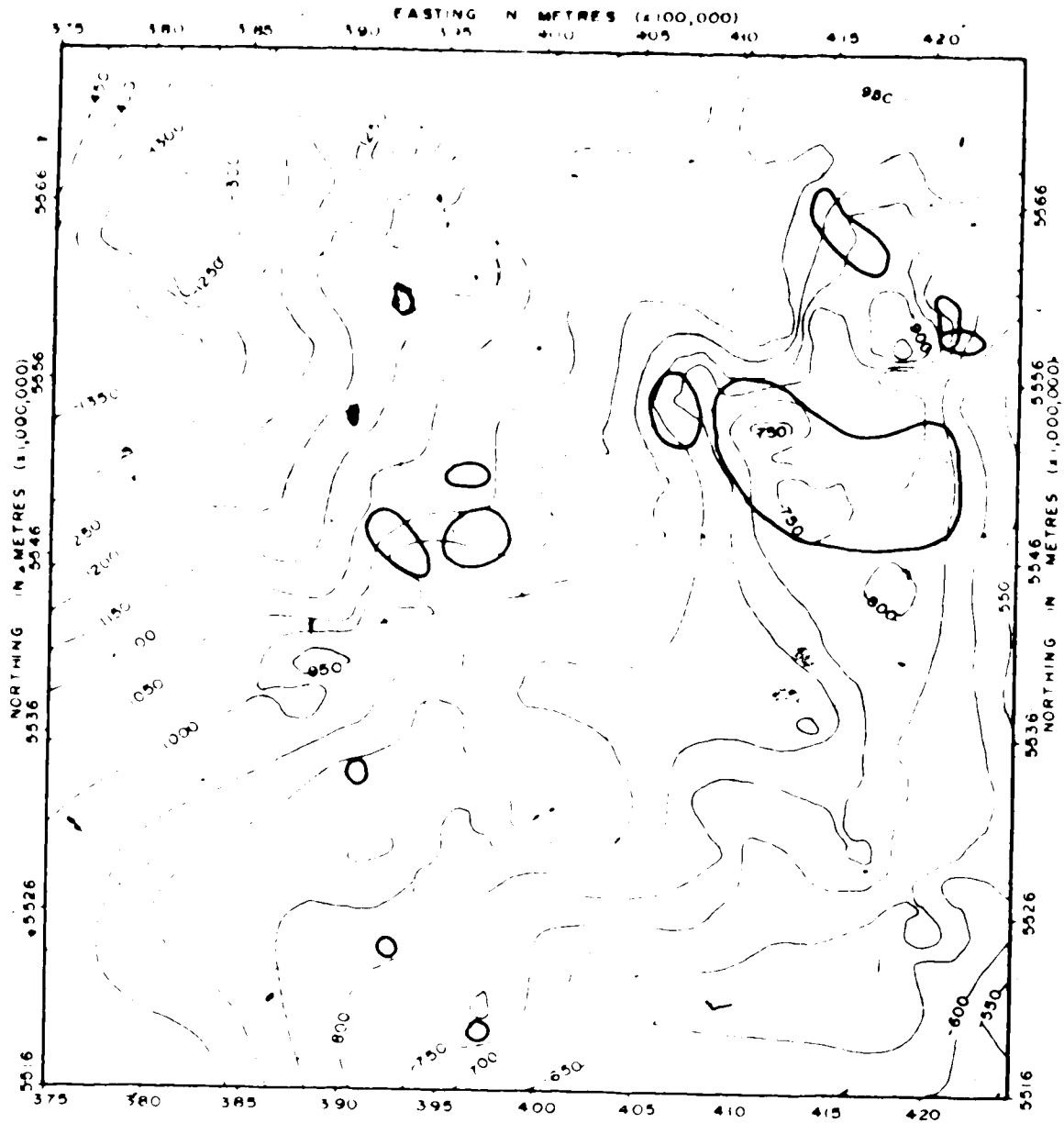
FIGURE 46

from the sandstones at the top of the Mannville Group, suggesting that marine Colorado shales may have been the source of the gas. The absence of sands in Interval 1 (Figure 40) over the Jurassic cuesta prevented comparable pools developing in the southwestern map area.

F. POST-MANNVILLE GROUP

Data on post-Mannville petroleum occurrences were not collected; however, inferences may be made from the distribution of gas in the Bow Island Formation as mapped by the Geological Survey of Canada (1970). Gas fields, when superimposed on the base of Mannville structure contour map (Figure 47), are seen to occur above pre-Mannville topographic highs of greatest relief. Differential compaction of Bow Island and underlying strata over the highs appears to have formed the traps. The largest occurrence is the Enchant field, which overlies Enchant Ridge; gas also occurs over the median Turin Valley Ridge (Retlaw field) and at the southeastern end of the Jurassic cuesta (Turin field).

Bow Island gas fields are also coincident with positive residuals on the base of the Mannville Group trend surface map (Figure 12). The Little Bow field (Mannville production) overlies the large northwestern residual, and the absence of Bow Island gas in this field is probably due to lack of an updip seal, permitting migration towards the Enchant field. The residual between the Little Bow field and the Enchant Ridge which is apparent on Figure 12, is absent on the trend surface map on the top of the Mannville Group (Figure 17), because of erosion of the high during late Mannville time. As a consequence, no structure is present at the Bow Island stratigraphic level, and no gas accumulation occurs.



PETROLEUM DISTRIBUTION : BOW ISLAND FORMATION

SHOWN ON BASE OF MANNVILLE GROUP STRUCTURE CONTOUR MAP (DATUM M.S.L.)

○ GAS POOLS, AFTER G.S.C. (1970)

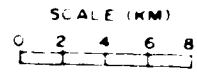


FIGURE 47

Chapter VIII

SUMMARY AND CONCLUSIONS

1) The Turin area lies at the margin of the Sweetgrass arch and the West Alberta basin. Continental sediments of the Mannville Group were deposited on an eroded surface of southwesterly-dipping Mississippian and Jurassic strata. The drainage pattern developed on this surface reflected the northwesterly strike of the bedding. The physiography was dominated by a Jurassic-capped Mississippian cuesta in the southwest and a fault-controlled Mississippian ridge in the northeast (Enchant Ridge), separated by the Turin Valley.

2) Sediments were derived from the Cordilleran region, which was subject to batholithic intrusion and uplift during the early Cretaceous. Sand deposition predominated initially, confined to pre-Mannville channels. Consequently, sand bodies are linear in form. Infilling of valleys and denudation of the ridges produced a land surface of low relief by late early Mannville time. Sand continued to be deposited along the axes of pre-Mannville valleys, while fine-grained sediments accumulated in lower energy depositional environments removed from active stream flow. Maturation of the source area is reflected in the progressive decrease in the volume of sand deposited, culminating in the widespread deposition of Ostracode Zone shales.

3) Differential compaction of Lower Mannville sediments produced an Upper Mannville depositional surface similar to, yet more subdued in form than that which existed during early Mannville time. Silts and muds were the main sediments deposited, but periodic uplift and erosion of the source area resulted in the influx of sand, the distribution of which was more variable than that of the underlying sequence. Drainage channels frequently coalesced to form wide valleys and floodplains of meandering streams. The section thickens regionally towards the southwest.

4) Mannville sedimentation was halted by the onset of the Colorado sea. The present structural configuration of the basin is the result of northwesterly tilting during the Tertiary.

5) Distribution of petroleum in the Mannville group is a function of pre-Mannville topography, sand distribution, and Tertiary tilting. Traps are stratigraphic, and are formed by channeling out of channel sands from a dip (southeasterly) direction. Fields are confined to the tops and flanks of structural highs, which correspond to ridges in the pre-Mannville surface. Production occurs mainly from the sandiest sandstone and the calcareous sandstone equivalent, capped by thin shales which have prevented the upward migration of petroleum into a reservoir. Gas in the uppermost sands of the Mannville was probably derived from marine shales of the Colorado group. Gas in the low island formation occurs in traps formed by differential compaction over upper Mannville beds, where closure exceeded the degree of Tertiary tilting.

6) Computer-generated structure and isopach maps were of a satisfactory standard for regional interpretation. Some of the subjectivity inherent in hand-drawn contouring was eliminated by the mechanical gridding and contouring algorithms used in the computer programs. Even though these mechanical techniques have a degree of "subjectivity" (e.g., the methods used to choose control points and interpolate to grid nodes), mapping is performed in exactly the same way each time. Trends were mapped which otherwise may have been overlooked due to geologic prejudice of the area. Sand percentage analysis, using proportionate and fixed slices through the Mannville Group, was an effective means of mapping gross sand distribution and the geometry of sand bodies. Trend surface analysis was useful in enhancing local features on structure contour maps, permitting a

more accurate interpretation of the Mannville drainage pattern. The irregular regional sand distribution prevented statistically valid surfaces being fitted to sand percentage data. The resulting residuals showed little that was not already apparent on raw data contour maps.

REFERENCES

- Acham, P.A., 1971, The Mannville Group (Lower Cretaceous) of the Hussar area, southern Alberta. Unpubl. M.Sc. Thesis, Univ. of Alberta, Edmonton.
- Allen, J.R.L., 1965, A Review of the Origin and Characteristics of Recent Alluvial Sediments. *Sedimentology* 5(2), 89-191.
- Baadsgaard, H., Folinsbee, R.E. and Lipson, J., 1961, Potassium - Argon Dates of Biotites from Cordilleran Granites. *Geol. Soc. Amer. Bull.*, 72(5), 689-701.
- Baars, D.L., 1972, Devonian System, In: Mallory, W.W. (Ed.), *Geologic Atlas of the Rocky Mountain Region*. Rocky Mountain Assoc. Geol., Denver, 90-99.
- Badgley, P.C., 1952, Notes on the Subsurface Stratigraphy and Oil and Gas Geology of the Lower Cretaceous Series in Central Alberta. *Geol. Surv. Canada, Paper* 52-11.
- Berger, A.D., 1974, A Note on the Discovery and Development of the Grand Forks Cretaceous Oil Field, Southern Alberta. *Bull. Can. Petrol. Geol.* 2(3), 325-339.
- Burwash, R.A., Baadsgaard, H., Peterman, Z.E. and Hunt, G.H., 1964, Precambrian, In: McCrossan, R.G. and Glaister, R.P. (Eds.), *Geological History of Western Canada*. Alberta Soc. Petrol. Geol., Calgary, 14-19.
- Burwash, R.A. and Krupicka, J., 1969, Cratonic Reactivation in the Precambrian Basement of Western Canada. I. Deformation and Chemistry. *Can. J. Earth Sci.* 6, 1381-1396.
- Burwash, R.A. and Krupicka, J., 1970, Cratonic Reactivation in the Precambrian Basement of Western Canada. II. Metasomatism and Isostasy. *Can. J. Earth Sci.* 7, 1275-1294.
- Burwash, R.A., Krupicka, J. and Culbert, R.R., 1973, Cratonic Reactivation in the Precambrian Basement of Western Canada. III. Crustal Evolution. *Can. J. Earth Sci.* 10, 283-291.
- Century, J.R., 1967, Oil Fields of Alberta Supplement. Alberta Soc. Petrol. Geol., Calgary, 136 pp.
- Chayes, F., 1970, On Deciding Whether Trend Surfaces of Progressively Higher Order are Meaningful. *Geol. Soc. Amer. Bull.*, 81, 1273-1278.
- Christopher, J.E., 1975, The Depositional Setting of the Mannville Group (Lower Cretaceous) in Southwestern Saskatchewan, In: Caldwell, W.G.E. (Ed.), *The Cretaceous System in the Western Interior of North America*. Geol. Assoc. Canada, Spec. Paper 13, 523-552.

- Cobban, W.A. and Reeside, J.B., Jr., 1952, Correlation of the Cretaceous Formations of the Western Interior of the United States. Geol. Soc. Amer. Bull., 63, 1011-1044.
- Cox, J.E. (Ed.), 1966, 17th Ann. Field Conf. Guidebook, Jurassic and Cretaceous Stratigraphic Traps, Sweetgrass Arch, Billings Geological Society, Great Falls, 227 pp.
- Craig, L.C., 1972, Mississippian System, In: Mallory, W.W. (Ed.), Geologic Atlas of the Rocky Mountain Region. Rocky Mountain Assoc. Geol., Denver, 100-110.
- Davis, J.C., 1973, Statistics and Data Analysis in Geology. John Wiley and Sons Inc., New York, 550 pp.
- Dayhoff, M.O., 1963, A Contour Map Program for X-ray Crystallography, C. ACM., 7, 620-622.
- Fox, L., 1962, Numerical Solution of Ordinary and Partial Differential Equations, Pergamon, Oxford, 509 pp.
- Geological Survey of Canada, 1970, Oil and Gas Pools of Western Canada (Southern Alberta), Map 1316A.
- Gill, J.R. and Cobban, W.A., 1966, The Red Bird Section of the Upper Cretaceous Pierre Shale in Wyoming. U.S. Geol. Surv., Prof. Paper 393A, 1-73.
- Glaister, R.P., 1959, Lower Cretaceous of Southern Alberta and Adjoining Areas. Bull. Amer. Assoc. Petrol. Geol., 34(9), 1795-1801.
- Harbaugh, J.W. and Bonham-Carter, G., 1970, Computer Simulation in Geology. John Wiley and Sons Inc., New York, 575 pp.
- Herbaly, E.L., 1974, Petroleum Geology of the Sweetgrass Arch, Alberta. Bull. Amer. Assoc. Petrol. Geol., 58(11), Pt. 1, 2227-2244.
- Krumbein, W.C., 1956, Regional and Local Components in Facies Maps. Bull. Amer. Assoc. Petrol. Geol., 40(9), 2163-2194.
- Krumbein, W.C., 1959, Trend Surface Analysis of Contour Type Maps with Irregular Control Point Spacing. J. Geophys. Res., 64(7), 823-834.
- Krumbein, W.C., 1969, The Computer in Geological Perspective, In: Merriam, D.F. (Ed.), Computer Applications in the Earth Sciences. Plenum Press, New York, 251-276.
- Larson, L.H. (Ed.), 1969, Gas Fields of Alberta. Alberta Soc. Petro]. Geol., Calgary, 407 pp.
- Loranger, D.M., 1951, Useful Blairmore Microfossil Zone in Central and Southern Alberta, Canada. Bull. Amer. Assoc. Petrol. Geol., 35(11), 2348-2367.

- Lowdon, J.A., 1960, Age Determinations by the Geological Survey of Canada, Rept. 1, Isotopic Ages. Geol. Surv. Can., Paper 60-17.
- Macauley, G., Penner, D.G., Procter, R.M. and Tisdall, W.H., 1964, Carboniferous, In: McCrossan, R.G. and Glaister, R.P. (Eds.), Geological History of Western Canada. Alberta Soc. Petrol. Geol., Calgary, 89-102.
- Maycock, I.D., 1967, Mannville Group and Associated Lower Cretaceous Clastic Rocks in Southwestern Saskatchewan. Sask. Dept. Min. Res., Rept. 96, 108 pp.
- McGookey, D.P., 1972, Cretaceous System, In: Mallory, W.W. (Ed.), Geologic Atlas of the Rocky Mountain Region. Rocky Mountain Assoc. Geol., Denver, 190-228.
- McLearn, F.H., 1932, Problems of the Lower Cretaceous of the Canadian Interior. Trans. Roy. Soc. Canada, 3rd Ser., Sec. 4, 26, 157-175.
- McLearn, F.H., 1944, Revision of the Palaeogeography of the Lower Cretaceous of the Western Interior of Canada. Geol. Surv. Can., Paper 44-17, 14 pp.
- Mellon, G.B., 1967, Stratigraphy and Petrology of the Lower Cretaceous Blairmore and Mannville Groups, Alberta Foothills and Plains. Res. Council Alberta, Bull. 21, 270 pp.
- Mellon, G.B. and Wall, J.H., 1961, Correlation of the Blairmore Group and Equivalent Strata. Edmonton Geol. Soc. Quart., 5(1).
- Merriam, D.F. and Harbaugh, J.W., 1963, Computer Helps Map Oil Structures. Oil and Gas J., 61(47), 158-163.
- Milner, R.L. and Thomas, G.E., 1954, Jurassic System in Saskatchewan, In: Clark, L.M. (Ed.), Western Canada Sedimentary Basin. Amer. Assoc. Petrol. Geol., Tulsa, 250-267.
- Milner, R.L. and Blaklee, G.W., 1958, Notes on the Jurassic of Southwestern Saskatchewan, In: Goodman, A.J. (Ed.), Jurassic and Carboniferous of Western Canada. Amer. Assoc. Petrol. Geol., Tulsa, 65-84.
- Nauss, A.W., 1945, Cretaceous Stratigraphy of Vermilion Area, Alberta, Canada. Bull. Amer. Assoc. Petrol. Geol., 29(11), 1605-1629.
- Obradovich, J.D. and Cobban, W.A., 1975, A Time Scale for the Late Cretaceous of the Western Interior of North America, In: Caldwell, W.G.E. (Ed.), The Cretaceous System in Western Interior of North America. Geol. Assoc. Can., Spec. Paper 13, 31-54.
- Peterson, J.A., 1972, Jurassic System, In: Mallory, W.W. (Ed.), Geologic Atlas of the Rocky Mountain Region. Rocky Mountain Assoc. Geol., Denver, 177-189.

- Potter, P.E., 1967, Sand Bodies and Sedimentary Environments: A Review. Bull. Amer. Assoc. Petrol. Geol., 51(3), 337-365.
- Price, L.L., 1963, Lower Cretaceous Rocks of Southeastern Saskatchewan. Geol. Surv. Can., Paper 62-69.
- Robinson, J.E., Charlesworth, H.A.K. and Ellis, M.J., 1969, Structural Analysis using Spacial Filtering in Interior Plains of Southeastern Alberta. Bull. Amer. Assoc. Petrol. Geol., 53, 2341-2367.
- Rudkin, R.A., 1964, Lower Cretaceous, In: McCrossan, R.G. and Glaister, R.P. (Eds.), Geological History of Western Canada. Alberta Soc. Petrol. Geol., Calgary, 156-168.
- Schumm, S.A., 1972, Fluvial Palaeochannels, In: Rigby, J.K. and Hamblin, W.K. (Eds.), Recognition of Ancient Sedimentary Environments. Soc. Econ. Paleontologists and Mineralogists, Spec. Publ. 16, 98-107.
- Springer, G.D., MacDonald, W.D. and Crockford, M.B.B., 1964, Jurassic, In: McCrossan, R.G. and Glaister, R.P. (Eds.), Geological History of Western Canada. Alberta Soc. Petrol. Geol., Calgary, 137-155.
- Stelck, C.R., 1975, Basement Control of Cretaceous Sand Sequences in Western Canada, In: Caldwell, W.G.E. (Ed.), The Cretaceous System in the Western Interior of North America. Geol. Assoc. Can., Spec. Paper 13, 427-440.
- Taylor, R.S., Mathews, W.H. and Kupsch, W.O., 1964, Tertiary, In: McCrossan, R.G. and Glaister, R.P. (Eds.), Geological History of Western Canada. Alberta Soc. Petrol. Geol., Calgary, 190-194.
- Thompson, R.L. and Crockford, M.B.B., 1958, The Jurassic Subsurface in Southern Saskatchewan, In: Goodman, A.J. (Ed.), Jurassic and Carboniferous of Western Canada. Amer. Assoc. Petrol. Geol., Tulsa, 52-64.
- Visher, G.S., 1972, Physical Characteristics of Fluvial Deposits, In: Rigby, J.K. and Hamblin, W.K. (Eds.), Recognition of Ancient Sedimentary Environments. Soc. Econ. Paleontologists and Mineralogists, Spec. Publ. 16, 84-97.
- Webb, J.B., 1964, Historical Summary, In: McCrossan, R.G. and Glaister, R.P. (Eds.), Geological History of Western Canada. Alberta Soc. Petrol. Geol., Calgary, 218-232.
- Weir, J.D., 1954, Marine Jurassic Formations of Southern Alberta Plains, In: Clark, L.M. (Ed.), Western Canada Sedimentary Basin. Amer. Assoc. Petrol. Geol., Tulsa, 233-249.
- Wermund, E.G. and Jenkins, W.A., Jr., 1970, Recognition of Deltas by Fitting Trend Surfaces to Upper Pennsylvanian Sandstones in North Central Texas, In: Morgan, J.P. (Ed.), Deltaic Sedimentation Modern and Ancient. Soc. Econ. Paleontologists and Mineralogists, Spec. Publ. 15, 256-269.

Whitten, E.H.T., 1969, Trends in Computer Applications in Structural Geology, In Merriam, D.F. (Ed.), Computer Applications in the Earth Sciences. Plenum Press, New York, 223-250.

Williams, G.D., 1963, The Mannville Group (Lower Cretaceous) of Central Alberta. Bull. Can. Petrol. Geol., 11, 350-368.

Williams, G.D., Baadsgaard, H. and Steen, G., 1962, Mineral Dates from the Mannville Group. J. Alberta Soc. Petrol. Geol., 10(6), 320-325.

Williams, G.D. and Burk, C.F., Jr., 1964, Upper Cretaceous History of Western Canada. Alberta Soc. Petrol. Geol., Calgary, 169-189.

Williams, G.D. and Stelck, C.R., 1975, Speculations on the Cretaceous Palaeogeography of North America, In: Caldwell, J.G. (Ed.), The Cretaceous System in the Western Interior of North America. Geol. Assoc. Can., Spec. Paper 13, 1-20.

White, R.J. (Ed.), 1960, Oil Fields of Alberta. Alberta Soc. Petrol. Geol., Calgary, 272 pp.

Wood, R.D., Wichmann, P.A. and Watt, H.B., 1974, Gamma Ray Neutron Log. Dresser Atlas Log Review 1, Sect. 8, 1-20.